1995

Hydrometeorological investigations on a small valley glacier in the Sawtooth Range, Ellesmere Island, Northwest Territories

Paul Michael Wolfe
Wilfrid Laurier University

NOTICE

The quality of this microform is heavily dependent upon the quality of the original thesis submitted for microfilming. Every effort has been made to ensure the highest quality of reproduction possible.

If pages are missing, contact the university which granted the degree.

Some pages may have indistinct print especially if the original pages were typed with a poor typewriter ribbon or if the university sent us an inferior photocopy.

Reproduction in full or in part of this microform is governed by the Canadian Copyright Act, R.S.C. 1970, c. C-30, and subsequent amendments.

AVIS

La qualité de cette microforme dépend grandement de la qualité de la thèse soumise au microfilmage. Nous avons tout fait pour assurer une qualité supérieure de reproduction.

S'il manque des pages, veuillez communiquer avec l'université qui a conféré le grade.

La qualité d'impression de certaines pages peut laisser à désirer, surtout si les pages originales ont été dactylographiées à l'aide d'un ruban usé ou si l'université nous a fait parvenir une photocopie de qualité inférieure.

La reproduction, même partielle, de cette microforme est soumise à la Loi canadienne sur le droit d'auteur, SRC 1970, c. C-30, et ses amendements subséquents.

Canada

HYDROMETEOROLOGICAL INVESTIGATIONS ON A SMALL VALLEY GLACIER IN THE SAWTOOTH RANGE, ELLESMERE ISLAND, NORTHWEST TERRITORIES.

by

PAUL MICHAEL WOLFE

THESIS

Submitted to the Department of Geography

in partial fulfilment of the requirements

for the Master of Arts degree

Wilfrid Laurier University

1995

ISBN 0-612-01828-8

Canada

ABSTRACT

Hydrometeorological techniques were employed during the summer of 1993 to study a small ($4.7km^2$) valley glacier in the Sawtooth Range, Fosheim Peninsula, Ellesmere Island, Northwest Territories.

The annual 1992-93 mass balance for Quviagivaa Glacier (unofficial name), and for the adjacent Nirukittuq Glacier (unofficial name) was -532mm and -530mm water equivalent respectively. The equilibrium line altitude was above the upper limit of the glaciers due to the exceptional warmth of the summer. Slight marginal shrinking in the areal extent of Quviagivaa Glacier since 1959 suggests that strongly negative mass balances such as those recorded in 1993 are not indicative of the last 46 years.

In order to determine the main factors influencing ablation and runoff on the glacier, statistical analyses were performed using daily runoff values, ablation data, and several hydrometeorological elements. Accumulated hourly temperature (melting degree hours) had the highest correlated with ablation. The best prediction of average daily discharge was achieved using a multiple regression of discharge with air temperature, wind speed, shortwave incoming radiation, and net radiation hours.

Superimposed ice formed on 95% of the surface of Quviagivaa Glacier during the melt season, and reached thicknesses of 30cm at the glacier terminus. A strong correlation was found between snow depth and superimposed ice formation. On average, 67% of the snowpack water equivalent formed superimposed ice. The net accumulation of superimposed ice occurred on <10% of the area of Quviagivaa Glacier, but evidence suggests that in 1992 this percentage was closer to 65%. It is likely that the primary form of net accumulation for the glaciers of the Sawtooth Range is superimposed ice.

ACKNOWLEDGMENTS

This project began as an idea, developed during discussions with Dr. Bea Alt, while at Hot Weather Creek in the summer of 1990. Dr. Michael English, my advisor, believed that the project was possible, and beginning in the fall of 1991 worked with me to bring this idea to fruition. Special thanks are due to Mike for his support and enthusiasm. I'm thankful for the assistance of Cameron Chadwick and LeeAnn Fishback, who lived and worked with me for three months at the glacier site. Thanks also to David Atkinson, who has been involved with this project since its conception. Dave named the glacier, and helped with the acquisition and set-up of the meteorological instruments. Thanks to Helen Taylor and Shannon Glenn for the loan of a water level recorder after the big storm and to James Hartshorn and Scott, who helped on the glacier during the 1994 field visit.

Many thanks must go to my committee members, Dr. Gordon Young, Dr. Kenneth Hewitt, Dr. Peter Adams, and Dr. Roy Koerner. Their expertise has been invaluable, and their example inspiring. Thanks also to Dr. Gracie at the University of Toronto for help with the photogrammetry.

The project was financially and logistically supported by the Northern Scientific Training Program, Wilfrid Laurier University, the Cold Regions Research Centre, and the generous support of the Polar Continental Shelf Project, Natural Resources, Canada. Scholarship assistance from Wilfrid Laurier University and the Ontario Graduate Scholarship program was much appreciated.

Thanks to all those at the Cold Regions Research Centre (Al, Rich, Cam, Corinne, and James), the Geography Department at Wilfrid Laurier University (Pam, Grant, Alex and Mike), and in the Arctic research community (Sylvia, Toni,

Hok, Bea, Fritz, Kelly, Fenja, Kathy, Bob, Steve, Catherine, Scott, Che, Jodi, LeeAnn, Miles, and others!), who I've had the pleasure of working with.

I'm very grateful for the loving support of my wife, Maria, my family, and my parents, Gerald and Diane Wolfe, and their expectations of good.

TABLE OF CONTENTS

ABSTRACT. i
ACKNOWLEDGMENTS. ii
TABLE OF CONTENTS. iv
LIST OF TABLES. viii
LIST OF FIGURES. ix

CHAPTER 1. INTRODUCTION. 1

1.1 The Scientific Problem. 1

1.2 Objectives. 1

1.3 Regional Setting of Study Location. 2

1.3.1 Physiography. 7
1.3.2 Climate. 11
1.3.3 Glaciers. 12

1.4 Organization of Thesis. 13

CHAPTER 2. LITERATURE REVIEW. 17

2.1 Glacier research in the Queen Elizabeth Islands. 17

2.2 Arctic glacier hydrology. 20

2.2.1 Glacier mass balance. 21
2.2.1.1 Mass balance systems 21
2.2.1.2 Mass balance field methods. 23
2.2.1.3 Determination of glacier mass balance. 27
2.2.2 Runoff from a glaciated catchment. 28
2.2.2.1 Hydrograph characteristics of Arctic catchments. 29
2.2.2.2 Streamflow lag effects. 31
2.2.2.3 Meteorological effects on glacier runoff. 33
2.2.3 Superimposed ice. 36

CHAPTER 3.

MANUSCRIPT 1: Mass balance of two small glaciers in the Sawtooth Range, Fosheim Peninsula, Ellesmere Island, Northwest Territories. 41

Abstract. 42

3.1 Introduction. 43

3.2 Mass balance methods and potential error. 43

3.3 Results. 47

3.3.1 Winter mass balance, Quviagivaa Glacier. 47
3.3.2 Summer mass balance, Quviagivaa Glacier. 49
3.3.3 Net mass balance, Quviagivaa Glacier. 50
3.3.4 Net mass balance, Nirukittuq Glacier. 58

3.4 Discussion. 60

3.4.1 Comparisons with other glaciers. 60
3.4.2 Representativeness of the 1992-93 mass balance year. 62

3.5 Conclusions. 63

CHAPTER 4.

MANUSCRIPT 2: Climate-ablation-runoff relationships on a small high Arctic glacier, Ellesmere Island, Northwest Territories, Canada. 66

Abstract. 67

4.1 Introduction. 68

4.2 Methods. 69

4.3 Results. 72

4.3.1 General observations of discharge. 72
4.3.2 Hydrometeorological conditions and ablation. 78
4.3.3 Ablation and runoff. 81
4.3.4 Hydrometeorological conditions and runoff. 83
4.3.4.1 Air temperature. 83
4.3.4.2 Precipitation. 85
4.3.4.3 Solar Radiation. 86
4.3.4.4 Albedo. 87
4.3.4.5 Wind. 90
4.3.4.6 Multiple variable prediction of runoff. 91

4.4 Discussion. 93

4.4.1 The extrapolation of hydrometeorological values across a glacier. 93
4.4.2 Comparisons with other basins. 95
4.5 Conclusions. 100

CHAPTER 5

MANUSCRIPT 3: The measurement and characteristics of superimposed ice on a small high Arctic glacier, Ellesmere Island, Northwest Territories, Canada. 102

Abstract. 103

5.1 Introduction. 104

5.2 Methods. 105

5.3 Results. 106

5.3.1 Superimposed ice formation and growth. 106
5.3.2 Snow distribution and depth. 109
5.3.3 Ice surface slope and roughness. 112
5.3.4 Meltwater delivery. 114
5.3.5 Snow-ice interface temperature. 117
5.3.6 Superimposed ice distribution and its importance. 119

5.4 Discussion. 122

5.5 Conclusions. 125

CHAPTER 6. SUMMARY AND CONCLUSIONS

6.1 Summary. 127

6.2 Implications for climate change. 130

6.3 Conclusions. 135

6.4 Recommendations for the future. 136

REFERENCES. 139

SELECTED REFERENCES NOT CITED. 147

LIST OF APPENDICES

Appendix A - Accuracy and natural variation of albedo measurements. 151

Appendix B - Average daily meteorological data from the Glacier meteorological station, 875m a.s.l. 158

Appendix C - Glacier meteorological station data: wind direction frequency by sector. 161

Appendix D - Average daily meteorological data from the Valley meteorological station, 230m a.s.l. 164

Appendix E - Air temperature lapse rates calculated from the Glacier and Valley meteorological stations for four different weather types. 167

Appendix F - Melting Degree Hour daily totals and estimated melt at glacier elevations from 550-1200m a.s.l. 170

Appendix G - Average daily temperature plot for Camp, Valley, Glacier, Hot Weather Creek, and Eureka sites, May 30-August 10, 1993. 173

Appendix H - Sawtooth Glacier Camp PCSP twice daily meteorological data, May 26-August 11, 1993. 175

Appendix I - Ablation station data from AS1-12, including surface lowering, snow and ice density, ablation water equivalent, albedo, and sky condition and comments. 181

Appendix J - Plot of seasonal albedo at AS1-12. 191

Appendix K - Scattergraphs of discharge vs. ablation for AS1-12. 193

Appendix L - Scattergraphs of ablation vs. absorptivity for AS1-10. 196

Appendix M - An analysis of the August, 1993 snowstorm. 199

Appendix N - Rating curves for Quviagivaa Creek. 202

Appendix O - Daily average and total discharge values for Quviagivaa Creek, June 14-August 9, 1993. 204

LIST OF TABLES

Table 1.1 Specifications of the Quviagivaa Creek catchment, and Quviagivaa and Nirukittuq glaciers. 6

Table 1.2 Mean July temperatures at Eureka and Hot Weather Creek, 1988-1993 12

Table 2.1 Properties of mass balance glaciers in the Queen Elizabeth Islands. 17

Table 2.2 Glacier mass balance measurement methods. 23

Table 2.3 Zonation on high Arctic glaciers 38

Table 3.1 Estimated and measured melt from 875-1200m a.s.l., June 29-August 3, 1993. 56

Table 4.1 Instrumentation of the glacier meteorological station. 70

Table 4.2 Arctic glacial runoff studies. 96

Table 5.1 Superimposed ice formation on Quviagivaa Glacier. 107

Table 5.2 Periods and amounts of maximum snow-ice interface warming at the glacier meteorological station. 117

LIST OF FIGURES

Figure 1.1 Location map of the Fosheim Peninsula, Ellesmere Island, showing the Sawtooth Range, Study Area and Quviagivaa Glacier. 3

Figure 1.2 Photograph of Quviagivaa Glacier, July 30, 1993. 4

Figure 1.3 Photograph of Nirukittuq Glacier, July 17, 1993. 4

Figure 1.4 Coverage of Quviagivaa and Nirukittuq glaciers by elevational range. 5

Figure 1.5 Hypsometric curves for Quviagivaa and Nirukittuq glaciers. 5

Figure 1.6 Photograph of the Sawtooth Range, early July, 1993. 8

Figure 1.7 Topographic map of the Quviagivaa Creek basin, showing Nirukittuq and Quviagivaa glaciers, and locations of ablation stakes, superimposed ice measurement sites, the glacier meteorological station, and the stream gauging site. 9

Figure 1.8 Photograph of Mt. Qalliq and the uppermost slopes of Quviagivaa Glacier, May 30, 1993 10

Figure 1.9 Air photograph of a glacier in the northern part of the Sawtooth Range, 1959. 14

Figure 1.10 Air photograph of several cirque glaciers in the southern part of the Sawtooth Range, 1959. 15

Figure 1.11 Photograph of an unnamed glacier in the central Sawtooth Range, July 31, 1993. All snow and superimposed ice have ablated on the glacier surface. 16

Figure 2.1 Photograph of cryoconite holes in ablating glacier ice, Quviagivaa Glacier. 25

Figure 2.2 Hydrographs of Hot Weather Creek for 1991 (A), and Quviagivaa Creek for 1993 (B). 30

Figure 2.3 Photograph of meltwater channels and slush flow deposits in deep snow at the terminus of Nirukittuq Glacier, July 9, 1993. 32

Figure 2.4 Photograph of supraglacial meltwater channels on Quviagivaa Glacier, July 17, 1993 34

Figure 2.5 Photograph of superimposed ice under a saturated snowpack at the terminus of Quviagivaa Glacier, July 6, 1993. 37

Figure 3.1 Photograph of an ablation station on Quviagivaa Glacier. 45

Figure 3.2 Map of winter mass balance, 1992-93 for Quviagivaa Glacier. . .48

Figure 3.3 Map of summer mass balance, 1993 for Quviagivaa Glacier. . . .51

Figure 3.4 Ablation as a function of altitude on Quviagivaa Glacier. A table is included, listing ablation stations, their elevations, and total ablation. 52

Figure 3.5 Ablation at AS5-7 (A) and at AS6, 8, and 9 (B) on Quviagivaa Glacier, 1993. 53

Figure 3.6 Surface albedo at AS5-7 (A) and at AS6, 8, and 9 (B) on Quviagivaa Glacier, 1993 54

Figure 3.7 Map of net mass balance, 1992-93 for Quviagivaa Glacier. 55

Figure 3.8 Ablation at AS10 as a function of melting degree hours accumulated during the period of measured ablation. 57

Figure 3.9 Map of net mass balance, 1992-93 for Nirukittuq Glacier. 59

Figure 3.10 Terminus locations of Quviagivaa Glacier for 1993, 1959, and the estimated ice margin during the Little Ice Age. 64

Figure 4.1 Photograph of the glacier meteorological station. 71

Figure 4.2 The total discharge record of Quviagivaa Creek for 1993, with major flow periods delineated. 73

Figure 4.3 Photograph of a large slush flow at the terminus of Quviagivaa Glacier, June 29, 1993 75

Figure 4.4 Photograph of an advancing slush flow on the central snout of Quviagivaa Glacier, July 5, 1993. 75

Figure 4.5 Photographs of Quviagivaa Glacier. A: June 1 (pre-melt); B: June 29 (start of main melt period); C: July 30 (end of melt season); D: August 5 (post-melt). 77

Figure 4.6 Plots of meteorological elements for the period of stream discharge. A: Average daily air temperature; B: Average daily incoming shortwave radiation and net radiation; C: Average daily wind speed; D: Average daily glacier albedo. 79

Figure 4.7 Ablation as a function of absorptivity at AS1-12 on Quviagivaa Glacier 80

Figure 4.8 Ablation at AS10 as a function of meting degree hours accumulated during the period of measured ablation. 80

Figure 4.9 Ablation versus discharge for periods of measured melt on Quviagivaa Glacier 82

Figure 4.10 Cumulative ablation at AS1-12 on Quviagivaa Glacier, 1993. . . .82

Figure 4.11 Scattergraph of average daily air temperature and average daily discharge for period of main melt on Quviagivaa Glacier. 84

Figure 4.12 Average daily temperature and discharge, June 12-August 9, 1993. 84

Figure 4.13 Scattergraph of net radiation days and average daily discharge for period of main melt on Quviagivaa Glacier. 88

Figure 4.14 Scattergraph of average glacier absorptivity and average daily discharge for the period of main melt on Quviagivaa Glacier 88

Figure 4.15 Surface conditions for Quviagivaa Glacier on four dates during the 1993 ablation season. 90

Figure 4.16 Scattergraph of average daily wind speed and average daily discharge for the period of main melt on Quviagivaa Glacier. 92

Figure 5.1 Superimposed ice growth curves for AS1-12 on Quviagivaa Glacier, 1993. 108

Figure 5.2 Map of winter mass balance, 1992-93 for Quviagivaa Glacier. .110

Figure 5.3 Maximum superimposed ice thickness as a function of snow depth at 23 sites on Quviagivaa Glacier 111

Figure 5.4 Daily melt rates at AS10, with periods of ice lense formation within the snowpack and superimposed ice formation delineated 116

Figure 5.5 Hourly air temperature and snow-ice interface temperature at four locations near the glacier meteorological station during the period of meltwater percolation 118

Figure 5.6 Mean daily snow-ice interface temperature change for four locations near the glacier meteorological station, for the pre-melt and meltwater percolation stages. 118

Figure 5.7 Map of maximum superimposed ice formation during the melt season and coverage at the termination of the season on Quviagivaa Glacier, 1993. 120

Figure A1 Photograph of a loose "weathering rind" glacier ice surface and the much darker, saturated ice beneath, Quviagivaa Glacier, June 29, 1993. . . .156

CHAPTER 1. INTRODUCTION

1.1 The Scientific Problem

Glaciers are one of the dominant physiographical features in mountainous regions of the Canadian high Arctic. Few intensive, field-based Arctic glacier studies exist. New records of accumulation, ablation and superiimposed ice formation on glaciers, and runoff from glacierized catchments are needed, both to better understand the complex interaction of glacier hydrological processes and climate, and to assess the sensitivity of such processes to changes in climate. Recent predictions of climate change for the Canadian high Arctic include increases in air temperature and precipitation. An increased understanding of glacio-hydrological processes and their interaction with climate on small glaciers should assist in determining how predicted climate change and the many potential negative and positive feedbacks will affect these glaciers.

1.2 Objectives

The primary objectives of this thesis are as follows;

a) To record in detail the hydrological cycle of a small high Arctic glacier in the Sawtooth Range, Fosheim Peninsula, Ellesmere Island, using:

   1) Winter accumulation and summer ablation measurements on the glacier.

   2) Meteorological data from stations on the glacier and on ice-free land 7km west of the glacier.

3) A continuous discharge record from the creek draining the glacier.

b) To relate runoff from the glacierized basin to ablation and various hydrometeorological parameters, such as air temperature, precipitation, solar radiation, albedo, and wind, in order to determine the relative importance of these factors in producing glacier runoff.

c) To examine hydrological processes occurring on the glacier, especially the extent, physical requirements for formation, and role of superimposed ice in the glacier mass balance.

1.3 Regional Setting of Study Location and Fieldwork

An 8.7km^2 glacierized catchment in the central Sawtooth Range, Fosheim Peninsula, Ellesmere Island (79° 33.98' N, 83° 20.48' W) (Fig. 1.1) was selected for study. The basin contains two small glaciers, Quviagivaa (unofficial name) (Fig. 1.2) and Nirukittuq (unofficial name) (Fig. 1.3). The specifications of the catchment and the glaciers are summarized in Table 1.1 and Figures 1.4 and 1.5 show the distribution of glacier ice by altitude, and the hypsometric curves of Quviagivaa and Nirukittuq glaciers, respectively.

Prior to 1993 no glaciological work had been carried out in the Sawtooth Range, although recent research on the Fosheim Peninsula lowlands has included climatological, hydrological, ground ice, geomorphic process, botanical, and paleo-glaciation studies. The selection of Quviagivaa Glacier from over 35 glaciers in the Sawtooth Range as a study glacier for mass balance and related studies was made when its fulfillment of the factors from

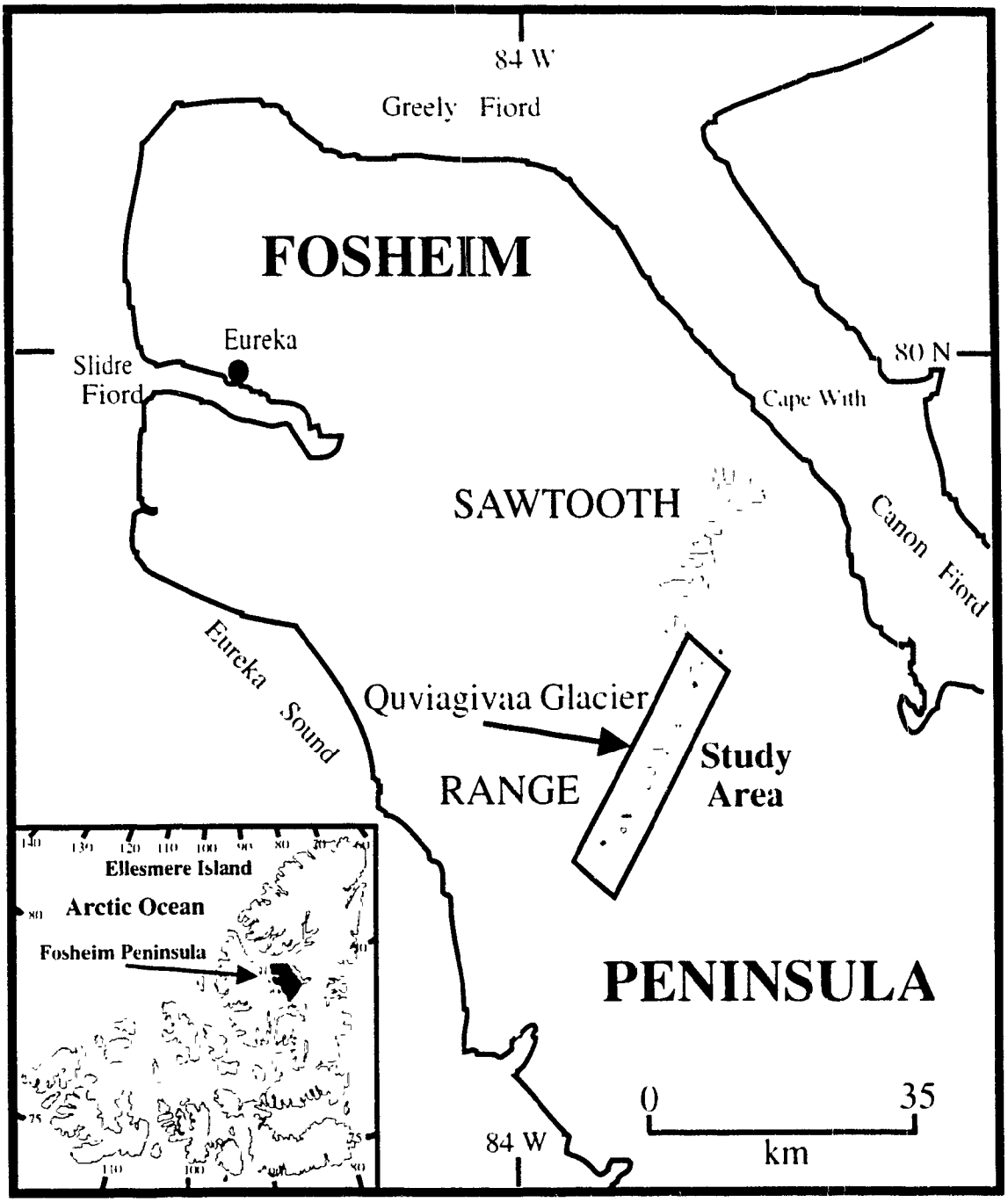

Figure 1.1. Location map of the Fosheim Peninsula, Ellesmere Island, showing the Sawtooth Range, Study Area and Quviagivaa Glacier

Figure 1.2. Photo of Quviagivaa Glacier and base camp, July 30, 1993.

Figure 1.3. Photo of Nirukittuq Glacier, July 17, 1993.

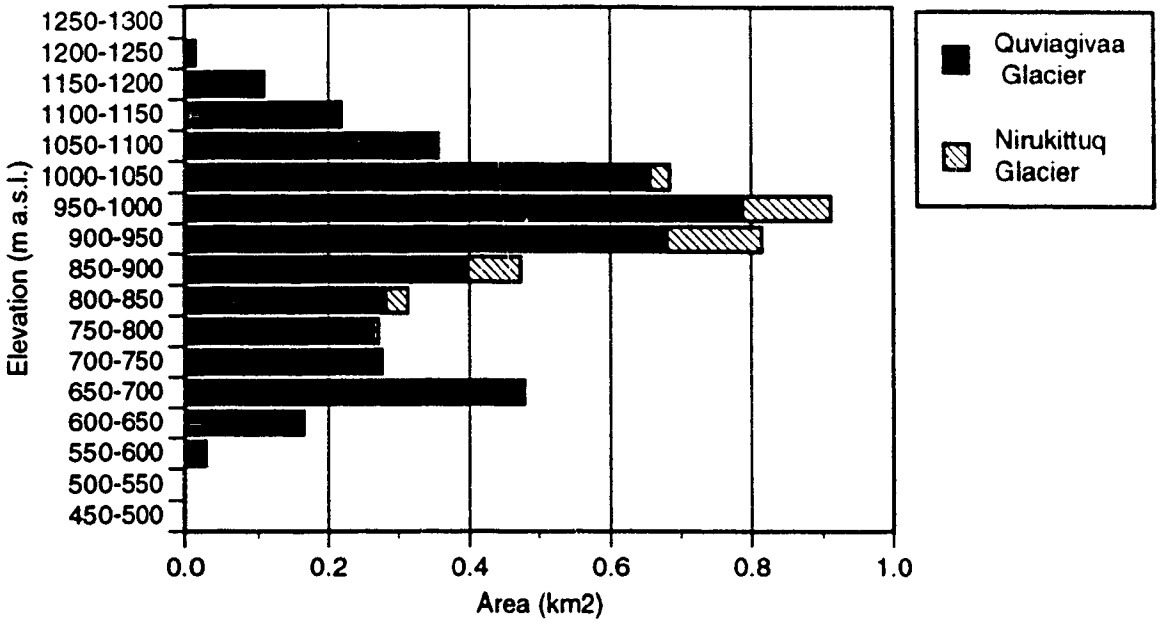

Figure 1.4. Areal coverage of Quviagivaa and Nirukittuq glaciers by elevational range.

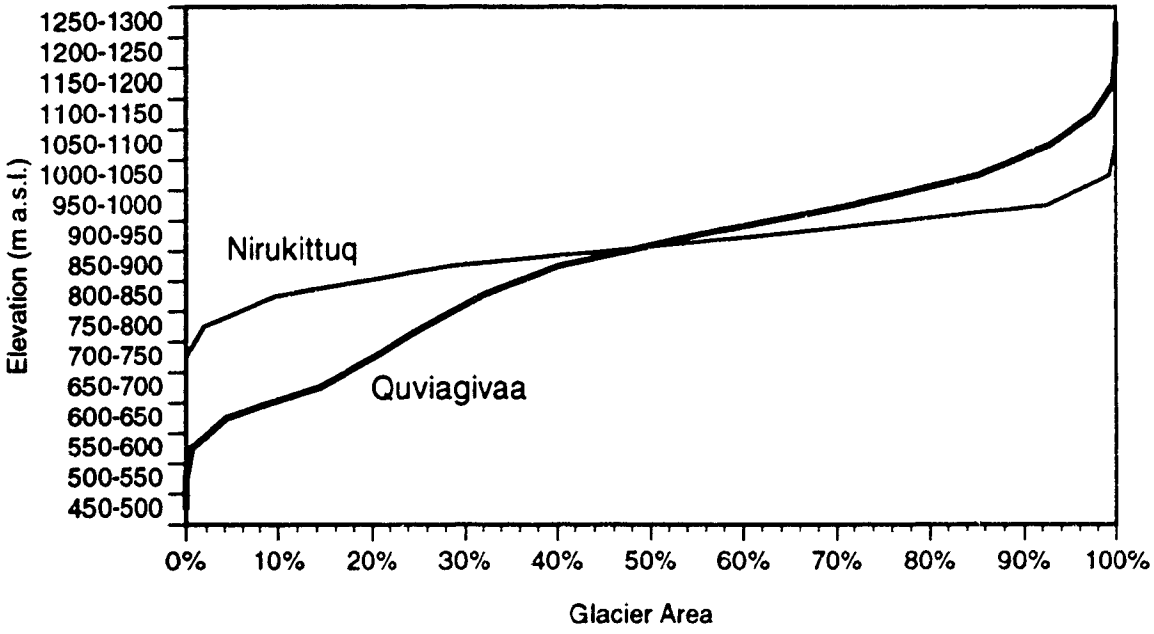

Figure 1.5. Hypsometric curves for Quviagivaa and Nirukittuq Glaciers.

TABLE 1.1

Specifications of the Quviagivaa Creek catchment, and Quviagivaa and Nirukittuq glaciers

	Quviagivaa Creek Catchment	**Quviagivaa**	**Nirukittuq**
Type	Proglacial	Mtn valley glacier	Niche glacier
Area	8.7km^2	4.7km^2	0.4km^2
Elevation	491-1271m a.s.l.	560-1250m a.s.l.	800-1110m a.s.l.
Latitude	79° 34'N	79° 34'N	79° 34'N
Longitude	83° 15'W	83° 15'W	83° 15'W
Orientation	West-northwest	West-northwest	Northwest
*Glacier Number**		46424 C7	46424 C6

*Glacier Atlas of Canada (1969)

Østrem and Brugman (1991) was considered. Namely, that the study glacier has:

1. A well-defined, highly-glacierized catchment.
2. A size comparable to adjacent glaciers, but small enough to be studied by a party of 2-3 people.
3. An elevational range from glacier terminus to upper limit as large as possible.
4. One meltwater stream draining it.
5. Relatively easy access.
6. Few crevasses.
7. Good maps, air photographs, and remote-sensing imagery.

Quviagivaa Glacier met all considerations except number seven, and this was somewhat rectified after the 1993 field season by the creation of a topographic

map of the basin from the 1959 air photographs using photogrammetric methods.

Field work was undertaken between May 25 and August 11, 1993, based from a camp located 900m west of the terminus of Quviagivaa Glacier. Most field work was concentrated on Quviagivaa Glacier, and to a much lesser extent Nirukittuq Glacier. Nine other nearby glaciers were visited. A brief visit was made to Quviagivaa Glacier on June 30, 1994, and several measurements were carried out.

1.3.1 Physiography

The Fosheim Peninsula, is an intermontane lowland, effectively divided into a western and an eastern region by the Sawtooth Range. The Sawtooth Range is a mountain chain of folded and faulted sedimentary rocks of Tertiary age. The range is 5-10km wide and 85km long, and trends in a SSW-NNE direction from the mouth of Vesle Fiord in the south to Cape With on Cañon Fiord in the north. Peaks are sharp and ridge crests are generally even, resembling the teeth of a saw when viewed from a distance (Fig. 1.6). Relief gradually decreases from approximately 1275m a.s.l. at the north end of the range to 975m a.s.l. at the south end. Many deeply incised creeks and rivers are fed throughout the summer by melting snow and ice in the Sawtooth Range, including the headwaters of the Slidre River, which drains most of the western Fosheim Peninsula. Creeks with their origin in the range eventually discharge their waters into Eureka Sound, and Cañon, Slidre and Vesle fiords.

The study basin (Fig. 1.7) is located on the west-facing, mid-section of the range, and contains Mt. Qalliq (unofficial name), the highest peak (1270m a.s.l.) in the southern half of the Sawtooth Range (Fig. 1.8). All ice within the basin

Figure 1 6 Photograph of the Sawtooth Range looking east, early July, 1993
Note: Nirukittuq and Quviagivaa glaciers are the first and second glaciers from left to right

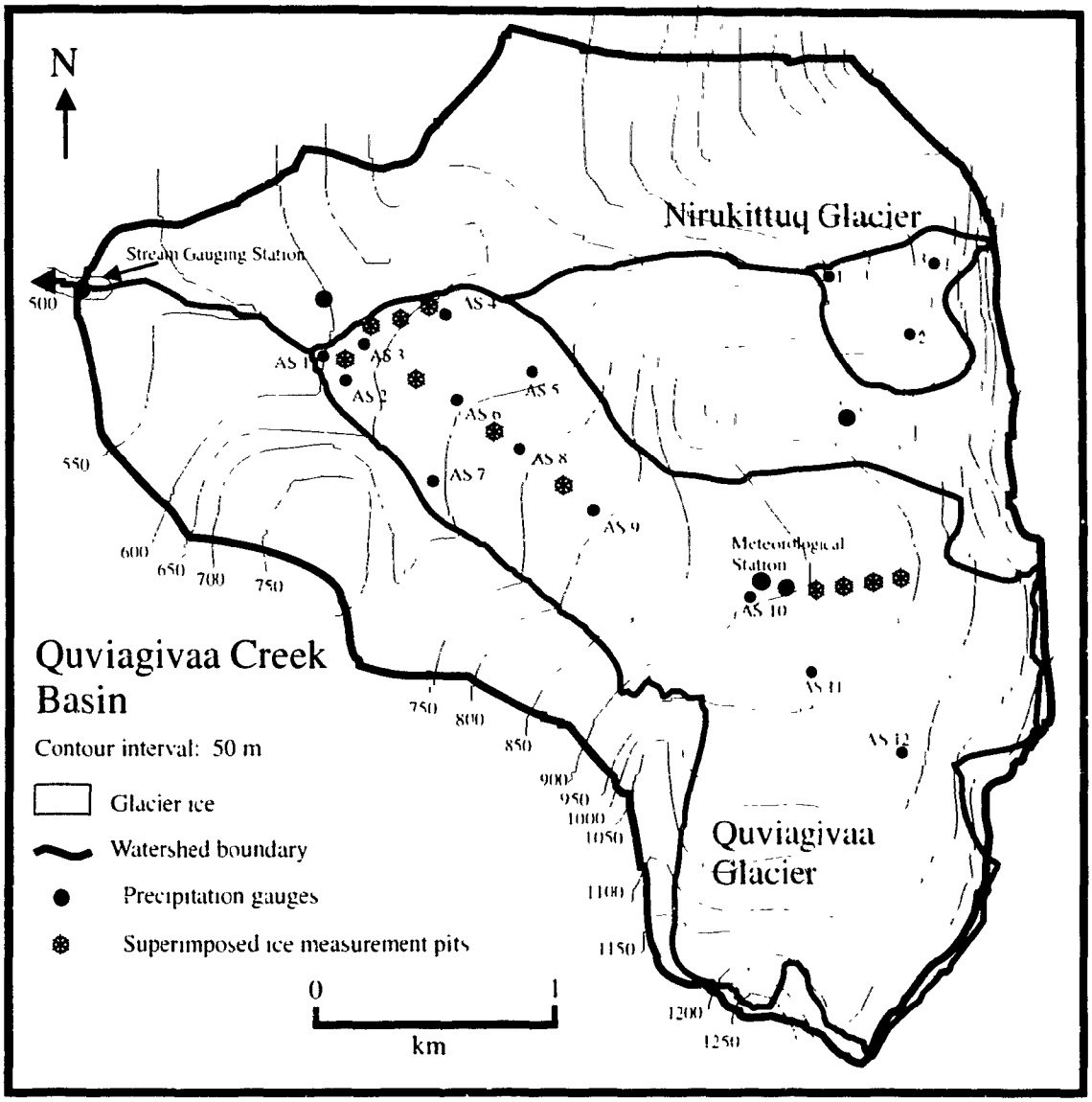

Figure 1.7. Topographic map of the Quviagivaa Creek basin, showing Nirukittuq and Quviagivaa glaciers, and locations of ablation stakes, precipitation gauges, superimposed ice measurement sites, the glacier meteorological station, and the stream gauging site.

Figure 1.8. Photograph of Mt. Qalliq and the uppermost slopes of Quviagivaa Glacier, May 30, 1993.

drains into Quviagivaa Creek (unofficial name), which is deeply incised into the underlying bedrock for its entire course through the basin.

1.3.2 Climate

The Fosheim Peninsula of west-central Ellesmere Island is one of the largest lowlands in the circumpolar Arctic, covering an area in excess of 10 000km^2. The peninsula is part of an intermontane lowland that stretches from the Lake Hazen area to the Svendsen Peninsula on Ellesmere Island, and includes the eastern lowlands of Axel Heiberg Island. Higher summer temperatures and lower amounts of cloud cover than surrounding regions are a result of the mountain ranges of Ellesmere and Axel Heiberg Islands, which tend to block or dissipate slow moving disturbances from the Arctic Ocean and Baffin Bay (Edlund and Alt, 1989). Eureka, located on the north shore of Slidre Fiord, 70km west-northwest of the study basin, has a mean annual temperature of -19.7°C, a mean July temperature of 5.4°C, and an annual temperature range of 43°C (AES, 1982).

Summer temperatures increase markedly inland from Eureka, away from the influence of the open fiords. Table 1.2 shows a comparison of mean July temperatures at Hot Weather Creek (75m a.s.l.), situated 15km from any large body of water or mountain, and Eureka, for 1988-1993. The 1993 fieldwork showed that these warm temperature conditions extend to the foothills of the Sawtooth Range, but that they quickly diminish on the glacierized surfaces. In 1993, mean July temperatures of 9.2 and 3.7°C were recorded at the basecamp (536m a.s.l.) and the meteorological station located on Quviagivaa Glacier (875m a.s.l.) respectively.

Annual precipitation at Eureka averages 64mm, although this value is

TABLE 1.2

Mean July temperatures at Eureka and Hot Weather Creek, 1988-1993

Year	Mean July Temperature (°C)	
	Eureka	Hot Weather Creek
1988	7.3	12.7
1989	4.1	6.3
1990	5.6	8.6
1991	6.3	10.3
1992	5.3	8.2
1993	7.3	12.5

likely an underestimation of actual precipitation caused by difficulties in the measurement of wind-blown snow (Woo et al., 1983). Snowfall is greater in the Sawtooth Range on account of the higher elevations and colder temperatures. The 1992-93 winter (August, 1992-May, 1993) snow survey on Quviagivaa Glacier measured an average value of 303mm snow water equivalent, compared to 46.7mm recorded at Eureka for the same period. Summer precipitation recorded at Quviagivaa Glacier in the Sawtooth Range is also higher, largely because of orographic effects. Total precipitation was 33.5mm at Quviagivaa Glacier for July, 1993, compared with 15.2mm for the same month at Hot Weather Creek, and 10.5mm at Eureka.

1.3.3 Glaciers

Ellesmere Island contains approximately 80 000km^2 of glacierized terrain, 53% of the total glacier ice cover in Canada (Haeberli et al., 1989). Unlike most of the island, the Fosheim Peninsula is largely ice-free, with the

exception of the Sawtooth Range and several ice caps and glaciers on the higher land of eastern Fosheim Peninsula. The Sawtooth Range supports over 35 separate ice fields, valley glaciers, and cirque glaciers, which range in size from $<0.5km^2$ to $20km^2$, and cover approximately $75km^2$. The majority of glaciers are located on the western side of the mountain range, although some glaciers which "saddle" the divide, also flow down the eastern slope. Most of the ice cover is found in the northern part of the range, where ice caps support valley glaciers up to 5km long (Fig. 1.9). In the southern Sawtooth Range, most ice masses are small niche glaciers with limited valley extension (Fig. 1.10). None of the glaciers reach above 1300m a.s.l., and it is likely that in warmer than average summers most of the ice in the range is below the equilibrium line (Fig. 1.11). Despite their close proximity to Eureka, and the plenitude of research activity in the area, no field studies have been carried out on the glaciers of the Fosheim Peninsula.

1.4 Organization of Thesis

Chapter 1 introduces the thesis, and chapter 2 provides a literature review. Chapters 3, 4 and 5, which constitute the main results of the thesis, are prepared as three manuscripts for publication. Chapter 3 (Manuscript 1) addresses the mass balance of Quviagivaa and Nirukittuq glaciers, Chapter 4 (Manuscript 2) examines the runoff record from Quviagivaa Creek, and relates ablation and various hydrometeorological elements with stream discharge, and Chapter 5 (Manuscript 3) discusses the characteristics and importance of superimposed ice on Quviagivaa Glacier. Chapter 6 includes a summary, the implications for climate change, the conclusion, and recommendations for the future.

Figure 1 9 Air photo showing an ice cap with several valley glacier extensions. in the northern part of the Sawtooth Range This aerial photograph (NAPL #A-16706-75) copyright 1959. Her Majesty the Queen in Right of Canada, reproduced from the collection of the National Air Photo Library with permission Natural Resources Canada

Figure 1 10. Air photo showing several small glaciers in the southern part of the Sawtooth Range. This aerial photograph (NAPL #A-16676-185) copyright 1959, Her Majesty the Queen in Right of Canada, reproduced from the collection of the National Air Photo Library with permission Natural Resources Canada.

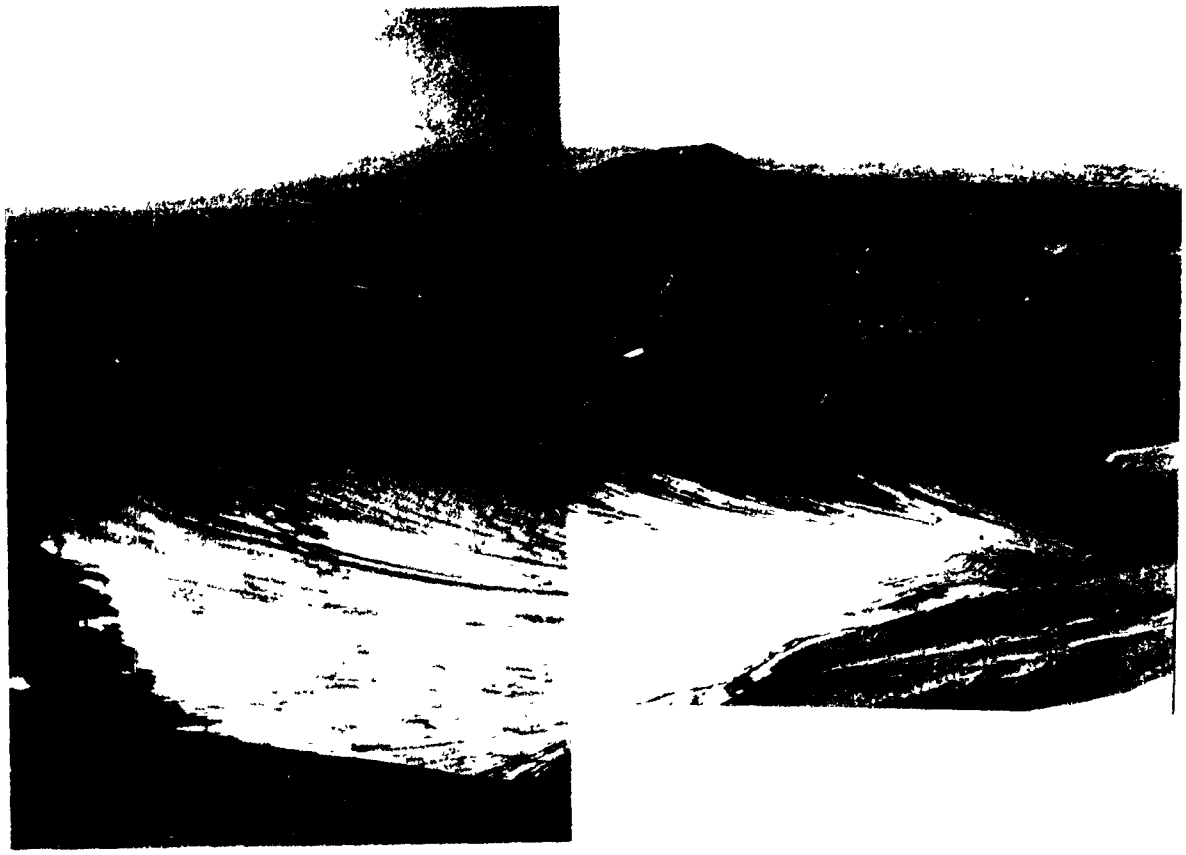

Figure 1.11. Photograph of unnamed Sawtooth Range glacier located 10km north of Quviagivaa Glacier, July 31, 1993. Note: All snow and superimposed ice has melted, and the entire glacier surface has a negative net mass balance.

CHAPTER 2. LITERATURE REVIEW

2.1 Glacier Research in the Queen Elizabeth Islands

Glacier studies were initiated in the Queen Elizabeth Islands in the late 1950s, usually as a component of large, multi-disciplinary research expeditions. Table 2.1 gives the specifications of the major study glaciers in the Queen Elizabeth Islands and the period of mass balance studies.

TABLE 2.1

Properties of mass balance glaciers in the Queen Elizabeth Islands

Name	Glacier Type	Long.	Lat.	Area (km^2)	Elev. Min.	Elev. Max.	First Year	Yrs	Locality
Gilman[1]	valley	-71.30	82.20	480	310	1850	1957	14	N Elles
Ward Hunt[1]	ice rise	-74.17	83.12	32			1958	22	N Elles
Meighen*[2]	ice cap	-99.13	79.95	85	70	267	1960	34	Meighen
Baby*[3]	niche	-90.97	79.43	0.6	715	1175	1960	34	Axel H
White*[3]	valley	-90.83	79.50	38.7	56	1782	1960	34	Axel H
Devon*[2]	ice cap	-82.50	75.33	1696	0	1800	1961	33	Devon
South Melville*[2]	ice cap	-115.02	75.42	66	490	715	1963	30	Melville
Per Ardua[2]	valley	-76.58	81.45	4.7	300	1700	1964	8	N Elles
St. Pat. Bay NE[4]	ice cap	-64.50	81.95	7.6	850	900	1972	12	NE Elles
Laika[5]	IC/valley	-79.17	75.90	9.8	0	530	1973	7	Coburg
Agassiz*[2]	ice cap	-71.55	80.50	n/a	437	1077	1977	17	NC Elles
Leffert/Unnamed[6]	valley	-75.02	78.69	593	20	700	1972	8	SE Elles
St. Pat. Bay SW[4]	ice cap	-64.53	81.93	3	740	820	1983	1	NE Elles
Quviagivaa*[7]	valley	-83.25	79.56	4.7	560	1250	1993	1	WC Elles

*denotes currently studied glaciers

Sources: 1, Young and Ommanney 1984; 2, Koerner, pers. comm., 1994; 3, Cogley et al. 1994; 4, Bradley and Serreze 1987; 5, Blatter and Kappenberger 1988; 6, Müller et al., 1980; 7, This work.

The first glaciological work was carried out as part of the Operation Hazen research expedition to northern Ellesmere Island, supported by the Defence Research Board. Mass balance measurements, snow pit studies, surveying, and glacial-meteorological studies were carried out on Gilman Glacier and an adjoining ice cap from 1957 into the late 1960s (Hattersley-Smith et al., 1961; Sagar, 1964; Arnold, 1968). Long term studies of mass balance and ablation were also initiated on the Ward Hunt Ice Rise and the non-land based Ward Hunt Ice Shelf off the northern coast of Ellesmere Island (Hattersley-Smith and Serson, 1970). In 1959 a field program was started on the Meighen Island ice cap in which mass balance and glacier flow (Arnold, 1965; Paterson, 1969), glacier energy balance (Alt, 1975), and ice core stratigraphy (Koerner, 1968; Koerner and Paterson, 1974) were studied. Also in 1959, members of the Jacobsen-McGill Axel Heiberg Island Expedition began work on the Thompson, Crusoe, Baby, and White glaciers in the Expedition Fiord area of Axel Heiberg Island (Müller, 1961). Working on the White and Baby glaciers from 1959-1961, Adams (1966) was one of the first researchers to study glacier ablation and runoff relationships in the Canadian Arctic. Other glaciological projects on the Axel Heiberg glaciers, over a time period of several decades, included studies of ablation (Müller, 1963; Arnold, 1981), glacier depth (Becker, 1963), glacier meteorology and climate (Andrews, 1964; Havens, 1964; Havens et al., 1965; Müller and Roskin-Sharlin, 1967), ice dammed lakes and glacier marginal drainage (Maag, 1969), glacier inventory (Ommanney, 1969), glacier movement (Iken, 1974), thermal regime (Müller,

1976; Blatter, 1985), and remote sensing of mass balance (Jung-Rothenhäusler, 1992).

In 1961, a glaciological program was initiated on the Devon Ice Cap, as part of the Arctic Institute of North America's expedition to Devon Island. This expedition eventually led to studies of mass balance (Koerner, 1970b), synoptic controls on mass balance (Alt, 1978; 1987), superimposed ice (Koerner, 1970a), accumulation (Koerner, 1966), and climate-ablation-runoff relationships on the ice cap and on the outlet Sverdrup Glacier (Keeler, 1964; Holmgren, 1971). In 1963, mass balance measurements began on South Ice Cap on Melville Island, and in 1964 a mass balance and mapping project began on Per Ardua Glacier in northern Ellesmere Island, as part of the International Hydrological Decade program (Young and Ommanney, 1984). Measurements on a small ice cap near St. Patrick Bay on Ellesmere Island in 1972 were initially limited to mass balance and were discontinued in 1977 (Hattersley-Smith and Serson, 1973), but were restarted along with glacio-climatic studies in 1982 (Bradley and Serreze, 1987b; Serreze and Bradley, 1987). As part of the North Water Project, which ran under the supervision of Fritz Müller from 1972-1980, mass balance, meteorological and thermal regime work was carried out on Laika Ice Cap, Coburg Island, from 1973-1980 (Müller et al., 1977; Blatter and Kappenberger, 1988).

Mass balance monitoring began on the Agassiz Ice Cap in 1977, and at a summit location, several surface to bedrock ice cores were drilled (Koerner et al., 1987). Several more recent short-term projects involving glacier runoff (Flugel, 1983), glacier inventory (Kraus, 1983), and glacier variations (Blake, 1981) have been carried out on Ellesmere Island.

The longest lasting projects have been the mass balance studies on the Meighen, South, Devon and Agassiz ice caps (Koerner, pers. comm., 1994),

and on White and Baby glaciers, Axel Heiberg Island (Ecclestone, pers. comm., 1994). These six mass balance monitoring projects have continued to the present, and at 34 years, the record from the Meighen Ice Cap is the longest mass balance study in the circumpolar high Arctic.

2.2 Arctic Glacier Hydrology

Glacier hydrology involves the study of the accumulation, ablation and movement of water, in both liquid and solid forms, on, under, and within glaciers. Arctic glaciers exist in a permafrost environment and most small glaciers are frozen to the bed, moving only through internal deformation although some mid-sized glaciers (e.g. White Glacier, Axel Heiberg Island, and Laika Glacier, Coburg Island), have a polythermal regime, whereby a temperate basal layer of ice exists in an otherwise cold glacier, allowing sliding over the bed (Blatter and Hutter, 1991). The brief summer season (June to August) is the period of greatest hydrological activity for Arctic glaciers, and understandably is the time frame of almost all hydrological research projects in the Arctic. Even in the summer season, cold temperatures result in processes which are distinct from those occurring on temperate ice masses. Although larger glaciers have internal drainage features such as moulins and artesian features which suggest that water is reaching the glacier bed (e.g. the White Glacier and the Gilman Glacier), Arctic glacier hydrology is simplified on most small glaciers because of the lack of internal water movement. On the smallest glaciers, such as those in the Sawtooth Range, crevasses do not normally drain to the bed, there are few moulins, and all runoff occurs over the glacier surface in supraglacial channels and in marginal channels (which often erode channels under stagnant glacier ice at the glacier terminus). One of the most important features of high Arctic

glaciers, which has a bearing on mass balance and the energy balance, is the refreezing of meltwater on the glacier surface as "superimposed ice". A review of glacier mass balance, glacier runoff, and superimposed ice are given as background for Chapters 3-5, which contain the main results of this study.

2.2.1 Glacier Mass Balance

The mass balance of a glacier is determined by the processes of accumulation and ablation of snow and ice, occurring throughout the balance year. The net mass balance (b_n) can be negative or positive, and in a simplified form, can be expressed as:

$$b_n = b_w + b_s$$

The winter mass balance (b_w) is dominated by accumulation processes (e.g. snowfall, avalanches), and is normally positive, while the summer mass balance (b_s) is dominated by ablation processes (e.g. melting followed by runoff, sublimation, calving of icebergs), and is normally negative. If the sum of the summer and winter balances for one mass balance year (e.g. September-August) is negative, then the glacier is losing mass (shrinking), while if the sum is positive, the glacier is gaining mass (growing).

2.2.1.1 Mass Balance Systems

The mass balance "year", and the "winter" and "summer" periods are variable in time and space. There are several different systems for the

measurement of mass balance which attempt to take into account this variability.

The most common system, and the one used in this study, is the "stratigraphic" system (Unesco, 1970). This involves measuring the annual minimum and maximum balance for each site, and integrating these values over the whole glacier in order to calculate the net mass balance. In the Arctic, the end of the "winter" season (the accumulation maximum), will occur in May or June, while the end of the "summer" season (the ablation maximum) may occur at any time from July to September. This system is difficult to put into practice if the glacier is remote and only a limited field season is possible. In addition, the summer and winter horizons are often not formed at the same time over the entire glacier, making the integration of stake values over the glacier surface difficult.

The "fixed-date" system (Unesco, 1970) was suggested by the International Association of Hydrological Sciences in order to simplify measurements made by the stratigraphic system. In this system, measurements of net change are made during one calendar year as defined by fixed dates of measurement (e.g. Oct. 1 to Sept. 30). Logistics make the use of this system impractical, and it is not widely used in Canadian studies (Østrem and Brugman, 1991).

Mayo et al. (1972) introduced a system combining the stratigraphic and fixed-date systems, which uses a more detailed identification of snow and ice types, and measures early and late-winter and early and late-summer balances. This system can be more accurate than the previously mentioned systems, but is more time consuming, and may not give the complete glacier mass balance.

2.2.1.2 Mass Balance Field Methods

A wide range of glacier mass balance measurement methods are used by field researchers. Table 2.2, based on Østrem and Brugman (1991), shows eleven different glacier mass balance measurement methods used by

TABLE 2.2

Glacier mass balance measurement methods

Measurement Methods	Glacier Measured	Details
A. Traditional	entire	surface stakes, snow probing, snow pit methods, snow coring, surveying locations
B. Snow-Cover	entire	same as A except measure only ablation less snow cover remaining at end of summer
C. Index Stake		
1. Balance/Elevation Integration	entire or portion	longitudinal profile of surface stakes, snow pit, coring, surveying locations
2. Stake Farm	portion	localized high density network of surface stakes, snow pit and ice core methods
3. Single Stake	portion	one stake, snow pit and ice core methods
D. Statistical Models		
1. Linear Balance Model	entire or portion	multivariate/statistical methods employed using data obtained from A & C based on site and yr
2. Parameter Correlation Model	entire or portion	similar to D1 but with additional correlations based upon model of most important melt parameters expected (e.g. topography, roughness, slope, aspect, etc.)
E. Reconnaissance 1. AAR 2. ELA 3. Runoff Line	entire	remote sensing using microwave to visible wavelengths, aerial photogrammetry, ground surveys of snow line & surface roughness, runoff/refreezing features, mapping of superimposed ice zones
F. Geodetic	entire	photogrammetry, remote sensing imagery, ground theodelite & EDM surveys and/or GPS, radar and laser altimetry
G. Hydrologic	entire	basin wide precipitation, evaporation and runoff
H. Terminus Position	entire	ground surveys, remote sensing or aerial photographs, glacier flow response model; often called the "inverse problem"
I. Cross-section	entire	mass continuity using successive glacier cross-sections, especially across ELA
J. Velocity Vector	entire or portion	ice flow in vertical & horizontal directions; topographic change
K. Climate Parameter Model	entire or portion	energy balance at surface, precipitation; temperature/precipitation at nearby locations

researchers around the world. The Traditional method, using a surface stake network, snow depth probing, and snow pits is the main method being used on small Arctic glaciers today (Ecclestone, pers. comm., 1994). In remote regions such as the Arctic, one visit per year to the glacier is standard. Measurements are usually made before the initiation of spring melt, and the previous summer mass balance is calculated by subtracting the net balance from the winter balance. The following paragraphs describe the Traditional methods of mass balance measurement for spring-only visits and melt season monitoring scenarios.

During the spring, prior to the onset of melt, pits are excavated or cores extracted to measure the snow water equivalent of the winter accumulation at stake locations. This involves identifying the previous summer surface, which is usually easily located in the ablation zone where the surface is often dust-laden and is comprised of low density, cryoconite glacier ice (Fig. 2.1) (Wharton et al., 1985). In the upper areas of the glacier, the summer surface may be composed of melt-affected superimposed ice or firn (Østrem and Brugman, 1991). Superimposed ice is normally clean and free from cryoconite, and on account of these characteristics can be distinguished from glacier ice. However, a firn surface may be confused with a melt layer within the winter snowpack, formed either in the previous fall or earlier in the spring. At this point it may be necessary to examine local meteorological records (if such records exist) to determine the likely time of formation of the problematic ice layers. In addition, in firn zones, summer melt may penetrate into the firn layer or layers of previous years, thereby leading to possible overestimation of ablation if surface lowering is simply read off the stake. The volume of meltwater percolation has been measured using trays, which are buried sufficiently deep to prevent them being exposed by the end of the melt season. The following spring, the amount of ice

Figure 2 1. Photograph of cryoconite holes in ablating glacier ice, Quviagivaa Glacier

in the tray and the change in density of the overlying firn must be measured to calculate total melt (Koerner, 1986). Trabant and Mayo (1985) in the accumulation area of the McCall Glacier, Alaska in 1971, found that more than 60% of the annual snow accumulation melted and refroze within firn layers from previous years. If percolation trays are not used, the density of several annual layers may need to be checked each year.

In ideal situations, researchers are at the study glacier for the entire period of melt. In such cases, the balance of the glacier can be measured in greater detail. Spring measurements are carried out as described previously. Summer ablation is normally monitored on a daily or weekly time frame, using the stake network (Østrem and Brugman, 1991). Measurements of ablation over short periods of time are subject to several errors caused by ablation stake effects and the characteristics of melting ice (Müller and Keeler, 1969). An error results when ablation is measured at the base of the stake caused by heat absorption and channeling of meltwater by the stake. Keeler (1964) addressed this problem by measuring surface lowering from wire strung between three stakes in triangle formation, although this setup is liable to errors caused by sagging of the wire. When single stakes are used experiments with different materials (steel, aluminum, PVC, and wood), have shown that wood stakes are the most reliable, although problems with the absorption of solar radiation and pole buoyancy still introduce some error (Østrem and Brugman, 1991). The short-term measurement of ablation in mm of water equivalent is complicated by to the presence of a "weathering rind", a less dense layer which develops in glacier ice under high solar radiation conditions. The weathering rind, which can reach densities as low as 0.5g cm^{-3}, fluctuates in depth based on the weather type, reaching maximum development during sunny conditions, and wasting away during warm, rainy, windy periods. This fluctuation introduces an

error when a constant ice density is assumed. When daily ablation values are required, it is often necessary to take repeated ice cores in order to quantify the density change. Over the period of an entire summer, the net change in ice surface density will be small, as the cycles of weathering rind formation and destruction tend to cancel each other out (Müller and Keeler, 1969).

2.2.1.3 Determination of Glacier Mass Balance

To determine the mass balance of the entire glacier, mass balance measurements from individual stakes are applied to the areas around them. Normally, the stake network should cover the entire glacier so that extrapolation beyond the stake network is minimized. In addition, glacier edges should be well represented to take account of marginal characteristics such as high snow accumulation and dirty, debris-covered ice. In Canadian Arctic studies, stake densities have ranged from several km^2 per stake on Devon ice cap (Koerner, pers. comm., 1994) to 14 stakes km^{-2} for the Boas Glacier, Baffin Island in 1970 (Jacobs et al., 1972). Keeler (1964) simulated a higher stake density by measuring surface lowering at 30 marked intervals from a wire strung between three stakes. For small glaciers, where the pattern of accumulation and ablation is well known, values of mass balance for each stake can be plotted on a map, and contours of equal balance drawn. The glacier mass balance is then determined by summing all the areally weighted balance values. This method is especially useful for glaciers which do not show a simple decrease in net balance with increasing altitude, such as was found for Laika Glacier (Blatter and Kappenberger, 1988).

The drawing of equiablation maps involves some subjectivity, and for larger glaciers which do not have a dense stake network, and are not monitored

throughout the melt season, it is not a preferred method. A common error on larger glaciers is the underrepresentation of areas with crevasses. These areas are undersampled because of the frequent loss of stakes in crevasses and the hazards of travel in such regions. For large glaciers, a common method is to average all stake measurements within an elevational band (e.g. 100m) to produce an average mass balance value for that elevational range. When this has been completed for all elevational bands, a graph is produced with elevation on the y-axis and mass balance (mm water equivalent) on the x-axis. A line is fitted through the points manually or using a computer line-fitting program, and the glacier mass balance is calculated from the intersection of the line through mid-points of each elevational band. Cogley et al. (1994), in a reexamination of the 32 year mass balance record of the White Glacier, fitted computer-generated polynomials to each annual set of grouped 100m-band means. For the 32 year period of observations, the authors found that the automated method produced an average mass balance estimate identical to that using the manual method (-100mm), while the difference for individual years ranged from an underestimate of 71mm to an overestimate of 24mm.

2.2.2 Runoff From a Glacierized Catchment

Streamflow from a glacierized catchment is controlled by winter precipitation, the summer energy balance, and summer precipitation events. The components of runoff from a glacierized basin are as follows:

$$Q_t = Q_s + Q_p + Q_g + Q_i$$

where Q_t is total discharge, Q_s is snowmelt from non-glacierized areas (including permafrost melt in warm summers), Q_p is runoff from rainfall, Q_g is ground water discharge (negligible in glacierized, continuous permafrost regions), and Q_i is the runoff from the glacier (ice melt, firn melt, and snowmelt) (Young, 1990). The proportions of these components to runoff will vary for any given year and depend on the percentage of ice cover in the basin. Stream discharge in basins which have over 50% ice cover will likely be dominated by ice melt in most years, and are called proglacial basins. Proglacial basins are important regulators of streamflow, as they store precipitation in the form of snow and ice in cold, wet years, and release that storage during warm, dry years through snow and ice melt.

2.2.2.1 Hydrograph Characteristics of Arctic Catchments

The shape of the hydrograph from any given proglacial catchment will vary from year to year in light of variations in winter snowfall and summer weather. However, several features are characteristic of hydrographs from proglacial catchments and are not found in neighbouring nival basins. Figure 2.2 shows hydrographs from Hot Weather Creek for 1991 and Quviagivaa Creek for 1993, two drainage basins located on the Fosheim Peninsula, Ellesmere Island. The two hydrographs illustrate the differences between ice-free, lowland catchments and higher elevated, partially glacierized catchments, respectively. The hydrograph for Hot Weather Creek, a 155km^2 basin with no permanent snow or ice, peaks early (June 3) because of snow melt, the diurnal variations in flow quickly decreasing as snow cover diminishes. Streamflow ceases in early July, but is recharged by a precipitation event (likely with some contribution from melting permafrost) in August. The hydrograph for Quviagivaa

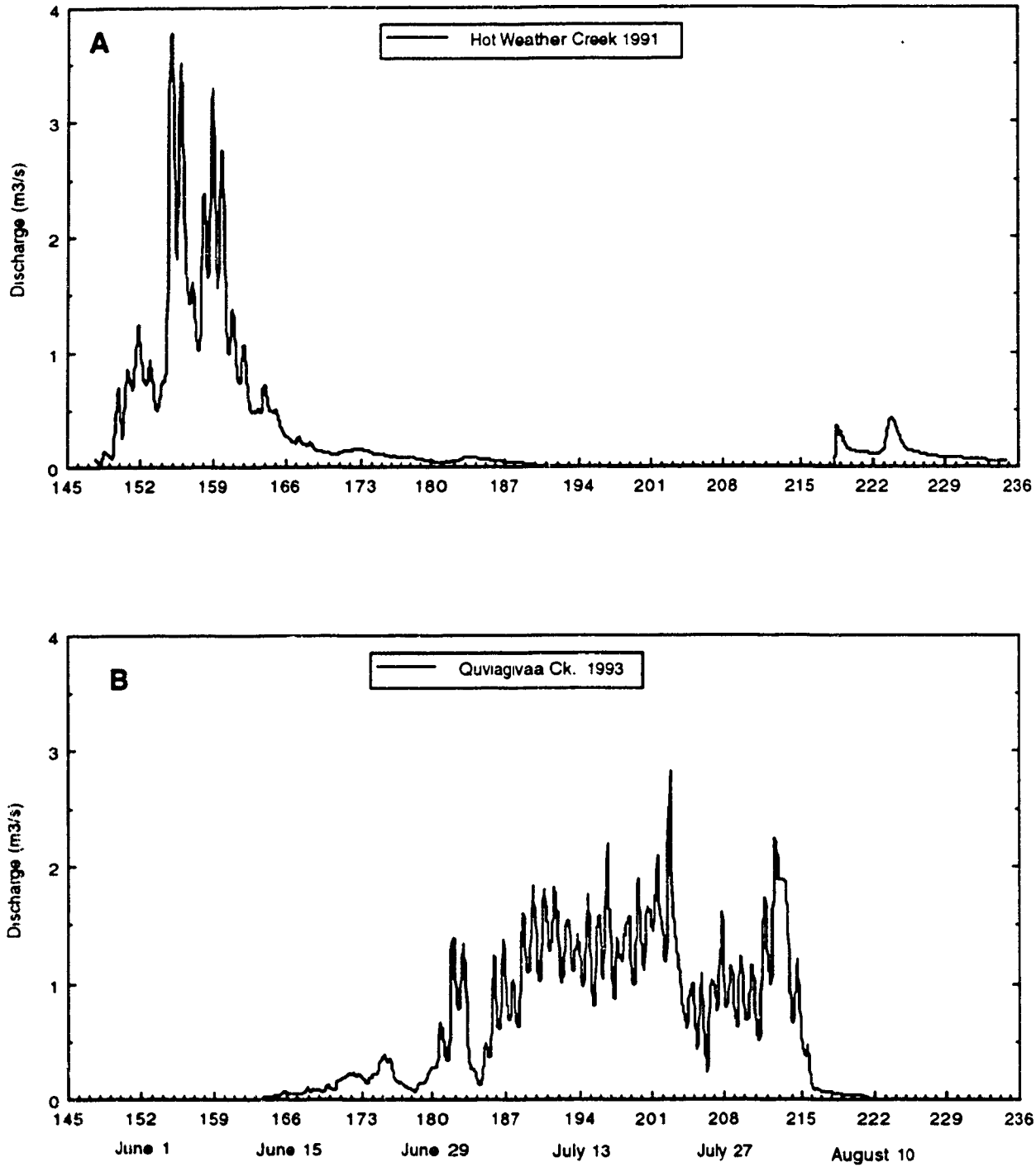

Figure 2.2. Hydrographs of Hot Weather Creek for 1991 (A), and Quviagivaa Creek for 1993 (B).

Creek, a 8.7km^2 basin with 59% permanent ice cover, shows a slow initiation of flow in mid-June with no diurnal variations in flow. Strong diurnal rhythms in discharge develop in late June and persist until early August, at which time flow quickly recedes to near zero on account of freezing temperatures and a significant snowfall. The peak discharge occurs on July 21, because of a rainfall event. Although from different years, the two hydrographs outline the typical differences between the nival and proglacial streamflow regimes. Namely, for proglacial basins:

1. Flow continues for the entire duration of >0°C temperatures,
2. Flow begins later and ends sooner by reason of higher elevations and colder temperatures,
3. Diurnal variations in flow last for the entire season after early snowmelt,
4. Peak discharges occur both during snowmelt and during ice melt, and are often caused by rain events or the bursting of slush pools.

2.2.2.2 Streamflow Lag Effects

As melt commences, streamflow from a glacierized catchment is affected by a strong lag on account of the refreezing of meltwater on the glacier surface as superimposed ice, the formation of large slush pools on the glacier surface, storage of water in crevasses, and the blockage of flow caused by deep snow on the glacier and snowdrifts in the stream channels downstream from the glacier terminus (Fig. 2.3). On a glacier in Arctic Sweden, Stenborg (1970) estimated that various lags resulted in the delay of 25% of total summer discharge from early to mid-summer. The effect of these lags and delayed melt in the upper elevations of the basin during the beginning stages of streamflow,

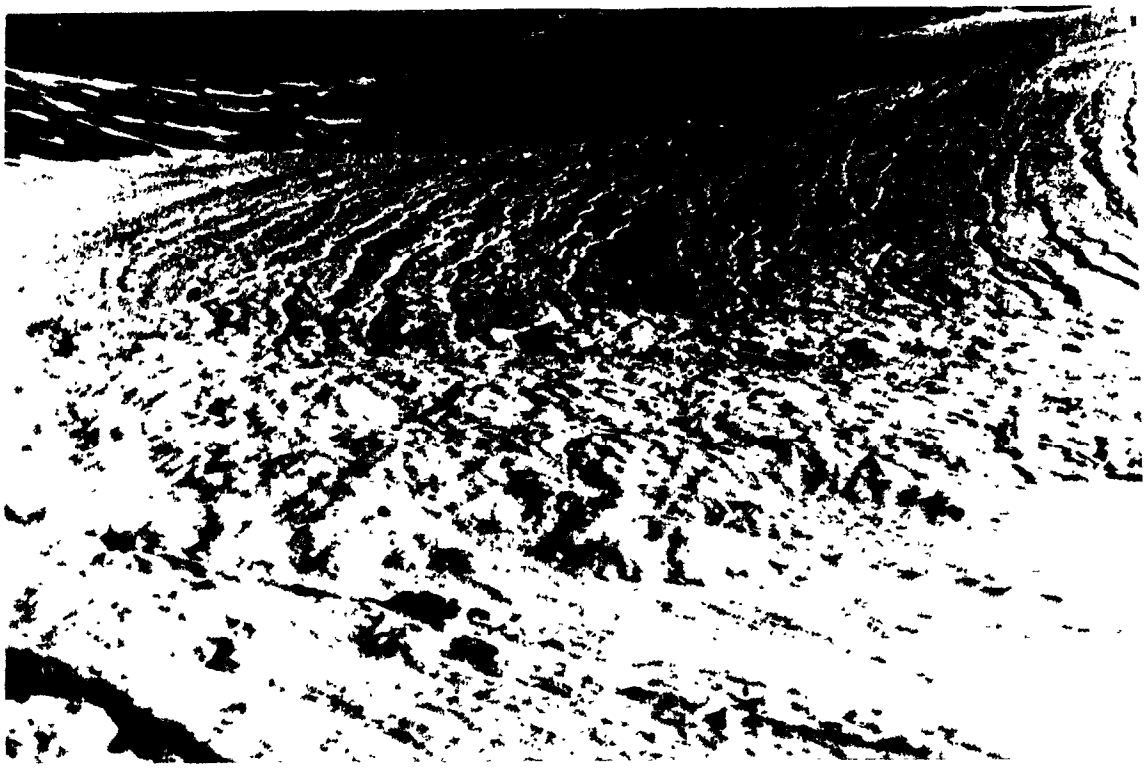

Figure 2.3. Photograph of meltwater channels and slush flow deposits in deep snow at the terminus of Nirukittuq Glacier, July 9, 1993.

is a contribution of flow to only a partial area of the basin. Later in the season, when flow pathways on and downstream from the glacier have been established, the meteorological elements causing melt have a more immediate influence on streamflow (Fig. 2.4). Lags caused by the formation of snowdams in non-glacierized catchments is common (Woo and Sauriol, 1980), and given a thick snowcover, most of the pro-glacial runoff-delay processes could also occur in catchments without perennial ice.

2.2.2.3 Meteorological Effects on Glacier Runoff

Munro (1991) states that generally applicable statistical relationships between glacier discharge and meteorological factors such as solar radiation and air temperature cannot be achieved. This by reason of the spatial variability of the glacier surface, which evolves over time and which results in uneven contributions to discharge. However, meteorological elements can be related to discharge for specific periods of runoff, as this study will show.

In order for melt and runoff to occur, the surface temperature must exceed 0°C. However, net solar radiation is the single largest heat source, and generally increases in importance with altitude and with the continentality of the climate (Braithwaite, 1981). Using four examples from the ablation zones of two glaciers in the Canadian Arctic (White Glacier, 1960-62 and Sverdrup Glacier, 1963), Braithwaite (1981) found that net radiation contributed an average of 55% of the energy for ablation, while sensible heat contributed 34% and latent heat 11%

Albedos are normally high (70-85%) early in the melt season given a complete snow coverage, and this results in low melt and runoff values. The albedo of the surface progressively decreases as wet snow (55-70%) is

Figure 2 4. Photograph of supraglacial meltwater channels on Quviagivaa Glacier, July 17, 1993.

replaced by superimposed ice (40-55%), and then by glacier ice (20-40%). As albedos decrease, a higher percentage of solar radiation is absorbed by the surface and melt proceeds in a much more efficient manner for a given radiation heat input, thereby enhancing streamflow (Church, 1972). Snowfall events are common on high Arctic glaciers during the summer, and in light of the albedo of fresh snow (80-90%), halt melt and result in a quick decline in streamflow (Adams, 1966).

Wind speed is an important factor in runoff generation because it increases the turbulent heat transfer at the glacier surface. Wind direction is also important, and several ablation-runoff studies on Arctic glaciers have shown that down-glacier winds are predominantly warmer than up-glacier winds (Keeler, 1964; Adams, 1966).

Often, the meteorological variable with the most dramatic effect on streamflow in glacierized basins is rainfall. The presence of continuous permafrost, and the steep gradient of most glacierized catchments, causes much of the liquid precipitation falling on the basin to be quickly routed into stream channels, resulting in a rapid rise in flow. In the White Glacier catchment in 1961, Adams (1966) recorded peak summer flows caused by a rain event on July 26-27, which removed the weir, terminating the continuous discharge record for the season. Seasonal peak flows caused by rainfall events also occurred in the Lewis and Decade glacier basins on Baffin Island in 1965, and in the McCall Glacier basin in 1969 and 1970 (Anonymous, 1967; Østrem et al., 1967; Wendler et al., 1972). Precipitation dominates daily discharge for days with major amounts of rainfall (>10mm). Although relatively rare during any single melt season, these events deliver greater quantities of water to the glacier basin per unit area per unit time than can be generated through snow and ice melt alone, even on the warmest days of the high Arctic melt season.

2.2.3 Superimposed Ice

From the initiation of Arctic glaciological studies, the refreezing of melt-water on glacier surfaces has been observed (Ahlmann and Tveten, 1923; Schytt, 1949; Baird, 1952). This process, first active when melt begins in the spring, superimposes an ice layer or layers on the impervious glacier surface (Fig. 2.5). This new "melt season" ice is known as superimposed ice, and by definition must form on the glacier ice surface, the melt being derived from a single season snowpack (Schytt, 1949). Superimposed ice usually forms below the firn line, although it can also form just above it where firn depths are <4m (Koerner, pers. comm., 1994). The formation of superimposed ice is not actually an accumulation process such as snowfall or freezing rain, but is a transfer of mass and energy on the glacier.

A large high Arctic glacier may consist of up to five zones (not including the dry snow zone, which only occurs consistently in the interior of Greenland and Antarctica), of which the superimposed ice zone is normally found between the firn edge and the equilibrium line (Müller, 1962) (Table 2.3). This zone will vary (somewhat) in size and location on a given glacier from year to year given differences in the amount and distribution of snow prior to melt and the varied temperature conditions and precipitation events during the melt season. The superimposed ice zone can normally be split into two distinctive sections: an upper region, where superimposed ice forms almost continuously through the melt season, and a lower region where some ablation of the superimposed ice occurs toward the end of the summer (Koerner, 1970a). It is also likely that sporadic zones of superimposed ice will exist both in protected hollows below the main region of superimposed ice, and on exposed ridges and mounds above the zone of superimposed ice (Adams, 1966).

Figure 2.5. Photograph of superimposed ice under a saturated snowpack at the terminus of Quviagivaa Glacier, July 6, 1993

TABLE 2.3

Zonation on high Arctic glaciers

Feature	Description
Dry Snow Zone	Snow is unaffected by melt. Does not exist in the Canadian Arctic with the exception of the highest ice caps during years with cold summers.
Percolation Zone A	The upper section of the percolation zone and upper limit of firn. Some melt occurs, but all meltwater refreezes within the snowpack of the reference year.
Percolation Zone B	The lower section of the percolation zone. The snowpack of the reference year is entirely within the 0°C isotherm. Some meltwater percolates into firn layers of previous years. There is no runoff.
Slush Zone	This zone becomes entirely soaked, and a portion of the meltwater becomes runoff. The lowest zone of firn. The upper limit of slush flows.
Superimposed Ice Zone	Situated between the firn line and the equilibrium line. Accumulation is in the form of ice formed during the reference year. A significant percentage of the snowpack becomes runoff.
Equilibrium Line	The point (usually a zone) at which annual accumulation equals annual ablation. Usually located at the lower limit of the superimposed ice zone.
Ablation Area	All snow and superimposed ice from the reference year ablate before the close of the melt season. Usually characterized by a net loss of glacier ice.

Areas of superimposed ice formation are highly variable in time and space. For example, in a colder than average year the superimposed ice zone will move to a lower elevation on the glacier, and the wet-snow zone will likely shift down-glacier to occupy parts of the former superimposed ice zone. In a warmer than average year, more melting will occur at higher elevations and the superimposed ice zone will shift somewhat into the wet-snow zone. However, the movement of the superimposed ice zone up-glacier will be limited on account of progressively deeper firn layers which require longer time periods to saturate, and refreezing will not likely be limited to the glacier ice surface. On a glacier which is largely located below the regional mean firn line, a warmer than average year may entirely eliminate the superimposed ice zone, bringing the entire glacier into the ablation zone (e.g. Baby Glacier, Axel Heiberg Island,

Adams, 1966 and Nirukittuq Glacier, this work). Conversely, a colder summer with frequent snowfalls followed by melting or rain, could result in the formation of superimposed ice on most surfaces (Arnold, 1965), and if such an event occurs close to the end of the melt season, a superimposed ice layer may remain on large areas of the glacier until the next melt season.

The formation of superimposed ice is generally understood to be a function of the temperature distribution of the top metre or more of ice underlying the snowpack, the snow depth, the slope and roughness of the ice surface, and the rate of melt-water delivery to the ice surface (Koerner, 1970a; Wakahama et al., 1976). The rate of meltwater delivery is itself a function of solar radiation inputs, sensible heat inputs, snow depth, and snow density. Through experimentation, Wakahama et al. (1976) found that the growth rate of superimposed ice increases in concert with increases in the rate of melt-water supply when it is less than 0.14g $cm^{-2}h^{-1}$, while the formation of superimposed ice becomes insensitive to melt-water delivery at higher values. This suggests that for the lower melt-water supply rates, the melt-water supply is the dominant factor, while for larger melt rates, the ice temperature is the dominant factor. This situation results in a decreasing rate of superimposed ice formation over time, as more of the melt-water goes towards runoff. A deep snowpack aids in the formation of superimposed ice by keeping the glacier ice surface cold during the initiation of melt, by acting as a barrier for slush flows, and as a source of meltwater as it ablates. In all cases, it is vital that the surface slope be relatively gentle, and that the micro-topography of the surface ice layer be somewhat irregular to facilitate the refreezing of the meltwater on the ice surface.

The formation of superimposed ice is a significant process on all Arctic glaciers and may in fact be the sole means by which a large number of low-

lying Arctic ice masses retain accumulation (Müller, 1962). In addition to the mass balance, the transformation of snow into glacier ice through the formation of superimposed ice is important in terms of the heat balance of Arctic glaciers. Latent heat is added to the glacier through the processes of refreezing of meltwater (80 calories for each gm of water), while the higher albedo of superimposed ice as compared to older glacier ice causes more reflection of solar radiation and a loss in energy. The refreezing of meltwater, dominant on cold Arctic glaciers, serves to create a lag in runoff measured at the snout of the glacier as compared to expected melt on the glacier surface. The presence of superimposed ice is especially problematic for glacier mass balance remote sensing studies, as ablating superimposed ice is often difficult to differentiate from glacier ice (Jung-Rothenhäusler, 1992). The equilibrium line is transitional in nature, and is sometimes located in the long-term zone of superimposed ice formation, which creates a problem in the determination of accumulation and ablation zone areas from satellite imagery.

CHAPTER 3

MANUSCRIPT 1

Mass balance of two small glaciers in the Sawtooth Range, Fosheim Peninsula, Ellesmere Island, Northwest Territories

ABSTRACT

Winter 1992-93, summer 1993, and annual 1992-93 mass balances were measured on a small ($4.7km^2$) valley glacier in the Sawtooth Range, Ellesmere Island, in the Canadian high Arctic during the summer of 1993. The 1992-93 net mass balance for the study glacier, Quviagivaa (unofficial name), was -532mm water equivalent. The 1992-93 net mass balance for Nirukittuq Glacier, a niche glacier adjacent to Quviagivaa, was -530mm. At the close of the melt season, both glaciers were entirely below the equilibrium line. The accumulation area ratio (AAR) for Quviagivaa was 0.06, reflecting the highly negative balance. At the termination of the melt season, several other smaller glaciers in the Sawtooth Range were visited, and most showed weathered glacier ice from snout to summit, suggesting an entire surface of net ablation. This condition suggests that many of the glaciers of the Sawtooth Range are now commonly entirely in the ablation zone. July 1993 was abnormally warm (the fourth warmest July in the 46 year record at Eureka), and Meighen, Melville South, and Agassiz ice caps as well as White and Baby glaciers on Axel Heiberg Island, had strongly negative mass balances, ranking 1992-93 as one of the top five most negative balance years on record (Koerner, pers. comm., 1994). Slight marginal shrinking in the areal extent of Quviagivaa Glacier since 1959 suggests that strongly negative mass balances such as those recorded in 1993 are not indicative of the last 46 years.

3.1 Introduction

Glacier mass balance measurements were initiated in the Canadian high Arctic in 1957 on the Gilman Glacier in northern Ellesmere Island (Hattersley-Smith et al., 1961). Since then, mass balance studies have been carried out on over a dozen different glaciers and ice caps (Bradley and Serreze, 1987; Blatter and Kappenberger, 1988; Cogley et al., 1994). Studies on White and Baby glaciers on Axel Heiberg Island (Ecclestone, pers. comm., 1994), and those by R.M. Koerner on Meighen, Melville, Devon, and Agassiz ice caps (Koerner, pers. comm., 1994), have been in operation for more than 30 years. The Meighen, South Melville and Devon ice cap, and White and Baby glacier mass balance records are the longest in the circumpolar high Arctic.

Quviagivaa Glacier (unofficial name), is located 70km east of Eureka, and 147km to the east of the White and Baby glaciers, on the Fosheim Peninsula of Ellesmere Island. This paper will discuss various aspects of the mass balance of Quviagivaa Glacier and to a lesser extent that of Nirukittuq Glacier (unofficial name) for the 1992-93 season.

3.2 Mass Balance Methods and Potential Error

The mass balance study on Quviagivaa Glacier was conducted within one field season (late May-mid August, 1993), which included the beginning and end of melt, and the measurement of the winter, summer, and net mass balances. The annual net mass balance was measured on Nirukittuq Glacier.

The winter snowcover of Quviagivaa Glacier for the 1992-93 season was measured on 9 and 11 June, 1993. A total of 635 snow depth measurements

and 66 snowpit-derived density measurements were used to draw a snow water equivalent isomap.

Surface lowering on the glacier was measured at 12 "ablation stations" (AS), representing different aspects and elevations, throughout the summer; on alternate days at AS1-10, and approximately once a week at AS11-12 (Fig. 3.1). Each AS consisted of plastic wire strung between three 1.8m long aluminum stakes, each side of the triangle measuring four metres. The wire was marked off at 40cm intervals, one metre in from each stake so as to avoid the disturbed snow around the stake and enhanced melting or channeling of meltwater by the stakes. As 15 surface lowering measurements were made at each AS, a simulated stake density of 38 stakes km^{-2} was obtained. The 15 measurements were averaged to give a single value for each site. The wires, which tend to slacken, were carefully reset on a weekly basis to reduce underestimation of surface lowering, and an error of 5mm attributable to the observer is suggested. An analysis of the standard deviations of surface lowering at each AS showed a range of 13 to 140mm and an average value of 34mm. This figure is the average error that *would* apply if only a single measurement was taken at each AS.

On Nirukittuq Glacier, three 1.8m long, 19mm diameter aluminum ablation stakes were installed, giving a stake density of 7.5 stakes km^{-2}. Stake measurements began prior to snow melt, and continued once a week until the end of the melt season.

A significant shortcoming of the stake network on Quviagivaa Glacier is that the elevations above 1000m are unrepresented (although a single stake was installed at 1100m in early August, 1993), leaving 27% of the glacier unmeasured. As an attempt to remedy this, the upper portion of the glacier was visited in late July and depths of firn were measured and the areal extent of

Figure 3.1. Photograph of an ablation station on Quviagivaa Glacier.

superimposed ice recorded. Although very good estimates of net ablation were made using a melting degree hours-ablation model (see Fig. 3.8), the mass balance isolines for the upper portions of the glacier are less certain than those for the snout region.

During snow ablation, snow density measurements were made to determine the water equivalent of melt by weighing a measured volume of snow from the melting portion of the snowpack. Snow density measurements are subject to error given the problem of obtaining an accurate volume of snow, and the difficulty of accurately leveling a scale on a windswept glacier. Given a common snow depth of 80cm, a possible overestimation in density of 0.05g cm^{-3} (e.g. from 0.35 to 0.40g cm^{-3}), would produce an overestimate in water equivalence of 40mm, or 5%. Other errors could occur because of the undersampling of the spatial variation of snow density. The standard deviation of all 66 density measurements on the glacier was found to be 0.03g cm^{-3}. When multiplied by the winter mass balance, the error becomes 9mm, or 3%. If a 5% error in density sampling is combined with a possible 3% error in the spatial variability of snow density, the resulting error is 24mm.

Snow density measurements were continued at the 12 ablation stations for the duration of snow melt and are subject to the same errors as the sampling done during the winter mass balance snow survey. Ice density measurements were not made, and a density of 0.88g cm^{-3} was applied to superimposed ice and 0.9g cm^{-3} for glacier ice. For short-term (e.g. daily) measurements of surface lowering, 0.9g cm^{-3} may not be sufficiently accurate when considering the development and destruction of a less dense "weathering rind", which often develops in the upper 20cm of the glacier surface (Müller and Keeler, 1969). Cogley et al. (1994) state that if the actual density for glacier ice is 0.85g cm^{-3} as opposed to 0.90g cm^{-3}, then an error of 6% results. It was observed that the

depth of weathering rind (measured using depths and coverage of cryoconite holes), was similar at most ablation stations at the beginning of the season and at the end, so a density of 0.9g cm^{-3} is likely appropriate.

The standard error for each ablation station, and the net mass balance, is considered to be the sum of the observer error and the snow density errors which give an error of about 70mm. This is an order of magnitude lower than the standard error of 200-250mm given for the White Glacier (Cogley et al., 1994), attained because of the higher stake density, the glacier-wide snow survey, and the lack of inaccessible regions on Quviagivaa Glacier.

3.3 Results

3.3.1 Winter Mass Balance, Quviagivaa Glacier

The winter accumulation of 1992-93 was very close to its maximum on June 9 and 11, when snow surveys were conducted on the glacier. In order to calculate the 1992-93 winter mass balance, an isomap of accumulation was produced (Fig. 3.2), which gave an average value of 303mm water equivalent.

The accumulation pattern is strongly influenced by the topography of the glacier. Accumulation does not show a close relationship with altitude but is strongly affected by the topographically-influenced deposition of wind-transported snow, both during and after snowfall events. Observations of snow transport and deposition were made during snowfalls and wind events in June and August, and snow depth probing identified the areas of snow scour and deposition. The greatest snow depths were recorded at the terminus of the glacier, which is sheltered from all winds excepting those blowing down-glacier. The snowpack is significantly reduced on the central snout of the glacier, which has a convex shape and is exposed to winds from all directions. The upper

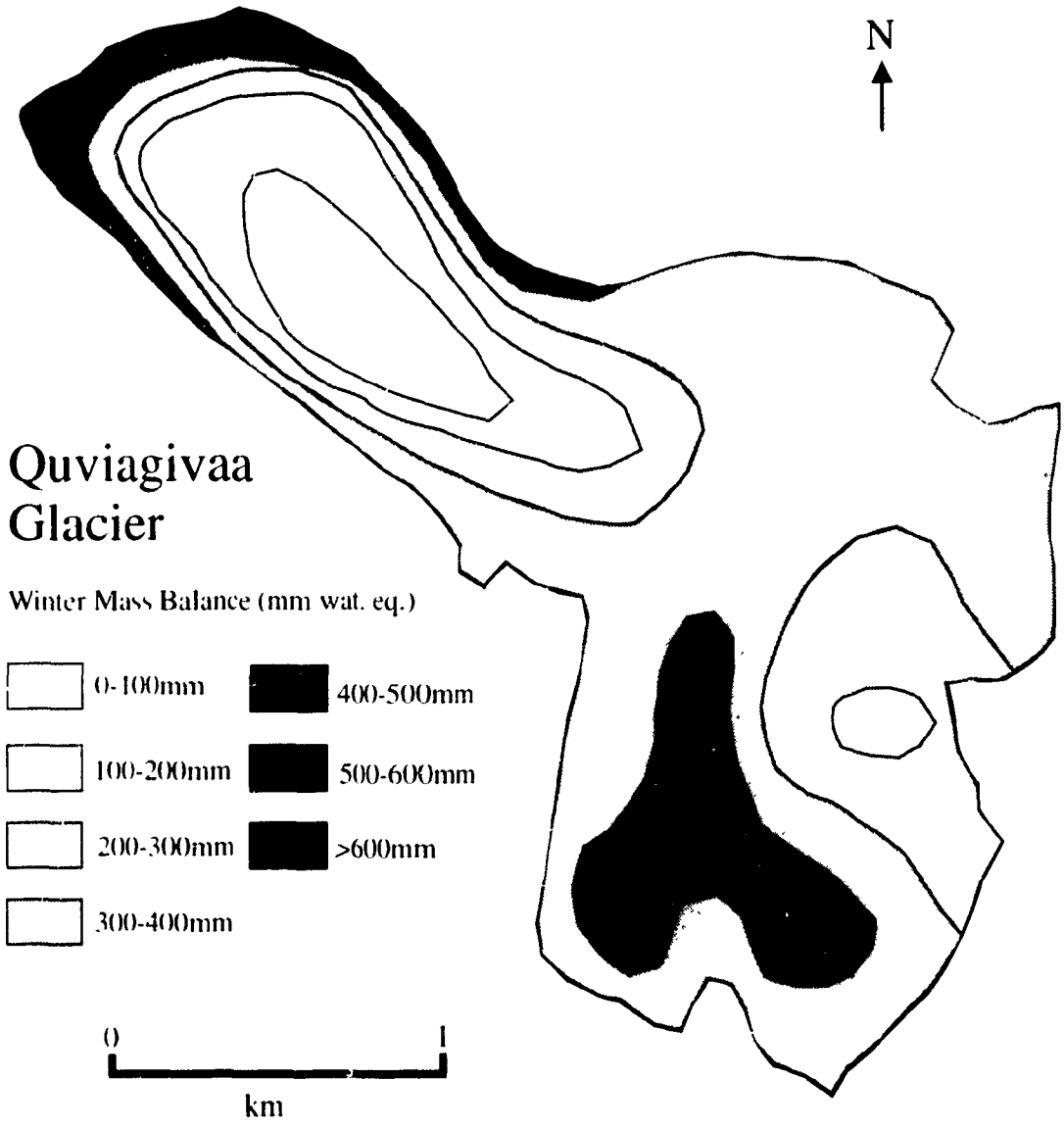

Figure 3 2. Map of winter mass balance, 1992-93 for Quviagivaa Glacier.

basin of the glacier is relatively sheltered by steep mountain sides which rise up to 130m above the glacier surface, although drifting over the southern ridge of the glacier basin produces a region of higher accumulation, and winds which enter the basin on the eastern side result in an area of reduced accumulation.

The 1993 melt season ended on August 3, and the 1993-94 accumulation season began abruptly on August 3 with a snowfall event. Snow, high winds, and sub-zero temperatures persisted from August 3 until the end of the field season (August 11). A snow depth survey carried out on the snout of the glacier on August 10 determined an average snow depth of 26cm and a range of depths from 0-98cm. The pattern of accumulation after strong winds from the southeast and east on August 8-9 respectively, produced an accumulation that closely resembles the pattern of the previous spring with highest accumulation at the terminus, and lower accumulation on the central snout.

3.3.2 Summer Mass Balance, Quviagivaa Glacier

Maximum temperatures rose briefly above freezing on the glacier in late May, and until late mid-June melt was minimal and sporadic because of high surface albedos and limited duration of above freezing temperatures. Melt was first measured on June 7 at AS1, at which time it is estimated that between 10-20mm of ablation had already occurred through sublimation and melting Melt continued almost uninterrupted from June 29 to August 3, as temperatures remained consistently above zero (excepting July 2). Temperature records from Eureka suggest that no further melt occurred at the glacier after August 3, when snowfall began.

Figure 3.3 shows the isomap of summer melt drawn using the 12 AS data points. A regression of stake elevation and total summer ablation at AS1-12, significant at the 99% confidence interval, shows decreasing melt with increasing altitude (r^2=0.8; n=12), although total melt is not dependent on altitude alone (Fig. 3.4). AS5-7 are located within 5m of elevation of each other, yet cumulative melt differs by 177mm at AS6 and AS7. Figure 3.5 shows that cumulative ablation varies a similar amount across the glacier snout at an altitudinal range of 684-688m a.s.l. as it does up the glacier snout from AS6 to AS9, where the altitudinal range is nearly 100m.

Much of the spatial difference in melt rate can be explained by the measured albedo at the sites (Fig. 3.6). Dirt bands at AS9 gave that location lower albedos than at AS6 or AS8 during the last several weeks of melt. Albedos were slightly lower at AS6 than at AS5 and AS7 on account of the dirt content of the ice, however slush flows into the AS7 area and the north-northwest aspect of AS5 likely also contributed to the lower ablation amounts at those stations.

3.3.3 Net Mass Balance, Quviagivaa Glacier

The small size of Quviagivaa Glacier, the availability of an equi-accumulation map for the winter mass balance, and the familiarity of the authors with patterns of melt on the glacier, allowed the production of an equi-ablation map as the potentially most accurate means of calculating the net mass balance (Fig. 3.7). Two-dimensional mapping is justified, as the mass balance (especially in the snout region), does not vary solely with elevation. One measurement of firn accumulation at 1100m at the end of the season gave a maximum value of accumulation on the glacier, but the graphical interpolations

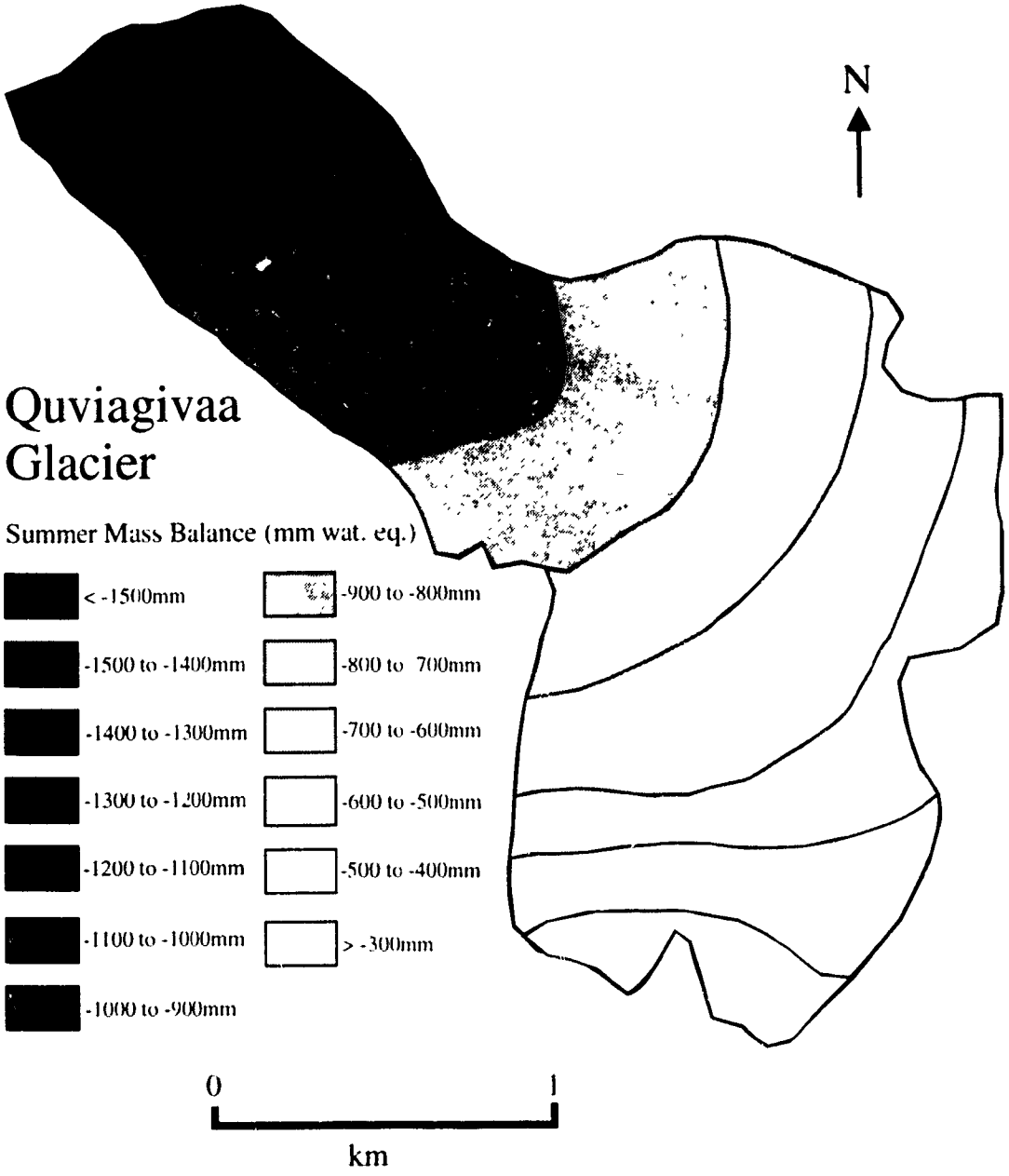

Figure 3.3. Map of summer mass balance, 1993 for Quviagivaa Glacier

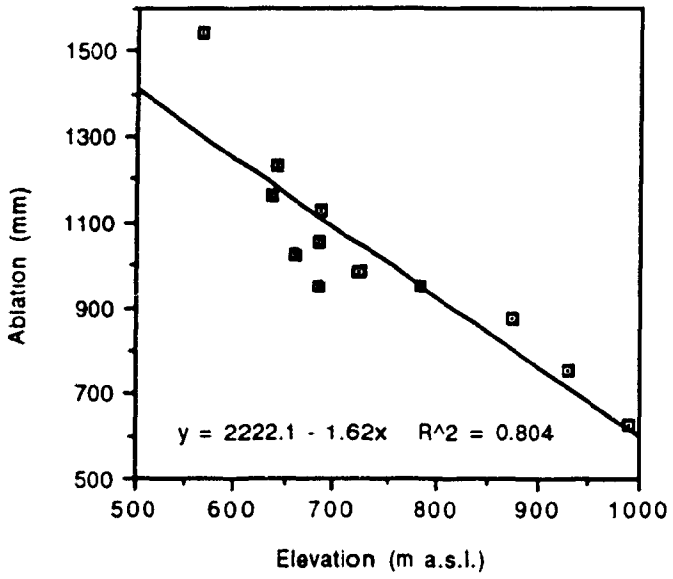

Ablation Station	Elevation (m a.s.l.)	Ablation (mm)
1	569	1540
2	635	1163
3	640	1231
4	659	1022
5	685	1054
6	688	1128
7	684	951
8	723	985
9	785	948
10	875	873
11	930	754
12	990	627

Figure 3.4. Ablation as a function of altitude on Quviagivaa Glacier with ablation values listed.

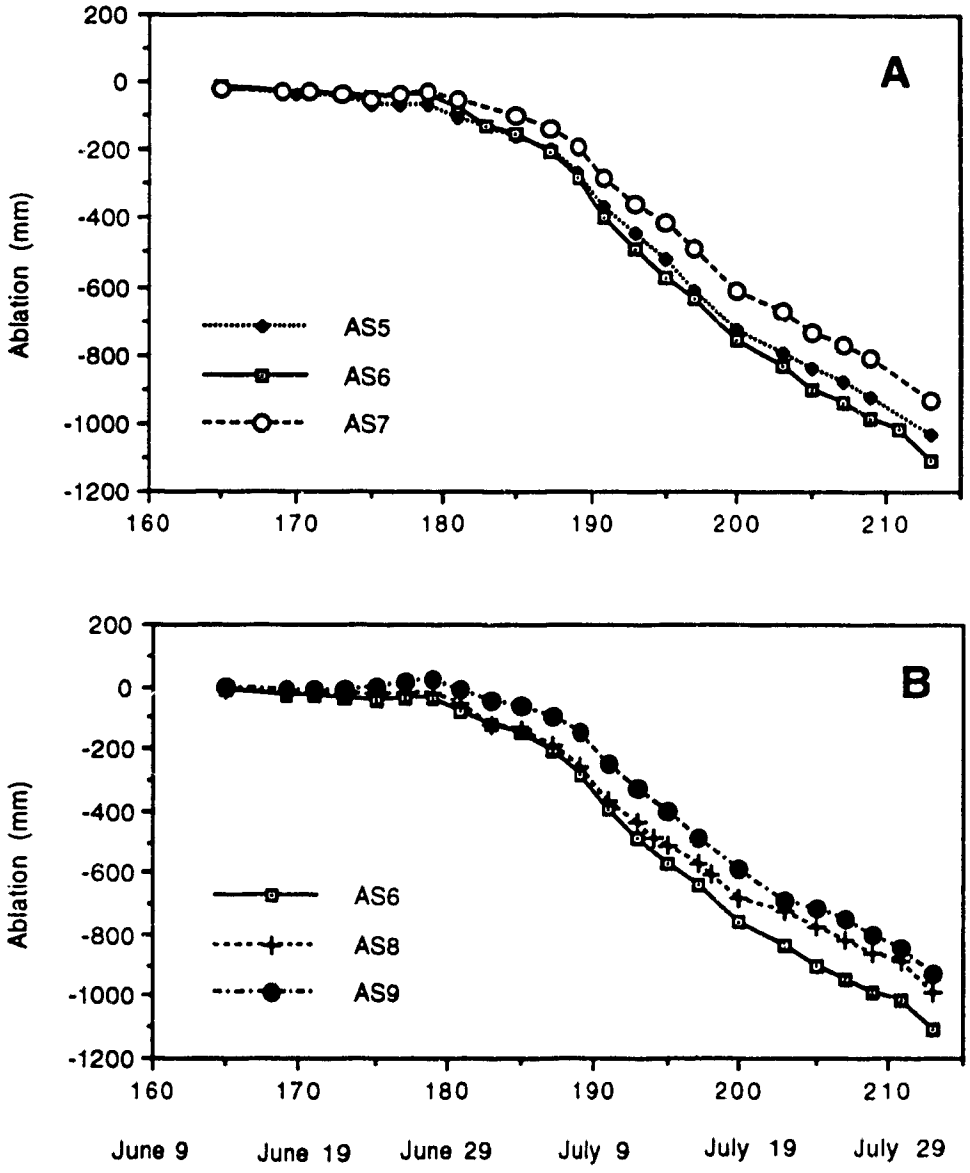

Figure 3.5. Ablation at AS5-7 (A) and at AS6, 8, and 9 (B).

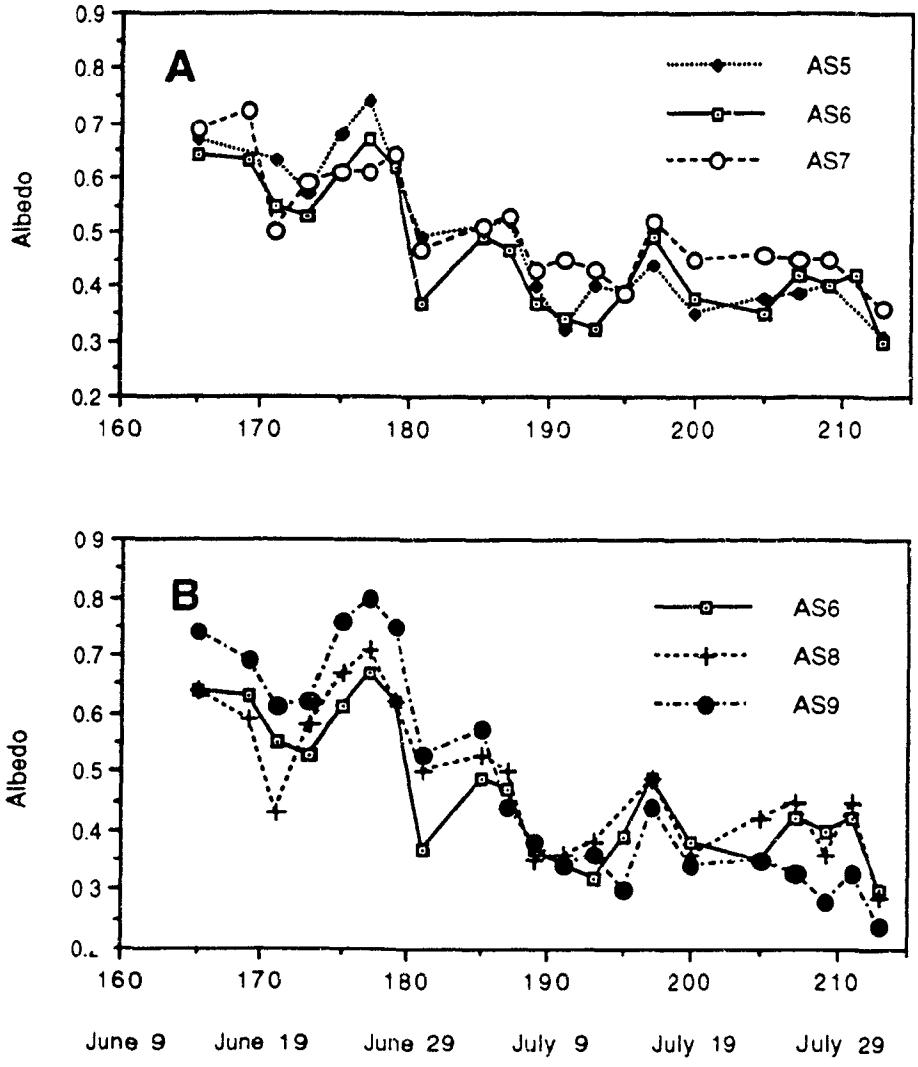

Figure 3.6. Albedos for AS5-7 (A) and for AS6, 8, and 9 (B).

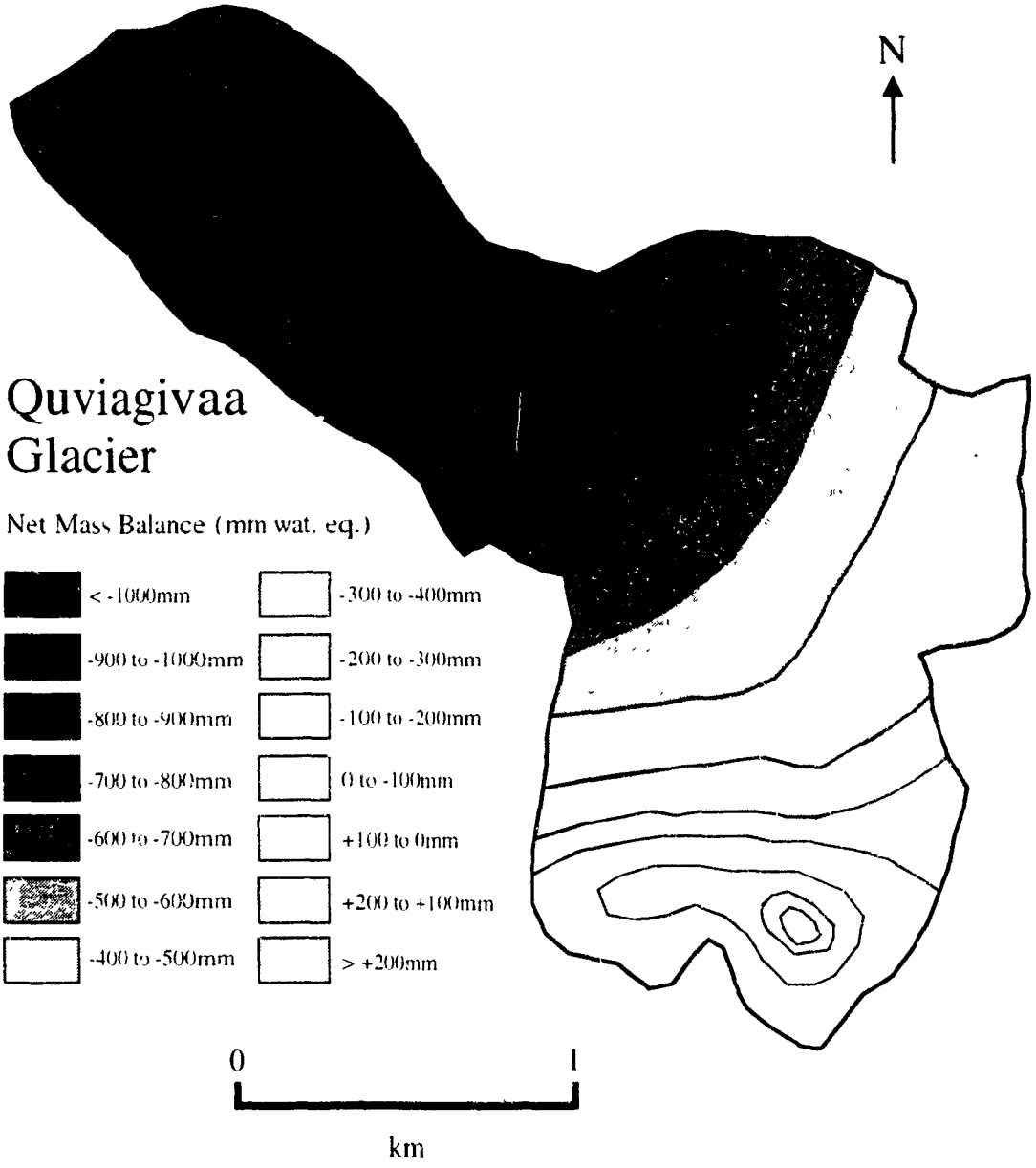

Figure 3.7. Map of net mass balance, 1992-93 for Quviagivaa Glacier

from 1000-1250m are still problematic. To justify the placing of the equi-ablation lines in the upper portions of the glacier, a simple model was developed to estimate melt at the unmeasured elevations. Melting degree hours (MDH), calculated as the sum of all hourly temperature values greater than 0°C at the glacier meteorological station, were related to periods of measured melt at AS10 (Fig. 3.8). With an r^2 value of 0.93, the relationship is significant at the 99% confidence interval.

MDH and estimated melt were calculated at 50m intervals to the top of the glacier using temperature lapse rates, which were taken from the difference in screen temperature between the glacier meteorological station (875m) and the valley meteorological station (230m), located seven km west of the glacier station. Estimated summer melt was 400mm at 1100m a.s.l., compared with 873mm of measured melt at the meteorological station. Table 3.1 shows estimated melt versus measured values from the meteorological station to the top of the glacier.

Considering the high degree of accuracy between estimated and measured melt at AS10-12, it is likely that estimated melt is within 5% of actual

TABLE 3.1

Estimated and measured melt from 875-1200m a.s.l.

June 29-August 3, 1993

Elevation (m a.s.l.)	Estimated Melt (mm)	Measured Melt (mm)	Estimated Melt as % of Meas.
875 (AS10)	868	878	99
900	813		
930 (AS11)	741	754	98
950	705		
990 (AS12)	619	627	99
1000	597		
1050	494		
1100	400		
1150	319		
1200	253		

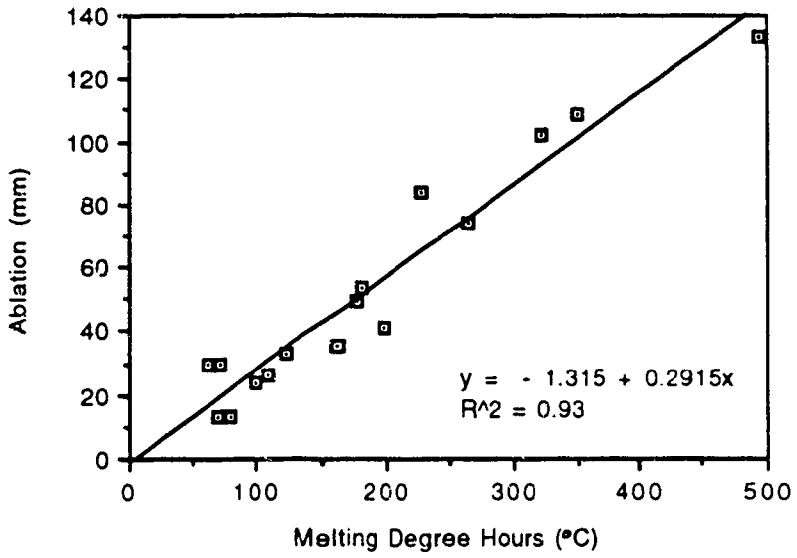

Figure 3.8. Ablation at AS10 as a function of melting degree hours accumulated during the period of measured ablation.

melt at upper elevations. If a value of 500mm is given (see Fig. 3.2) for snow accumulation at the accumulation outlier site (1100m a.s.l.), then it is evident that some firn would remain at this site, where only 400mm of melt is estimated. An estimate of 130mm of snow water equivalent for the end of the melt season was calculated for 1100m a.s.l. using the model. The maximum amount of firn measured at the accumulation outlier at the end of the season was 131mm water equivalent, above an undetermined thickness of superimposed ice. The areal coverage of melting superimposed ice was limited to a narrow band encompassing the firn patch. It is probable that the steep slopes (30-35°) and the limited meltwater supply from upslope resulted in only minor formation of superimposed ice at the site. If an estimated thickness of 10cm of superimposed ice (0.88g cm^{-3}) is given for the area under the firn patch, then the maximum estimated accumulation at the site is 219mm, which equates to the 200mm isoline on the equi-ablation map. A band of net ablation exists at the top of the glacier despite the fact that estimated MDH totals for elevations at the top of the glacier are only 30% of those at the meteorological station. This is likely because of heat advection from the surrounding slopes which become snow-free in mid-July, and a reduction in albedo caused by rock falls, sediment carried by runoff, and aeolian deposits from the adjacent rock slopes.

3.3.4 Net Mass Balance, Nirukittuq Glacier

The net mass balance of Nirukittuq Glacier was performed using the equi-ablation map method, and was calculated to be -530mm for 1992-93. Three stake measurements were used to draw the isomap (Fig. 3.9). Nirukittuq Glacier is a small, sheltered ice mass, which is steeply-inclined towards the northwest. Slope angles of 30-35° on much of the glacier result in large mass

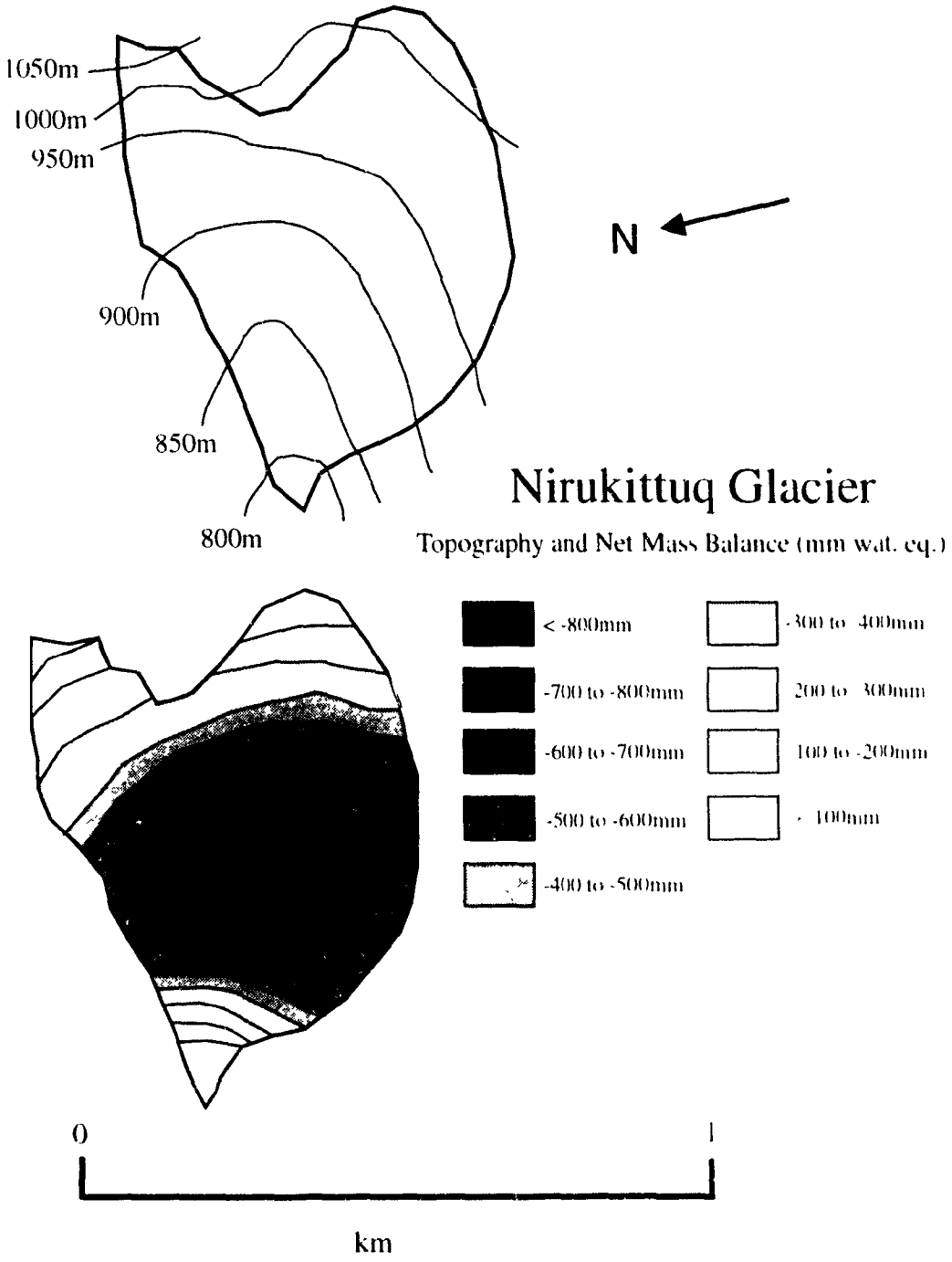

Figure 3.9. Map of net mass balance, 1992-93 for Nirukittuq Glacier

movements from the upper portions of the glacier to the terminus in the form of slush flows. The formation of superimposed ice is limited on the steep slopes, but enhanced on account of deep snow (80cm on June 22) and the refreezing of slush flows at the lowest elevations of the glacier, creating a pattern of maximum net ablation in the central portions of the glacier, and minimum net ablation conditions at the terminus and the upper limits of the glacier. For the elevational range of 850-950m a.s.l., larger net ablation values were measured on Nirukittuq Glacier than those from identical elevations on Quviagivaa Glacier. Higher ablation on Nirukittuq is likely a result of its steep slope, which causes the quick removal of most of the snowpack as slush flows, induced by early melt and runoff from the ice-free surfaces upslope of the glacier. Small slush flows continue during the period of ablating superimposed ice. Superimposed ice crystals are equant and lack the "grain growth" of glacier ice, and because of this, melting superimposed ice forms a loose slush which is easily moved down-glacier by the supraglacial runoff.

When measurements were made on August 1, the entire glacier was within the ablation area. However, several patches of melting superimposed ice remained at the top of the glacier at the end of the melt season. These were likely formed in 1992, which was the fifth coldest summer since 1948 according to climate records from Eureka, and likely a positive mass balance year on Nirukittuq Glacier.

3.4 Discussion

3.4.1 Comparisons With Other Glaciers

During the last decade no new glacier mass balance studies have been initiated in the Canadian high Arctic, and currently, no other small, valley

glaciers are being investigated in the Canadian high Arctic. The closest comparable studied glaciers in the Canadian high Arctic are White and Baby glaciers on Axel Heiberg Island.

One of the most significant factors influencing the mass balance of Quviagivaa Glacier is high snow accumulation at the glacier terminus. This serves to reduce net ablation at the terminus and to maintain the areal extent of the glaciers. This pattern has also been observed on Icewall Glacier, an outlet of the Laika Ice Cap on Coburg Island, which, because of its lee slope and concave topography, accumulates the largest amount of firn on the entire ice cap (Blatter and Kappenberger, 1988). The high snow accumulations at the glacier terminus stop slush flows at the snout. This was especially evident on Nirukittuq Glacier, where slush mounds at the terminus measured over 80cm deep. Baby Glacier, similar in shape to Nirukittuq, also experiences large snow and slush flow deposits at the snout, and this resulted in near equilibrium conditions at the snout in 1991 (Dicks et al., 1992).

Differences in albedo rather than differences in altitude were found to be the main factors causing variations in melt at ablation stations on the central snout of Quviagivaa Glacier This agrees with the findings of Van de Wal et al. (1992), who found that differences in ablation on profiles across the tongue of Hintereisferner could be explained almost entirely by differences in albedo.

The equilibrium line was located above the upper elevations of Quviagivaa Glacier in 1993. This has also been recognized for other glaciers which do not reach above about 1200m a.s.l., and for which ablation and accumulation processes are more important than elevation to the net mass balance (Blatter and Kappenberger, 1988). However, it must be noted that accumulation, and especially ablation are controlled to a degree by elevation. In a cool summer with a positive net balance, Quviagivaa Glacier would likely

have net accumulation both at the top and the bottom of the glacier and net ablation in the exposed central snout region. This pattern has also been found on Baby Glacier in cool years (Cogley et al., 1994). This pattern does not develop on larger glaciers such as White and Gilman, which extend several hundred metres above the highest measured equilibrium line (1444m and 1240m a.s.l. respectively), and have exposed terminus locations, at elevations below 350m (Hattersley-Smith et al., 1961; Cogley et al., 1994).

3.4.2 Representativeness of the 1992-93 Mass Balance Year

For the 1992-93 mass balance year, the mass balances of White and Baby glaciers were strongly negative. In fact, Baby Glacier, which reaches 1175m a.s.l., was found to be entirely below the equilibrium line. In addition, Koerner (pers. comm., 1994) measured large amounts of melt on several of the ice caps on the Queen Elizabeth Islands. On the Meighen Ice Cap, the 1992-93 mass balance was -600mm, the third most negative balance since records were started in 1960, and on the Agassiz Ice Cap and the Melville Island ice cap (South), average melt values were the highest since measurements began in 1977 and 1963 respectively. The melting degree day (daily maximum+daily minimum) totals for the summer of 1993 at Eureka ranked 14th in the 1948-1993 record, while the average July temperature was 7.3°C, the fourth warmest on record. In the Arctic, July is the month when most glacier melt occurs, and the above average July temperature at Eureka corresponds with the above average melt measured on northern Ellesmere, Axel Heiberg, Meighen, and Melville Islands. This suggests that the melt on Quviagivaa in 1993 was not indicative of the long-term situation. For the White Glacier, Cogley et al. (1994) give a long-term balance normal derived from 29 annual measurements of

-100±48mm, and for the high Arctic estimate -82mm a^{-1}. The slightly negative long-term balance that Cogley et al. (1994) suggest for high Arctic glaciers agrees with the slight marginal retreat at the terminus of Quviagivaa Glacier (maximum of 150m) detected from photographs taken in 1959 and 1994 (Fig. 3.10).

3.5 Conclusions

The winter, summer, and net mass balance were measured on Quviagivaa Glacier in 1993, and were found to be +303mm, -771mm, and -532mm respectively. The mass balance was measured using standard stratigraphic techniques, using a glacier-wide snow survey to calculate the winter mass balance, and a network of 12 ablation stations to monitor melt. The error in the net mass balance is about 70mm, and accounts for the discrepancy between the three mass balance values. The net mass balance of Nirukittuq Glacier was -530mm, remarkably close to that of Quviagivaa considering the elevational and size differences between the two glaciers. Accumulation is strongly influenced by the topography of Quviagivaa Glacier, which controls the scour and deposition of wind-blown snow. The general altitude-net balance relationships which standard mass balance calculations depend upon are not found on Quviagivaa or Nirukittuq glaciers.

Climate records from Eureka, a weather station located 70km west-northwest of the glacier, place the summer of 1993 as the 14th warmest in the period 1948-1993. However, the month of July was the fourth warmest on record. Interestingly, the mass balance of Devon Ice Cap was only slightly negative, and did not apply to the whole Queen Elizabeth Islands. Very strong negative mass balances from White and Baby glaciers on Axel Heiberg Island

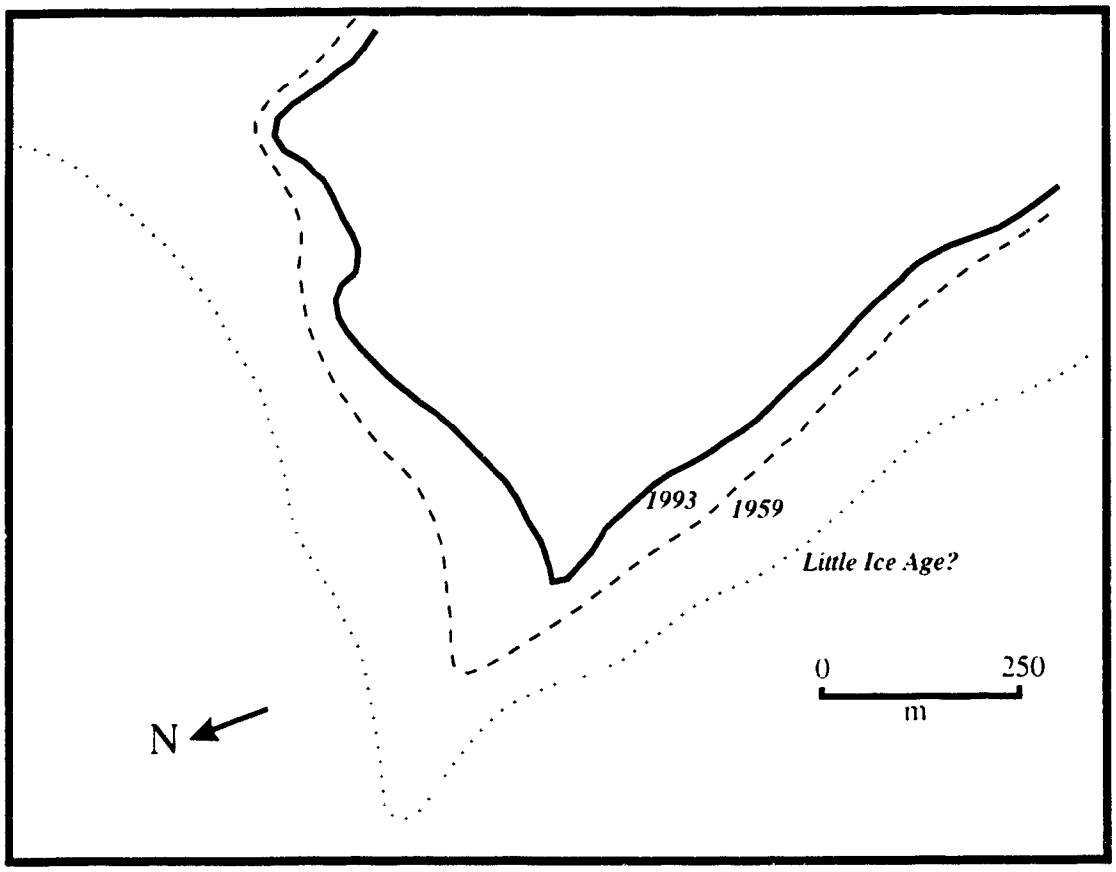

Figure 3 10. Terminus locations of Quviagivaa Glacier for 1993, 1959, and the estimated ice margin during the Little Ice Age

and from the South Melville, Meighen, and Agassiz ice caps suggest that the summer of 1993 was much warmer than usual and that the 1993 mass balance of Quviagivaa Glacier was not typical of the last 45 years, during which time only slight retreat at the terminus can be detected.

CHAPTER 4

MANUSCRIPT 2

Climate-ablation-runoff relationships on a small high Arctic glacier, Ellesmere Island, Northwest Territories, Canada

ABSTRACT

Runoff from a small glacierized catchment (8.7km^2) in the Canadian high Arctic was monitored throughout the 1993 melt season. The stream discharge record is one aspect of a larger project involving glacier mass balance, superimposed ice formation, and local climate, that was carried out in the summer of 1993 on Quviagivaa Glacier (unofficial name), a small glacier in the Sawtooth Range, Fosheim Peninsula, Ellesmere Island.

In order to determine the main factors influencing ablation and runoff on the glacier, statistical analyses are performed using daily runoff values, ablation data, and several hydrometeorological elements. Measured at 12 ablation stations (AS) across the glacier, absorptivity (1-albedo) is a good indicator of ablation (r^2=0.79) for the entire melt period (June 7-August 3), although melting degree hours show the highest correlation with ablation, explaining 87% of the variance (r^2=0.93). Ablation shows a good correlation with discharge at AS2-10 (r^2=0.74), although absorptivity is the meteorological factor with the highest correlation with discharge (r^2=0.47). When the July 20-21 rainstorm days are removed from the regressions, temperature becomes the best predictor of runoff (r^2=0.58). The best prediction of average daily discharge was achieved using a multiple regression of discharge with air temperature, wind speed, shortwave incoming radiation, and net radiation hours (r^2=0.84). Precipitation events (>10mm day^{-1}) can dominate daily discharge when they occur during the period of ice melt, as was evidenced by a 40mm rain event on July 20-21, which resulted in the maximum discharge values for the season.

4.1 Introduction

Glacierized catchments comprise the majority of the watersheds in mountainous Arctic regions, yet very few records of runoff from glacierized basins exist. Studies by Adams (1966) on Axel Heiberg and Wendler et al. (1972) in northern Alaska, obtained partial stream discharge records in proglacial basins for two consecutive seasons. Studies in the late 1960s in the Decade Glacier basin and the Lewis Glacier basin, both on Baffin Island, also obtained records of runoff from glacierized watersheds (Østrem et al., 1967; Church, 1972). These studies included traditional glacier mass balance measurements and some limited correlations made between discharge and meteorological elements. During the last several decades no published work on proglacial watersheds in the high Arctic has been produced, excepting two in which measurements were made in proglacial streams but not on the glaciers in the stream basin studies (Cogley and McCann, 1976; Flugel, 1983). Although several discharge records exist from Ellesmere Island nival catchments (Ambler, 1974; Woo, 1976; Flugel, 1983; Lewkowicz and Wolfe, 1994), this study presents the first complete discharge record from an Ellesmere proglacial stream.

The prediction of runoff and ablation from meteorological variables in an Arctic proglacial catchment has not been attempted in the Canadian Arctic. This paper will examine the discharge record of Quviagivaa Creek and the relationships between hydrometeorological conditions, ablation, and runoff in the Quviagivaa Creek basin. The prediction of runoff from ablation measurements, and several meteorological variables is attempted for the main melt period only (June 29-August 3) because of the complicating influence of snowcover, which causes runoff lags during the initiation of melt.

4.2 Methods

A gauging station was set up in Quviagivaa Creek, approximately 900m downstream from the glacier portal. A stilling well (45 gallon drum), was placed in an excavated hole in the frozen stream bed and rocks were piled around it to keep it secure. Stage was recorded using a float and a counterweight connected to a potentiometer. From June 17 to July 21, the potentiometer was connected to a Campbell Scientific CR21 datalogger, which recorded the stage every 30 minutes. The datalogger malfunctioned on July 21, and a battery-operated Stevens Type F water level recorder was used until flow became too low to measure on August 8.

To convert stages to discharge, a stage-discharge curve was created using velocity-area measurements. A Marsh-McBirney current meter was mounted on a current rod and velocity of flow and depth were measured at 50 cm intervals along a marked cross-section of the creek 2m upstream from the stilling well. High flows on July 21 resulted in the aggradation of the streambed, necessitating two separate stage-discharge curves: one for the period of June 14 to July 21 (A), and one the period of July 22 to August 10 (B). The best fit for the two stage-discharge curves was achieved using third-order polynomial fits (A: r^2=0.98, n=15; B: r^2=0.99, n=13).

Discharge measurements were carried out in the marginal stream at the northwest side of the glacier (June 14, 29 and July 9), at the glacier terminus (June 29), and in Nirukittuq Creek (June 29 and July 9), using the Marsh-McBirney current meter and measured stream cross-sections.

When the diurnal flow patterns became evident, daily discharge values were calculated from the hydrograph by summing hourly discharge from trough

to trough, which takes into account the time needed for glacier runoff to travel up to several kilometres through a system with many lag effects.

Meteorological data were collected at a station on the glacier at 875m a.s.l. (Fig. 4.1). Instruments were connected to a Campbell Scientific CR21X datalogger and hourly values of air temperature, wind speed and direction, incoming shortwave radiation, and net radiation were recorded. On July 10, the glacier station was moved 40m to the north on account of problems with slush flows and melt water streams. The instrumentation of the glacier meteorological station is given in Table 4.1.

TABLE 4.1

Instrumentation of the glacier meteorological station

Measurement	Instrument and Model	Instrument Height
Air temperature	Campbell Scientific Inc. 207F temperature/relative humidity	0.5m
Wind speed and direction	R.H. Young wind monitor	0.5m
Incoming shortwave radiation	Li-Cor LI 200SZ pyranometer	1.8m
Net radiation	REBS Q*6 net radiometer	1.3m
Snow-ice interface temperature	Campbell Scientific Inc. 107 temperature probe	snow-ice interface

Meteorological elements such as air temperature, incoming shortwave radiation, net radiation, albedo, and wind speed, and precipitation vary across the surface of the glacier. Except for albedo and precipitation, the meteorological variables were recorded at one location on the glacier. The meteorological station was positioned at a middle elevation and in the centre of the glacier in an effort to obtain representative values for the largest area of the glacier as possible. However, it would have been preferable to have two or more meteorological stations functioning in the basin, especially for periods when areas contributing to runoff were located below the elevation of the

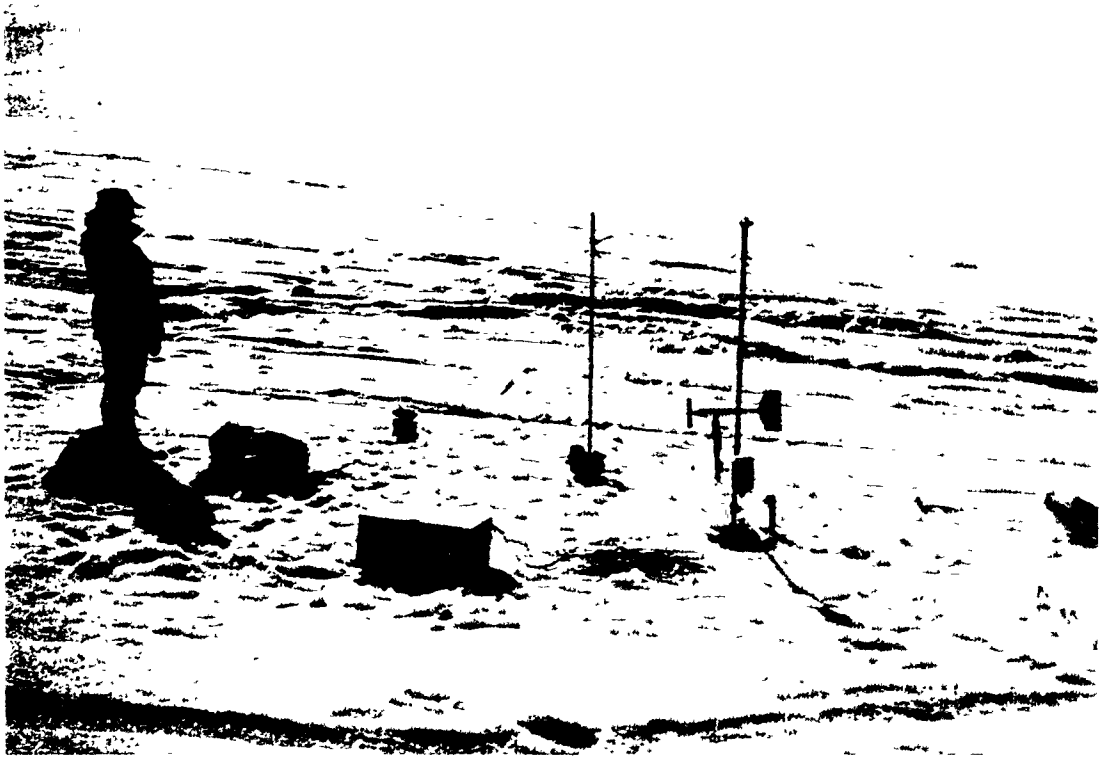

Figure 4 1 Photograph of the glacier meteorological station, July 10 1993

meteorological station. To attempt to rectify this situation, regressions of discharge and meteorological variables were limited to the main period of melt

Albedo measurements were made at each ablation station every other day using a portable solarimeter, mounted on a 75cm long wooden rod, from which voltage was read using a multimeter. The solarimeter was held level, approximately 60cm from the user and 150cm off the ground, pointing toward the sun so as to avoid the shadow of the user. Measurements were always taken in the late morning, between 0900h and 1200h to avoid possible "cosine errors" caused by low solar elevations (Dirmhirn and Eaton, 1975).

Precipitation was measured with Atmospheric Environment Service standard rain gauges at four sites within the basin: the camp meteorological station (550m); the glacier terminus (590m); the glacier meteorological station (875m); and a ridge top between the two glaciers (1000m).

Ablation measurements were taken at 12 locations on the glacier as described in chapter 3.

4.3 Results

4.3.1 General Observations of Discharge

The runoff record from the 8.7 km^2 Quviagivaa Creek drainage basin, encompassing the entire period of streamflow, is shown in Figure 4.2. The discharge record can be separated into three main periods: early melt, main melt, and recession.

The early melt period was characterized by daily discharges below 0.5 $m^3 s^{-1}$ and the absence of a diurnal flow pattern. This period began with the initiation of flow at the gauging station on June 12. Small amounts of runoff were observed adjacent to the glacier as early as May 28 on a south-facing,

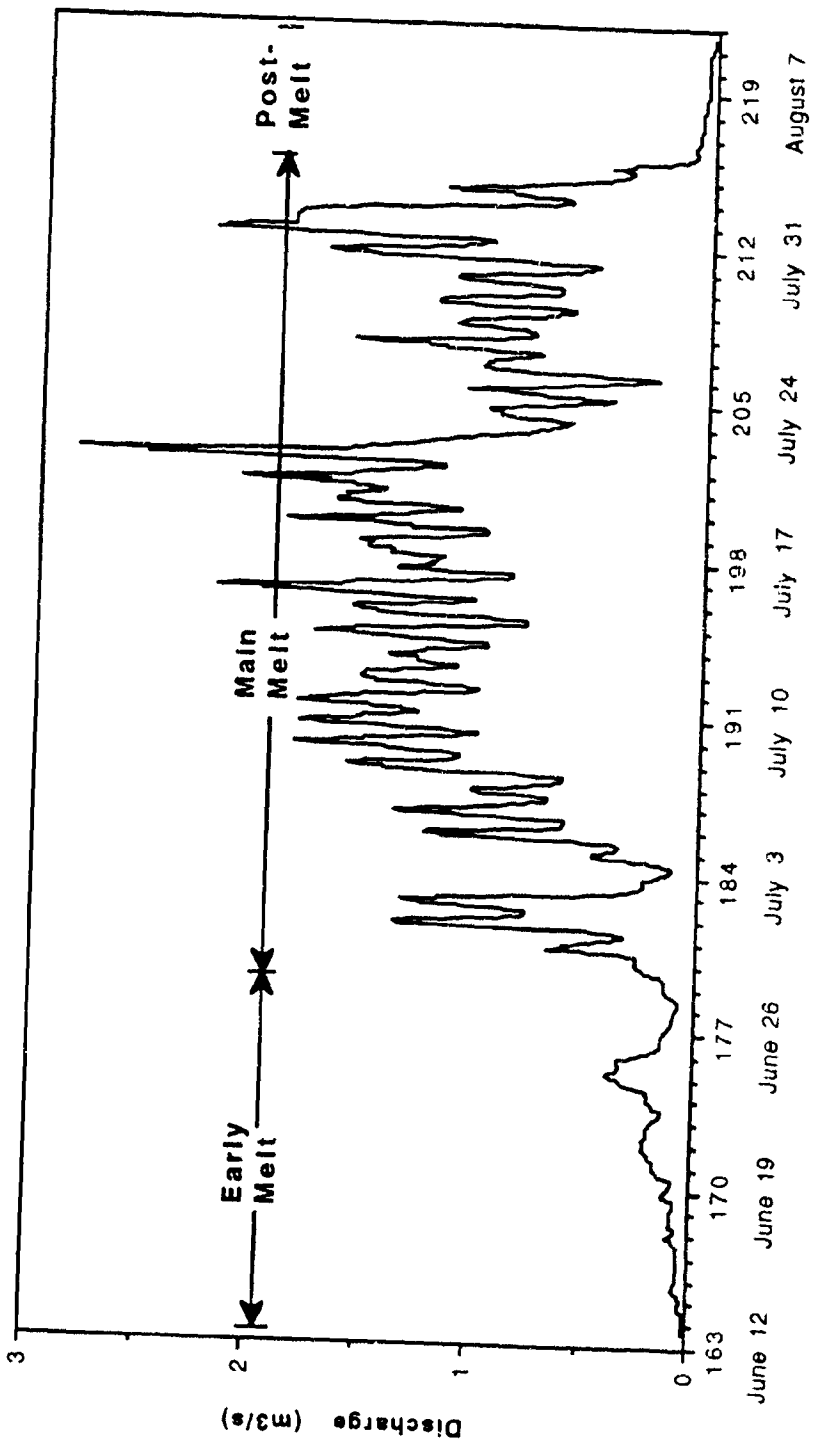

Figure 4.2. The total discharge record of Quviagiaa Creek for 1993 with major flow periods delineated.

partially snow-free slope. During the first week of flow, the source of meltwater was snowpack melt from the ice-free areas below the glacier terminus. However, very little flow from the glacier portal reached the gauging station before June 19. Melt from the glacier was contained in the Quviagivaa Creek channel by snowdrifts (<2m thick in places), which resulted in a series of snowdams between the glacier portal and the gauging station. During this period, temperatures on the glacier dropped below freezing most nights creating a heat deficit that had to be overcome each day before melt could occur. In addition, snowfall events on 26-28 June increased glacier albedo and interrupted melt.

The main melt period was characterized by strong diurnal fluctuations in discharge, and daily peak discharges ranging between 0.5 and 3.0$m^3 s^{-1}$. This period, lasting from June 29-August 3, comprised 94% of all flow measured in 1993. Discharge measurements at the glacier terminus at the beginning of the main melt period (June 29), revealed that approximately 50% of flow was derived from snowmelt on the non-glacierized slopes downslope from the glacier. Late on 29 June a large slush flow (Fig. 4.3) occurred on the lower snout of the glacier which fully established a pathway for flow from the northern glacier ice margin to Quviagivaa Creek and moved a large mass of saturated snow off the glacier. By reason of warm temperatures and high radiation values, melt proceeded rapidly from June 29 onwards (with the exception of July 2), and on July 5 a large slush pool that had been forming near the glacier meteorological station burst, creating numerous slush flows (Fig. 4.4), and opening flow pathways from the upper portions of the glacier. Discharge measurements made at the glacier terminus on July 9 showed that approximately 90% of flow was derived from the glacier surfaces. Consistently warm temperatures in early July meant that by the middle of July non-ice

Figure 4.3. Photograph of a large slush flow at the terminus of Quviagivaa Glacier, June 29, 1993.

Figure 4.4. Photograph of an advancing slush flow on the central snout of Quviagivaa Glacier, July 5, 1993.

surfaces in the basin were predominantly snow-free. In mid-July, new supraglacial meltwater channels were becoming established on the glacier (most of the shallow channels formed during the previous cold summer had been largely filled with superimposed ice), and flow pathways were unobstructed up to 950m on the glacier. The last half of July was characterized by generally overcast skies, slightly cooler temperatures, and several rain events. The seasonal peak discharge of 3.0 $m^3 s^{-1}$ on July 21 occurred during a prolonged rainy period in which up to 40mm of rain fell on the largely snow-free glacier. The second highest discharge (2.3 $m^3 s^{-1}$) occurred on July 31 during a brief period of high glacier melt caused by warm temperatures, high radiation, low glacier albedo, and strong winds (see Fig. 4.6). By the beginning of August the drainage network had extended over virtually the entire glacier, some supraglacial channels reaching depths of 2m.

Melt on the glacier ended abruptly on August 3 because of a snowfall. The recession period of discharge is defined as the period from August 4-9, and is characterized by a rapid recession of meltwater flow on August 4 followed by a gradual recession in flow, primarily composed of discharge from non-glacierized areas. Temperatures remained below zero after August 3, and flow during this period was likely comprised predominantly of active layer drainage from the non-glacierized areas of the basin. Flow declined relatively quickly to levels below 0.01 $m^3 s^{-1}$ by August 9. Figure 4.5 presents the changing condition of Quviagivaa Glacier in 1993 for periods of early melt (June 1), the first stages of main melt (June 29), the end of main melt (July 30), and post-melt (August 5).

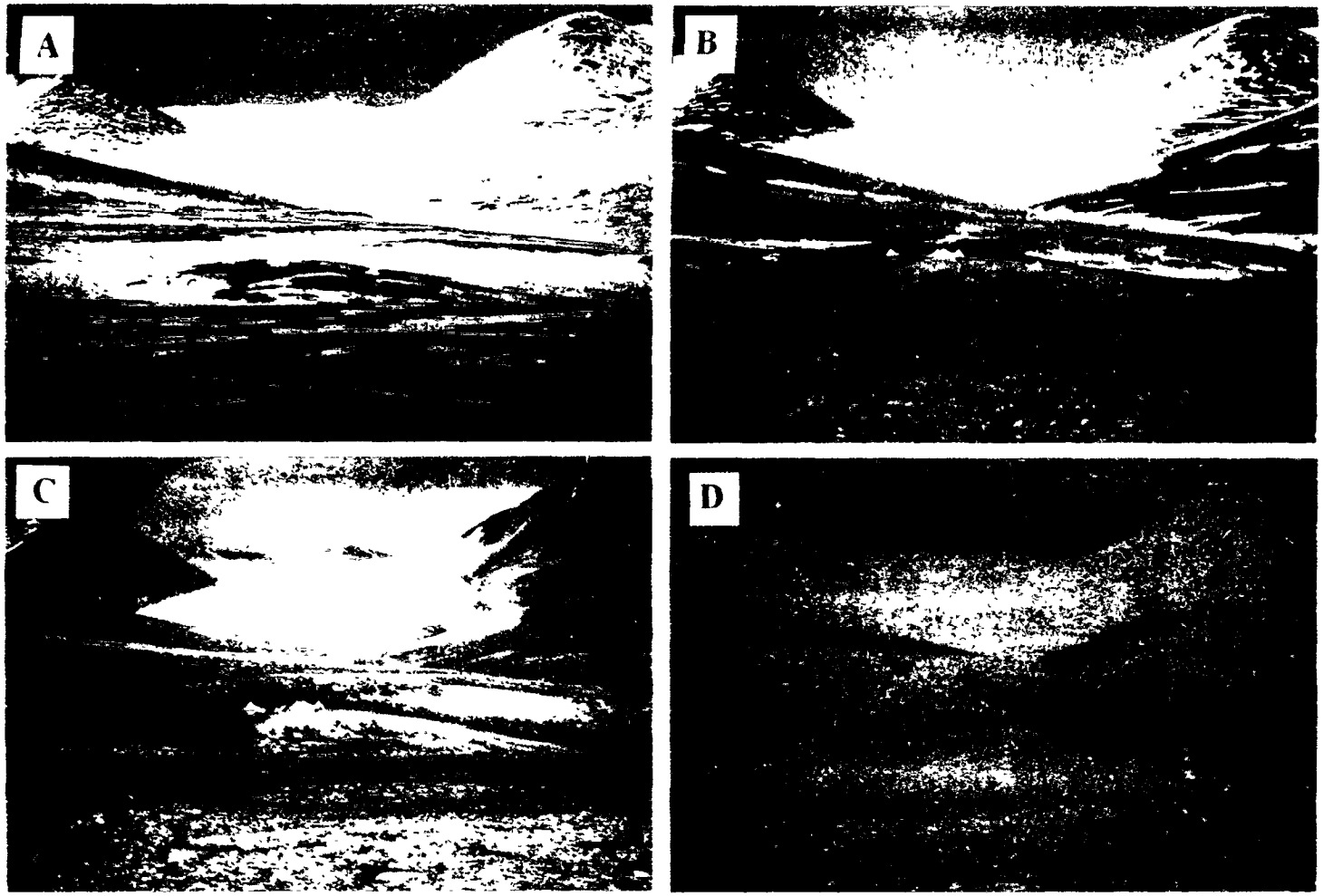

Figure 4.5. Photographs of Quviagivaa Glacier. A: June 1 (pre-melt): B: June 29 (start of main melt period): C: July 30 (end of melt season): D: August 5 (post-melt).

4.3.2 Hydrometeorological Conditions and Ablation

Figure 4.6 graphs average daily air temperature, shortwave incoming radiation, net radiation, and wind speed, measured at the glacier meteorological station, and average albedo measured at AS1-12 for the period of stream discharge (June 12-August 9).

Figure 4.7 illustrates that albedo, or absorptivity (1-albedo), is correlated well with ablation, and the relationship is significant at the 99% confidence interval. The r^2 value in the relationship is lowered on account of AS1. At this site, late-lying snow and superimposed ice elevated albedos by 3-10% between June 30 and July 10 compared with the rest of the glacier snout, while the exposure of dark, sediment-rich glacier ice after July 10 lowered the local albedo by 3-10% compared with the rest of the glacier snout. The relationship between absorptivity and ablation is improved by removing the unrepresentative AS1 site.

Unlike albedo, meteorological data was collected at only one site on the glacier, and correlations between hourly meteorological data and ablation were attempted at an adjacent ablation station (AS10). A strong relationship, significant at the 99% confidence interval, was obtained between ablation at AS10 and melting degree hours (Fig. 4.8). This relationship showed a closer fit than all other measured meteorological factors, including shortwave incoming radiation hours (hourly sums of shortwave incoming radiation between ablation measurements), and net radiation hours.

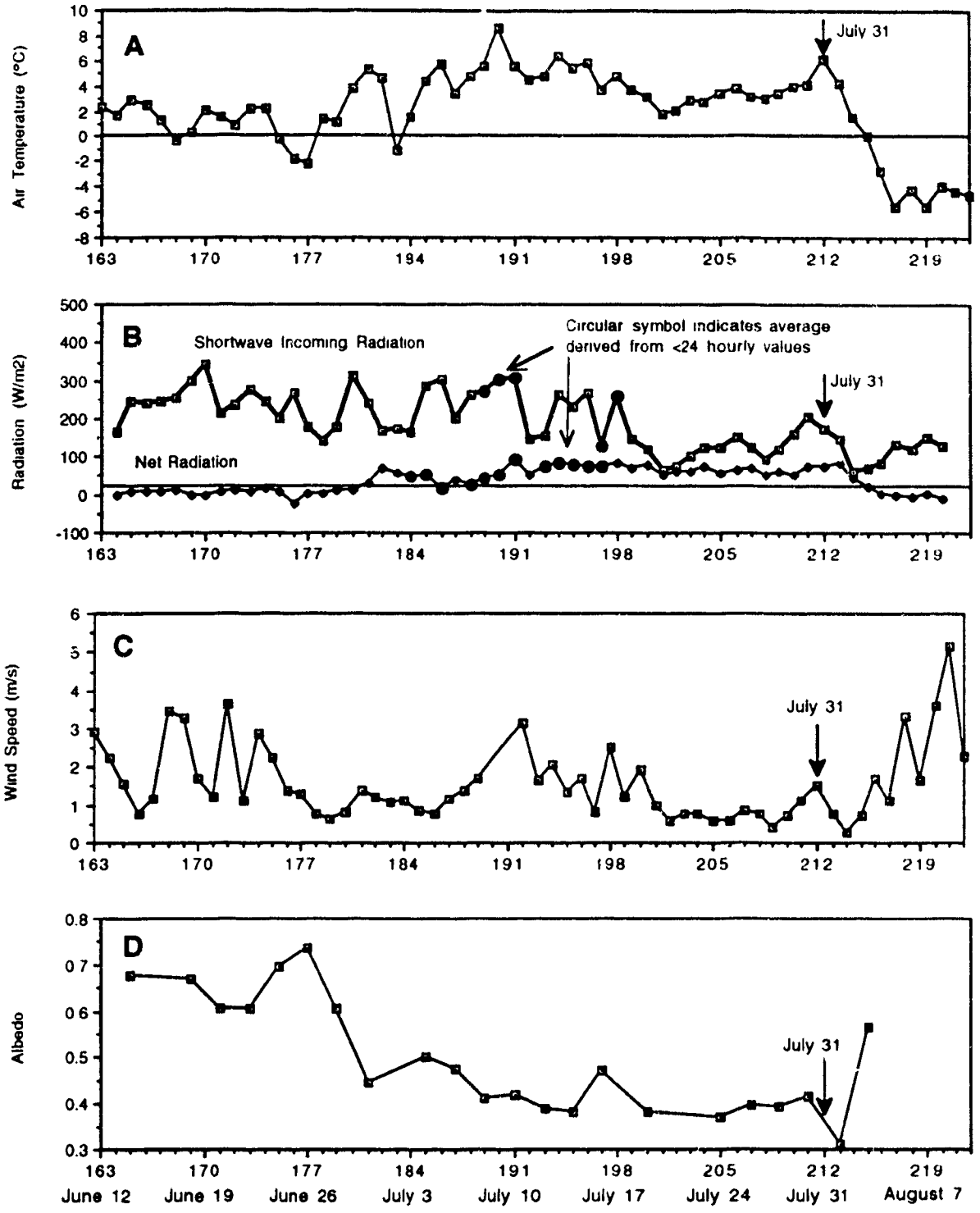

Figure 4.6. Plots of meteorological elements for the period of stream discharge. A: Average daily air temperature; B: Average daily incoming shortwave radiation and net radiation; C: Average daily wind speed; D: Average daily glacier albedo.

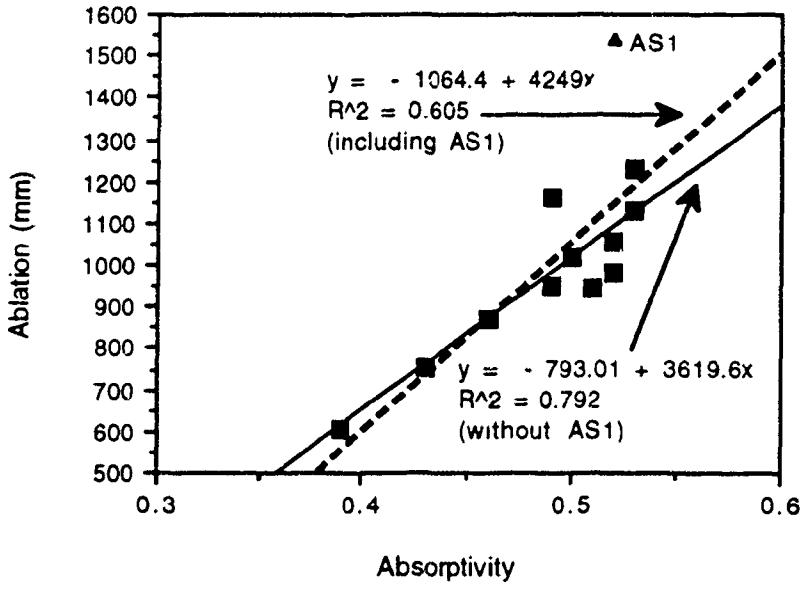

Figure 4.7. Ablation as a function of absorptivity at AS1-12 on Quviagivaa Glacier.

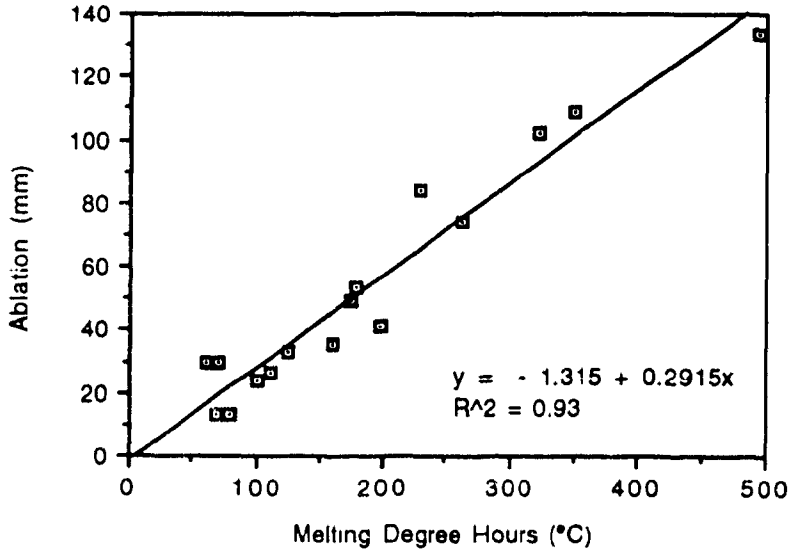

Figure 4.8. Ablation at AS10 as a function of melting degree hours accumulated during the period of measured ablation.

4.3.3 Ablation and Runoff

Scattergraphs of ablation and runoff (totals of hourly discharge measured at the gauging station during periods of ablation measured on the glacier) were produced for each AS. Linear fits were applied to each discharge-ablation scatterplot, and r^2 values from 0.31 to 0.84 were obtained. The discharge and ablation values for July 22 were removed from every plot on account of the overwhelming effect of the July 20-22 rain event on discharge. Glacier-wide ablation measurements were plotted against discharge (Fig. 4.9). The r^2 value for AS2-10 is 0.74, significant at the 99% confidence interval. The significance of this relationship is reduced with the addition of AS1, 11, and 12.

The discharge-ablation regression illustrates that ablation at most stations (AS2-10) closely represents discharge at the stream gauging site, while at AS1, 11 and 12, ablation is a rather poor predictor of discharge. In Figure 4.10 a plot of cumulative ablation at AS1-12 is shown. The unrepresentativeness of AS1 and 12 is evident. AS12 is near the east edge of the glacier and is not affected by glacier winds. On several occasions, calm conditions persisted at AS12 while a brisk down-glacier wind was blowing at AS11. The lower wind velocities at AS12, although unmeasured, likely reduced melt rates and runoff production. In addition, runoff from the site was forced to pass through areas of deep snow upslope from AS11, as well as several crevasses.

The reasonably high r^2 values for the discharge-ablation relationship during the main melt period calculated for most of the ablation stations, suggests that there is a good possibility of estimating runoff from ablation measurements using a single representative location on the glacier. For

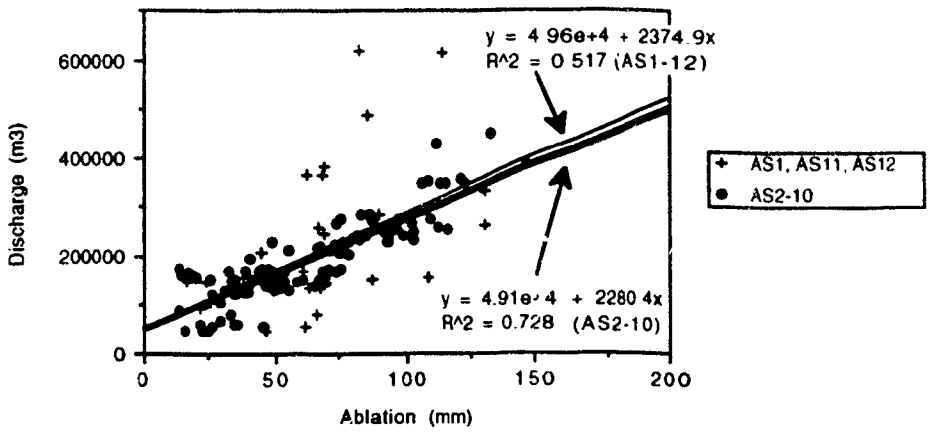

Figure 4.9. Ablation versus discharge for periods of measured melt on Quviagivaa Glacier.

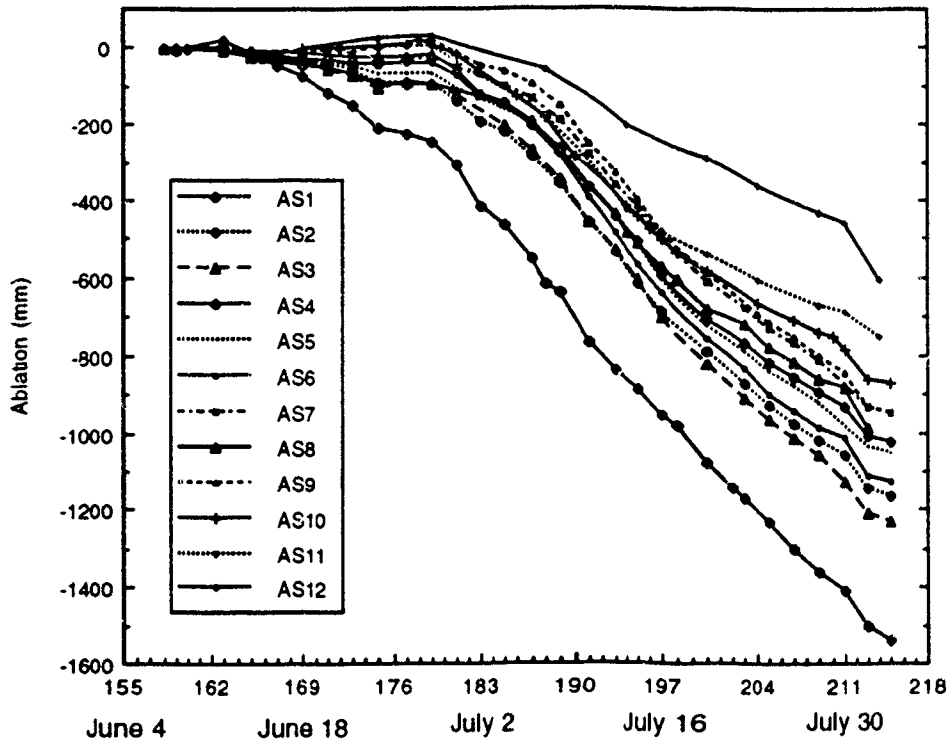

Figure 4.10. Cumulative ablation (mm wat. eq.) at ablation stations 1-12.

Quviagivaa Glacier, the central snout area from approximately 530-930m a.s.l. appears to be the most representative region.

4.3.4 Hydrometeorological Conditions and Runoff

For the purpose of relating runoff to individual meteorological parameters, the period of main melt (June 29-August 3; Julian Day 180-215), when 94% of runoff occurred, was used.

4.3.4.1 Air Temperature

A scattergraph of average daily temperature versus average daily discharge was produced for the main melt period (Fig. 4.11). The relationship, significant at the 99% confidence interval, is improved when the July 20-21 rainstorm days are removed from the plot, which indicates the importance of rain events on stream discharge. In Figure 4.12, the temporal changes in the temperature-discharge relationship, which reduce the r^2 value in Figure 4.11, are more easily seen. Although melt is occurring throughout the basin from June 12 onwards, a significant lag effect is produced primarily because of snow dams in the stream bed, retention of meltwater within the snowpack and crevasses, and the formation of superimposed ice on the glacier. During the first week of streamflow, snow dams in the creek channel are the main cause of the melt-runoff lag effect. The length of free-flowing channel is confined to the ice-free slopes below the glacier, thereby restricting the area of contribution of flow to <10% of the drainage basin. When runoff begins in the upper basin (early July), it is initially impeded by numerous transverse crevasses until they fill with water and no longer delay runoff. Storage of runoff as superimposed ice

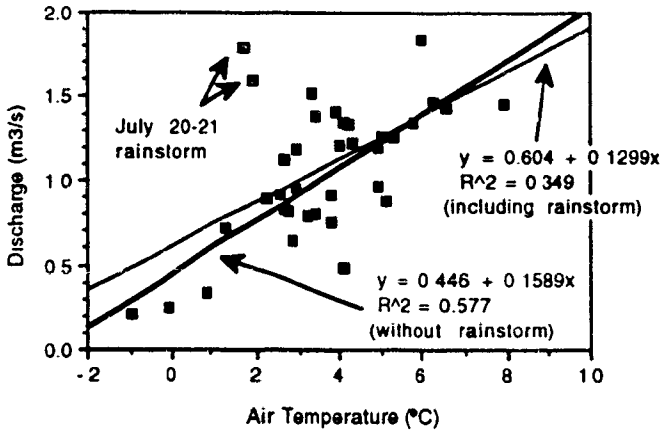

Figure 4.11. Scattergraph of average daily air temperature and average daily discharge.

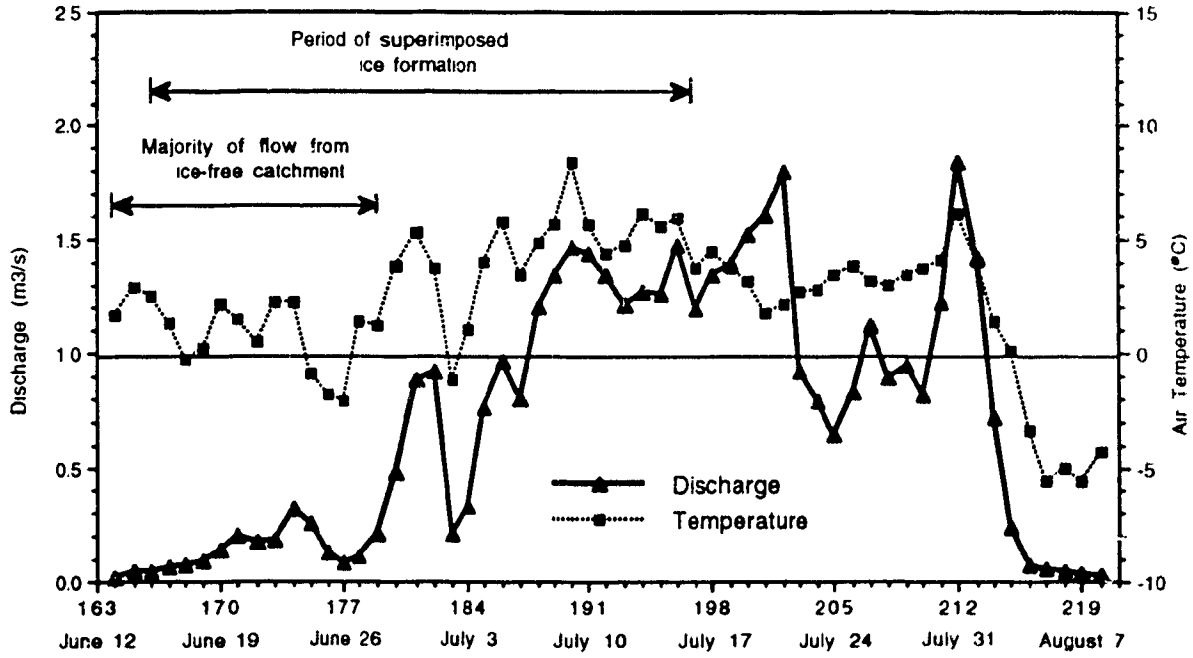

Figure 4.12. Average daily temperature and discharge, June 12-August 9, 1993.

is likely a major factor on days such as June 30 and July 5 (see Fig. 4.6) when high temperatures did not result in peaks in discharge as high as for days with similar temperatures in late July, when the formation of superimposed ice was no longer occurring on most of the glacier. The formation of superimposed ice is widespread early in the season, when meltwater percolating through the winter snowpack refreezes immediately as it reaches the still-cold glacier surface, and is less common when the snow has disappeared and the glacier surface has warmed to 0°C. The formation of superimposed ice varies in time and space on the glacier surface, occurring in the latter part of the time frame shown in Figure 4.12 at the higher elevations and in areas with deeper snowpacks. Superimposed ice was studied in some detail on the glacier, and was found to achieve thicknesses exceeding 30cm in some of the deep snow areas on the glacier snout. In the ablation zone of the glacier, this ice eventually melted and contributed to runoff, some 2-4 weeks after it was formed. In regions of net accumulation, the formation of superimposed ice may create a lag which lasts into the next melt season or longer. In 1993, a small patch of superimposed ice in the uppermost reaches of Quviagivaa did not entirely disappear, largely because of the early termination of the melt season the first week of August.

4.3.4.2 Precipitation

During periods of rainfall (associated with overcast skies and cooler temperatures), fog and low cloud are often present over the glacier, thereby reducing the influence of solar radiation. The great improvement in the r^2 value when the precipitation days were removed from the regression between daily discharge and temperature underscores the importance of rain events on

discharge. However, a plot of daily totals of precipitation regressed against discharge shows a poor relationship. The use of hourly values of precipitation would likely show a much better relationship with daily discharge by reason of the quick response of the glacier hydrological system to rain events (when most of the snow has ablated). With the exception of July 20-21, most of the precipitation events during the 1993 melt season were short in duration and contributed less than 3mm. Although producing small rises in the hydrograph, these minor events likely did not constitute the primary contribution to daily discharge and therefore do not entirely explain the average discharge during the days in question. Events such as the July 20-21 rain event, consisting of some 30-40mm of rain in a 48 hour period, produced the highest instantaneous discharge of the season (3.0 $m^3 s^{-1}$), and likely resulted in most of daily flow.

Continuous permafrost, the highly glacierized catchment, and its steep gradient, result in very little storage of precipitation (given the ablation of the snowpack), and the response time in the hydrograph is rapid. For instance, at 1700h on July 22, exactly 24 hours after the peak discharge of the season, flow had dropped from 3.00 to 0.95 $m^3 s^{-1}$.

4.3.4.3 Solar Radiation

Studies of glacier ablation and runoff in the high Arctic have stressed the importance of receipt of solar radiation on the glacier surface to melt and runoff production (e.g. Keeler, 1964; Braithwaite, 1981). However, no statistically significant relationship between discharge and shortwave incoming radiation was found. This is primarily on account of the timing of peak solar radiation inputs around the summer solstice (depending on cloud conditions), at which time the high glacier surface albedo results in a loss of 60-85% of the radiation.

Runoff on high Arctic glaciers with altitudinal ranges such as Quviagivaa is usually just beginning in late June, with maximum runoff commonly occurring in July (July 21, 1993 on Quviagivaa), often a full month after the peak in incoming shortwave radiation (Adams, 1966).

Although statistically significant at the 99% confidence interval, net radiation displays a rather weak relationship with average daily discharge. There is only a marginal improvement in the r^2 value when the July 20-21 rainstorm days are removed (Fig. 4.13). Compared with incoming shortwave radiation, net radiation should more closely approximate runoff, as maximum net radiation and discharge values occur during July. The weak relationship is likely caused by the unrepresentativeness of the net radiation site measurements compared with the large variance in net radiation across the glacier surface at any given time caused by aspect, shading, and albedo.

4.3.4.4 Albedo

Average glacier albedo is second only to air temperature in explaining average daily discharge for the glacier basin, and the relationship is significant at the 99% confidence interval (Fig. 4.14). Albedo was measured only on rain-free days. The glacier albedo values were arrived at by averaging daily values measured at 8-12 ablation stations on the glacier. On account of the spatially-averaged value obtained, the r^2 value is higher than that obtained using the single site net radiation values. It is likely that with a more comprehensive survey of daily glacier albedo or net radiation, a further improvement in the prediction of daily discharge would be possible.

Figure 4.15 shows the surface conditions of the glacier for four dates through the melt season. The average glacier albedo is reduced from 0.69 on

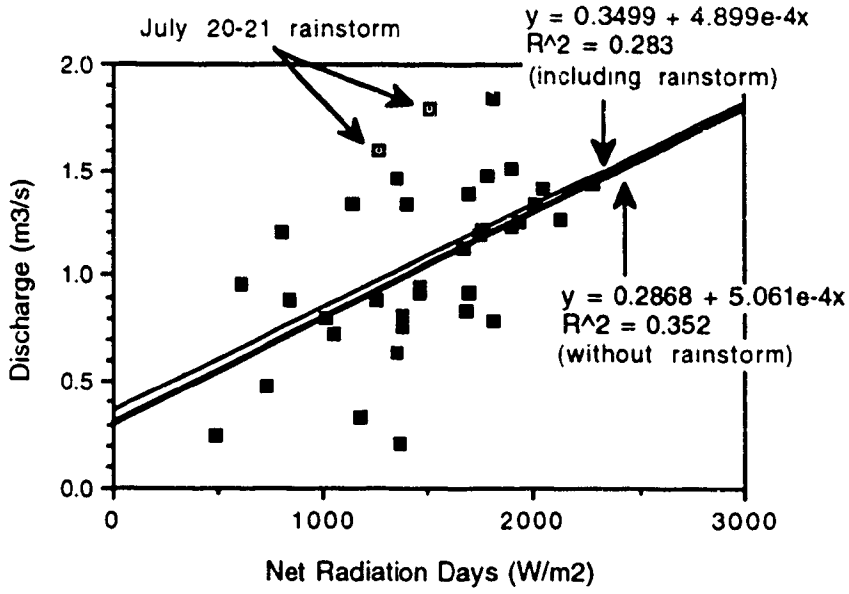

Figure 4.13. Scattergraph of net radiation days and average daily discharge.

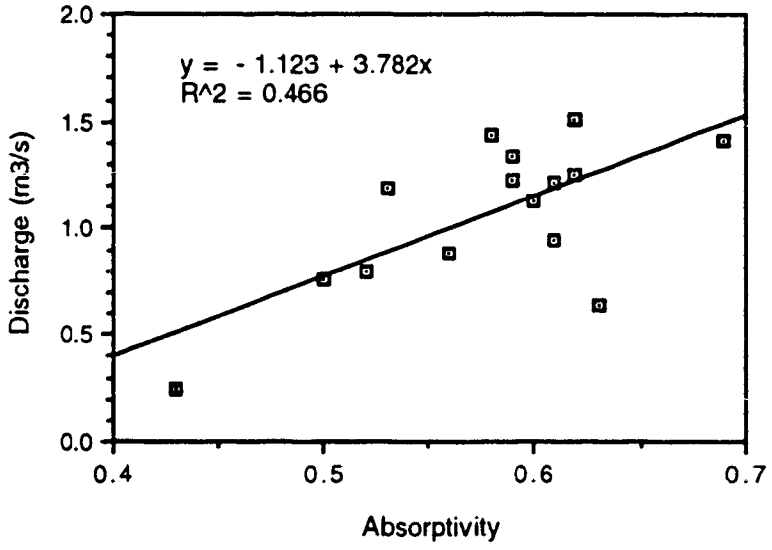

Figure 4.14. Scattergraph of averge glacier absorptivity (1-albedo) and average daily discharge.

June 24, when the glacier was still predominantly snow-covered, to 0.31 on August 1 when the glacier was largely dust-encrusted, ablating glacier ice. The percentage cover of remnant superimposed ice and firn from previous melt seasons have a bearing on the average glacier albedo for the latter part of the melt season. In Figure 4.15, most of the superimposed ice remaining on August 1 was formed in previous years, and has the effect of increasing the average glacier albedo.

Melt and runoff proceed much more efficiently for a given radiation heat input when the snow and superimposed ice have ablated, and darker glacier ice is exposed. The lower albedos in late July and early August compensate for the lower values of incoming shortwave radiation at this time. This effect is demonstrated by comparing discharge and weather conditions on July 8 and 31. Although both days have similar mean temperatures, the average glacier albedo decreases from 0.41 on July 8 to 0.31 on July 31. The darker surface (largely as a result of more exposed glacier ice) on July 31 results in a greater percentage of solar radiation absorbed by the glacier, producing a slightly higher average discharge, even though average incoming shortwave radiation is 100W m^{-2} lower. Therefore, the exposure of the dark-coloured glacier ice early in the melt season increases the likelihood of a high runoff year.

4.3.4.5 Wind

Another important factor in the generation of runoff from a glacier is wind. Winds were almost constant on Quviagivaa, occurring 99% of the time at the glacier meteorological station. A melting glacier cools the air directly above it, which acts as a negative feedback, slowing melt. However, if a wind develops it will mix the cold surface layer of air with warmer air which has not been in

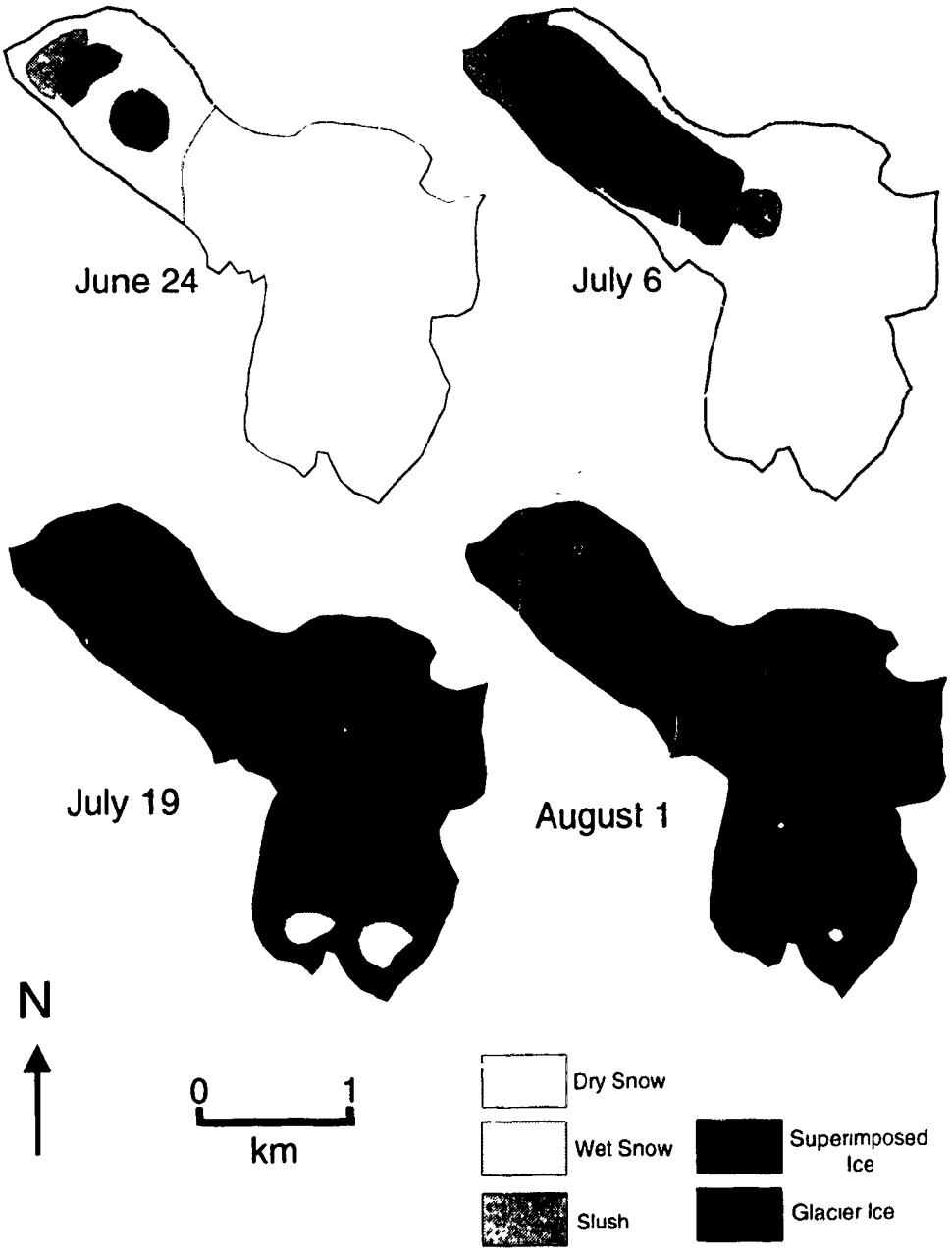

Figure 4.15. Surface conditions for Quviagivaa Glacier on four dates during the 1993 ablation season.

contact with the glacier ice. Greater wind speeds increase the mixing of warm air heated by the surrounding ice-free land, with the colder air sitting over the glacier, and this increases melt and runoff. The correlation between average discharge and average wind speed on the glacier, significant at the 99% confidence interval (Fig. 4.16), is relatively low, but the nearly continuous presence of wind on the glacier during the melt season underlines the importance of wind and melting conditions. As was the case with air temperature, incoming shortwave radiation, and net radiation, the removal of the July 20-21 rainstorm days from the relationship increases the r^2 value.

It is likely that peaks of discharge on July 15 and 31 were caused in part by strong winds (averaging above 1.5m s^{-1}) observed on those days. In the first case winds were up-glacier, while in the second they were down-glacier. This difference in wind direction is probably significant given higher temperature lapse rates for descending air (which is not significant at the top of the glacier where down-glacier winds form). Nearly constant winds measured at the Quviagivaa Glacier meteorological station during the period of observation, were blowing down-glacier 74% of the time.

4.3.4.6 Multiple Variable Prediction of Runoff

The best prediction of average daily discharge during the main melt period was achieved using a multiple regression of discharge with air temperature, wind speed, shortwave incoming radiation, and net radiation hours. The resulting equation, significant at the 99% confidence interval (r^2=0.84), was:

$$y = 0.315\ (T) + 0.11767\ (W) - 0.00248\ (K) + 0.000217\ (NRH)$$

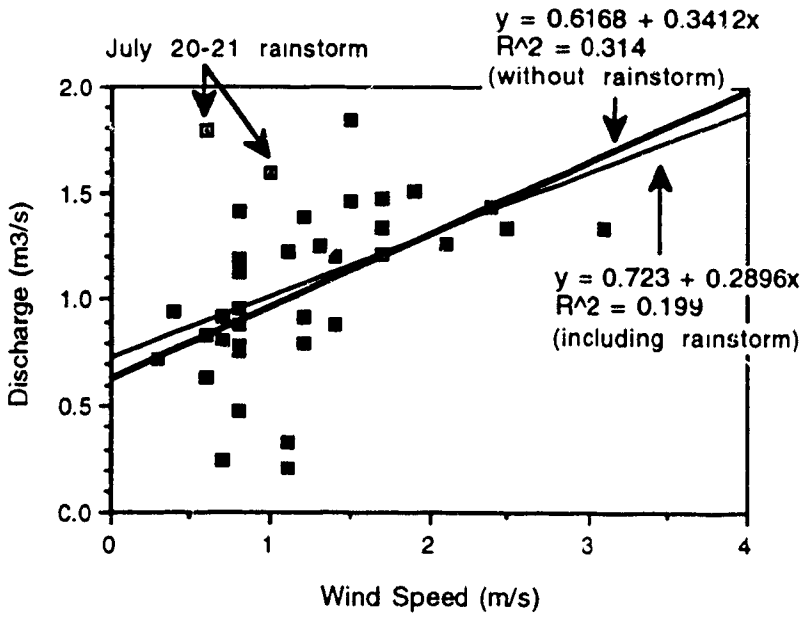

Figure 4.16. Scattergraph of average daily wind speed and average daily discharge.

where:

T = average daily air temperature (°C)
W = average daily wind speed (m s^{-1})
K = average daily shortwave incoming radiation (W m^{-2})
NRH = daily net radiation hours (W m^{-2})

Using these four variables the resulting standard error is ±0.165 m^3 s^{-1}.

4.4 Discussion

4.4.1 The Extrapolation of Hydrometeorological Values Across a Glacier

In any study of the natural environment, where site measurements are the basis of quantitative comparisons, one must determine what extrapolations are acceptable. In this study, hydrometeorological variables are regressed with ablation, and ablation, air temperature, incoming shortwave radiation, net radiation, albedo, and wind speed are regressed against discharge, with the assumption that the aforementioned elements are reasonably representative of conditions on the glacier as a whole. Air temperature, radiation, and wind speed, were measured only at the glacier meteorological station, while ablation and albedo values are averaged from measurements at twelve ablation stations.

Although the measurement of ablation was made at twelve locations across the glacier, it was only related to meteorological parameters at the glacier meteorological station. Screen air temperature (expressed as melting degree hours) was the element with the best relationship with ablation. Air temperature varies mainly with elevation across the glacier with the exception of a border tens of metres wide around the glacier which is affected by the advection of warmer air from non-ice surfaces. The meteorological station was placed near the median elevational range of the glacier to more accurately

represent the average of the total temperature range. The ablation-melting degree hours relationship (Fig. 4.8), developed at the meteorological site, estimated ablation to within 98% of actual measured values at AS11 and AS12, thereby suggesting the extrapolation of this relationship across the glacier surface to be well-founded. The good fit of the air temperature-discharge relationship can be anticipated, considering the high correlation between ablation and melting degree hours (air temperature). It should be noted that because of the inefficiency of the temperature screen, the air temperature values probably include some of the radiation effect. However, nearly constant winds at the site likely reduce the error caused by the radiation absorption of the temperature screen.

Shortwave incoming radiation is difficult to extrapolate across the glacier due to the effects of shading by adjacent mountain slopes and due to the range of aspects and slope angles. Without the construction of a terrain model it is difficult to accurately estimate the percentage of glacier surface in shade for any one time. However, observations at the glacier through the night on July 13-14 determined that up to 50% of the glacier surface was in shadow at the time of maximum shading (0300h). Additionally, radiation contrasts between the upper glacier and snout are heightened on clear days through the local formation of low clouds at the top of the glacier, while the glacier snout experiences partial or total sunshine (conditions experienced on approximately 16 days during the 1993 melt season).

The surface albedo must be accounted for in the extrapolation of net radiation values across the glacier. The better fit achieved with discharge using albedo (Fig. 4.14), as compared with the related element, net radiation, is primarily on account of the measurement of albedo at twelve sites across the glacier, compared with one location for net radiation.

Attempts to choose a representative location to measure wind speed must always take into account the predominance of glacier-generated winds, which commonly develop on even the smallest glaciers (Ohata, 1989). Locations where the fetch is small, such as near the top of the glacier or along the upper margins, will have little glacier wind, and therefore will not represent the general wind conditions on the glacier. Conversely, locations with the longest fetch (along the terminus), or areas in which winds are channeled by topography, will experience the most persistent and strong glacier winds. Wind conditions at the meteorological station were likely close to the mean for the entire glacier. The relatively low correlation between discharge and wind speed suggests that other meteorological elements influence discharge to a greater degree than wind speed (Fig. 4.16).

4.4.2 Comparisons With Other Glacier Basins

The record of discharge in this paper is significant simply on account of the paucity of glacier runoff data from the Canadian Arctic islands. Table 4.2 lists the only published studies from glacierized basins in the North American Arctic. Reasons for the small number of studies include the logistical constraints and high costs of reaching study sites, and the many difficulties which can arise when attempting to measure glacier runoff from a glacierized basin. These include snow-filled streams, aufeis deposits, and extreme flows due to rain events and periods of warm and sunny weather which tend to rearrange channel geometry, wash away weirs, stilling wells, and recording devices. On

TABLE 4.2

Arctic glacial runoff studies

Author	Glacier basin	Basin area (km^2)	% ice-covered	Period of discharge record
Adams, 1966	White, Axel Heiberg I.	54	75	Jun 8-26, 1960 Jun 15-Jul 13, 1961
Anonymous, 1967	Lewis, Baffin I.	182	90	Jun 25-Aug 23, 1963 May 31-Aug 14, 1964 May 29-Aug 13, 1965
Østrem et al., 1967	Decade, Baffin I.	12.8	68	Jun 7-Aug 20, 1965
Wendler et al., 1972	McCall, N. Alaska	30.6	30	Jun 22-Aug 3, 1969 Jul 12-18, 22-Aug 30, 1970

account of these difficulties, and the frequent continuation of runoff after the close of the field season, records from the White Glacier, McCall Glacier, and the Lewis Glacier in 1964 and 1965, are partial.

Most of the difficulty in predicting runoff from glacier meteorological data lies in the complexity of melt and runoff at the start of the season. Complexity is introduced on account of the partial areas of the basin which contribute to flow at the outset of melt, and because of a lag from melt to runoff which varies spatially and temporally. For this study, the relationships between discharge and ablation and meteorological elements, were studied for the period of main melt, in which the entire basin was contributing to runoff. However, by the start of the main melt period on June 29, lags caused by the formation of superimposed ice, and slush ponds were still affecting stream discharge. In a study on Mikkaglaciarenin Arctic Sweden, Stenborg (1970) estimated that 25% of the total summer discharge was delayed from the early to the middle part of the summer. Factors which create this lag are given by Stenborg (1970), and are listed in the order of their approximate quantitative importance on Quviagivaa Glacier for the summer of 1993:

1. The formation of superimposed ice, which caused storage across most of the glacier surface in June and early July,
2. Slush pools in the upper basin; formed by rapid melting of the snowpack in early July,
3. Snowdams in the glacier marginal streams and in the streambed below the glacier, which caused partial to total restriction of flow in June,
4. Storage of meltwater in crevasses on the upper half of the glacier which do not drain to the bed,
5. The limited number of supraglacial channels at the beginning of the melt season (after the formation of superimposed ice and especially in years following cold summers), forcing the meltwater to move across the rough glacier surface,
6. Capillary storage of meltwater in the snowpack throughout its existence on the glacier.

When the snowpack has largely ablated, capillary storage of meltwater is very small, and after crevasses fill up with water (predominantly the crevasses which run perpendicular to the down-slope direction), they no longer create a significant lag in discharge. Superimposed ice formation is largely completed, and flow pathways in the basin are established. The prediction of runoff from ablation and meteorological elements is then more straightforward (Colbeck, 1977).

Although runoff-ablation-climate relationships are described in most Arctic glacier studies (Keeler, 1964; Adams, 1966), none exist which correlate unit values of stream discharge with meteorological elements in a glacierized basin. One of the most significant findings of this work is that during the main

period of melt, average discharge can be most accurately predicted using values of average air temperature on the glacier. Several studies have shown a positive relationship between temperature and runoff in alpine basins, however the runoff-temperature relationship is not simple, and many other factors such as albedo, radiation, wind speed, and precipitation can affect the relationship (Collins, 1984).

Net radiation is in most cases the largest energy source for ablation on Arctic glaciers (Braithwaite, 1981). However, as has been found on other Arctic glaciers, on Quviagivaa Glacier net radiation is not correlated with ablation or discharge as well as air temperature. Braithwaite and Olesen (1984) argue that the typically poor relationship between the ablation rate and global radiation is caused by the low variability of global radiation compared with other energy sources, and the negative relationship between global radiation and the longwave radiation balance.

The relationship of albedo to glacier runoff has not been examined closely in Arctic basins. However, the importance of the surface albedo to ablation is well known. Van de Wal et al. (1992) found that variations in albedo across the snout of Hintereisferner explained most of the difference in ablation during the melt season. If the surface albedo is the prime determining factor for ablation differences across the glacier at similar altitudes, it will also be the principal element determining runoff differences.

During the melt season the temperature of the glacier ice surface can never exceed 0°C. If the glacier is located in a region of relative warmth and the general circulation winds are weak, a local, down-glacier wind will often develop, resulting in an increase of the vertical temperature gradient and in sensible heat transfer to the glacier surface (Ohata, 1989). Down-glacier winds are created by the drainage of cold, heavy air down the glacier surface

(sometimes called katabatic winds). Working on the Greenland ice sheet margin, Duynkerke and Broeke (1994) found that the combined effect of the katabatic and thermal wind effect (induced by the adjacent warm tundra surface), was to enhance the transport of sensible heat to the ice surface. On the Devon Ice Cap, Holmgren (1971) found that at noon, down-glacier winds were on average 2.5°C warmer than up-glacier winds. The predominance of katabatic winds when synoptic conditions favour low gradient winds suggests the importance of stable fair weather systems for the production of strong down-glacier winds, which result in increased runoff from ice and snow ablation (Ohata, 1989).

Keeler (1964), working on the Sverdrup Glacier, Devon Island, found that the greatest ablation rates occurred because of the turbulent transfer of heat during periods of high winds (in this case, winds are caused by general circulation and are not necessarily down-glacier), high temperatures and high humidities. The presence of wind (especially strong winds), must therefore be an important factor which enhances ablation and runoff, despite the low correlation between average wind speed and discharge attained in this study (see Fig. 4.16).

In numerous proglacial basins, precipitation events are related to peak annual discharges. Peak flows occurred on account of a rain event in the White Glacier catchment in 1961, which washed out the weir, terminating stream discharge measurements for the season (Adams, 1966). Summer peak flows due to rain events also occurred in the Lewis and Decade glacier basins in 1965, and in the McCall Glacier basin in 1969 and 1970 (Anonymous, 1967; Østrem et al., 1967; Wendler et al., 1972). Cogley and McCann (1976) describe an exceptional storm which produced peak flows in the proglacial "Sverdrup" and "Schei" rivers at Vendom Fiord, Ellesmere Island, on account of

54.6mm of rain which fell from July 21-23, 1973. The authors note that the exceptional storm of 1973 would have gone unnoticed without measurements at research stations located away from the official high Arctic weather stations. In 1993, a similar situation occurred on July 19-22, when 9.2mm of rain was recorded at Eureka, while 34.1mm was measured at the terminus of Quviagivaa Glacier. This suggests that summer precipitation events play a much greater role in runoff in glacierized catchments than would be expected from the precipitation records from the near-sea level official weather stations.

4.5 Conclusions

The characteristics of the runoff season in the Quviagivaa Creek basin were discussed and average daily discharge values were related with snow and ice ablation, air temperature, precipitation, wind speed, net radiation, incoming shortwave radiation, and albedo for the period of main melt (June 29-August 3, 1993) on Quviagivaa Glacier. The main conclusions can be summarized as follows:

1. Snow dams, meltwater retention in the snowpack, slush pools, and the formation of superimposed ice produce a lag in runoff during the early melt period, and are mainly responsible for the weak temperature-discharge relationship at the outset of the runoff season,
2. Slush flows (of snow and melting superimposed ice) are an important part of the set of processes involved with slush ponds, snow damming, and superimposed ice formation, and result in the relocation of mass to lower elevations on the glacier and in the removal of mass from the glacier,

3. Ablation is closely related to discharge at several locations on the central snout of the glacier, but is not a good predictor of discharge at locations which are unrepresentative of the glacier as a whole in terms of average snow depth, superimposed ice formation, and albedo,

4. For the main melt period, average daily air temperature on the glacier is the single best indicator of average discharge on days unaffected by significant rainfall (>10mm),

5. The best prediction of glacier runoff can be achieved using a multiple regression of air temperature, wind speed, shortwave incoming radiation, and net radiation hours (r^2=0.84),

6. Rain events strongly influence the hydrograph due to the impermeable rock and ice surfaces in the steeply-inclined Quviagivaa Creek basin, and are likely responsible for peak flows in the majority of years.

CHAPTER 5

MANUSCRIPT 3

The measurement and characteristics of superimposed ice on a small high Arctic glacier, Ellesmere Island, Northwest Territories, Canada

ABSTRACT

The formation and ablation of superimposed ice were studied on a small glacier (4.7km^2) on the Fosheim Peninsula, Ellesmere Island, N.W.T.. The formation of superimposed ice was monitored at twelve locations on the glacier through the melt season, and maximum thicknesses were measured at several additional locations. Hourly snow-ice interface temperatures were recorded at a meteorological station on the glacier, and snow-ice interface temperatures were monitored periodically at several locations on the lower portions of the glacier. Approximately 95% of the glacier area sampled evidenced some superimposed ice formation during the melt season, maximum thicknesses reaching in excess of 30cm in the deep snow at the glacier terminus. An isolated area of net accumulation of superimposed ice and firn remained at the end of the melt season, representing <10% of the glacier area. Remnant superimposed ice formed in 1992 (or earlier), was exposed during the 1993 melt season, and covered approximately 65% of the glacier surface. Approximately 67% of spring snowpack water equivalent contributed to the formation of superimposed ice, although percentages ranged from <20% to >100%. The formation of superimposed ice showed a positive relationship with snow depth (r^2=0.83; n=23). Factors which enhanced superimposed ice growth included low snow-ice interface temperatures, the continuous supply of melt-water to the snow-ice interface, low surface slope and high surface roughness.

5.1 Introduction

The refreezing of meltwater on the ice surface of glaciers during the ablation season is a dominant hydrological process in the Canadian high Arctic. The formation of this superimposed layer of ice, or superimposed ice, is a key process on high Arctic glaciers, which serves to:

1. Create a lag in runoff measured at the terminus of the glacier as compared to melt measured on the glacier surface,
2. Add latent heat to the snow-pack and glacier surface through its formation,
3. Elevate glacier albedo (when the snowpack has ablated),
4. Constitute the only means of net accumulation on glaciers which lie predominantly below the regional firnline,
5. Frustrate efforts to locate the equilibrium line from air photos and satellite imagery on account of its probable location within the long-term superimposed ice zone.

Many workers on Arctic glaciers (Schytt, 1949; Wakahama et al., 1976) and high Arctic glaciers (Baird, 1952; Adams, 1966; Koerner, 1970a, 1970b; Palosuo, 1987; Jonsson and Hansson, 1990; Bøggild et al., 1994) have studied superimposed ice within mass balance, modeling, runoff, and process studies.

Aspects of the formation and ablation of superimposed ice were studied in the summer of 1993 in the Canadian high Arctic as part of a project to investigate the mass balance, and ablation-climate-runoff relationships on a small high Arctic glacier. The glacier project was undertaken largely because of the absence of a glaciological component in the current research on the Fosheim Peninsula,

Ellesmere Island, primarily based out of Hot Weather Creek, a Geological Survey of Canada research camp located 50km northwest of the study area.

The objective of this paper is to examine the extent, physical requirements for formation, and hydrological importance of superimposed ice on a small high Arctic glacier.

5.2 Methods

Superimposed ice formation was monitored at all 12 ablation stations (see chapter 3 for description of ablation stations). Snow pits were dug at 10 locations prior to melt, and the bottom of each pit was marked with red or blue chalk before being refilled with snow. Just prior to the total ablation of the snowpack, the snow pit locations were excavated to the depth of the chalk layer, thereby allowing the measurement of superimposed ice thickness. This method was not used in areas with a shallow snowpack, because of the potential for the chalk layer to absorb solar radiation and to melt the surrounding snow and ice. Weller and Schwerdtfeger (1970) state that about 10% of the incoming radiation reaches a depth of 25cm in snow. In firn zones, the measurement of superimposed ice thicknesses using the two described methods can create error given the percolation of meltwater into the firn layers of previous summers. Trabant and Mayo (1985), working on McCall Glacier in northern Alaska, found that the percolation of meltwater into porous firn accounts for an average of 64% of annual accumulation at such sites. The error caused by internal accumulation is minimized on Quviagivaa because of the high regional elevation of the equilibrium line (1000-1200m a.s.l. in the Sawtooth Range), which results in high density, icy firn on glacier surfaces which do not extend higher than this limit (Miller et al., 1975). On Quviagivaa Glacier it is assumed that the superimposed

ice formed preferentially on top of the firn rather than within it on account of the low porosity.

Four thermistors were installed at the snow-ice interface near the glacier meteorological station (see description of the meteorological station in chapter 4) for the purpose of recording the snow-ice interface thermal conditions prior to, and during the formation of superimposed ice. The thermistors were connected to a Campbell Scientific CR21X datalogger, which recorded hourly values of temperature until the ablation of the snowpack was nearly complete.

The glacier was visited briefly on June 30, 1994, at the height of superimposed ice development, and measurements of superimposed ice thickness and snow depth were taken.

5.3 Results

5.3.1 Superimposed Ice Formation and Growth

The formation of superimposed ice on a glacier depends on several factors, which include slope angle, surface roughness, snow-ice interface temperature, meltwater delivery rate to the snow-ice interface, and snow depth (Wakahama et al., 1976). After melt has advanced such that meltwater is able to percolate to the snow-ice interface without refreezing within the snowpack, the following function applies.

$$Si = f(Sd+Ti+Ss+Sr+Md)$$

where:
- Si = superimposed ice
- Sd = snow depth
- Ti = temperature at the snow-ice interface
- Ss = ice surface slope
- Sr = ice surface roughness
- Md = meltwater delivery rate

The formation of superimposed ice was monitored on alternate days at 12 glacier ablation stations (AS1-12). The approximate growth curves (by eye) for superimposed ice at AS1-12 are shown in Figure 5.1. Growth is least rapid at stations with thin snow cover (e.g. AS6 and AS8), possibly because of significant warming of the snow-ice interface prior to meltwater percolation, or resulting from some percolation of meltwater into the porous surface ice at those locations.

The specifics of superimposed ice formation on Quviagivaa Glacier are listed in Table 5.1.

TABLE 5.1

Superimposed ice formation on Quviagivaa Glacier

Location	Elevation (m a.s.l.)	Max. s.i. thickness	Initial snow depth (cm)	Period of formation	Days	Date of disappearance
AS1	569	32	150	Jun 22-Jul 8	18	July 19
AS2	635	11	37	Jun 15-Jun 29	15	July 6
AS3	640	17	43	Jun 18-Jun 27	10	July 6
AS4	659	19	38	Jun 15-Jun 26	12	July 8
AS5	685	7	37	Jun 27-Jul 5	10	July 8
AS6	688	4	17	Jun 15-Jun 21	7	June 30
AS7	684	6	16	Jun 15-Jun 21	7	July 4
AS8	723	2	23	Jun 19-Jun 21	3	June 29
AS9	785	14	30	Jun 27-Jul 4	9	July 10
AS10	875	13	58	Jun 28-Jul 6	8	July 11
AS11	930	20	77	Jul 8-Jul 16	9	July 23
AS12	990	18	65	Jul 5-Jul 12	8	July 19
Snowpit 3	620	30	82	-	-	-
Snowpit 3A	630	24	87	-	-	-
Snowpit 3B	640	28	83	-	-	-
Snowpit 3C	645	10	38	-	-	-
Snowpit 4	655	1	19	-	-	-
Snowpit 5	685	3	16	-	-	-
Snowpit 6	700	8	19	-	-	-
Chalkpit A	900	17	65	-	-	-
Chalkpit B	910	20	52	-	-	-
Chalkpit C	915	21	60	-	-	-
Chalkpit D	920	17	59	-	-	-

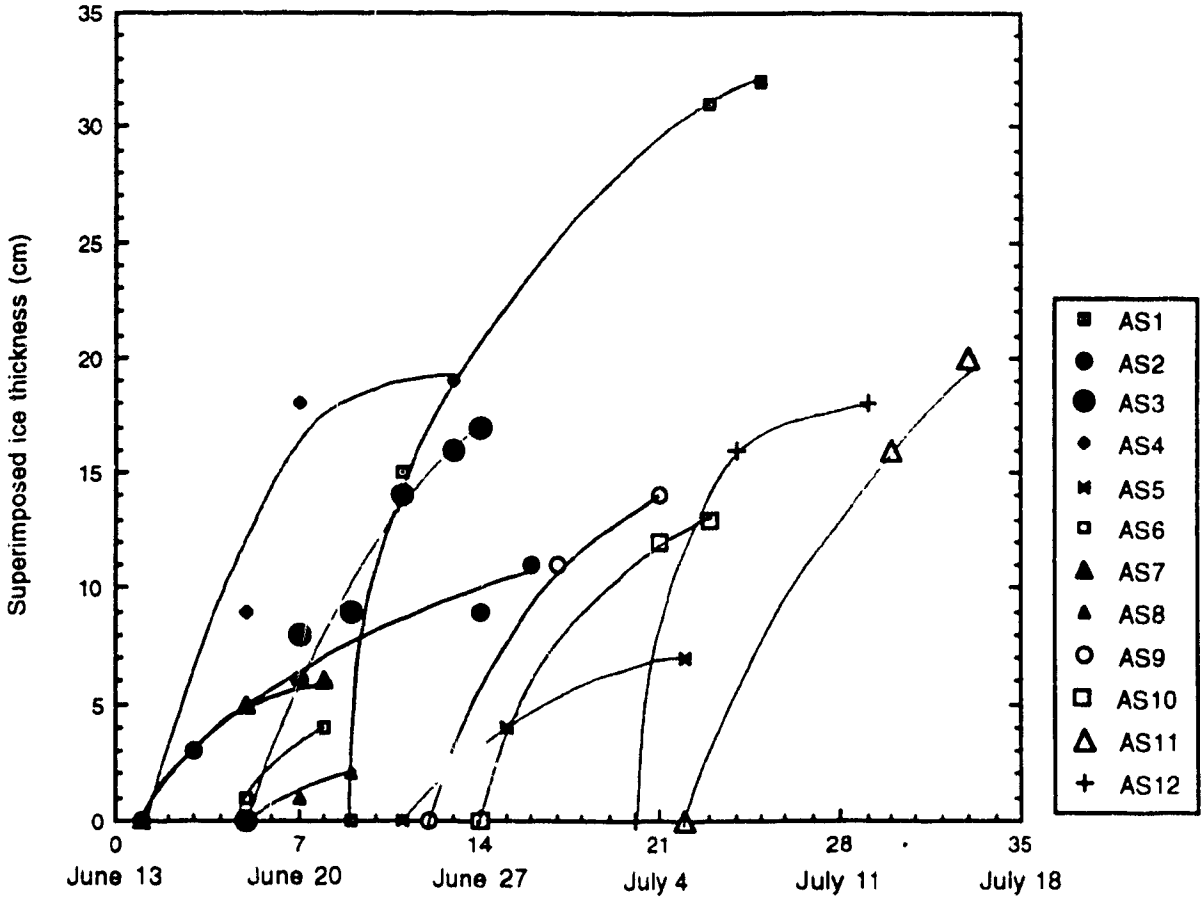

Figure 5.1. Superimposed ice growth curves at ablation stations 1-12.

5.3.2 Snow Distribution and Depth

An isomap of snow water equivalence was created for winter 1992-93 (Fig. 5.2). As evidenced during the snow survey in early June and during several snow events in late June and early August, drifting of snow on the glacier is frequent during and after snow events, and deposition follows a predictable pattern. Snow tends to be eroded from the highest and most exposed sections of the glacier snout and to be deposited along the glacier margins, reaching maximum thickness at the sheltered glacier terminus. Deep snow was also measured in the upper basin, where regional winds are often lessened by the surrounding mountain ridges. The deepest snow occurs at the terminus and the shallowest snowpacks midway up the snout, resulting in no statistical relationship between snow depth and altitude. Likewise, no relationship was found between maximum superimposed ice formation and altitude. The best relationship, significant at the 99% confidence interval, was obtained plotting snow depth against maximum superimposed ice thickness (Fig. 5.3). A semi-logarithmic plot, with snow depth on the logarithmic scale proved to be the best fit, with an r^2 value of 0.83. No superimposed ice was detected in areas with snow depths approximately 15cm or less, while in the deepest snow packs proportionally more superimposed ice was formed. In deeper snowpacks, meltwater can be held until it freezes more easily than in shallow snowpacks. Probably one of the main factors resulting in greater thicknesses of superimposed ice in the deeper snowpacks at the glacier terminus, is the transport of meltwater and slush flows from higher to lower elevations. At Quviagivaa, surface runoff was first witnessed after the ablation of the shallow snow in the central snout region of the glacier. This meltwater had to pass through the deep snow along the glacier margins on

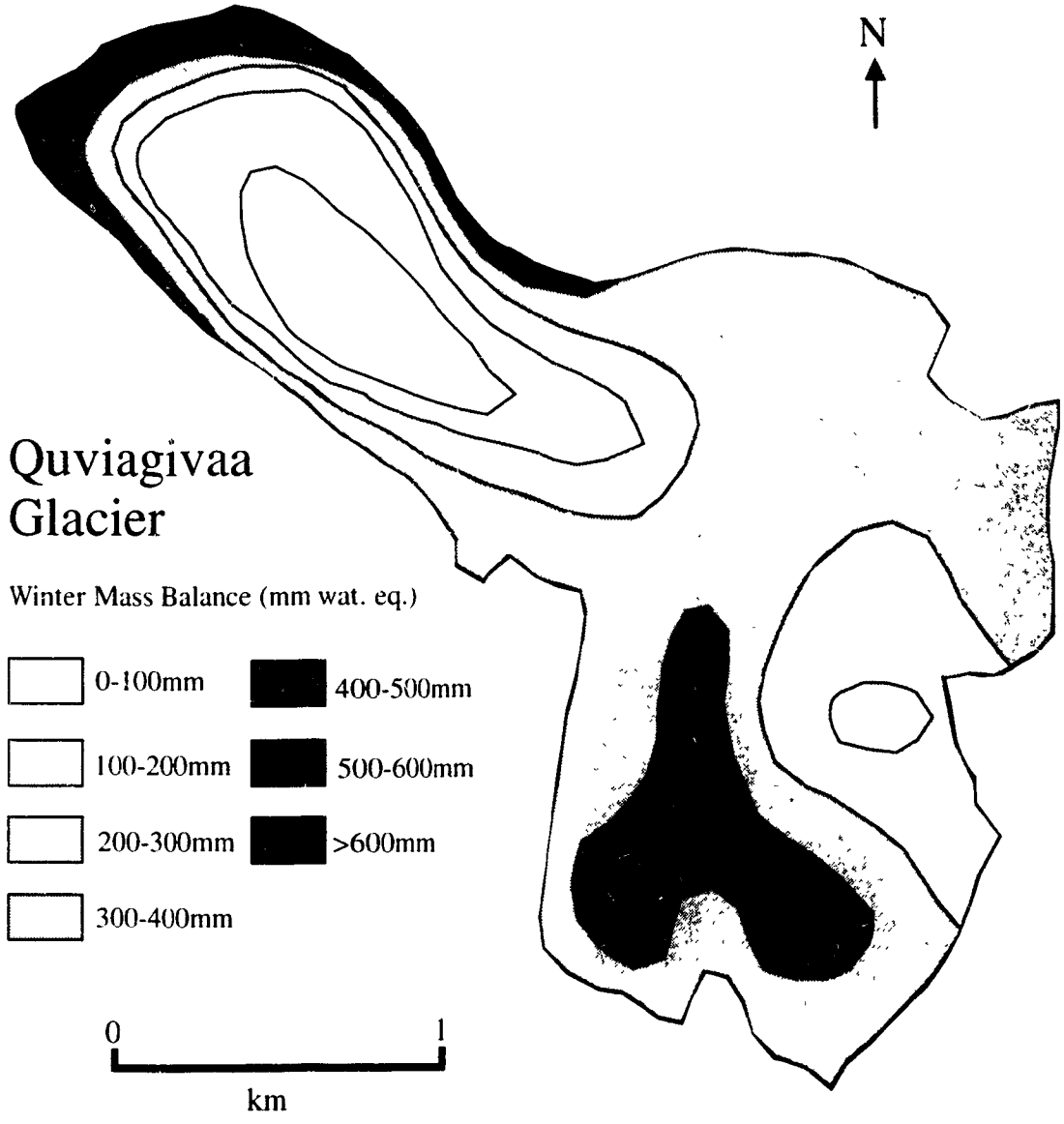

Figure 5.2. Map of winter mass balance, 1992-93 for Quviagivaa Glacier.

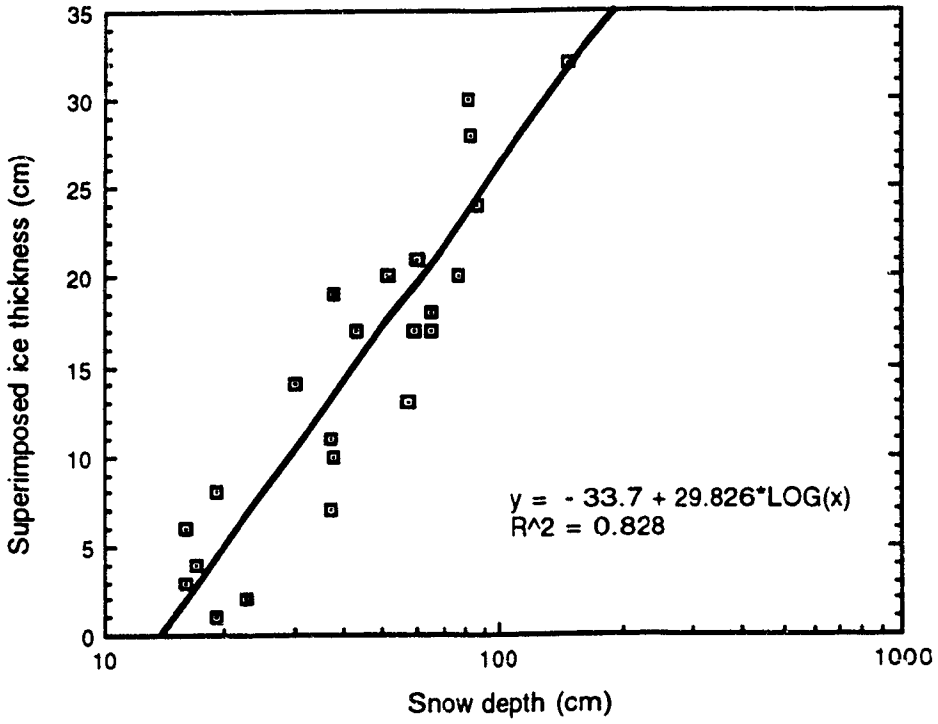

Figure 5.3. Maximum superimposed ice thickness as a function of snow depth at 23 sites on Quviagivaa Glacier.

its way downslope, providing additional sources of meltwater for the formation of superimposed ice.

At Nirukittuq Glacier, the greatest snow depths were also observed at the glacier terminus. Slush flows were a dominant mass transfer process on this relatively steep glacier (35-40°), and superimposed ice in excess of 30cm was formed beneath the slush deposits, where the initial snow depth had been 77cm.

The relationship will also change depending on the summer climate. It is probable that during cool summers, if large enough snow depths were present on a glacier, a semi-logarithmic relationship between snow depth and superimposed ice formation would not apply because of limited percolation of meltwater to the snow-ice interface and a subsequent reduction in the refreezing of meltwater. The relationship will also not apply for regions which are above the long-term regional firnline. In these locations superimposed ice formation is limited because of small amounts and short periods of snowmelt, and most meltwater refreezes within the snowpack. However, this would be an unlikely situation on Quviagivaa Glacier, where substantial melt occurs to the top of the glacier (1250m a.s.l.) and snow depths seldom exceed 1.5m.

5.3.3 Ice Surface Slope and Roughness

Quviagivaa Glacier has a gently-sloping ice surface, most slope angles ranging between 2-15°. Marginal areas of the snout and the north-facing sides of the upper basin, which cover <15% of the glacier area, reach 20-30°. All ablation stations and snow pits were located on sections of the glacier with slopes between 2-12° or account of difficulty of measurement and crevasses on the steeper slopes. Therefore, a comparison of thicknesses of superimposed ice on gentler slopes as opposed to steeper slopes could not be made. However, it is

probable that on the steepest slopes the formation of superimposed ice is reduced because of enhanced runoff of the melt water. Compensating somewhat for their large slope angles, the steepest slopes (30° in the upper basin), contain numerous transverse crevasses, generally 5-50cm wide, which tend to trap meltwater flowing along the steeply-inclined ice surface. These crevasses tend to fill with water soon after the start of melt, and it is assumed that they do not drain to the bed. At the meteorological station, 5-20cm wide crevasses were sealed with new ice within a week of the initiation of superimposed ice formation.

Roughness of the ice surface, both on a small (<1m) and a large (1-100m) scale, is also important in the formation of superimposed ice. In general, large surface features such as hollows, narrow crevasses, and old supra-glacial stream channels are areas where superimposed ice will preferentially form. Surface roughness is high over much of the ablation area at the end of the summer as a result of differential melting and supraglacial melt channels. This surface is then very well suited for superimposed ice formation in the following melt season. Large ice surface irregularities were measured during the snow survey during snow depth probing. In an area with an undulating, but apparently smooth snow surface, snow depths differed by up to 20cm over a distance of 1m. Roughness differences on a medium scale between the upper basin and the lower snout region were noted during the snow surveys conducted prior to snow melt. Standard deviation from the mean snow depth on a 250m transect (n=25) on the lower snout region was 19cm, compared with 8cm on a 250m transect (n=25) in the upper basin. On a smaller scale, the glacier ice surface in parts of the ablation area were rough-textured and cryoconite-affected because of radiation-induced melt and the preferential melting of dirt patches during the last stages of the 1992 melt season. The upper sections of the glacier had patches of firn

remaining from the 1992 melt season, creating significant surface roughness, and thereby increasing the probability of superimposed ice formation. On Quviagivaa Glacier, it is probable that much of the percolating meltwater refroze on top of the moerately icy firn rather than within it. Once superimposed ice has started to form in areas of small scale roughness (e.g. pitted firn or cryoconite areas), the surface roughness is quickly reduced, thereby decreasing the runoff-melt ratio. Surface irregularities in the ablation area formed during the 1992 melt season and measured during the pre-melt snow survey, were entirely filled with new superimposed ice by the time the snow pack ablated. Not only does this process reduce the subsequent formation of superimposed ice, but it also increases the albedo of the surface, thereby negatively affecting the energy budget.

Conflicting with the findings in 1993, a cursory survey of the snout of the glacier on June 30, 1994 revealed that most of the meltwater channels formed during the previous summer were still present, although the formation of superimposed ice was nearly complete. This result may have been on account of the greater quantity and size of meltwater channels formed in the warm summer of 1993 which aided the removal of meltwater from the glacier the following spring.

5.3.4 Meltwater Delivery

The rate of meltwater delivery is a function of absorbed solar radiation, air temperature, liquid precipitation, and snow depth and density. This rate is variable in time given the fact that melt occurs first at the lowest elevations of the glacier, and because of diurnal fluctuations in radiation and temperature, which result in peak melt rates around the daily peak in temperature and absorbed

radiation. The rate is spatially variable because of the heterogeneous nature of the snowpack. Meltwater percolation is impeded where there are ice layers, and routed more quickly in isothermal, ice layer-free snowpacks. Although meltwater delivery was not measured directly, surface lowering, and the main meteorological and physical elements governing melt were. Figure 5.4 shows a graph of estimated daily melt in mm water equivalent at AS10, with the period of ice lense formation within the snowpack, and superimposed ice formation delineated. The daily melt values were calculated with a linear ablation-melting degree hours model (significant at the 99% confidence interval; r^2=0.93) using ablation measurements from AS10 and temperature data from the glacier meteorological station. At AS10, where the pre-melt snow depth was 60cm, approximately 90mm of melt, or 38% of the snowpack water equivalent, occurred before the arrival of meltwater at the snow-ice interface, and the start of superimposed ice formation. High melt rates were important for the initiation of superimposed ice formation, which lasted approximately nine days, but became rapidly less important as the snowpack became isothermal and ablated completely (see Fig. 5.1). At locations with less snowcover (e.g. AS6), meltwater percolation produced superimposed ice more quickly on account of the reduced time required for meltwater to move through the shallow snowpack. At the terminus of the glacier the lag between high surface melt rates and the initiation of superimposed ice formation is greatest on account of the early but discontinuous initiation of melt, and the greater snow depths. Meltwater delivery is delayed because of complex flow pathways through an often highly stratified snowpack and refreezing of meltwater on impeding horizons. Most days with high melt rates occur in July, when most of the glacier is snow-free. At this time, most meltwater is producing runoff rather than contributing to the formation of superimposed ice. The consistently high melt rates measured in mid-July likely

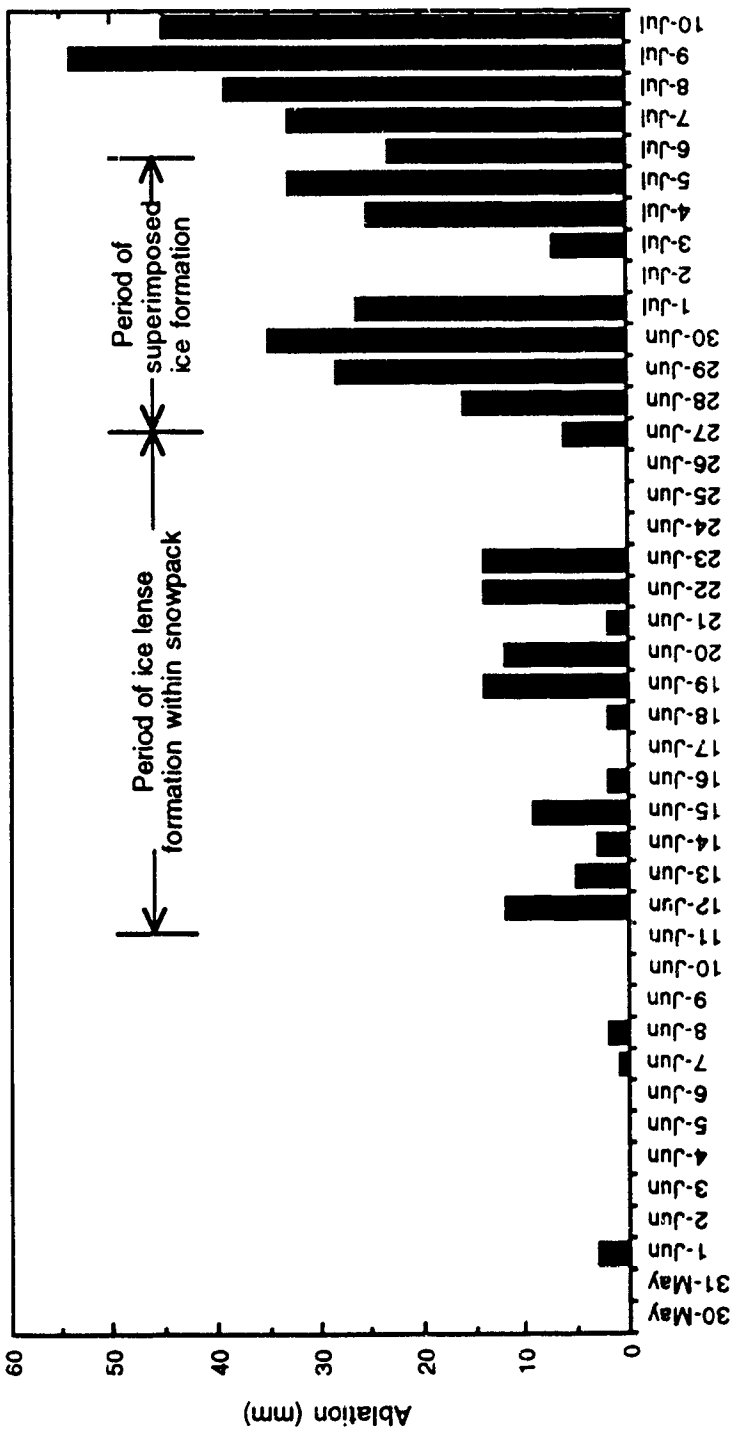

Figure 5.4. Daily melt rates at AS10, showing approximate periods of ice lense formation within the snowpack and superimposed ice formation.

reduced overall superimposed ice formation in the upper areas of the glacier given the rapid warming of the snow-ice interface, which would increase the runoff component (Colbeck, 1977; Marsh and Woo, 1984a).

5.3.5 Snow-Ice Interface Temperature

Figure 5.5 shows a plot of hourly snow-ice interface temperatures at four locations within an area of $100m^2$ surrounding the meteorological station, and hourly air temperatures at 50cm above the glacier surface. Figure 5.6 shows the mean change in temperature per day for the four snow-ice interface locations. The gradual warming, averaging 0.1-0.3°C day^{-1} in the first four weeks of measurements rises to an average of 1.3°C day^{-1} by the fifth week of measurements, as meltwater finally reaches the snow-ice interface. Most warming occurred from June 28-July 2 when average temperatures rose from -9.8 to -0.2°C. This time period corresponds directly with the onset of meltwater percolation to the snow-ice interface and superimposed ice formation at AS10. Despite close proximity, each temperature probe recorded different rates of warming, suggesting varying rates of melt water percolation. The most significant rates of snow-ice interface warming (indicating the major period of melt water percolation) for each temperature probe are given in Table 5.2.

TABLE 5.2

Periods and amounts of maximum snow-ice interface warming

Temperature Probe	Temperature Rise (°C)	Warming (°C)	Warming Rate (°C $hour^{-1}$)	Date and Time
A	-6.9 to -2.7	4.2	1.4	1100-1400 June 29
B	-9.1 to -0.6	8.5	2.1	1300-1700 June 30
C	-4.1 to -0.2	3.9	2.0	0800-1000 July 1
D	-8.0 to -2.7	5.3	1.3	1500-1900 June 30

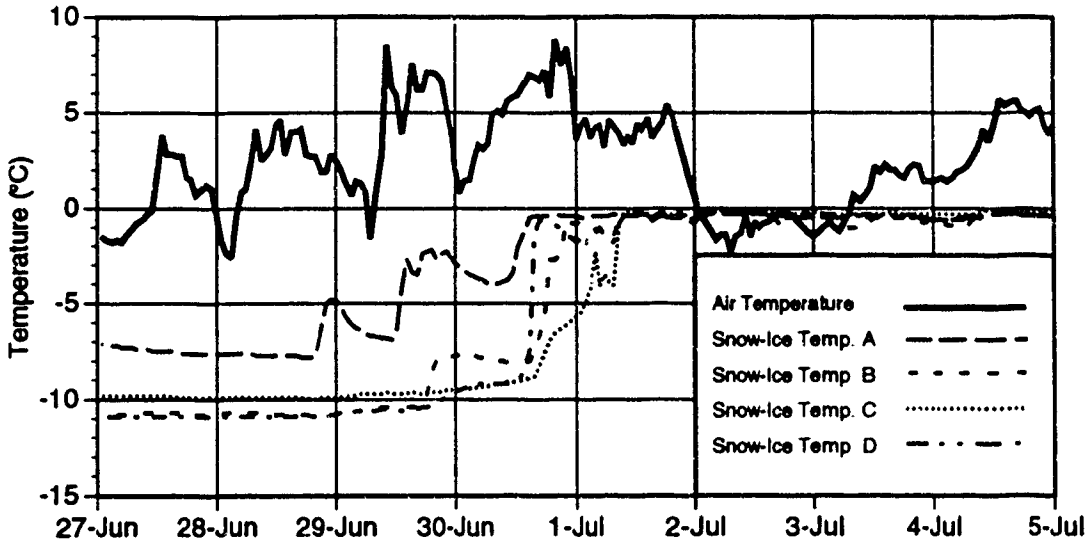

Figure 5.5. Hourly air temperature and snow-ice interface temperature at four locations near the glacier meteorological station during the period of meltwater percolation.

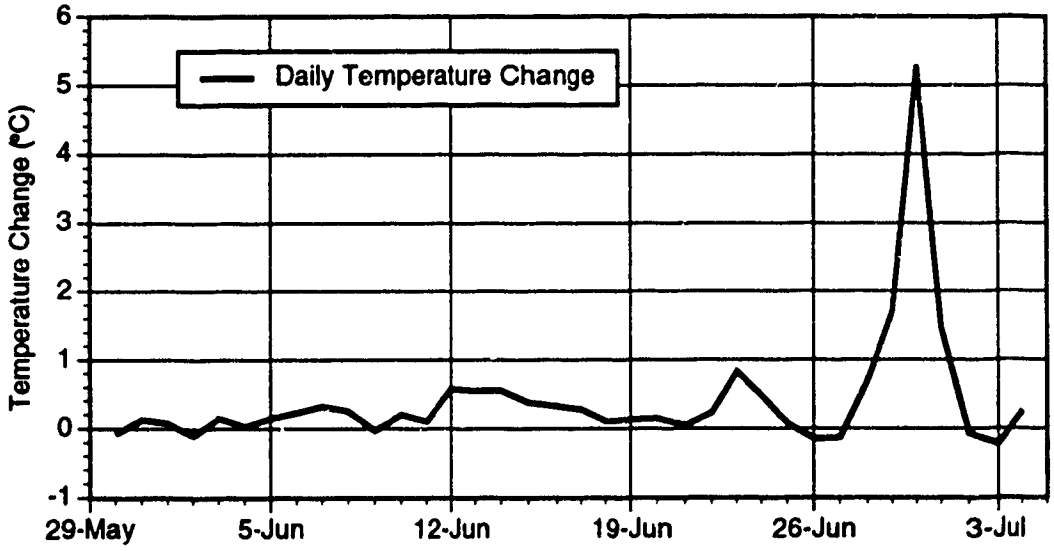

Figure 5.6. Mean daily snow-ice interface temperature change for pre-melt and meltwater percolation stage.

Temperature increases range from 1.3 to 2.1°C $hour^{-1}$ over a three day period within an area of 100m^2, showing the temporal and spatial variability of meltwater delivery to the ice surface in an area with little variation in snowpack depth and density.

5.3.6 Superimposed Ice Distribution and its Importance

The distribution of superimposed ice on Quviagivaa Glacier at time of maximum formation is shown in Figure 5.7. This map is not a "snapshot in time", because of the time-transgressive nature of superimposed ice formation, which is heterogeneous given the uneven distribution of snowfall with elevation on the glacier. Although superimposed ice forms to some degree on almost all surfaces on the glacier, it is very short-lived in areas of shallow snow, while it may persist throughout the summer in upper elevation areas with high snow accumulation. In general, the distribution of superimposed ice shown in Figure 5.7 resembles the map of snow depth (Fig. 5.2), which supports the strong relationship between snow depth and superimposed ice. On August 3, the last day of melt on the glacier, only a small patch of superimposed ice surrounding and underlying an even smaller area of firn remained on the glacier (Fig. 5.7).

Several glaciers adjacent to Quviagivaa were visited late in the melt season and no remnant firn was evident. The smaller glaciers were entirely net ablation surfaces, while the larger ice bodies had small patches of ablating superimposed ice. Summer ablation in the upper basin of Quviagivaa exposed thicknesses of superimposed ice in excess of 40cm, formed in previous summers, suggesting that as much as 65% of the glacier experiences a net accumulation of superimposed ice in cool summers, such as 1992. In addition, several strips of superimposed ice along the lower margins of the glacier survived

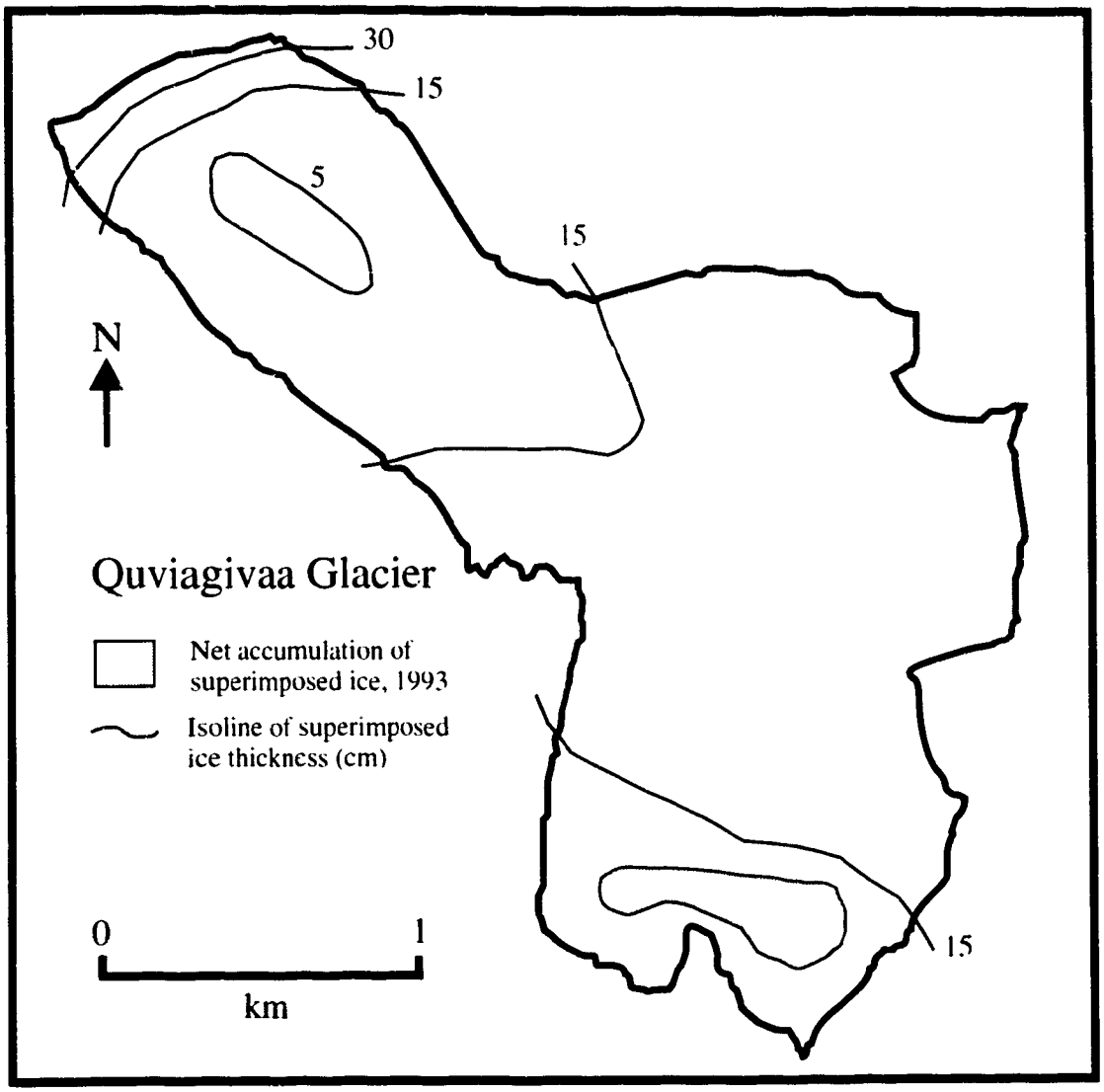

Figure 5.7. Map of maximum superimposed ice formation during the melt season and coverage at the termination of the season on Quviagivaa Glacier, 1993.

into the final week of July (probably formed in 1992), and it is likely that in cooler summers, this region is an area of net accumulation of superimposed ice, thereby helping to maintain the areal extent of the snout. In the summer of 1993, conditions were such that approximately 67% of snowpack water equivalent, measured at 23 sites, went to the formation of superimposed ice. In other words, at an average location on the glacier, 67% of the snowpack had to be melted twice - first as snow, then as superimposed ice. This process is vital for the survival of glaciers in a region where snow accumulation is low.

A short visit to the glacier on June 30, 1994 determined that superimposed ice thicknesses were, on the whole, less than those measured in 1993. Shallow pits dug in the ice on the central snout area revealed superimposed ice thicknesses of 2-7cm beneath an isothermal snowpack measuring 5-30cm thick. At AS10, <1cm of superimposed ice was recorded beneath 40cm of wet snow, compared with up to 10cm of superimposed ice under a similar amount of snow at the same time in 1993.

Superimposed ice has been recognized as the dominant process promoting the survival of several Arctic glaciers which do not reach the altitude of the mean snow line: Meighen Ice Cap, Meighen Island (Paterson, 1969), Barnes Ice Cap, Baffin Island (Baird, 1952), and Storoyjokulen, Svalbard (Jonsson and Hansson, 1990). Müller (1962) states that all the glaciers on Axel Heiberg Island which do not reach higher than 900 to 1000m a.s.l. have no net gain of snow and firn, and rely entirely on the net gain of superimposed ice for their existence. While Quviagivaa reaches 1250m a.s.l., in warmer than average years the regional firnline lies somewhere above the highest point on the glacier, and it is probable that in the majority of years accumulation is predominantly in the form of superimposed ice.

5.4 Discussion

Very few studies of superimposed ice have been carried out in the Canadian high Arctic. However, several researchers mention it within studies focusing on other aspects of glaciology. Baby Glacier, a 0.6km^2 niche glacier on Axel Heiberg Island, is the closest comparable, currently studied glacier to Quviagivaa Glacier in the Canadian high Arctic. Baby Glacier (particularly the lower part of the glacier, which is inclined at 35°), is steeper than Quviagivaa, and likely sheds more of the meltwater which would ordinarily form superimposed ice. It is estimated that on average, superimposed ice forms 15% of net accumulation on Baby Glacier, although the contribution of superimposed ice to net accumulation ranges from 0 to nearly 100%. In 1960, following a winter with little snowfall (96mm), no formation of superimposed ice was observed. In 1969, superimposed ice formed 96% of net accumulation (Cogley et al., 1994 citing Alean and Müller, 1977). A similar substantial variation in superimposed ice formation on Quviagivaa Glacier from year to year is likely reduced somewhat on account of the less steep surface, and sheltered areas on the glacier where snow accumulation is invariably enhanced by drifting in winters with low snowfall.

The White Glacier, 10km from Baby Glacier, has a mass balance record from 1960 to present, and superimposed ice has been studied in some detail (Adams, 1966). Adams (1966) found a strong relationship between the amount of spring snow and the maximum thickness of superimposed ice in the vicinity of the equilibrium line, with at least some superimposed ice formation at snow depths greater than four cm. The same strong snow depth-superimposed ice relationship was found over the entire area of Quviagivaa Glacier. Koerner (1970a) also suggests that one of the most important variables in the formation of superimposed ice is snow depth, and states that there is an optimum snow depth

for any summer melt condition for the production of a maximum thickness of superimposed ice. Since superimposed ice formation seems to be largely determined by snow depth, one would not necessarily expect a significant relationship between maximum superimposed ice formation and altitude on smaller glaciers such as Quviagivaa.

Most of the superimposed ice formation curves for AS1-12 on Quviagivaa Glacier begin steep and gradually level off (see Fig. 5.1), suggesting that the initial coldness of the glacier ice results in rapid superimposed ice growth, which slows as the latent heat released raises the snow-ice interface temperature to near freezing. Measurements of superimposed ice formation and snow-ice interface temperature have been made by Ward and Orvig (1952) on the Barnes Ice Cap, Baffin Island. The initiation of superimposed ice formation caused rapid increases in the temperature of the snowpack to near freezing and the temperature at a depth of 25cm in the ice rose from -12 to -3°C over a period of several days. Like the findings on Quviagivaa Glacier, the superimposed ice growth curves begin steep, and quickly level out as the snowpack temperatures moderate (Ward and Orvig, 1952).

Excepting an isolated patch of superimposed ice at the top of the glacier (1100m a.s.l.), no zone of superimposed ice formation was present on Quviagivaa Glacier in the warmer than average summer of 1993. Ablation of the 1993 snow and superimposed ice uncovered large areas of superimposed ice formed in 1992 (or in earlier years), suggesting that in cooler summers a significant superimposed ice zone can exist on the glacier. On the Gilman Glacier, Hattersley-Smith et al. (1961) found that from 1957-59 accumulation exclusively by superimposed ice occurred from approximately 1200m to 1280m a.s.l., with the interfingering of superimposed ice and firn occurring to 1450m a.s.l.. On the Devon Ice Cap, Koerner (1970a) remarks that the zone of

superimposed ice formation is highly variable in elevation from year to year, as well as in any given year on different sides of the ice cap. In 1963, a relatively cool summer, Koerner (1970a) recorded net gains of superimposed ice from 700m to 1300m a.s.l. The mass balance record of the White Glacier from 1960 to 1991 gives a mean equilibrium line altitude (which denotes the lower limit of the zone of net accumulation of superimposed ice), of 974m a.s.l., which ranges from 470m a.s.l. to 1444m a.s.l. (Cogley et al., 1994).

While significant zones of net superimposed ice have been identified on the White Glacier, Gilman Glacier, and the Devon Ice Cap, the situation of Quviagivaa Glacier is distinctly different. Quviagivaa Glacier does not reach a high enough altitude to support a contiguous zone of net superimposed ice accumulation from year to year. Areas of net superimposed ice formation are often confined to sectors where high snow accumulation, and lower rates of melt caused by shading by the adjacent mountains, support its formation and persistence.

Measurements of the percentage of snowpack water equivalent used to form superimposed ice on Arctic glaciers are few. Measurements on McCall Glacier in northern Alaska, show that approximately 50% of the pre-melt snowpack water equivalent contributes to the formation of superimposed ice (Wakahama et al., 1976). Laboratory experiments were carried out by Wakahama et al. (1976) in order to form superimposed ice in a controlled environment. A block of snow 0.048m^3 in volume, inclined 8°, was cooled to -10°C, then melted using a heat lamp for 24 hours before being refrozen. It was discovered that 37% of the snow formed superimposed ice. It is likely that the lower percentages of snowpack water equivalent going to the formation of superimposed ice on McCall Glacier and in the laboratory experiment are at least in part caused by the slightly higher snow-ice interface temperatures in those

studies compared with those that occur in the high Arctic. However, the experience on Quviagivaa Glacier shows that the variability from site to site can be high, ranging from <20 to >100% of the snowpack water equivalent in 1993.

5.5 Conclusions

Several conclusions can be reached as to the characteristics, formation, and distribution of superimposed ice on Quviagivaa Glacier:

1. Snow depth is the major control on superimposed ice growth where steep slope i.e. >20°, is not a limiting factor: the deeper the snowpack, the thicker the superimposed ice.
2. Given an adequate snowpack, the most important condition for the formation of superimposed ice is that the snow-ice interface is below 0°C: the colder the ice surface, the greater the thickness of superimposed ice which can form before the latent heat of freezing raises the snow-ice interface to 0°C. High surface roughness and low slope angle are two additional conditions which support the formation of superimposed ice.
3. Superimposed ice formation can occur at any time during the melt season, but is most efficient during the initial phases of spring snowpack ablation as the meltwater first reaches the snow-ice interface.
4. From the beginning to the end of the melt season, superimposed ice forms on most surfaces of the glacier, although it is most significant where thicknesses are sufficient to increase the glacier albedo (>1-2cm), thus changing the surface energy balance, and additionally resulting in a substantial lag in the runoff of snowmelt.

5. The formation of superimposed ice over time occurs first in areas with the shallowest snowpacks on the lowest elevations of the glacier, and last in the areas of deepest snow and in the upper portions of the glacier.

6. The percentage of snowpack water equivalent that goes towards the formation of superimposed ice can range between <20% to >100% depending on the degree to which the site is affected by the mass transport of snow and slush. On average, 67% of the snowpack water equivalent on Quviagivaa Glacier formed superimposed ice.

7. Superimposed ice is the predominant form of accumulation on the glaciers of the Sawtooth Range, although in cool summers and on account of the shading effects of mountains, firn also contributes to accumulation.

CHAPTER 6. SUMMARY AND CONCLUSIONS

6.1 Summary

The purpose of this study is to examine mass balance, ablation-climate-runoff relationships, and superimposed ice on a small high Arctic glacier in the Sawtooth Range, Fosheim Peninsula, Ellesmere Island. Hydrological and climatological data were collected over a 77 day period during the summer of 1993 at the site. The absence of glaciological work in the Sawtooth Range, and the usefulness of small glaciers as quick indicators and indexes of climatic change gave impetus to the study (Grudd, 1989).

The annual net mass balance measurements for 1992-93, carried out on Quviagivaa (unofficial name) and Nirukittuq (unofficial name) glaciers, were -532mm and -530mm respectively. The winter and summer mass balances for Quviagivaa Glacier were +303mm and -771mm respectively. The error in the net mass balance is about 70mm, which accounts for the fact that the sum of the winter and summer mass balance values does not equal the net mass balance. On the study glaciers, hydrological processes such as superimposed ice formation and slush flows reduce the altitude-net mass balance relationship. Equilibrium zones can exist both at the top and terminus of both glaciers owing to wind-transported snow and slush flows. The whole of Nirukittuq Glacier was a net ablation surface at the end of the melt season, while only a small patch of firn surrounded by a thin border of superimposed ice remained on Quviagivaa Glacier by August 3. Climate records from Eureka (70km west-northwest of the study site) show that the summer of 1993 was the 14th warmest overall and had the fourth warmest July in the 46 year record. The summer of 1993 was an above average melt year, despite the early end of melt the first week of August

on account of a prolonged snowstorm. Strongly negative mass balances were recorded on the White and Baby glaciers on Axel Heiberg Island, and on Melville and Meighen Island ice caps. High melt was also recorded on the Agassiz Ice Cap in northern Ellesmere Island (Koerner, pers. comm., 1994), suggesting that the negative mass balance of the Sawtooth study glaciers reflected the regional situation. Assuming retreat is proportional to warming, the slight retreat at the terminus of Quviagivaa Glacier (reaching a maximum of 4.3m yr^{-1} at the point of greatest retreat), evidenced from the 1959 air photos, suggests that the normal mass balance situation for the Sawtooth glaciers is only slightly negative. The trim lines (about 40m above the glacier surface at 850m a.s.l.) (see Fig. 1.2), are assumed to represent the most recent period of maximum ice extent, reached during the Little Ice Age (the trim line marks the border between rocks colonized by lichens and those not colonized). At that specific location, the height of the trim line suggests that average summer melt since the Little Ice Age has been less than half that measured in 1993.

Streamflow in Quviagivaa Creek began on June 14, and continued until the end of measurements on August 10, 1993. During the first two weeks of flow, discharges were low because of freezing temperatures at night, snowdams in the channel, and lags in runoff from the glacier. Lags on the glacier were caused by the restriction of melt to the lower altitudinal zones of the basin, the formation of superimposed ice, the storage of meltwater in crevasses, and ponding of water on the glacier surface. Almost 95% of streamflow occurred in the period from June 29 to August 3, which was characterized by predominantly above freezing temperatures and an absence of snowfall. Streamflow was typified by a diurnal rhythm and daily peaks which occurred at 2150h local time in early July and four hours earlier, 1745h local time, in late

July on account of the establishment of supraglacial channels across most of the glacier surface.

For the June 29-August 3 period of main melt, measured ablation, average daily air temperature, net radiation, albedo, and wind speed, showed varying relationships to average daily discharge. The controls on ablation were investigated, and melting degree hours were found to show the highest correlation with ablation (r^2=0.93). With July 20-21 removed from the regressions (a 40mm rainstorm caused high flows on those days), air temperature was the best predictor of runoff (r^2=0.58). The best prediction of average daily discharge was achieved using a multiple regression of discharge with air temperature, wind speed, shortwave incoming radiation, and net radiation hours (r^2=0.84). Precipitation events in July had an immediate effect on streamflow because of the impermeable nature of the basin. A rain event on July 21 resulted in the maximum discharge of the season ($3.0 m^3 s^{-1}$).

The measurement of superimposed ice on Quviagivaa Glacier determined a positive relationship between snow depth and maximum superimposed ice formation (r^2=0.83; n=23). Other factors which enhanced superimposed ice growth were a cold snow-ice interface (insulated by a deep snowpack), a continuous meltwater supply, a gentle slope, and a rough glacier surface. Growth of superimposed ice was found to follow a curve where most rapid accretion occurred in the first few days of formation, given the coldness of the glacier ice, the growth curve flattening out after that despite the higher meltwater supply. The maximum thickness of superimposed ice was measured at the terminus of Quviagivaa (32cm), where initial snow depths were in excess of 1.5m. Areas of low superimposed ice formation (<1cm) were located on the central snout of the glacier, where initial snow depths were less than 15cm.

Deep snow and the accumulation of slush flow deposits along the lower margins of both glaciers resulted in the thickest superimposed ice on the glacier, some of which survived into mid-July. At the end of the melt season, only a small patch of superimposed ice, representing <10% of the glacier area, remained at the top of Quviagivaa Glacier, although additional areas of superimposed ice exposed at the end of the melt season (likely formed in 1992), indicated the possibility for the net accumulation of superimposed ice on 65% of the glacier. At 23 sites on Quviagivaa Glacier, an average of 67% of the snowpack water equivalent formed superimposed ice. The average percentage of snow water equivalent forming superimposed ice was the same for the upper and lower portions of the glacier, although there was higher measured variability on the snout of the glacier given the greater redistribution of mass through slush flows and the larger variation in snow depth. All of the superimposed ice formed in 1993 on Nirukittuq Glacier ablated by the end of the melt season. However, patches of superimposed ice at the top and the terminus of both glaciers persisted into the last week of the melt season, which suggests a large percentage cover of superimposed ice in summers of average or below average warmth.

6.2 Implications for Climate Change

Climate change and the extent to which this perceived change will impact the glaciers of the high Arctic is currently a topic of widespread interest. Most global circulation models agree on the general direction of change for Arctic regions - that it will result in increased surface warming with the greatest warming occurring in the winter, increases in precipitation and evaporation, and decreases in sea ice extent and thickness. The most recent Canadian high

resolution global circulation model (GCM2), predicts that for a doubling of atmospheric CO_2, Arctic regions will be 8-12°C warmer in the winter, 1-6°C warmer in the summer, and will show increases in precipitation (AES, 1994).

During the past 32 years, the ice caps of the Queen Elizabeth Islands have not shown significant trends in mass balance, ablation, or accumulation, although the overall record shows slightly negative mass balances (Koerner, 1994). The summer of 1993 was one of exceptional warmth in the context of the last three decades of glacier research in the Queen Elizabeth Islands. Although average July temperatures at Eureka were only 2°C warmer than the 46 year average, Koerner (Pers. comm., 1994) measured the highest ever (1977-1993) values of ablation on the Agassiz Ice Cap, and the most negative mass balance since 1962 on the Meighen Ice Cap. Measurements of glacier climate, runoff, accumulation and ablation were underway during the summer of 1993 on Quviagivaa Glacier, and because of this, arguable predictions can be made for the still warmer summer conditions that could persist in a scenario of global warming.

The 4-6°C increase in average summer temperatures (June, July and August), which is forecast for the central Queen Elizabeth Islands (AES, 1994), should both lengthen and intensify the melting season on glaciers. Considering the temperature conditions and the resulting glacier ablation experienced across much of the Queen Elizabeth Islands in 1993, an increase in summer temperature of 4-6°C (with no change in precipitation) would likely create strong negative mass balance conditions for all glaciers in the Sawtooth Range (because of their limited elevational extent), and possibly for most of the glaciers in the high Arctic. Glenday (1989) developed a mass balance model for White Glacier, Axel Heiberg Island, using temperature, precipitation and radiation data from Eureka. The result was a mass balance sensitivity of

-74mm $°C^{-1}$ to change in temperature at Eureka. Given a 4°C warming, a net mass balance of -296mm results. Using a glacier surface energy balance sensitivity test, Oerlemans (1991) obtained net mass balance values of -450mm yr^{-1} per degree warming for glaciers located in dry climates. If a warming of 4°C is considered, this results in an average net mass balance of -1800mm yr^{-1}. This value is significantly larger than the most negative annual mass balances ever recorded in the Canadian Arctic (Cogley et al., 1994). This situation would result in a retreat of ice margins until a new state of balance could be reached, and would likely entail the eventual disappearance of most small, low-lying glaciers and ice caps. The amount of summer warming considered exceeds the approximate 2°C warmer conditions experienced during the Climatic Optimum (Koerner and Fisher, 1990), when it is thought that most current small, relatively low elevation glaciers in the high Arctic did not exist (Koerner and Paterson, 1974).

Precipitation has a higher regional variability than air temperature, and the application of rainfall and snow projections is more difficult. Although different models show both increases and decreases in Arctic precipitation, the probability of a precipitation increase exceeds 0.75 (Schlesinger, 1993). Moisture availability in Arctic regions should be heightened on account of the reduction in sea ice cover, and because of the warmer air in the winter months of December, January and February (+8-10°C according to GCM2), it will be able to hold more moisture. During months with consistently sub-zero average temperatures (September to May), any increase in precipitation will likely occur as snow, thereby increasing the winter glacier mass balance. An increase in snow depth on glaciers should result in higher superimposed ice formation, leading to higher average glacier albedos, lower net ablation, and increased snowmelt runoff. However, precipitation events during the summer will likely

increasingly be in a liquid form. The frequency of summer snowfalls (which raise albedo and often halt melt for several days) will likely drop substantially, thereby allowing the uninterrupted procession of ablation during the melt season.

It is possible that a warmer and wetter climate could result in glacier growth. Mayo and March (1990) working on the Wolverine Glacier in southern Alaska, have recorded increases in glacier mass balance during a two decade period of increasing air temperatures (0.76°C decade^{-1}) and increasing annual precipitation (420mm decade^{-1}). The warming occurred primarily in the winter, when temperatures were substantially below -5°C, and the increase in accumulation was not accompanied by an increase in ablation. A case for the growth of high Arctic glaciers could be argued given an increase in annual precipitation with little change in summer temperatures.

In a scenario of global warming, temperatures will likely increase in both winter and summer. However, negative feedbacks exist which could serve to substantially decrease the effect of warming during the melt season. On numerous occasions during the 1993 melt season on Quviagivaa Glacier, days with warm ambient air temperatures and predominantly clear-sky conditions were accompanied by the formation of low cumulus clouds over the mountain peaks. The orographically-induced clouds formed only over the mountain range, often casting a shadow over 50-100% of Quviagivaa Glacier. On ten days during the melt season when this phenomenon was observed, hourly shortwave incoming radiation values at the glacier meteorological station dropped by an average of 46% from clear-sky values earlier in the same day when the sun was at a similar altitude. Daily ablation values calculated from melting degree hours at the glacier meteorological station, were reduced by 40-60% on days affected by orographically-induced clouds. Cloud formation was

most often observed in the early afternoon when radiation values should have been highest. Inputs of solar radiation are more important to glacier melt in late July when the albedo of the ice surface is normally at the lowest level, and in a scenario of warmer summer air temperatures and higher absolute humidity, the negative feedback caused by the orographic formation of clouds would be a significant factor for mountain glaciers.

Positive feedbacks could also affect the glaciers in a situation of climate warming. The disappearance of the regional snowpack (although an originally thicker snowpack) earlier in the season, would increase the annual frequency of aeolian sediment transport onto the glacier surface, thereby lowering the glacier albedo. The likely increase of debris flows and higher volumes of sediment-laden slope runoff would also result in a reduction of the glacier albedo. Lower glacier albedos earlier in the season would lead to higher absorption of radiation when solar radiation values are near the potential maximum. In addition, the likely increase in consecutive negative mass balance years would result in higher concentrations of dust and dirt in the ablation zone, thereby lowering the average glacier albedo.

It is probable that given the substantial increase in average annual air temperature accompanied by an increase in precipitation, Arctic glaciers such as Quviagivaa will experience more frequent occurrences of extreme negative mass balances than at present and will eventually disappear. Given the estimated future annual mass balance of -1800mm, an approximate six fold increase in current accumulation would be required to produce a positive balance - a situation which is highly unlikely. However, negative feedback mechanisms such as enhanced summer cloud formation, added snowfall, and higher superimposed ice formation will slow the otherwise rapid wasting of the smaller glaciers.

6.3 Conclusions

The hydrological cycles of two high Arctic glaciers were studied for the duration of the melt season in a small catchment (8.7km^2) in the Sawtooth Range, Fosheim Peninsula, Ellesmere Island. The following conclusions can be reached based on the primary objectives of this study;

a) Accumulation on Quviagivaa (4.7km^2) and Nirukittuq (0.4km^2) glaciers is predominantly in the form of wind-blown snow, and is controlled primarily by topography. The highest snow accumulations occur at the sheltered terminus areas of each glacier. Melt is sensitive to altitude, although albedo variations across the glacier surface strongly influence ice ablation, and degrade the general decreasing ablation with increasing altitude relationship. The net mass balances of Quviagivaa and Nirukittuq glaciers for 1992-93 were -532mm and -530mm respectively. Meteorological records from Eureka, a weather station 70km west-northwest of the glacier site, show that 1993 had the fourth warmest July in the 46 years of record, thereby suggesting that the normal mass balance for the Sawtooth glaciers is less negative. A photo comparison of the snout of Quviagivaa Glacier between 1959 and 1994 revealed a maximum retreat of 150m at the terminus perhaps indicating that small negative balances were normal for the period.

b) Runoff from the glacierized catchment was recorded from June 14-August 9, 1993, and totaled 3 522 900m^3. Daily ablation was found to be a good predictor of daily runoff at AS2-11. Daily average air temperature from the glacier meteorological station was found to be the best meteorological indicator of daily runoff (r^2=0.58), although a better relationship was produced (r^2=0.84)

using a multiple regression of discharge with air temperature, wind speed, shortwave incoming radiation, and net radiation hours. Precipitation, which introduces considerable scatter in the runoff-air temperature relationship, was found to have the most dramatic effect on runoff, producing the highest discharge of the season on July 21.

c) The formation of superimposed ice was found to be a vital factor in the survival of Quviagivaa Glacier, as on average, 67% of the snowpack water equivalent formed superimposed ice. Maximum superimposed ice thicknesses ranged from 0-32cm on the glacier, and showed a strong, positive relationship with snow depth. A small patch of superimposed ice remained on Quviagivaa Glacier at the end of the season representing <10% of the total glacier area, while all superimposed ice formed during the 1993 melt season ablated on Nirukittuq Glacier.

6.4 Recommendations for the Future

The long-term monitoring of glaciers has been recognized as important in the identification of changes in climate (Cogley et al., 1994). Mass balance records from the Meighen, Melville (South), Devon and Agassiz ice caps, and the White and Baby glaciers have been measured largely on an annual basis since the 1960s. Today these records are invaluable as they provide a background against which the effects of future climatic change may be anticipated. Many glacier studies, however, start with great enthusiasm only to have interest wane after the initial few years. Often, funding for the project runs out and work is finally canceled. Several glacier projects in the Canadian high Arctic such as those at Per Ardua Glacier and St. Patrick Bay Ice Cap come to

mind as examples of this phenomenon. The work at Quviagivaa Glacier may simply be next in the line of projects initially pursued with vigor, only to be deleted when the primary researcher(s) moves on to new work. Quviagivaa Glacier is, however, an attractive study glacier for several reasons, and it is strongly suggested that the work undertaken so far at Quviagivaa Glacier i.e. mass balance, runoff, and climate data collection, be continued in a reduced format.

Glacier mass balance is the most common long-term measurement, as it is a relatively simple, but meaningful, procedure. The argument for the continuation of mass balance measurements at Quviagivaa Glacier is valid simply on account of the great value of field measurements in a data-sparse region such as the Canadian high Arctic. Small glaciers, due to the fact that a large percentage of their area is at or below the long-term equilibrium line, react more quickly to changes in climate than larger glaciers and ice caps. Quviagivaa is the only small ($<10 km^2$) valley glacier presently being studied in the Canadian Arctic. In addition, the glacier meets all the qualifications for a long-term study site. The basin is well-defined, drained by a single stream, and is relatively safe to work on because of the lack of heavily-crevassed regions.

Quviagivaa Glacier is the study glacier which is closest to a long-term meteorological station (Eureka) in the Canadian Arctic. This supports the possibility of the development of mass balance models from Eureka climate data, which would allow good estimates of mass balance for years when the glacier could not be visited. The installation of an automatic weather station on the glacier and the development of accumulation and ablation functions would allow high quality mass balance measurements to be continued with only a brief field visit to download the data.

The predicted increases in air temperature and precipitation in the Canadian Arctic will surely create responses from the glaciers which are not entirely expected, simply on account of the complexities of the natural world. This basic supposition provides sufficient justification for continued study and exploration.

REFERENCES

Adams, W.P. (1966). Ablation and run-off on the White Glacier,Axel Heiberg Island, Canadian Arctic Archipelago. Glaciology, No. 1, Axel Heiberg Research Reports. McGill University, Montreal. Jacobsen-McGill Arctic Research Expedition 1959-1962. 77 p.

Ahlmann, H.W. and Tveten, A. (1923). The recrystallization of snow into firn and the glaciation of the latter. Geografiska Annaler . **5** : 51-58.

Alean, J. and Müller, F. (1977). Zum Massenhaushalt des Baby Glacier, kanadische Hocharktis. Geogr. Helv. **32**:: 203-207.

Alt, B.T. (1975). The energy balance climate of Meighen Ice Cap, N.W.T. Ottawa: Polar Continental Shelf Project, Energy, Mines and Resources Canada. 2 vol.s.

Alt, B.T. (1978). Synoptic climate controls of mass balance variations on Devon Island Ice Cap. Arctic and Alpine Research. **10** (1): 61-80.

Alt, B.T. (1987). Developing synoptic analogs for extreme mass balance conditions on Queen Elizabeth Island ice caps. Journal of Climate and Applied Meteorology. **26** (12): 1605-1623.

Ambler, D.C. (1974). Runoff from a small Arctic watershed. Permafrost Hydrology: Proceedings of the Workshop Seminar. pp. 45-49.

Andrews, R.H. (1964). Meteorology and heat balance of the ablation area, White Glacier, Canadian Arctic Archipelago - Summer 1960. Meteorology No. 1, Axel Heiberg Island Research Reports. McGill University, Montreal. 107p.

Anonymous (1967). Hydrology of the Lewis Glacier, north-central Baffin Island, N.W.T., and discussion of reliability of the measurements. Geographical Bulletin. **9** (3): 232-261.

Arnold, K.C. (1965). Aspects of the glaciology of Meighen Island, Northwest Territories, Canada, Journal of Glaciology. **5** (40): 399-410.

Arnold, K.C. (1968). Determination of changes of surface height, 1957-1967, of the Gilman Glacier, Northern Ellesmere Island, Canada. M.Sc. thesis. Interdisciplinary Glaciology, McGill University, Montreal, Québec. 74p.

Arnold, K.C. (1981). Ice ablation measured by stakes and terrestrial photogrammetry - a comparison on the lower part of the White Glacier, Axel Heiberg Island, Canadian Arctic Archipelago. Glaciology No. 2, Axel Heiberg Island Research Reports. McGill University, Montreal. 98p.

Atmospheric Environment Service. (1982). Canadian Climate Normals - Volume 2 - Temperature 1951-1980. Canadian Climate Program, Environment Canada, Ottawa. 306p.

Atmospheric Environment Service. (1994). Modelling the Global Climate System. Climate Change Digest CCD 94-01, Environment Canada, Ottawa. 20p.

Baird, P.D. (1952). The glaciological studies of the Baffin Island Expedition, 1950. Part 1: method of nourishment of the Barnes Ice Cap, Journal of Glaciology. **2** (11): 2-9.

Becker, A. (1963). On the determination of glacier depth. Ph.D. thesis, Department of Physics, McGill University, Montreal. 84p.

Blake, W. (1981). Neoglacial fluctuations of glaciers, southeastern Ellesmere Island, Canadian Arctic Archipelago. Geografiska Annaler. **63A** (3-4): 201-218.

Blatter, H. (1985). On the thermal regime of Arctic glaciers: a study of the White Glacier, Axel Heiberg Island, and the Laika Glacier, Coburg Island, Canadian Arctic Archipelago, Glaciology No. 6, Axel Heiberg Island Research Reports, McGill University, Montreal. 107p.

Blatter, H. and Kappenberger, G. (1988). Mass balance and thermal regime of Laika Ice Cap, Coburg Island, N.W.T., Canada. Journal of Glaciology. **34** (116): 102-110.

Blatter, H. and Hutter, K. (1991). Polythermal conditions in Arctic glaciers. Journal of Glaciology. **37** (126): 261-269.

Bøggild, C.E., Reeh, N. and Oerter, H. (1994). Modelling ablation and mass-balance sensitivity to climate change of Storstrømmen, Northeast Greenland. . Global and Planetary Change. **9** (1-2):79-90.

Bradley, R.S. and Serreze, M.C. (1987a). Mass balance of two High Arctic plateau ice caps. Journal of Glaciology. **33** (113): 123-128.

Bradley, R.S. and Serreze, M.C. (1987b). Topoclimatic studies of a High Arctic plateau ice cap. Journal of Glaciology. **33** (114): 149-158.

Braithwaite, R.J. (1981). On glacier energy balance, ablation, and air temperature. Journal of Glaciology. **27** (97): 381-391.

Braithwaite, R.J. and Olesen, O.B. (1984). Ice ablation in west Greenland in relation to air temperature and global radiation. Zeitschrift für Gletscherkunde und Glazialgeologie. **Band 20**, S. 155-168.

Church, M. (1972). Baffin Island Sandurs: A Study of Arctic Fluvial Processes. Geological Survey of Canada Bulletin 216. 208p.

Cogley, J.G. and McCann, S.B. (1976). An exceptional storm and its effects in the Canadian high Arctic. Arctic and Alpine Research. **8** (1): 105-110.

Cogley, J.G., Adams, W.P., Ecclestone, M.A., Jung-Rothenhäusler, F., and Ommanney, C.S.L. (1994). Mass balance of Axel Heiberg glaciers, 1960-1991: A reassessment and discussion. NHRI Science Report No. 6. Environment Canada, Saskatoon, Sask.

Colbeck, S.C. (1977). Short-term forecasting of water runoff from snow and ice. Journal of Glaciology. **19** (81): 571-587.

Collins, D.N. (1984). Climatic variation and runoff from alpine glaciers. Zeitschrift für Gletscherkunde und Glazialgeologie. **Band 20**, S. 127-145.

Dicks, W., Adams, W.P., and Ecclestone, M.A. (1992). Mass balance and ablation season processes, Baby Glacier, Axel Heiberg Island, N.W.T. Musk-Ox. **39**: 15-23.

Dirmhim, I. and Eaton, F.D. (1975). Some characteristics of the albedo of snow. Journal of Applied Meteorology. **14**: 375-379.

Duynkerke, P.G. and van den Broeke, M.R. (1994). Surface energy balance and katabatic flow over glacier and tundra during GIMEX-91. Global and Planetary Change. **9** (1-2):17-28.

Edlund, S.A. and Alt, B.T. (1989). Regional congruence of vegetation and summer climate patterns in the Queen Elizabeth Islands, Northwest Territories, Canada. Arctic. **42** (1): 3-23.

Flugel, W.A. (1983). Summer water balance of a high Arctic catchment area with underlying permafrost in Oobloyah Valley, northern Ellesmere Island, N.W.T., Canada. Permafrost: Proceedings, Fourth International Conference. National Academy Press, Washington, D.C. pp. 295-300.

Glenday, P.J. (1989). Mass Balance Parameterization, White Glacier, Axel Heiberg Island, N.W.T., 1970-1980. B.Sc. thesis, Department of Geography, Trent University, Peterborough, Ontario. 120p.

Grudd, H. (1990). Small glaciers as sensitive indicators of climatic fluctuations. Geografiska Annaler. **72A** (1): 119-123.

Haeberli, W., Bosch, H., Scherler, K., Ostrem, G., and Wallen, C.C. (1989). World Glacier Inventory. Status 1988. IAHS (ICSI) - UNEP - UNESCO.

Hattersley-Smith, G., Lotz, J.R., and Sagar, R.B. (1961). The ablation season on Gilman Glacier, northern Ellesmere Island. Union Géodésique et Géophysique Internationale. Association Internationale d'Hydrologie Scientifique. Assemblée général de Helsinki. 25-7-6-8. 1960. Commission des Neiges et Glaces. 152-168.

Hattersley-Smith, G. and Serson, H. (1970). Mass balance of the Ward Hunt ice rise and ice shelf: a 10 year record. Journal of Glaciology, **9** (56): 247-252.

Hattersley-Smith, G. and Serson, H. (1973). Reconnaissance of a small ice cap near St. Patrick Bay, Robeson Channel, northern Ellesmere Island, Canada. Journal of Glaciology, **12** (66): 417-421.

Havens, J.M. (1964). Meteorology and heat balance of the accumulation area, McGill Ice Cap. Canadian Arctic Archipelago - Summer 1960. Meteorology No. 2. Axel Heiberg Island Research Reports. McGill University, Montreal. 87p.

Havens, J.M., Müller, F., and Wilmot, G.C. (1965). Comparative meteorological survey and short term heat balance study of the White Glacier, Canadian Arctic Archipelago - Summer 1962. Meteorology No. 4. Axel Heiberg Island Research Reports. McGill University, Montreal. 68p.

Holmgren, B. (1971). Climate and energy exchange on a sub-polar ice cap in summer. Arctic Institute of North America Devon Island Expedition, 1961-1963. Part A. Physical Climatology. Meddelanden fran Uppsala Universitets Meteorologiska Institution. Nr 107. 83p.

Iken, A. (1974). Velocity fluctuations of an Arctic valley glacier, a study of the White Glacier, Axel Heiberg Island, Canadian Arctic Archipelago. Glaciology No. 5. Axel Heiberg Island Research Reports. McGill University, Montreal. 116p.

Jacobs, J.D., Andrews, J.T., Barry, R.G., Bradley, R.S., Weaver, R. and Williams, L.D. (1972). Glaciological and meteorological studies on the Boas Glacier, Baffin Island, for two contrasting seasons (1969-70 and 1970-71). In: The Role of Snow and Ice Hydrology. Proceedings of the Banff Symposia. September 1972. IAHS Vol. I. pp. 371-382.

Jonsson, S. and Hansson, M. (1990). Identification of annual layers in superimposed ice from Storoyjokulen in northeastern Svalbard. Geografiska Annaler, **72A** (1): 41-54.

Jung-Rothenhäusler, F. (1992). Prospects for remote sensing of the annual mass balance: White Glacier, Axel Heiberg Island, N.W.T., Canada. M.Sc. thesis, Watershed Ecosystems Graduate Programme, Trent University, Peterborough, Ontario. 187p.

Keeler, C.M. (1964). Relationship between climate, ablation and runoff on the Sverdrup Glacier, 1963, Devon Island, N.W.T. Arctic Institute of North America, Research Paper No. 27. 80p.

Koerner, R.M. (1966). Accumulation on the Devon Island ice cap, Northwest Territories, Canada. Journal of Glaciology **6** (45): 383-392.

Koerner, R.M. (1968). Fabric analysis of a core from the Meighen Ice Cap, N.W.T., Canada. Journal of Glaciology **7** (51): 421-430.

Koerner, R.M. (1970a). Some observations on superimposition of ice on the Devon Island Ice Cap, N.W.T. Canada. Geografiska Annaler. **52A** (1): 57-67.

Koerner, R.M. (1970b). The mass balance of the Devon Island Ice Cap, Northwest Territories, Canada, 1961-66. Journal of Glaciology. **9** (57): 325-336.

Koerner, R.M. (1986). Novyy metod ispol' zovaniya lednikov dlya monitoringa izmeneniy klimata/A new method for using glaciers as monitors of climate. Materialy Glyatsiologicheskiy Issledovanii/Data of Glaciological Studies No. 57, Akademii Nauk SSSR, Moskva, (in Russian) 47-52; (in English) 175-179.

Koerner, R.M. (1994). Glaciers in the context of global warming. In: Abstracts, Workshop on Mass Balance of Arctic Glaciers, International Arctic Science Committee, Working Group on Arctic Glaciology. Wisla, Poland, 18-22 September, 1994.

Koerner, R.M. and Fisher, D.A. (1990). A record of Holocene summer climate from a Canadian high-Arctic ice core. Nature. **343**: 630-631.

Koerner, R.M. and Paterson, W.S.B. (1974). Analysis of a core through the Meighen Ice Cap, Arctic Canada, and its paleoclimatic implications. Quaternary Research. **4**: 253-263.

Koerner, R.M., Fisher, D.A. and Paterson, W.S.B. (1987). Wisconsinan and pre-Wisconsinan ice thicknesses on Ellesmere Island, Canada: inferences from ice cores. Canadian Journal of Earth Sciences. **24**: 296-301.

Kraus, P. (1983). Glacier inventory of southeast Ellesmere Island, N.W.T., Canada and its application for estimating the annual run-off. Geographisches Institut Eidgenössische Technische Hochschule Zürich. Heft 9. 103p.

Lewkowicz, A.G. and Wolfe, P.M. (1994). Sediment transport in Hot Weather Creek, Ellesmere Island, N.W.T., 1990-1991. Arctic and Alpine Research. **26** (3): 213-226.

Maag, H. (1969). Ice dammed lakes and marginal glacial drainage on Axel Heiberg Island, Axel Heiberg Island Research Reports. McGill University, Montreal. 147p.

Marsh, P. and Woo, M.-K. (1984). Wetting front advance and freezing of meltwater within a snow cover. 1. Observations in the Canadian Arctic. Water Resources Research. **20** (12): 1853-1864.

Mayo, L.R. and March, R.S. (1990). Air temperature and precipitation at Wolverine Glacier, Alaska: glacier growth in a warmer, wetter climate. Annals of Glaciology. **14**: 191-194.

Mayo, L.R., Meier, M.F., and Tangborn, W.V. (1972). A system to combine stratigraphic and annual mass balance systems: a contribution to the International Hydrological Decade. Journal of Glaciology. **11** (61): 3-14.

Miller, G.H., Bradley, R.S., and Andrews, J.T. (1975). The glaciation level and lowest equilibrium line altitude in the high Canadian Arctic: maps and climatic interpretation. Arctic and Alpine Research. **7** (2): 155-168.

Müller, B.S. Ed. (1961). Preliminary Report of 1959-60, Jacobsen-McGill Research Expedition to Axel Heiberg Island, Queen Elizabeth Islands. McGill University, Montreal. 219p.

Müller, F. (1962). Zonation in the accumulation area of the glaciers of Axel Heiberg Island, NWT, Canada. Journal of Glaciology. **4** (33): 302-311.

Müller, F. (1963). Englacial temperature measurements. Preliminary Report of 1961-62, Jacobsen-McGill Research Expedition to Axel Heiberg Island, Queen Elizabeth Islands. McGill University, Montreal. pp81-89.

Müller, F. (1976). On the thermal regime of a high Arctic valley glacier. Journal of Glaciology. **16** (74): 119-133.

Müller, F. and Keeler, C.M. (1969). Errors in short-term ablation measurements on melting ice surfaces. Journal of Glaciology. **8** (52): 91-105.

Müller, F. and Roskin-Sharlin, N. (1967). A high Arctic climate study on Axel Heiberg Island. Canadian Arctic Archipelago - Summer 1961. Meteorology No. 3, Axel Heiberg Island Research Reports. McGill University, Montreal. 82p.

Müller, F., Ohmura, A. and Braithwaite, R.J. (1977). The North Water Project (Canadian-Greenland Arctic). Polar Geography. **1** (1): 75-85.

Müller, F., Berger, P., Ito, H., Ohmura, A., Schroff, K., Steffen, K. (1980). Chapter 5: Glaciological observations in the North Water Area. In: North Water Project: Progress Report VI, 1 April to 31 December, 1979. Unpublished report. pp. 90-105.

Munro, D.S. (1991). On modelling surface meltwater discharge from Arctic and alpine glaciers. In: Northern Hydrology: Selected Perspectives. Proceedings of the Northern Hydrology Symposium, NHRI Symposium No. 6. Prowse, T.D. and Ommanney, C.S.L. (Ed.s), National Hydrology Research Institute, Environment Canada, Saskatoon, Saskatchewan, pp. 253-262.

Oerlemans, J. (1991). A model for the surface balance of ice masses: Part I. Alpine glaciers. Zeitschrift für Gletscherkunde und Glazialgeologie. **Band 27-28**: 63-83.

Ohata, T. (1989). The effect of glacier wind on local climate, turbulent heat fluxes, and ablation. Zeitschrift für Gletscherkunde und Glazialgeologie. **Band 25**, Heft 1: 49-68.

Ommanney, C.S.L. (1969). A study in glacier inventory. The ice masses of Axel Heiberg Island, Canadian Arctic Archipelago. Glaciology, No. 3, Axel Heiberg Island Research Reports. McGill University, Montreal. 105p.

Østrem, G. and Brugman, M. (1991). Glacier Mass-Balance Measurements. National Hydrology Research Institute, Science Report No. 4. 224p.

Østrem, G., Bridge, C.W. and Rannie, W.F. (1967). Glacio-hydrology, discharge and sediment transport in the Decade Glacier area, Baffin Island, NWT, Geografiska Annaler. **49A** (3): 268-282.

Palosuo, E. (1987). Ice layers and superimposition of ice on the summit and slope of Vestfonna, Svalbard. Geografiska Annaler **69A** (2): 289-296.

Paterson, W.S.B. (1969). The Meighen Ice Cap, Arctic Canada: accumulation, ablation and flow. Journal of Glaciology **8** (54): 341-351.

Paterson, W.S.B. (1981). The Physics of Glaciers. 2nd Edition, Oxford: Pergamon Press Ltd. 380p.

Sagar, R.B. (1964). Meteorological and glaciological observations on the Gilman Glacier, northern Ellesmere Island, 1961. Geographical Bulletin. **22**: 13-56.

Serreze, M.C. and Bradley, R.S. (1987). Radiation and cloud observations on a High Arctic plateau ice cap. Journal of Glaciology. **33** (114): 162-168.

Schlesinger, M.E. (1993). Model projections of CO_2 -induced equilibrium climate change. In: Climate and sea level change: observations, projections and implications. Warrick, R.A., Barrow, E.M. and Wigley, T.M.L. (Ed.s), Cambridge University Press, Cambridge, U.K. pp169-191.

Schytt, V. (1949). Re-freezing of the melt-water on the surface of glacier ice, Geografiska Annaler. **31** (1-4): 222-227.

Stenborg, T. (1970). Delay of runoff from a glacier basin. Geografiska Annaler. **52A** (1): 1-30.

Trabant, D.C. and Mayo, L.R. (1985). Estimation and effects of internal accumulation on five glaciers in Alaska. Annals of Glaciology. **6**: 112-117.

Unesco. (1970). Combined heat, ice and water balances at selected glacier basins, a guide to measurement and data compilation. Technical Papers in Hydrology. No. 5, Unesco, Paris, 20pp.

Van de Wal, R.S.W., Oerlemans, J. and Van der Hage, J.C. (1992). A study of ablation variations on the tongue of Hintereisferner, Austrian Alps. Journal of Glaciology. **38** (130): 319-323.

Wakahama, G., Kuroiwa, D., Hasemi, T. and Benson, C.S. (1976). Field observations and experimental and theoretical studies on the superimposed ice of McCall Glacier, Alaska Journal of Glaciology. **16** (74): 135-149.

Ward, W.H. and Orvig, S. (1952). The glaciological studies of the Baffin Island Expedition, 1950. Part 4: The heat exchange at the surface of the Barnes Ice Cap during the ablation period. Journal of Glaciology **2** (13): 158-168.

Weller, G. and Schwerdtfeger, P. (1970). Thermal properties and heat transfer processes of the snow of the central Antarctic plateau. IASH. **86**: 284-298.

Wendler, G., Trabant, D. and Benson, C. (1972). Hydrology of a partly glacier-covered Arctic watershed. In: The Role of Snow and Ice Hydrology. Proceedings of the Banff Symposia, September 1972. IAHS Vol. I. pp. 417-434.

Wharton, R.A. Jr., McKay, C.P., Simmons, G.M. Jr. and Parker, B.C. (1985). Cryoconite holes on glaciers. Bioscience. **35**(8): 499-503.

Woo, M.-K. (1976). Hydrology of a small Canadian high Arctic basin during the snowmelt period. Catena. **3** (2): 155-168.

Woo, M.-K. and Sauriol, J. (1980). Channel development in snow-filled valleys, Resolute, N.W.T., Canada. Geografiska Annaler. **62A** (1-2): 37-56.

Woo, M.-K., Heron, R., Marsh, P., and Steer, P. (1983). Comparison of weather station snowfall with winter snow accumulation in high Arctic basins. Atmosphere-Ocean. **21** (3): 312-325.

Young, G.J. (1990). Glacier Hydrology. In: Northern Hydrology: Canadian Perspectives. NHRI Science Report No. 1. Prowse, T.D. and Ommanney, C.S.L. (Ed.s), National Hydrological Research Institute, Environment Canada, Saskatoon, Saskatchewan, pp. 135-162.

Young, G.J. and Ommanney, C.S.L. (1984). Canadian glacier hydrology and mass balance studies; a history of accomplishments and recommendations for future work. Geografiska Annaler. **66A** (3): 169-182.

SELECTED REFERENCES NOT CITED

Ambach, W. (1974). The influence of cloudiness on the net radiation balance of a snow surface with high albedo. Journal of Glaciology. **13** (67): 73-84.

Bradley, R.S. (1975). Equilibrium-line altitudes, mass balance, and July freezing-level heights in the Canadian high Arctic. Journal of Glaciology. **14** (71): 267-274.

Bradley, R.S. and England, J. (1978a). Recent climatic fluctuations in the Canadian high Arctic and their significance for glaciology. Arctic and Alpine Research. **10** (4): 715-731.

Bradley, R.S. and England, J. (1978b). Volcanic dust influence on glacier mass balance at high latitudes. Nature. **271**: 736-738.

Braithwaite, R.J. (1984). Calculation of degree-days for glacier-climate research. Zeitschrift für Gletscherkunde und Glazialgeologie. **Band 20**, S. 1-8.

Braithwaite, R.J. (1986). Assessment of mass balance variations within a sparse stake network, Qamanârssûp sermia, west Greenland. Journal of Glaciology. **32** (110): 50-53.

Braithwaite, R.J. and Olesen, O.B. (1984). Ice ablation in west Greenland in relation to air temperature and global radiation. Zeitschrift für Gletscherkunde und Glazialgeologie. **Band 20**, S. 155-168.

Braithwaite, R.J. and Olesen, O.B. (1988). Winter accumulation reduces summer ablation on Nordbogletscher, South Greenland. Zeitschrift für Gletscherkunde und Glazialgeologie. **Band 24**, S. 21-30.

Braithwaite, R.J. and Olesen, O.B. (1989). Detection of climate signal by inter-stake correlations of annual ablation data, Qamanârssûp sermia, west Greenland. Journal of Glaciology. **35** (120): 253-259.

Braithwaite, R.J. and Olesen, O.B. (1990). A simple energy-balance model to calculate ice ablation at the margin of the Greenland ice sheet. Journal of Glaciology. **36** (123): 222-228.

Clarke, G.K.C. (1987). A short history of scientific investigations on glaciers. Journal of Glaciology. **Special Issue**. 4-24.

Dubreuil, M.-A. and Woo, M.-K. (1984). Problems of determining snow albedo for the high Arctic. Atmosphere-Ocean. **22** (3): 379-386.

Etzelmüller, B., Vatne, G., Odegard, R.S., and Sollid, J.L. (1993). Dynamics of two subpolar valley glaciers - Erikbreen and Hannabreen, Liefdefjorden, northern Spitsbergen. Geografiska Annaler. **75A** (1-2): 41-54.

Föhn, P.M.B. and Meister, R. (1983). Distribution of snow drifts on ridge slopes: measurements and theoretical approximations. Annals of Glaciology. **4**: 52-57.

Hagen, J.O. and Liestøl, O. (19). Long-term glacier mass-balance investigations in Svalbard, 1950-1988. Annals of Glaciology. **14** : 102-106.

Hall, D.K., Ormsby, J.P., Bindschadler, R.A. and Siddalingaiah, H. (1987). Characterization of snow and ice reflectance zones on glaciers using Landsat Thematic Mapper data. Annals of Glaciology. **9** : 104-108.

Hattersley-Smith, G.F. (1963). Climatic inferences from firn studies in northern Ellesmere Island. Geografiska Annaler. **45** (2-3): 139-51.

Hattersley-Smith, G.F. (1969). Glacial features of Tanquary Fiord and adjoining areas of northern Ellesmere Island, N.W.T. Journal of Glaciology. **8** (52): 23-50.

Hooke, R.L. (1976). Near-surface temperatures in the superimposed ice zone and lower part of the soaked zone of polar ice sheets. Journal of Glaciology. **16** (74): 302-304.

Hooke, R.L., Gould, J.E. and Brzozowski, J. (1983). Near-surface temperatures near and below the equilibrium line on polar and subpolar glaciers. Zeitschrift für Gletscherkunde und Glazialgeologie. **Band 19**, Heft 1: S. 1-25.

Hubley, R.C. (1955). Measurements of diurnal variations in snow albedo on Lemon Creek Glacier, Alaska. Journal of Glaciology. **2**: 560-563.

Koerner, R.M. (1977). Ice thickness measurements and their implications with respect to past and present ice volumes in the Canadian high Arctic ice caps. Canadian Journal of Earth Sciences. **14** (12): 2697-2705.

Koerner, R.M. (1979). Accumulation, ablation, and oxygen isotope variations on the Queen Elizabeth Islands ice caps, Canada. Journal of Glaciology. **22** (86): 25-41.

LaChapelle, E.R. (1959). Errors in ablation measurements from settlement and sub-surface melting. Journal of Glaciology. **3** (26): 458-467.

Letréguilly, A. and Reynaud, L. (1989). Spatial patterns of mass-balance fluctuations of North American glaciers. Journal of Glaciology. **35** (120): 63-68.

Meier, M.F. (1984). Contribution of small glaciers to global sea level. Science. **226**: 1418-1421.

McGuffie, K. and Henderson-Sellers, A. (1985). The diurnal hysteresis of snow albedo. Journal of Glaciology. **31** (108): 188-189.

Oerlemans, J., Van de Wal, R.S. and Conrads, L.A. (1992). A model for the surface balance of ice masses: part II. Application to the Greenland Ice Sheet. Zeitschrift für Gletscherkunde und Glazialgeologie. **Band 27/28**, S. 85-96.

Ohmura, A., Kasser, P. and Funk, M. (1992). Climate at the equilibrium line of glaciers. Journal of Glaciology. **38** (130): 397-411.

Pffefer, W.T., Illangasekare, T.H., and Meier, M.F. (1990). Analysis and modelling of melt-water refreezing in dry snow. Journal of Glaciology. **36** (123): 238-246.

Rogerson, R.J. (1986). Mass balance of four cirque glaciers in the Torngat Mountains of northern Labrador, Canada. Journal of Glaciology. **32** (111): 208-218.

Röthlisberger, H.B. and Lang, H. (1987). Glacial Hydrology. In: Glacio-Fluvial Sediment Transfer: an Alpine Perspective. Gurnell, A.M. and Clark, M.J. (Ed.s), John Wiley and Sons Ltd., Toronto. pp207-284.

Sagar, R.B. (1966). Glaciological and climatological studies on the Barnes Ice Cap, 1962-64. Geographical Bulletin. **8** (1): 3-47.

Spector, A. (1966). A gravity survey of the Melville Island ice caps. Journal of Glaciology. **6** (45): 393-400.

Tangborn, W.V., Krimmel, R.M. and Meier, M.F. (1972). A comparison of glacier mass balance by glaciological, hydrological and mapping methods, South Cascade Glacier, Washington. In: Snow and Ice-Symposium-Neiges et Glaces. Proceedings of the Moscow Symposium, August 1971. IAHS-AISH publ. no. 104. pp. 185-195.

Walker, E.R. and Lake, R.A. Runoff in the Canadian Arctic Archipelago. In: Climate of the Arctic. Weller, G. and Bowling, S.A. (Ed.s). Proceedings of the 24th Alaska Science Conference, Fairbanks, Alaska, August 15-17, 1973. pp. 374-378.

Ward, W.H. and Baird, P.D. (1954). Studies in glacier physics on the Penny Ice Cap, Baffin Island, 1953. Part 1: a description of the Penny Ice Cap, its accumulation and ablation. Journal of Glaciology **2** (15): 342-356.

Weaver, R.L. (1975). "Boas" glacier (Baffin Island, N.W.T., Canada). Mass balance for the five budget years 1969-1974. Arctic and Alpine Research. **7** (3): 277-284.

Wendler, G. and Ishikawa, N. (1973). Experimental study of the amount of ice melt using three different methods: a contribution to the international hydrological decade. Journal of Glaciology. **12** (66): 399-410.

Wendler, G. and Ishikawa, N. (1974a). The effect of slope, exposure and mountain screening on the solar radiation of McCall Glacier, Alaska: a contribution to the International Hydrological Decade. Journal of Glaciology. **13** (68): 213-226.

Wendler, G. and Ishikawa, N. (1974b). The combined heat, ice and water balance of McCall Glacier, Alaska: A contribution to the International Hydrological Decade. Journal of Glaciology. **13** (68): 227-241.

Wendler, G. and Kelley, J. (1988). On the albedo of snow in Antarctica: A contribution to I.A.G.O. Journal of Glaciology. **34** (116): 19-25.

Wendler, G. and Weller, G. (1974). A heat-balance study on McCall Glacier, Brooks Range, Alaska: a contribution to the International Hydrological Decade. Journal of Glaciology. **13** (67): 13-26.

Wendler, G., Fahl, C., and Corbin, S. (1972). Mass balance studies on McCall Glacier, Brooks Range, Alaska. Arctic and Alpine Research. **4** (3): 211-222.

Williams, R.S., Hall, D.K. and Benson, C.S. (1991). Analysis of glacier facies using satellite techniques. Journal of Glaciology. **37** (125): 120-128.

APPENDIX A

ALBEDO ACCURACY AND VARIABILITY

The Accuracy and Natural Variation of Albedo Measurements

On Quviagivaa Glacier, albedo measurements were made at ablation stations 1-10 on alternate days using a portable solarimeter, mounted on a 75cm long wooden rod, from which voltage was read using a multimeter. The solarimeter was leveled using two spirit levels attached to the solarimeter, and was held approximately 60cm from the user and 120cm off the ground, pointing in the direction of the sun so as to avoid the shadow of the user. Measurements were always taken in the late morning, between 0900h and 1200h when solar elevations were always greater than 15°, thereby avoiding possible "cosine errors" due to low solar elevations (Dirmhirn and Eaton, 1975).

On a cloud-free day (July 9, 1993), several albedo measurements were made on the snout of the glacier to check the reliability of measurements and the variability of albedo on different snow and ice types in the late morning (0930-1000h) and in the afternoon (1645-1700h). The five measurements sites and the measured albedos are listed in the table below.

July 9 albedo test

Site	Surface Type	Morning Albedo	Afternoon Albedo	Difference in Albedo
1	patch of rocks surrounded by dirty ice at glacier margin	0.34	0.32	-0.02
2	rippled, melting snow	0.50	0.64	+0.14
3	newly-formed and exposed, wet superimposed ice	0.28	0.44	+0.16
4	slushy, ablating superimposed ice	0.40	0.61	+0.21
5	porous, ablating glacier ice	0.34	0.55	+0.21

At Sites 1, 2, and 3, several tests were performed to determine the accuracy of the measurement techniques. At Site 1, the instrument was lowered

to 60cm over the surface (60cm lower than using normal measurement techniques). Lowering the instrument meant that it sensed more of the dark rock surface and less of the ice, thereby reducing the albedo by 4%. Raising the solarimeter by 40cm allowed the instrument to sense proportionally more ice, thereby raising the albedo by 4%. At Site 2, lowering and raising the instrument had no effect on the readings, likely due to the homogeneity of the surface. Although the instrument is equipped with a spirit level, an experiment was carried out to determine the potential errors if the solarimeter was pointing slightly into or away from the sun. At Site 1, pointing the solarimeter into the sun caused a 2% decrease in albedo, while pointing the instrument away from the sun caused a 2% increase in surface albedo. It is likely that the error due to leveling during normal measurements was insignificant, as the instrument was always carefully leveled before a reading was taken, and the maximum error based on the tests described above should be considered ±4%.

As shown in the above table, albedo measurements made in the morning and the evening were highest on the melting snow. The next highest values were measured on melting superimposed ice, and porous, ablating glacier ice. In the morning, the rocky margin of the glacier ice had the same albedo as the glacier ice, and the lowest albedo was measured on the newly exposed, wet superimposed ice. These albedos approximate snow and ice albedos measured in other glacier studies (Wendler and Weller, 1974). Although the solar elevation was identical to that in the morning, all albedos increased markedly in the afternoon, except for that measured on the rocky margin of the glacier, which dropped by 2%. Albedo values for the melting snow, newly-exposed superimposed ice, melting superimposed ice, and melting glacier ice increased by 14%, 16%, 21%, and 21% respectively. This finding does not coincide with the results of other researchers working on snow and ice.

Several researchers have shown that the albedo of snow and ice surfaces varies during the course of one day (Hubley, 1955; Dirmhirn and Eaton, 1975; Dubreuil and Woo, 1984; McGuffie and Henderson-Sellers, 1984; Wendler and Kelley, 1988). In a study of snow albedo at Resolute, N.W.T., Dubreuil and Woo (1984) found that the albedo of snow varied by about 20% over one day. They determined these variations to solar elevation (increasing albedo with decreasing solar elevation), snow metamorphism during the day (albedo usually decreasing due to larger snow grains), and instrument error (albedo measurements unreliable at low solar elevations due to the deviation of the solarimeter response from the cosine law). Since the measurements at Quviagivaa Glacier were taken at relatively high and equal solar elevations (3.5-4.0 hours both before and after solar noon), the cause of the albedo variations must be due to changes in the physical characteristics of the glacier surface.

Several researchers note that albedos on melting snow and ice surfaces will be lower in the afternoon than in the morning at identical solar elevations due to the metamorphism of the surface and its increased roughness (Dirmhirn and Eaton, 1975; McGuffie and Henderson-Sellers, 1985). Hubley (1955) states that the maximum diurnal variation of albedo should occur over smooth, melting glacier ice, although he found that afternoon albedos were lower due to increased surface roughness. Keeler (1964) working on the Sverdrup Glacier, Devon Island, found that on clear days (i.e. July 21, 1963) the surface albedo varied only by 2-3% between mid-morning and mid-afternoon readings.

The most likely cause of the marked increase in albedo from morning to afternoon is the development of a weathering crust. Temperatures were well above zero during the night preceding the measurements, and during the morning of July 9, strong melt was occurring. Water was flowing over the surface of the newly-exposed superimposed ice, giving the very low albedo. The ablating

glacier ice and superimposed ice had slightly lower albedos, as they were saturated within several cms of the surface. The melting snow was also very wet, and melting rapidly. July 9 was completely sunny, and under such high radiation conditions, internal melt occurs within ice, creating a "weathering rind" (Müller and Keeler, 1969). This weathering rind has a density <0.9g cm^{-3}, can be up to 20cm deep, and is white due to the lowering of the water table within the glacier ice surface (Fig. A1). In addition, during radiation melt, dust particles melt down into the ice, creating cryoconite holes, which makes the surface whiter. This process likely accounts for the 21% increase in albedo. Van de Wal et al. (1992) observed this phenomena on the snout of Hintereisferner, where, during a four day period in July, a white crusty layer developed, and albedos were lowered by up to 20%. In West Greenland, Braithwaite and Olesen (1984, 1990) observed that the ice appears whiter when there is a deep "weathering rind" and darker blue on overcast or stormy days. When fresh, superimposed ice is exposed to solar radiation, melting occurs along the crystal boundaries, and a white, icy, slush results. This phenomena was observed across the entire surface of Quviagivaa Glacier as superimposed ice was exposed and began to melt, and likely accounts for the 16% increase in albedo at Site 3 on July 9. An increase in the thickness of melting ice and a decrease in the water content at the surface at Site 4 likely accounts for the large increase in albedo, while the 14% increase measured at Site 2 is likely due to draining of water from the surface, and the accumulation of slush flows of melting glacier ice crystals.

Higher snow and ice albedos in the afternoon as compared with albedos at equal solar elevations in the morning likely occurs on days when the weathering crust is developing. If melting is occurring through the night due to sensible heat, this will likely degrade the weathering rind somewhat, thereby causing the water table to rise nearer to the surface, giving lower albedos in the

Figure A1. Photograph of a loose "weathering rind" glacier ice surface and the much darker, saturated ice just beneath, Quviagivaa Glacier, June 29, 1993.

morning. As the weathering rind is deepened during the day due to radiation melting, albedos should increase, as was observed on Quviagivaa Glacier on July 9.

References quoted in Appendix A

Braithwaite, R.J. and Olesen, O.B. (1984). Ice ablation in west Greenland in relation to air temperature and global radiation. Zeitschrift für Gletscherkunde und Glazialgeologie. **Band 20**, S. 155-168.

Braithwaite, R.J. and Olesen, O.B. (1990). A simple energy-balance model to calculate ice ablation at the margin of the Greenland ice sheet. Journal of Glaciology. **36** (123): 222-228.

Dirmhirn, I. and Eaton, F.D. (1975). Some characteristics of the albedo of snow. Journal of Applied Meteorology. **14**: 375-379.

Dubreuil, M.-A. and Woo, M.-K. (1984). Problems of determining snow albedo for the high Arctic. Atmosphere-Ocean. **22** (3): 379-386.

Hubley, R.C. (1955). Measurements of diurnal variations in snow albedo on Lemon Creek Glacier, Alaska. Journal of Glaciology. **2**: 560-563.

Keeler, C.M. (1964). Relationship between climate, ablation and runoff on the Sverdrup Glacier, 1963, Devon Island, N.W.T. Arctic Institute of North America, Research Paper No. 27. 80p.

McGuffie, K. and Henderson-Sellers, A. (1985). The diurnal hysteresis of snow albedo. Journal of Glaciology. **31** (108): 188-189.

Müller, F. and Keeler, C.M. (1969). Errors in short-term ablation measurements on melting ice surfaces. Journal of Glaciology. **8** (52): 91-105.

Van de Wal, R.S.W., Oerlemans, J. and Van der Hage, J.C. (1992). A study of ablation variations on the tongue of Hintereisferner, Austrian Alps. Journal of Glaciology. **38** (130): 319-323.

Wendler, G. and Kelley, J. (1988). On the albedo of snow in Antarctica: A contribution to I.A.G.O. Journal of Glaciology. **34** (116): 19-25.

Wendler, G. and Weller, G. (1974). A heat-balance study on McCall Glacier, Brooks Range, Alaska: a contribution to the International Hydrological Decade. Journal of Glaciology. **13** (67): 13-26.

APPENDIX B

GLACIER METEOROLOGICAL STATION DATA

Average Daily Meteorological Data from the Glacier Meteorological Station, Quviagivaa Glacier, 875m a.s.l., 1993

Date	Air Temp. (°C)	MDD (°C)	K down (W/m2)	KDD (W/m2)	Net Rad. (W/m2)	NRD (W/m2)	Wind Speed (m/s)	Wind Dir.	Glacier Albedo
30-May	-3.5	1	316	7579	-18.2	212			
31-May	-4.2	3	326	7820	-10.7	293			
1-Jun	-2.5	15	340	8163	-17.7	304			
2-Jun	-5.3	0	305	7320	-33.8	98			
3-Jun	-5.4	0	349	8368	-37.4	100	2.1	NE-E	
4-Jun	-4.3	5	340	8158	-24.8	226	0.9	NE-E	
5-Jun	-3.2	6	350	8396	-23.4	256	1	E-SE	
6-Jun	-2.2	5	305	7311	-5.4	306	0.8	E-SE	
7-Jun	-1	7	192	4605	-0.3	124	0.4	NE-E	
8-Jun	-0.7	11	275	6599	-4.6	189	1.2	NE-E	
9-Jun	-2.5	3	346	8299	-21.2	289	2.7	NE-E	
10-Jun	-2.6	0	228	5460	-19.1	59	5.4	NE-E	
11-Jun	-2.1	0	317	7596	-20.9	127	5.7	NE-E	
12-Jun	1.7	44	299	7185	-9.7	208	2.9	NE-E	
13-Jun	0.9	22	162	3898	-1.8	103	2.2	NE-E	
14-Jun	0.2	14	244	5860	6.4	384	1.6	NE-E	0.68
15-Jun	1	36	239	5743	8.2	298	0.8	NE-E	
16-Jun	0.2	11	245	5887	5.8	325	1.2	NE-E	
17-Jun	-0.4	5	253	6070	12.1	395	3.4	NE-E	
18-Jun	0	12	297	7134	-2.7	279	3.3	E-SE	0.67
19-Jun	1.8	52	343	8221	-3.4	491	1.7	NE-E	
20-Jun	1.8	47	215	5171	7.6	410	1.2	E-SE	0.61
21-Jun	0.4	11	235	5639	12	464	3.6	NE-E	
22-Jun	2.1	54	276	6635	6.6	417	1.1	NE-E	0.61
23-Jun	2.1	51	243	5822	17.2	570	2.9	NE-E	
24-Jun	-0.6	1	199	4768	5.6	136	2.2	E-SE	0.69
25-Jun	-2.1	0	268	6423	-25.4	27	1.4	SE-S	
26-Jun	-1.5	0	178	4261	2.3	124	1.3	SE-S	0.73
27-Jun	0.4	24	143	3432	1.2	97	0.8	SE-S	
28-Jun	2.1	58	178	4277	11	403	0.6	E-SE	0.61
29-Jun	4.1	100	311	7467	13.8	732	0.8	E-SE	
30-Jun	5.1	123	241	5777	29.8	844	1.4	W-NW	0.44
1-Jul	3.8	92	168	4042	71	1704	1.2	E-SE	
2-Jul	-1	0	172	4125	56.7	1360	1.1	W-NW	
3-Jul	0.9	27	166	3973	*48.9*	*1174*	1.1	W-NW	
4-Jul	3.8	90	284	6806	*52.7*	*1379*	0.8	E-SE	0.5
5-Jul	4.9	117	305	7313	*17*	*604*	0.8	E-SE	
6-Jul	3.4	82	199	4771	38.9	1022	1.2	E-SE	0.48
7-Jul	4.9	119	264	6347	*27*	*811*	1.4	E-SE	
8-Jul	5.8	138	*272*	*6520*	*41.4*	*1137*	1.7	NE-E	0.41
9-Jul	7.9	190	*301*	*7233*	*51.9*	*1347*	1.5	E-SE	

10-Jul	6.6	158	*308*	*7399*	*90.6*	*2277*	2.4	E-SE	0 42
11-Jul	4.2	100	147	3537	50.5	1400	3.1	E-SE	
12-Jul	4	97	155	3718	*73.4*	*1762*	1.7	E-SE	0.39
13-Jul	5.3	127	263	6322	*84.6*	*2138*	2.1	NE-E	
14-Jul	5	121	233	5585	*76.9*	*1936*	1.3	E-SE	0.38
15-Jul	6.3	152	265	6362	*73.3*	*1787*	1.7	W-NW	
16-Jul	2.9	69	*130*	*3112*	*72.4*	*1743*	0.8	E-SE	0.47
17-Jul	4.1	99	*257*	*6162*	82.6	2006	2.5	W-NW	
18-Jul	3.4	81	147	3537	68.8	1696	1.2	E-SE	
19-Jul	3.3	80	118	2842	79.1	1898	1.9	SW-W	0.38
20-Jul	1.9	46	51	1215	52.5	1260	1	SW-W	
21-Jul	1.7	41	70	1683	63	1511	0.6	E-SE	
22-Jul	2.5	59	104	2486	60 8	1464	0.7	E-SE	
23-Jul	3.2	77	125	3001	75.6	1813	0.8	E-SE	
24-Jul	2.8	66	122	2932	55.9	1347	0.6	SE-S	0.37
25-Jul	2.6	63	152	3653	67.7	1690	0.6	NE-E	
26-Jul	2.6	62	124	2970	69.9	1677	0.8	E-SE	0.4
27-Jul	2.2	52	91	2179	52.4	1258	0.8	E-SE	
28-Jul	2.9	70	122	2920	61	1464	0 4	NE-E	0.39
29-Jul	2.7	65	158	3795	54.4	1378	0.7	NE-E	
30-Jul	4.3	103	203	4862	74.4	1897	1.1	E-SE	0.41
31-Jul	6	143	173	4155	73.5	1811	1.5	SE-S	
1-Aug	3.9	93	149	3573	81.7	2049	0.8	E-SE	0.31
2-Aug	1.3	32	58	1395	44.1	1059	0.3	NE-E	
3-Aug	-0.1	2	72	1739	20.2	486	0.7	SE-S	0.57
4-Aug	-2.8	0	84	2027	4.2	104	1.7	SW-W	
5-Aug	-5.5	0	134	3220	-2.3	38	1.1	SE-S	
6-Aug	-4.9	0	119	2851	-6.2	5	3.3	E-SE	
7-Aug	-5.9	0	149	3567	4.9	226	1.7	S-SW	
8-Aug	-4.5	0	129	3096	-8.7	1	3.6	E-SE	
9-Aug	-4.3	0	115	2749	-5.9	2	5.2	N-NE	
10-Aug	-4.6	0	124	2987	-5.8	0	2.3	SW-W	

Notes for previous table:

Air Temp., Net Rad., and Wind Speed are average values, taken from hourly measurements.
MDD is Melting Degree Days, the sum of all positive hourly temperatures .
K down is incoming shortwave radiation.
KDD is K Down Days, the sum of all hourly incoming shortwave radiation values.
NRD is Net Radiation Days, the sum of all positive hourly net radiation values.
Wind Speed is an average value from hourly values.
Wind Direction is the predominant wind direction for the day.
Glacier Albedo is the average albedo using measurements from 6-12 ablation stations.
Italicized values are estimated due to missing data.

APPENDIX C

GLACIER METEOROLOGICAL STATION DATA:
WIND DIRECTION FREQUENCY BY SECTOR

Glacier Meteorological Station Wind Direction Frequency by Sector, 1993

		Down-glacier winds				Up-glacier winds			
Date	N-NE	NE-E	E-SE	SE-S	S-SW	SW-W	W-NW	NW-N	% windy
3-Jun	0%	46%	38%	14%	1%	1%	0%	0%	100.00%
4-Jun	2%	36%	36%	5%	11%	7%	2%	0%	99.99%
5-Jun	3%	31%	33%	29%	4%	1%	0%	0%	99.99%
6-Jun	1%	11%	48%	8%	4%	17%	10%	1%	99.98%
7-Jun	11%	24%	12%	11%	13%	20%	8%	1%	99.99%
8-Jun	11%	59%	21%	5%	1%	1%	1%	1%	99.98%
9-Jun	4%	77%	18%	0%	0%	0%	0%	0%	100.00%
10-Jun	2%	74%	23%	0%	0%	0%	0%	0%	100 00%
11-Jun	6%	90%	4%	0%	0%	0%	0%	0%	100.00%
12-Jun	8%	68%	10%	3%	1%	1%	7%	3%	100 00%
13-Jun	11%	73%	7%	0%	8%	1%	0%	1%	99.85%
14-Jun	5%	38%	17%	5%	3%	11%	18%	4%	100.35%
15-Jun	5%	31%	11%	5%	6%	28%	13%	1%	99.99%
16-Jun	3%	63%	21%	7%	2%	3%	0%	1%	99.87%
17-Jun	9%	58%	22%	7%	3%	1%	0%	0%	99.99%
18-Jun	1%	17%	67%	15%	0%	0%	0%	0%	99.98%
19-Jun	19%	35%	19%	4%	3%	4%	11%	6%	99.86%
20-Jun	4%	24%	34%	22%	10%	5%	0%	1%	99.99%
21-Jun	1%	49%	43%	7%	1%	0%	0%	0%	99.98%
22-Jun	5%	48%	37%	6%	1%	1%	1%	1%	99.72%
23-Jun	4%	68%	24%	3%	0%	0%	0%	1%	100.13%
24-Jun	1%	22%	37%	28%	11%	1%	0%	0%	99.98%
25-Jun	1%	2%	14%	56%	22%	4%	0%	0%	99.97%
26-Jun	0%	0%	20%	58%	13%	7%	0%	0%	100.00%
27-Jun	4%	4%	26%	28%	22%	12%	3%	1%	99.98%
28-Jun	8%	23%	50%	10%	4%	2%	2%	1%	99.85%
29-Jun	2%	19%	43%	5%	7%	18%	5%	1%	100.00%
30-Jun	2%	21%	19%	5%	5%	7%	38%	3%	99.98%
1-Jul	1%	19%	55%	3%	6%	9%	7%	0%	99.98%
2-Jul	2%	5%	2%	1%	4%	37%	47%	2%	99.99%
3-Jul	0%	24%	16%	4%	11%	17%	27%	0%	99.99%
4-Jul	7%	18%	34%	13%	1%	2%	16%	9%	99.85%
5-Jul	10%	20%	41%	11%	4%	6%	5%	4%	99.97%
6-Jul	0%	11%	68%	20%	0%	0%	0%	0%	99 99%
7-Jul	2%	26%	59%	14%	0%	0%	0%	0%	99.99%
8-Jul	2%	76%	22%	0%	0%	0%	0%	0%	100.00%
9-Jul	6%	43%	50%	1%	0%	1%	0%	0%	99.98%
10-Jul	7%	32%	60%	1%	0%	0%	0%	0%	100.01%
11-Jul	0%	4%	90%	5%	0%	0%	0%	0%	100.00%
12-Jul	4%	44%	46%	4%	1%	0%	0%	1%	99 98%
13-Jul	2%	70%	26%	0%	1%	1%	0%	0%	100.00%
14-Jul	2%	32%	37%	1%	0%	1%	23%	4%	100.00%
15-Jul	2%	12%	5%	2%	3%	18%	52%	6%	99.98%
16-Jul	2%	42%	47%	4%	2%	1%	2%	1%	100.00%
17-Jul	0%	85%	15%	0%	0%	0%	0%	0%	100.00%

Date	N-NE	NE-E	E-SE	SE-S	S-SW	SW-W	W-NW	NW-N	% windy
18-Jul	1%	**32%**	**35%**	2%	8%	18%	2%	1%	100.00%
19-Jul	5%	**16%**	**4%**	1%	7%	65%	1%	1%	99.98%
20-Jul	1%	**14%**	**24%**	0%	3%	47%	10%	0%	100.00%
21-Jul	3%	**29%**	**58%**	2%	0%	4%	2%	1%	99.99%
22-Jul	9%	**26%**	**40%**	15%	3%	2%	1%	3%	99.98%
23-Jul	4%	**9%**	**26%**	21%	11%	22%	5%	3%	99.98%
24-Jul	5%	**11%**	**18%**	29%	12%	10%	11%	4%	100.00%
25-Jul	11%	**42%**	**27%**	12%	4%	2%	1%	1%	99.84%
26-Jul	4%	**26%**	**57%**	8%	1%	1%	2%	2%	99.74%
27-Jul	1%	**39%**	**54%**	2%	1%	1%	3%	0%	99.85%
28-Jul	10%	**32%**	**25%**	11%	4%	6%	8%	3%	99.71%
29-Jul	4%	**50%**	**35%**	3%	2%	2%	2%	1%	99.86%
30-Jul	3%	**23%**	**43%**	25%	4%	1%	1%	0%	99.98%
31-Jul	3%	**5%**	**20%**	36%	26%	7%	3%	1%	99.85%
1-Aug	6%	**29%**	**37%**	13%	5%	8%	1%	1%	99.98%
2-Aug	9%	**42%**	**16%**	4%	3%	9%	11%	6%	99.99%
3-Aug	2%	**5%**	**25%**	32%	14%	11%	9%	2%	100.01%
4-Aug	0%	**0%**	**0%**	1%	6%	53%	38%	1%	100.00%
5-Aug	1%	**11%**	**22%**	27%	15%	16%	8%	0%	100.00%
6-Aug	0%	**22%**	**41%**	10%	11%	16%	0%	0%	99.98%
7-Aug	1%	**0%**	**6%**	22%	40%	28%	2%	0%	99.98%
8-Aug	0%	**8%**	**49%**	41%	1%	0%	0%	0%	100.00%
9-Aug	1%	**76%**	**23%**	0%	0%	0%	0%	0%	100.00%
10-Aug	0%	**5%**	**13%**	6%	31%	44%	1%	0%	100.00%
Average	3.80%	**32.27%**	**30.77%**	10.92%	5.86%	8.93%	6.11%	1.29%	99.97%

APPENDIX D

VALLEY METEOROLOGICAL STATION DATA

Average Daily Meteorological Data from the Valley Meteorological Station, 230m a.s.l., 1993

Date	Air Temp. (°C)	MDD (°C)	K down (W/m2)	KDD (W/m2)	Wind Speed (m/s)	Wind Direction
4-Jun	0.8	25	307	7377	0.8	S-SW
5-Jun	1.2	35	329	7900	1.1	SW-W
6-Jun	2	48	320	7681	1.1	SW-W
7-Jun	2.1	50	141	3395	1.9	N-NE
8-Jun	3.1	74	235	5637	4.3	N-NE
9-Jun	4	96	329	7905	3.3	N-NE
10-Jun	2.8	66	144	3448	5.2	NE-N
11-Jun	4	95	334	8015	8.3	NE-N
12-Jun	6.6	158	279	6685	4.3	NE-N
13-Jun	3.1	75	148	3547	2.6	N-NE
14-Jun	3	73	237	5698	3.1	N-NE
15-Jun	3.6	87	254	6103	4.3	N-NE
16-Jun	3.7	88	149	3577	0.8	S-SW
17-Jun	5	120	221	5293	3.6	NE-N
18-Jun	5.7	136	281	6749	4.2	SE-S
19-Jun	6.5	157	331	7946	4.3	NE-N
20-Jun	7	167	267	6407	3.1	N-NE
21-Jun	6.5	155	212	5085	2.7	SE-S
22-Jun	7.3	175	271	6514	1.2	NE-E
23-Jun	8.4	202	264	6346	3.7	NE-E
24-Jun	3.6	86	123	2959	3.3	S-SW
25-Jun	2	49	202	4848	6.1	S-SW
26-Jun	3.1	75	174	4178	3	S-SW
27-Jun	3.7	88	140	3363	0.7	W-NW
28-Jun	7.2	172	196	4694	1	N-NE
29-Jun	9.9	238	304	7286	1.3	W-NW
30-Jun	11.9	287	250	5991	1.1	N-NE
1-Jul	11	265	165	3958	1.6	NW-N
2-Jul	3	73	184	4424	1.8	NW-N
3-Jul	5.2	126	155	3712	2.3	N-NE
4-Jul	9.1	218	267	6401	4.2	N-NE
5-Jul	10.9	262	310	7445	2.6	N-NE
6-Jul	12.7	306	334	8010	1.5	W-NW
7-Jul	13.4	322	272	6539	1.3	W-NW
8-Jul	14.4	345	293	7038	2	E-SE
9-Jul	14.8	356	314	7530	2.4	NE-E
10-Jul	14.6	350	316	7576	3.1	NE-E
11-Jul	12.1	291	170	4073	2.9	SE-S
12-Jul	10.1	243	176	4233	1.5	W-NW
13-Jul	13.6	327	278	6671	2.5	N-NE

14-Jul	13.3	319	282	6757	1.6	W-NW
15-Jul	13.4	322	270	6468	4.2	NW-N
16-Jul	8.9	214	159	3810	1.7	W-NW
17-Jul	9.2	221	242	5807	2.5	N-NE
18-Jul	11.3	272	195	4689	1.4	W-NW
19-Jul	9.3	224	158	3783	1.6	SW-S
20-Jul	5.3	126	49	1175	0.6	NW-N
21-Jul	6.1	146	100	2407	0.3	NW-N
22-Jul	7	168	97	2325	0.6	NW-N
23-Jul	8.4	202	136	3263	3.8	W-NW
24-Jul	7.2	172	177	4254	1.7	W-NW
25-Jul	8	192	201	4813	0.4	NW-N
26-Jul	9.4	226	148	3555	0.8	E-SE
27-Jul	9.3	223	111	2670	0.4	E-SE
28-Jul	6.6	158	162	3883	0.4	NW-N
29-Jul	6.3	150	174	4168	0.2	NW-N
30-Jul	8.6	207	217	5197	0.3	NW-N
31-Jul	9.9	238	177	4246	4	W-NW
1-Aug	9.6	231	105	2520	2	W-NW
2-Aug	4.7	113	66	1585	0.2	NW-N
3-Aug	2	48	69	1647	0.8	NW-N
4-Aug	-0.4	8	44	1064	1.2	NE-E
5-Aug	-1.6	0	90	2165	4.3	W-NW
6-Aug	-1.4	0	97	2338	6.4	W-NW
7-Aug	-2.7	0	151	3612	10.5	W-NW
8-Aug	0	19	90	2157	6.6	SW-S
9-Aug	0.4	13	106	2539	5.8	SE-S
10-Aug	-1.7	0	91	2181	5.7	W-NW

Notes:

Air Temp., K down, and Wind Speed are average values from hourly measurements.
MDD is Melting Degree Days, the sum of all hourly temperatures above 0°C.
K down is incoming shortwave radiation.
KDD is K Down Days, the sum of all hourly incoming shortwave radiation values.
Wind Direction is the predominant wind direction for the day.

APPENDIX E

AIR TEMPERATURE LAPSE RATES FOR FOUR WEATHER TYPES

Air Temperature lapse rates calculated from the Glacier and Valley meteorological stations for four different weather types, 1993

Calm and Clear

Date	Lapse Rate (°C/m)	Stn. Dev. (°C/m)	MDD (°C)	Glacier Temp. (°C)	Valley Temp. (°C)	Valley-Glacer (°C)
5-Jun	0.0077	0.0051	5	-4.3	0.8	5.1
6-Jun	0.0068	0.0037	6	-3.2	1.2	4.5
30-Jun	0.0089	0.0028	100	4.1	9.9	5.8
05-Jul	0.0081	0.0010	90	3.8	9.1	5.3
06-Jul	0.0092	0.0025	117	4.9	10.9	6.0
Average	*0.0082*	*0.0030*	*64*	*1.1*	*6.4*	*5 3*
Early Melt	*0.0073*	*0.0044*	*5*	*-3.7*	*1 0*	*4 8*
Main Melt	*0.0088*	*0.0021*	*102*	*4.3*	*10.0*	*6.0*

Calm and Cloudy

Date	Lapse Rate (°C/m)	Stn. Dev. (°C/m)	MDD (°C)	Glacier Temp. (°C)	Valley Temp. (°C)	Valley-Glacer (°C)
07-Jun	0.0065	0.0024	5	-2.2	2.0	4.2
08-Jun	0.0047	0.0021	7	-1.0	2.1	3.1
16-Jun	0.0040	0.0030	36	1.0	3 6	2.6
28-Jun	0.0050	0.0014	23	0.4	3.7	3 3
29-Jun	0.0077	0.0022	58	2.1	7.2	5 0
17-Jul	0.0093	0.0023	69	2.9	8.9	6.1
21-Jul	0.0051	0.0012	46	1.9	5.3	3.3
22-Jul	0.0067	0.0006	41	1.7	6.1	4.4
23-Jul	0.0069	0.0016	59	2.5	7.0	4.5
24-Jul	0.0080	0.0006	77	3.2	8.4	5.2
25-Jul	0.0068	0.0022	66	2.7	7.2	4 4
26-Jul	0.0082	0.0032	63	2.6	8.0	5.4
27-Jul	0.0104	0.0015	62	2.6	9.4	6.8
28-Jul	0.0109	0.0009	52	2.2	9.3	7.1
29-Jul	0.0056	0.0018	70	2.9	6.6	3.7
30-Jul	0.0054	0.0035	65	2.7	6.3	3 6
02-Aug	0.0088	0.0018	93	3.9	9.6	5.8
03-Aug	0.0052	0.0011	32	1 3	4.7	3.4
Average	*0.0069*	*0.0019*	*51*	*1.9*	*6.4*	*4 5*
Early Melt	*0.0050*	*0.0022*	*18*	*-0.4*	*2.8*	*3.3*
Main Melt	*0.0075*	*0.0017*	*61*	*2.5*	*7.4*	*4.9*

Windy and Clear

Date	Lapse Rate (°C/m)	Stn. Dev. (°C/m)	MDD (°C)	Glacier Temp. (°C)	Valley Temp. (°C)	Valley-Glacer (°C)
10-Jun	0.0099	0.0024	3	-2.5	4.0	6 5
12-Jun	0.0092	0.0005	0	-2.1	4.0	6.1
13-Jun	0.0075	0.0019	43	1.6	6 6	4 9
19-Jun	0.0087	0.0005	12	0.0	5.7	5 7

20-Jun	0.0072	0.0017	52	1.8	6.5	4.7
08-Jul	0.0130	0.0018	119	4.9	13.4	8.5
09-Jul	0.0132	0.0012	138	5.7	14.4	8.6
10-Jul	0.0105	0.0018	190	7.9	14.8	6.9
11-Jul	0.0122	0.0027	158	6.6	14.6	8.0
14-Jul	0.0127	0.0027	127	5.3	13.6	8.3
15-Jul	0.0126	0.0024	121	5.0	13.3	8.3
16-Jul	0.0108	0.0014	152	6.3	13.4	7.1
18-Jul	0.0078	0.0040	99	4.1	9.2	5.1
Average	*0.0104*	*0.0019*	*93*	*3.4*	*10.3*	*6.8*
Early Melt	*0.0085*	*0.0014*	*22*	*-0.2*	*5.4*	*5.6*
Main Melt	*0.0110*	*0.0024*	*138*	*5.8*	*13.0*	*7.2*

Windy and Cloudy

Date	Lapse Rate (°C/m)	Stn. Dev. (°C/m)	MDD (°C)	Glacier Temp. (°C)	Valley Temp. (°C)	Valley-Glacer (°C)
09-Jun	0.0058	0.0024	11	-0.7	3.1	3.8
11-Jun	0.0082	0.0011	0	-2.6	2.8	5.4
14-Jun	0.0034	0.0014	23	0.9	3.1	2.2
15-Jun	0.0044	0.0024	13	0.2	3.0	2.9
17-Jun	0.0053	0.0014	11	0.2	3.7	3.4
18-Jun	0.0082	0.0006	5	-0.4	5.0	5.4
21-Jun	0.0079	0.0021	47	1.7	7.0	5.2
22-Jun	0.0093	0.0006	12	0.4	6.5	6.1
23-Jun	0.0080	0.0013	54	2.1	7.3	5.2
24-Jun	0.0096	0.0009	53	2.1	8.4	6.3
25-Jun	0.0064	0.0013	1	-0.6	3.6	4.2
26-Jun	0.0063	0.0012	0	-2.1	2.0	4.1
27-Jun	0.0070	0.0008	0	-1.5	3.1	4.6
01-Jul	0.0104	0.0022	123	5.1	11.9	6.8
02-Jul	0.0110	0.0033	92	3.8	11.0	7.2
03-Jul	0.0061	0.0018	0	-1.0	3.0	4.0
04-Jul	0.0067	0.0019	27	0.9	5.2	4.4
07-Jul	0.0142	0.0022	82	3.4	12.7	9.3
12-Jul	0.0122	0.0016	100	4.1	12.1	8.0
13-Jul	0.0093	0.0015	97	4.0	10.1	6.1
19-Jul	0.0121	0.0010	81	3.4	11.3	7.9
20-Jul	0.0092	0.0015	80	3.3	9.3	6.0
31-Jul	0.0066	0.0022	103	4.3	8.6	4.3
01-Aug	0.0060	0.0035	143	6.0	9.9	3.9
Average	*0.0081*	*0.0017*	*48*	*1.5*	*6.8*	*5.3*
Early Melt	*0.0069*	*0.0013*	*18*	*0.0*	*4.5*	*4.5*
Main Melt	*0.0098*	*0.0019*	*84*	*3.1*	*9.5*	*6.4*

Notes:

MDD (melting degree days) are calculated for the Glacier Meteorological Station, as the daily sum of all positive hourly air temperatures.

Early Melt is the period of June 4-27 and Main Melt is the period from June 28-August 3.

APPENDIX F

MELTING DEGREE HOUR TOTALS FOR QUVIAGIVAA GLACIER AT 50M INTERVALS

Melting Degree Hour daily totals for elevations from 550-850m a.s.l.
Estimated melt at said elevations, 1993

Date	Lapse Rate (°C/m)	ICE MDH	550m MDH	Melt	600m MDH	Melt	650m MDH	Melt	700m MDH	Melt	750m MDH	Melt	800m MDH	Melt	850m MDH	Melt
4-Jun	0 0077	5	9	1	8	1	7	1	6	0	5	0	5	0	5	0
5-Jun	0 0068	6	14	3	12	2	10	2	9	1	8	1	7	1	6	0
6-Jun	0.0065	5	18	4	15	3	13	2	11	2	9	1	7	1	6	0
7-Jun	0.0047	7	20	5	18	4	15	3	13	2	11	2	9	1	8	1
8-Jun	0.0058	11	32	8	28	7	24	6	20	5	17	4	14	3	12	2
9-Jun	0.0099	3	32	8	26	6	21	5	16	3	11	2	7	1	4	0
10-Jun	0.0082	0	7	1	3	0	1	0	0	0	0	0	0	0	0	0
11-Jun	0 0092	0	33	8	25	6	18	4	12	2	6	0	1	0	0	0
12-Jun	0 0075	43	98	27	89	25	80	22	71	19	62	17	54	14	47	12
13-Jun	0 0034	23	47	12	43	11	39	10	35	9	31	8	27	7	24	6
14-Jun	0.0044	13	38	10	33	8	28	7	24	6	20	5	17	4	14	3
15-Jun	0 004	36	57	15	52	14	48	13	44	12	41	11	39	10	37	9
16-Jun	0 0053	11	46	12	40	10	34	8	28	7	22	5	17	4	13	3
17-Jun	0 0082	5	55	15	46	12	36	9	27	6	19	4	12	2	7	1
18-Jun	0.0087	12	67	18	57	15	46	12	36	9	27	7	20	5	14	3
19-Jun	0 0072	52	100	28	91	25	82	23	74	20	66	18	60	16	54	15
20-Jun	0 0079	47	106	30	97	27	87	24	78	21	69	19	61	16	52	14
21-Jun	0.0093	12	79	22	68	19	57	15	46	12	35	9	24	6	15	3
22-Jun	0.008	54	116	32	106	30	96	27	87	24	77	21	68	18	59	16
23-Jun	0.0096	53	124	35	113	31	101	28	90	25	78	22	67	18	56	15
24-Jun	0.0064	1	33	8	27	6	21	5	16	3	11	2	6	0	2	0
25-Jun	0 0063	0	8	1	4	0	1	0	0	0	0	0	0	0	0	0
26-Jun	0.007	0	24	6	17	4	11	2	7	1	3	0	1	0	0	0
27-Jun	0 005	23	51	13	45	12	40	10	36	9	32	8	28	7	25	6
28-Jun	0 0077	58	114	32	105	29	96	27	88	24	80	22	72	20	64	17
29-Jun	0 0089	100	168	48	157	44	146	41	135	38	124	35	114	32	104	29
30-Jun	0 0104	123	208	59	195	56	183	52	170	48	158	45	145	41	133	37
1-Jul	0 011	92	170	48	158	45	145	41	132	37	119	33	107	30	94	26
2-Jul	0 0061	0	26	6	19	4	14	3	8	1	4	0	1	0	0	0
3-Jul	0 0067	27	77	21	69	19	61	16	53	14	46	12	39	10	32	8
4-Jul	0 0081	90	156	44	147	41	137	39	127	36	117	33	108	30	98	27
5-Jul	0 0092	117	189	54	178	50	166	47	155	44	143	40	132	37	121	34
6-Jul	0.0142	82	193	55	176	50	159	45	142	40	125	35	108	30	91	25
7-Jul	0.013	119	222	63	207	59	191	54	176	50	161	46	145	41	130	37
8-Jul	0.0132	138	241	69	225	64	209	60	193	55	177	50	162	46	146	41
9-Jul	0 0105	190	274	78	261	75	248	71	236	67	223	64	211	60	198	56
10-Jul	0 0122	158	250	72	235	67	221	63	206	59	191	54	176	50	161	46
11-Jul	0 0122	100	193	55	178	51	164	47	150	42	136	38	121	34	107	30
12-Jul	0 0093	97	172	49	160	45	149	42	138	39	126	36	115	32	104	29
13-Jul	0 0127	127	224	64	208	59	193	55	178	50	162	46	147	42	132	37
14-Jul	0 0126	121	223	64	208	59	193	55	178	50	163	46	148	42	132	37
15-Jul	0 0108	152	232	66	219	63	206	59	193	55	180	51	167	47	154	44
16-Jul	0 0093	69	138	39	128	36	117	33	106	30	95	27	85	23	74	20
17-Jul	0 0078	99	162	46	152	43	143	40	133	37	123	35	113	32	104	29
18-Jul	0 0121	81	175	50	161	46	147	41	132	37	118	33	103	29	89	25
19-Jul	0 0092	80	149	42	138	39	127	36	117	33	106	30	95	26	84	23
20-Jul	0 0051	46	85	23	79	22	73	20	66	18	60	16	54	14	48	13
21-Jul	0 0067	41	93	26	85	24	78	21	70	19	62	17	54	14	46	12
22-Jul	0 0069	59	115	32	107	30	99	27	90	25	82	23	73	20	65	18
23-Jul	0 008	77	137	39	128	36	118	33	109	30	100	28	90	25	81	22
24-Jul	0.0068	66	119	33	110	31	102	28	94	26	86	24	78	21	69	19
25-Jul	0.0082	63	129	36	119	33	108	30	98	27	88	24	78	21	68	19
26-Jul	0 0104	62	143	41	131	37	118	33	106	29	93	26	81	22	68	18
27-Jul	0 0109	52	136	38	124	35	111	31	98	27	85	23	72	20	59	16
28-Jul	0 0056	70	112	31	105	29	99	28	92	26	86	24	80	22	73	20
29-Jul	0 0054	65	108	30	102	28	95	26	88	24	81	22	74	20	67	18
30-Jul	0 0066	103	156	44	148	42	141	40	133	38	126	35	118	33	111	31
31-Jul	0.006	143	191	54	184	52	177	50	169	48	162	46	155	44	147	42
1-Aug	0 0088	93	158	45	148	42	137	39	126	35	116	32	105	29	94	26
2-Aug	0 0052	32	68	19	62	17	56	15	50	13	45	12	39	10	33	8
3-Aug	0.0032	2	22	5	19	4	15	3	10	2	9	1	6	0	3	0

		550m		600m		650m		700m		750m		800m		850m	
June 29-August 3	3135	5616	1590	5229	1477	4844	1365	4460	1253	4077	1141	3697	1031	3320	922
Total melt period.	3614	6943	6943	6396	1784	5858	1629	5331	1476	4818	1327	4321	1185	3842	1048

Melting Degree Hour daily totals for elevations from 900-1200m a.s.l.
Estimated melt at said elevations, 1993

Date	Lapse Rate (°C/m)	ICE MDH	900m MDH	Melt	950m MDH	Melt	1000m MDH	Melt	1050m MDH	Melt	1100m MDH	Melt	1150m MDH	Melt	1200m MDH	Melt
4-Jun	0 0077	5	4	0	4	0	4	0	4	0	3	0	3	0	3	0
5-Jun	0.0068	6	5	0	5	0	5	0	5	0	5	0	5	0	5	0
6-Jun	0.0065	5	4	0	3	0	2	0	2	0	1	0	1	0	1	0
7-Jun	0.0047	7	7	1	6	0	5	0	5	0	4	0	3	0	3	0
8-Jun	0.0058	11	9	1	7	1	5	0	4	0	4	0	3	0	3	0
9-Jun	0.0099	3	2	0	1	0	0	0	0	0	0	0	0	0	0	0
10-Jun	0.0082	0	0	0	0	0	0	0	0	0	0	0	0	0	0	0
11-Jun	0.0092	0	0	0	0	0	0	0	0	0	0	0	0	0	0	0
12-Jun	0.0075	43	40	10	35	9	30	7	26	6	22	5	20	4	17	4
13-Jun	0.0034	23	21	5	17	4	15	3	13	3	12	2	10	2	9	1
14-Jun	0 0044	13	13	2	11	2	10	2	10	2	9	1	9	1	9	1
15-Jun	0.004	36	35	9	33	8	31	8	30	8	29	7	28	7	27	7
16-Jun	0 0053	11	9	1	6	0	4	0	2	0	2	0	1	0	1	0
17-Jun	0.0082	5	4	0	2	0	0	0	0	0	0	0	0	0	0	0
18-Jun	0.0087	12	9	1	5	0	2	0	0	0	0	0	0	0	0	0
19-Jun	0.0072	52	49	13	44	12	40	10	36	9	31	8	27	7	23	5
20-Jun	0.0079	47	44	11	35	9	29	7	24	6	19	4	15	3	11	2
21-Jun	0.0093	12	6	0	1	0	0	0	0	0	0	0	0	0	0	0
22-Jun	0.008	54	51	14	43	11	36	9	29	7	24	6	19	4	15	3
23-Jun	0.0096	53	44	12	33	8	23	5	14	3	7	1	2	0	0	0
24-Jun	0.0064	1	0	0	0	0	0	0	0	0	0	0	0	0	0	0
25-Jun	0.0063	0	0	0	0	0	0	0	0	0	0	0	0	0	0	0
26-Jun	0.007	0	0	0	0	0	0	0	0	0	0	0	0	0	0	0
27-Jun	0.005	23	22	5	19	4	17	4	15	3	13	3	12	2	10	2
28-Jun	0.0077	58	56	15	49	13	41	11	34	9	28	7	22	5	18	4
29-Jun	0.0089	100	94	26	84	23	77	21	70	19	65	18	59	16	54	14
30-Jun	0.0104	123	120	34	108	30	95	27	84	23	73	20	62	17	52	14
1-Jul	0.011	92	81	22	69	19	56	15	44	11	31	8	20	4	12	2
2-Jul	0 0061	0	0	0	0	0	0	0	0	0	0	0	0	0	0	0
3-Jul	0.0067	27	26	6	19	4	13	2	7	1	3	0	1	0	0	0
4-Jul	0 0081	90	88	24	78	22	69	19	59	16	50	13	42	11	35	9
5-Jul	0.0092	117	109	31	98	27	87	24	76	21	65	18	55	15	46	12
6-Jul	0.0142	82	73	20	56	15	39	10	23	5	10	2	5	0	2	0
7-Jul	0.013	119	114	32	99	28	84	23	69	19	55	15	42	11	34	9
8-Jul	0.0132	138	130	37	114	32	98	27	82	23	67	18	51	13	35	9
9-Jul	0.0105	190	185	53	173	49	160	45	148	42	135	38	122	34	110	31
10-Jul	0.0122	158	147	41	132	37	117	33	102	29	88	24	76	21	65	18
11-Jul	0.0122	100	93	26	79	22	64	17	50	13	36	9	22	5	11	2
12-Jul	0.0093	97	92	26	81	22	70	19	58	16	47	12	36	9	25	6
13-Jul	0.0127	127	116	33	101	28	86	24	70	19	56	15	43	11	33	8
14-Jul	0.0126	121	117	33	102	29	87	24	72	20	59	16	48	13	39	10
15-Jul	0 0108	152	141	40	128	36	115	32	102	28	89	25	77	21	65	18
16-Jul	0 0093	69	63	17	53	14	42	11	32	8	22	5	14	3	10	2
17-Jul	0 0078	99	94	26	84	23	74	20	64	17	55	15	46	12	38	10
18-Jul	0.0121	81	75	20	60	16	46	12	32	8	19	4	11	2	4	0
19-Jul	0 0092	80	74	20	63	17	52	14	42	11	31	8	22	5	13	2
20-Jul	0 0051	46	42	11	36	9	29	7	24	6	19	4	16	3	12	2
21-Jul	0.0067	41	38	10	30	7	22	5	14	3	9	1	5	0	2	0
22-Jul	0.0069	59	57	15	48	13	40	10	32	8	23	6	16	3	9	1
23-Jul	0 008	77	71	19	62	17	52	14	43	11	34	8	24	6	16	3
24-Jul	0.0068	66	61	17	53	14	45	12	37	9	29	7	21	5	13	3
25-Jul	0.0082	63	58	16	48	13	38	10	28	7	22	5	18	4	15	3
26-Jul	0.0104	62	55	15	43	11	30	8	20	4	12	2	6	0	2	0
27-Jul	0.0109	52	46	12	34	8	21	5	11	2	7	1	4	0	2	0
28-Jul	0.0056	70	67	18	60	16	54	14	47	12	41	11	34	9	29	7
29-Jul	0.0054	65	60	16	54	14	47	12	41	11	35	9	31	8	27	7
30-Jul	0.0066	103	103	29	95	26	88	24	82	23	76	21	70	19	64	17
31-Jul	0.006	143	140	40	133	37	126	35	118	33	111	31	104	29	97	27
1-Aug	0.0088	93	83	23	73	20	62	17	52	14	44	12	38	10	31	8
2-Aug	0 0052	32	27	7	22	5	17	4	12	2	8	1	5	0	2	0
3-Aug	0 0032	2	1	0	0	0	0	0	0	0	0	0	0	0	0	0

		900m		950m		1000m		1050m		1100m		1150m		1200m	
June 29-August 3	3135	2944	813	2571	705	2202	597	1847	494	1526	400	1245	319	1007	253
Total melt period	3614	3379	915	2932	787	2502	664	2100	548	1740	444	1427	355	1162	282

APPENDIX G

GRAPH OF AVERAGE DAILY AIR TEMPERATURE FOR FIVE LOCATIONS ON THE FOSHEIM PENINSULA, SUMMER 1993

Average daily mean temperatures for Camp, Valley, Glacier, Hot Weather Creek, and Eureka weather stations, Summer 1993

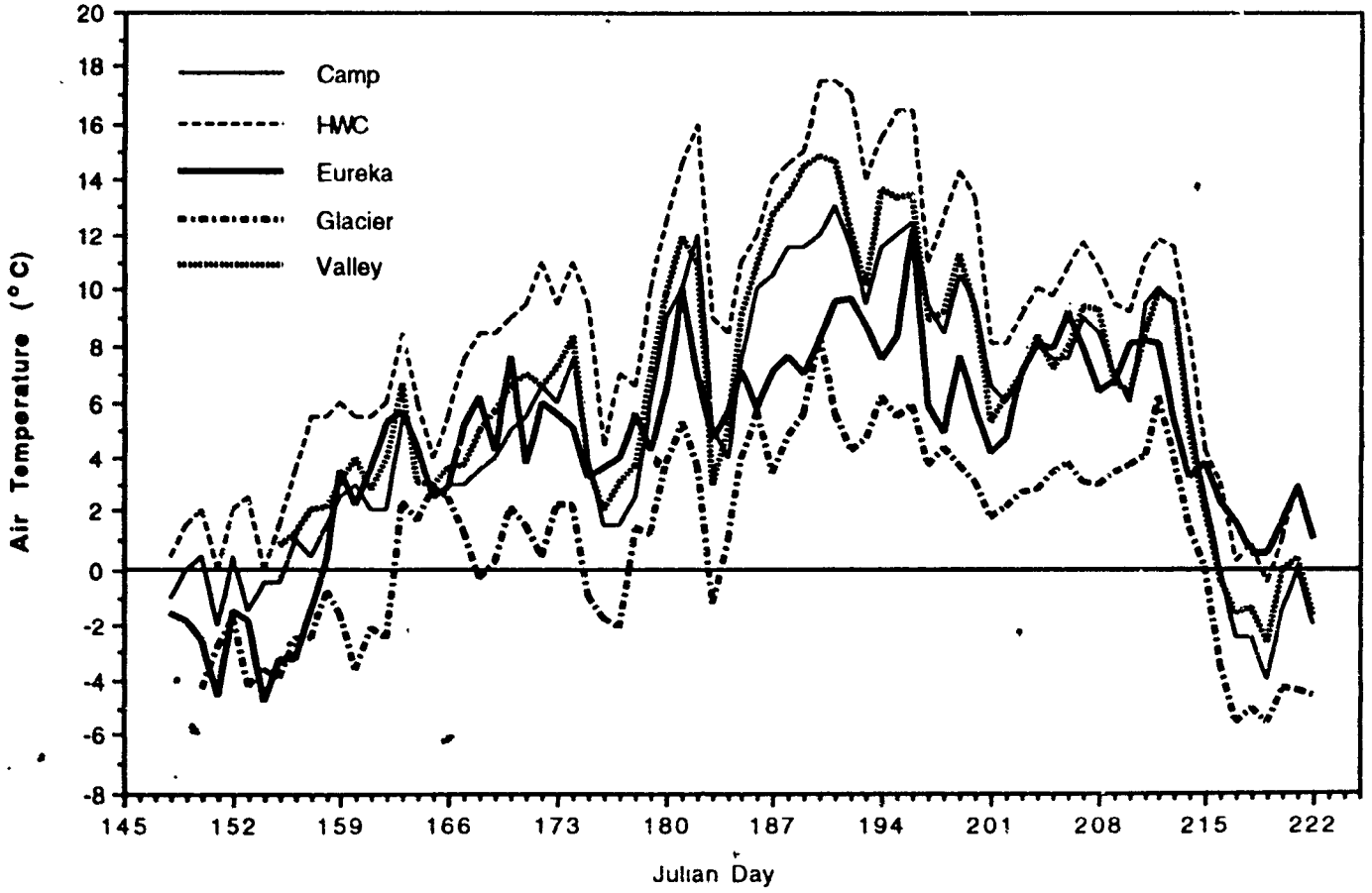

APPENDIX H

SAWTOOTH GLACIER TWICE DAILY METEOROLOGICAL DATA

MAY 26-AUGUST 11, 1993

Sawtooth Glacier Base Camp twice daily meteorological data, May 26 to August 11, 1993

Date	Time	Sky Conditions	Visibility	Obs. to Visibility	Temp. (°C)	Wind	Clouds	Max. (°C)	Min. (°C)	Precip. (mm)	Remarks
May-26	1900	E20OVC	15		-3	0	ST10			T snow	FOG most of day
May-27	700	E30OVC	10	S--	-3	0	ST10			0.5cm S	
	1900	E30BKN	15		-2	1710	ST8				
May-28	700	E40SCT200OVC	15		-3	0	ST2CS8	0	-4		
	1900	E200-SCT250SCT	15		-2	0	CS2CI1	2	-3		
May-29	700	E200BKN	15		-1	0	CS6	2	-3		
	1900	CLR	15		1	0		3	-1		
May-30	700	E150BKN	15		-1	0	AS7	0	-2		
	1900	E30SCT150SCT	15		-1	3302	SC2AS1	3	-2		ST around mtns during day
May-31	700	CLR	15		-4	0		0	-5		
	1900	E100SCT250BKN	15		-1	0	AS4CI3	1	-5		
Jun-01	700	E150SCT200SCT	15		-1	0	AS1CI1	1	-3		
	1900	E100SCT200SCT	15		1	2402	AS1CI1	4	-1		
Jun-02	700	E20OVC	10	S	-4	2707	ST10	2	-4	T	S--drg nite w/cold front pass
	1900	E150SCT	15		-2	0	AS1	-1	-5		
Jun-03	700	E200SCT	15		-3	1204	CI3	-1	-4		
	1900	E40SCT	15		0	0	SC1	3	-4		
Jun-04	700	E100SCT	15		-1	0	AS1	1	-3		
	1900	E40SCT200SCT	15		1	1801	SC1CI1	2	-2		
Jun-05	700	E200SCT	15		1	0	CI1	2	-2		
	1900	E100SCT200SCT	15		2	0	AC3CI1	4	-1		
Jun-06	700	CLR	15		2	0		3	-2		
	1900	E70BKN	15		2	0	AS7	3	0		
Jun-07	700	E60OVC	15		1	0	ST10	3	0		
	1900	E60BKN	15		1	3003	SC9	3	0		
Jun-08	700	E50BKN60BKN	15		2	904	ST5SC3	3	0		
	1900	E60BKN	15		3	3206	SC6	5	2		
Jun-09	700	CLR	15		3	0		4	1		
	1900	E50SCT	15		4	406	SC2	5	2		
Jun-10	700	E50BKN100OVC	15		3	714	ST8AS2	4	0		

	1900	E30SCT50BKN	15		1	912	SF3ST5	3	0	0.5cm S	winds all day gusting 30 kts
Jun-11	700	E35SCT200SCT	15		1	717	ST1CI1	2	-1		
	1900	E40SCT100BKN	15		5	712	ST1AS4	5	1		
Jun-12	700	E40SCT100BKN	15		4	709	ST4AS3	5	3		
	1900	E50SCT200BKN	15		6	3208	SC4CI1	8	3		
Jun-13	700	E35OVC	15		3	2502	ST10	7	2	T	v light rain
	1900	E30BKN	15		4	0	ST9	5	2	2	
Jun-14	700	E25SCT60BKN	10	S	2	2904	ST2ST7	4	1		
	1900	E30BKN200BKN	15		3	3208	ST5CI2	3	1	T	light snow for 3 hr in aft.
Jun-15	700	E100SCT200OVC	15		2	3004	AS3CS7	4	0		
	1900	E50BKN100BKN200OVC	15		4	3001	ST6AS3CS1	6	1		
Jun-16	700	E30SCT100BKN	15		2	0	ST4AS5	4	1	T	light snow this morning
	1900	E40BKN80BKN	15		4	2203	ST5AS4	5	2	T	
Jun-17	700	E50SCT100SCT200BKN	15		3	811	ST1AS3CS2	5	2		
	1900	E80SCT100BKN	15		5	907	AS2AC3	5	2		
Jun-18	700	E50SCT100BKN200BKN	15		3	1614	ST3AS2CS2	6	2		
	1900	E50SCT	15		5	1205	SC2	6	3		
Jun-19	700	CLR	15		4	203		6	2		
	1900	E100SCT200SCT	15		7	3007	AS1CI1	8	3		
Jun-20	700	E100SCT200BKN	15		5	1003	AS3CS5	7	2		
	1900	E45BKN200BKN	15		9	1803	SC6CI1	9	4		
Jun-21	700	E45SCT100SCT200BKN	15		4	1202	SC2AC2CI2	9	4		
	1900	E45SCT100BKN	15		4	1013	SC4AC3	7	4		
Jun-22	700	E45SCT200BKN	15		4	403	SC3CI3	5	3		
	1900	E60SCT180BKN200BKN	15		8	505	SC3CS5CI1	9	3		
Jun-23	700	E180SCT200BKN	15		6	0	CS3CI2	9	6		
	1900	E45SCT100BKN200BKN	15		7	508	SC2AC5CI1	9	6		
Jun-24	700	E30OVC	5	FOG	3	703	FOG10	7	3	1.4	
	1900	E30BKN100BKN	10	S	2	1503	ST7AS2	5	1	T	intermittent snow all day
Jun-25	700	E30BKN100OVC	15		1	1804	ST7AS3	2	0	T	wind gusting 29 kts drg night
	1900	E30BKN100BKN	15		1	1809	SC6AC2	3	0	T	light snow showers in morning
Jun-26	700	E35SCT50BKN	15		1	2203	ST3ST6	2	0		
	1900	E50SCT100OVC	15		2	1110	ST4AC6	3	1	T	light snow in morning
Jun-27	700	E35SCT40OVC	15		2	1606	SF1ST9	3	1		
	1900	E30BKN40BKN80OVC	15		4	0	ST5SC3AS2	4	1	0.4	sun dim vis

Jun-28	700	E40SCT80BKN	15		5	3203	ST3AC5	5	3	
	1900	E80BKN100BKN	15		6	2202	AS5AC4	9	4	
Jun-29	700	E50SCT	15		6	904	SC2	8	6	
	1900	CLR	15		10	2305		12	6	
Jun-30	700	E80BKN	15		8	902	AS9	11	7	
	1900	E50SCT100SCT200BKN	15		13	3208	SC1AC3CI3	13	8	
Jul-01	700	E100OVC	15		10	0	AS10	14	10	
	1900	E80BKN100BKN	15		12	3010	AS5AC4	13	10	
Jul-02	700	E30BKN	15		0	0	ST9	11	-1	2 cold front pass; clring to W
	1900	E35BKN	15		3	3403	ST9	3	0	
Jul-03	700	E20OVC	5	FOG	2	2706	FOG10	3	1	
	1900	E35BKN200BKN	15		6	605	ST6CI2	7	2	
Jul-04	700	E50BKN100BKN	15		6	606	SC6AC3	7	5	
	1900	E200SCT	15		9	3212	CS1	10	6	
Jul-05	700	E100SCT	15		8	2703	AS1	10	7	
	1900	CLR	15		11	3007		13	8	
Jul-06	700	E200SCT	15		10	2203	CI1	12	8	
	1900	E80BKN	15		10	1405	AC7	13	9	
Jul-07	700	E80SCT100SCT	15		11	903	AS1AC1	13	9	
	1900	E80SCT	15		13	708	AC2	14	10	
Jul-08	700	E80SCT	15		12	903	AC1	13	9	
	1900	E80BKN200BKN	15		13	607	AC5CI1	14	10	
Jul-09	700	CLR	15		12	703		13	9	
	1900	CLR	15		14	1006		15	12	
Jul-10	700	CLR	15		12	1006		15	11	
	1900	E200SCT	15		13	807	CI2	15	12	
Jul-11	700	E100SCT180BKN200BKN	15		10	708	AS3CC2CI2	14	9	
	1900	E80BKN100OVC	15		10	505	AS6AC4	12	9	
Jul-12	700	E80BKN100OVC	15		8	0	AS7AC3	10	7	
	1900	E50SCT100BKN200BKN	15		12	0	SC3AS3CI1	12	7	0.3
Jul-13	700	E200SCT250BKN	15		11	707	CC1CI5	12	8	
	1900	E50SCT200BKN	15		14	2507	SC4CI1	15	10	
Jul-14	700	E200SCT	15		10	0	CI1	14	9	
	1900	E50BKN200BKN	15		14	3005	SC6CI1	15	10	
Jul-15	700	E200SCT	15		12	3006	CI4	15	10	

	1900	E100SCT200SCT250BKN	15		11	2608	AC1CC4CI4	14	11		
Jul-16	700	E100SCT200SCT250BKN	15		10	0	AS3CC1CI1	12	7		
	1900	E30SCT50OVC	15		7	0	SF2ST8	11	7		v light rain at present
Jul-17	700	Indef. Obs.	0.125	FOG	6	0	FOG10	7	4	2.3	
	1900	E50SCT	15		11	907	SC2	13	6		
Jul-18	700	E100BKN	15		9	0	AC7	12	9		
	1900	E50SCT60BKN200BKN	15		11	2407	SF1CU6CI2	12	9	0.8	
Jul-19	700	E50BKN100BKN	15		9	2505	SC6AS3	12	7	0.9	
	1900	E40SCT60OVC	15		8	2004	SF4ST6	10	8	T	
Jul-20	700	Indef. Obs.	0.125	FOG	5	2402	FOG10	8	5	4.7	light rain all night
	1900	Indef. Obs.	0.125	FOG	5	2802	FOG10	6	5	6	light to mod rain drg day
Jul-21	700	Indef. Obs.	0.125	FOG	5	0	FOG10	5	5	2.4	light rain during the night
	1900	Indef. Obs.	0.125	FOG	6	2303	FOG10	7	5	8 2	rain all day
Jul-22	700	Indef. Obs.	0.125	FOG	4	2403	FOG10	6	4	2.4	light rain during the night
	1900	E40BKN100BKN	15		8	1807	ST5AC4	10	4	1 9	
Jul-23	700	E40BKN100OVC	15		7	1610	ST8AS2	9	7		
	1900	E50BKN100BKN	15		7	1906	ST6AC3	9	7		
Jul-24	700	E30SCT50OVC	15		5	0	ST3ST7	8	5		
	1900	E50SCT200BKN	15		8	2005	SC4CS4	10	5		
Jul-25	700	E100SCT200SCT	15		7	0	AS1CI1	8	6		
	1900	E50BKN	15		8	2202	SC8	9	6		
Jul-26	700	E50OVC	15		7	0	SC10	10	7		
	1900	E40SCT50BKN100BKN	15		9	1404	ST4SC3AS2	11	7	0.1	intermittent showers drg day
Jul-27	700	E40SCT50OVC	15		7	802	ST2ST8	9	7	1.5	
	1900	E40SCT50OVC	15		8	2502	ST7SC3	10	7		
Jul-28	700	E50SCT100SCT200BKN	15		7	0	SC3AS1CI1	9	6		
	1900	E30SCT50BKN100-OVN	15		6	2204	ST1ST6AC3	9	5		
Jul-29	700	E60BKN100BKN	15		4	0	ST7AS1	6	3		
	1900	E80SCT100BKN200-OVC	15		8	0	AS2AS6CS2	9	3		
Jul-30	700	E100SCT200-OVC	15		10	0	AS2CS8	11	7		
	1900	E150SCT200BKN250BKN	15		9	2502	AC2CS4CC2	12	7		
Jul-31	700	E150SCT	15		9	1903	AS4	11	7		
	1900	E150SCT180BKN200BKN	15		11	1804	AS2CC3CS3	13	9		winds gusting 20 kts drg aft
Aug-01	700	E40SCT50BKN200BKN	15		8	1610	ST2SC6CS1	11	8		winds gusting 20 kts drg night
	1900	E50BKN80BKN200BKN	15		8	0	SC5AC3CI1	11	8		

Aug-02	700	E30OVC	15		5	1802	ST10	8	5	T	v light rain at present
	1900	E28OVC	15		3	1802	ST10	5	3		
Aug-03	700	E25SCT50OVC	15		1	0	ST4ST6	3	1	0.7	
	1900	E30BKN50OVC	15		3	2204	ST6ST4	4	1		
Aug-04	700	Indef. Obs.	1	FOG+S	0	2205	FOG10	3	0	0.9	v light snow at present
	1900	Indef. Obs.	2	S	-3	2502	ST10	0	-3	3.8	snow drg day, S on ground
Aug-05	700	Indef. Obs.	0 25	S	-4	2208	FOG10	-3	-4	T	snow was likely > trace
	1900	E25BKN	10	S-	-2	1810	SC9	-1	-4	T	S- drg day, vis 2 miles to N
Aug-06	700	Part.Obs.E20OVC	0.5	S+BS	-2	1216	SNOW10	-1	-3	T	wind 27 kts drg nite, >T snow
	1900	Part.Obs.E20OVC	1	S+BS	-3	1710	SNOW10	-1	-4	T	light-mod S all day, >T snow
Aug-07	700	E35BKN	15		-4	1808	ST6	-3	-5	T	winds gusting 19 kts drg night
	1900	Part.Obs.E30OVC	2	S+BS	-3	1813	SNOW10	-3	-5	T	light snow in afternoon, >T
Aug-08	700	Part.Obs.E30OVC	5	S+BS	-3	1223	SNOW10	-3	-4	T	wind gusting 27 kts presently
	1900	E30BKN80BKN180OVC	10	BS	1	1220	ST5AS3CI2	1	-3	T	wind gusting 32 kts drg aft
Aug-09	700	Indef. Obs.	0 125	S+BS	-2	1020	SNOW10	2	-2	T	wind gusting 30 kts drg nite
	1900	E35SCT50OVC	15		0	612	ST2ST8	1	-2	T	wind gusting 36 kts drg day
Aug-10	700	Indef. Obs.	1	S	-2	1802	SNOW10	0	-2	5cm S	five cm of snow, no drifting
	1900	E40SCT50BKN80OVC	10	BS	-4	1615	ST2ST6AS2	-1	-4	T	improved vis to S
Aug-11	700	E40SCT50OVC	5	S	-3	1611	ST2ST8	-3	-4	T	sun dim vis, > T snow

Notes:

Visibility is in miles.
Restrictions to visibility are: S=snow, S-=light snow, S--=very light snow, BS=blowing snow, FOG=fog
Wind is in knots and is in the format: direction, speed
Precipitation is in mm except when labeled otherwise

APPENDIX I

ABLATION AND ALBEDO DATA FROM AS1-12

Ablation Station data from all stations and comments, Quviagivaa Glacier, 1993
Surface lowering, density, albedo, sky condition, surface condition

Date	Dec. Day	Surf (mm)	Low	Density (g/cm3)	Wat Eq. (mm)	Albedo	Sky Condition and Surface Condition
AS1							
6-Jun	157	35					
7-Jun	158	40	15	0.388	5 7		
8-Jun	159	36	6	0 343	2 2		hard crust on snow from last nite, wet just underneath, still dry below 3cm
12-Jun	163	40	-76	0.465	-26 2	0 57	Clr, snow v wet, fresh drifted snow 10-14cm thick
14-Jun	165	38	74	0.508	34 6	0 65	5000 OVC-, snow v wet
16-Jun	167	46	60	0.513	30 6		S-/R-, snow v wet
18-Jun	169	38	56	0.535	28.9	0.72	Clr, surf froze last nite, still crunchy, snow about 140cm deep
20-Jun	171	50	74	0 546	39 4	0 63	bright sun, SC around, snow a bit crusty on top, v wet to about 80cm
22-Jun	173	47	67	0.585	36 6	0 66	CS, a few light shadows being cast, v wet snow and saturated to ice (125cm deep)
24-Jun	175	54	102	0 623	59 6	0 65	S--, totally saturated snow, mushy and 1m deep, about 15cm si formed since last measurement
26-Jun	177	48	26	0.465	16 2	0.76	BKN SC, sun not vis, fresh snow 1-3cm, very slushy under
28-Jun	179	47	42	0.585	19 5	0.55	sunny, bit of SC around, v saturated, sm crystal slush
30-Jun	181	38	105	0 711	61 4	0.51	cloudy, AC, snow very wet and slushy
2-Jul	183	50	152	*0 675*	108 1		deep snow very wet and slushy, ice at around 70cm depth
4-Jul	185	48	69	0 616	46.8	0 56	sun part in cloud, v saturated snow, water at 65cm down pit
6-Jul	187	48	141	0 623	87 1	0 47	AC sun on edge of cloud, snow 30 cm deep, v wet si, flow vis on ice surf at depth
7-Jul	188	68	106	*0.640*	65 9		total sun, stakes melting out
8-Jul	189	48	35	*0.650*	22 2	0 49	AC obscurring sun, slush 15cm, water flowing everywhere under surf
10-Jul	191	63	201	*0.680*	130 9	0 50	Clr, slush pile-up at #1-3,11-14, 17cm to ice, v slushy + sat
12-Jul	193	47	107	0 687	72 8	0.40	var SC, v large grained, sm bits of remnant snow around, exposed rx above AS1
14-Jul	195	42	65	*0 740*	44.9	0.39	melting si 7cm deep, si below that, crystal slush band around 40m wide
16-Jul	197	48	94	*0.810*	69.3	0 44	slushy si becoming dry crunchy ice in places, si almost gone, v dirty ice14cm down, few tiny c holes
17-Jul	198	46	32	*0.840*	25.7		si disappearing
19-Jul	200	54	112	*0.900*	94 4	0.28	still ST OVC, surf much dirtier, rx and sm flecks, si all gone, N of stn still some si covering dirtier surf
21-Jul	202	47	74	*0.900*	66.9		raining heavier, looking even dirtier on glacier now
22-Jul	203	48	29	*0 900*	25 8		FOG, surf is dirty, ice under is clean, v dense, surf streams flowing well
24-Jul	205	48	70	*0.900*	63 3	0.28	OVC ST, surf much dirtier 30m above AS1, sm chnls flwng, porous ice 1-2cm thick cryoc shallow, surf dry
26-Jul	207	48	76	*0.900*	68.1	0 29	OVC SC, surf v dirty, more rx exposed, melt channels on both sides of stn, v thin abl surf, dense ice below
28-Jul	209	50	67	*0 900*	60 6	0.32	ST OVC 3000, v dirty, no si left around, flow by stn in channel, hard, sm crystal surf, rx still appearing
30-Jul	211	51	56	*0.900*	50.1	0 29	sun bright, surf v dirty, flow in channels on either side, surface only 1cm thick, smaller crystal size
1-Aug	213	50	100	*0.900*	90 0	0.24	sun behind SC + variable, streams flowing well, v thin white unsat crystal, most of surf is sat, dirty as usual
3-Aug	215	48	43	*0 900*	38 7	0 40	ST 3000 OVC, dirty surf showing, most snow melted, ice surf wet, chnls flowing well both sides stn
10-Aug	222	14					wind blown snow but not as hard-packed as up gl, depths from 39-52cm at stn
	Total	2180		1539.8			

AS2

6-Jun	157 36					
7-Jun	158 42	4	0 436	1 7		icy snow surf, was melting recently, dry below 2-3cm
8-Jun	159 38	1	0 484	0.3		
9-Jun	160 35	8	*0 480*	3 9		
12-Jun	163 42	-17	*0 480*	-8 2		v thin Cl, snow v wet, some drifting and accumulation
14-Jun	165 38	38	0.477	18 1	0.67	ST5000, sun dimly vis, snow v wet
16-Jun	167 47	13	0.550	6 2		flow on sı surface
18-Jun	169 39	16	0 528	8.6	0.66	trace of thin cloud, 7cm of crusty snow over ice layer
20-Jun	171 48	24	0.518	12 7	0 80	sunny w/ thin cloud, water flowing on ice surf beneath 22cm snow
22-Jun	173 46	28	0 556	14 5	0 64	thin CS, sun dim vis, snow crusty but wet just below surf
24-Jun	175 52	57	0.669	31 9	0 59	v light snow falling, slushy and wet snow, surf appears blue
26-Jun	177 46	0	0 563	-0 2	0.76	OVC, not much fresh snow (0-2cm thick)
28-Jun	179 46	11	0.729	6 0	0 52	sunny, but on edge of SC, snow wet and crystally 5-15cm deep, sı becoming exposed
30-Jun	181 39	63	0 757	45 9	0 44	cloudy, AC, very slushy and wet
2-Jul	183 48	69	*0.825*	52 2		saturated ice with icy layer (lg crystals) over it, quite a bit of flow, only few slushy patches (melting sı)
4-Jul	185 48	31	*0 900*	25 3	0.45	sunny, crunchy surf, porous lg crystal 3cm, wt at 8cm
6-Jul	187 48	75	*0 900*	67 2	0 46	AC mostly sunny, saturated at 2cm, hard, porous on top, still some melting sı around
8-Jul	189 47	79	*0 900*	74 7	0.48	some AC, dry crystal surf, 2-3cm of porous ice, sı all gone
10-Jul	191 63	113	*0 900*	113 0	0 54	Clr, cryoc 10-13cm deep, porous ice 13cm, wt=5cm, some sat surf
12-Jul	193 46	85	*0 900*	76 5	0 41	OVC w/ SC, cryoc , wt=6cm, few sat patches, most white, dry porous, larger crystals than AS3
14-Jul	195 65	92	*0.900*	82 5	0 39	Clr, cryoconite 6-11cm deep, wt=6cm, some cryo coalescing, surf dry crunchy, irregular topography
16-Jul	197 48	75	*0 900*	71 3	0 45	ST OVC, sun bright, wt=2-7cm, flow w/in ice, less c holes, up to 15cm deep, dirty ice margin albedo=0 16
19-Jul	200 52	120	*0 900*	108 0	0 36	ST OVC breaking up a bit, surf flecked w dirt, sat surf near, some c dry, one hole 11cm deep + full w/water
22-Jul	203 48	87	*0 900*	76.6		FOG, light rain some cryoc dirty flecked surf wt=6cm in 9cm cyroconite
24-Jul	205 47	62	*0 900*	54 3	0 40	OVC40ST, surf much cleaner, flecked w dirt, c holes10cm, dry surf1-2cm thick flow in channel + sat areas
26-Jul	207 48	55	*0 900*	48 1	0 44	OVCSC surf flecked w dirt, channels flowing by stn, dry porous ice only 1-2cm some areas sat to surface
28-Jul	209 48	49	*0 900*	43 4	0 41	ASOVC- bright, surf flecked w dirt, chnls flowing well in slush, c holes merging to 6cm, wt=3cm, dry crystal surf1-2cm
30-Jul	211 50	40	*0 900*	34 1	0 44	sun bright, few c holes, wt=8cm, chnl flowing well, dry crystal surf larger like AS3, loosely bonded 3cm thick surf
1-Aug	213 48	96	*0 900*	88 3	0 35	sun behind SC but variable, chnl flowing well, few c holes to 8cm, wt=0, crystal surf 1-2cm thick + wt=10+cm
3-Aug	215 48	23	*0 900*	21 3		STOVC 0 5cm fresh snow, c holes visible, sm trickle of flow in channel to N
10-Aug	222 13					wind blown snow, depths from 29-33cm at stn
	Total	1393		1178 3		

AS3

6-Jun	157 48					
7-Jun	158 43	6	0 290	1 6		ice layer on snow surf 1cm thick dry snow starts at 3cm depth
8-Jun	159 38	-3	0 346	-0 8		
12-Jun	163 52	16	0 452	5 4		snow wet to 10cm depth
14-Jun	165 47	41	0 473	18 7	0 71	cloudy and just below cloud level snow quite wet

15-Jun	166 65	-2	*0 450*	-0 9		snow 25-28cm deep, snow-ice interface still dry
18-Jun	169 40	40	0 482	18.0	0 65	Clr, cystalline hard snow 34cm thick over hard ice, ice layers in snow, no si yet
20-Jun	171 47	32	0 514	15 6	0 59	some sun, v mushy wet snow, 22cm deep, 1cm thick ice layer at 8cm
22-Jun	173 46	33	0 518	16 8	0 62	CS, sun dim vis, crunchy, small grain snow, snow 19cm deep
24-Jun	175 52	61	0.528	31 7	0.54	v light snow falling, v wet and slushy snow, saturated underneath
26-Jun	177 44	-30	0.335	-15 8	0 81	snow/ice crystals falling, 0-3cm fresh snow
28-Jun	179 44	16	0.546	5 4	0 50	sunny, but SC next to sun, saturated melting superimposed ice (si)
30-Jun	181 40	50	0 757	27.1	0.34	sun on edge of AC, vv slushy (melting si), and water flowing thru it
4-Jul	185.47	104	*0.900*	78 7	0.46	ST variable sun/cloud, 3cm slushy melting si, numerous melt channels
6-Jul	187 47	75	*0.900*	56 5	0 43	AC mostly sunny, hard, white dry surf, wt at 11cm, porous surf = 3cm thick, all si gone
8-Jul	189 47	84	*0.900*	63 3	0.40	bright sun, 2-3cm rolling, bumpy porous ablating ice, good flow nearby
10-Jul	191 60	125	*0.900*	93 5	0.50	Clr, cryoc 10-15cm deep, white porous surf, wt=5cm, some wet, slushy areas adjacent to stn, mostly dry
12-Jul	193 44	81	*0.900*	61.0	0.40	SC-OVC breaking up, surf dry+v bumpy, dirtier, mostly hard, porous ice
14-Jul	195 40	83	*0.900*	62.3	0.31	Clr, lots of cryoc, some dry at 11cm, surf v irregular, crunchy stuff, general wt=5cm, surf a bit dirtier
16-Jul	197 47	110	*0 900*	82.3	0.43	ST,AS cloudy, surf flecked w/ dirt, numerous c, some dry to 5cm, surf dry + crunchy + irregular, wt=0 to 17cm
19-Jul	200 52	135	*0.900*	111 4	0.31	OVC, but breaking a bit, surf v bumpy and flecked w dirt, flow by one stake, sm cryoconite
22-Jul	203 47	96	*0 900*	79 2		FOG, undulating surf, had to redrill stake, water flow on surf, some areas ice is dry to 10cm, sm c and melted c holes
24-Jul	205.47	58	*0.900*	50.5	0 30	OVC40ST sun not vis, surf v rough btw AS4+3, dirty, some dark blue sat ice, thin white dirty ice 1cm thick
26-Jul	207 47	55	*0.900*	45 7	0 38	OVCSC, sm flow by stn, surf v dirty in bands, channels merged c holes and are dirty, wt=0, dry crystal surf=1-2cm
28-Jul	209 48	50	*0.900*	43 5	0.40	thin ACOVC someST, similar surf to last time, trickle of flow thru stn, lots micro c holes, saturated in depression areas
30-Jul	211 50	78	*0 900*	64 5	0 39	sun bright, good flow + periodic slush flows, dirt at surf + in micro c holes, few merged larger holes, wt=3cm
1-Aug	213 48	92	*0 900*	69 3	0 34	sun behind SC, stream thru stn, surf flow, micro c holes, whitish crystally ice 2cm thick, most surf is sat + dirty
3-Aug	215.47	22	*0 900*	18 4		STOVC, 0 5cm of new snow, still dirty patches showing, flow in channel to S
7-Aug	219 36					below freezing and blowing snow, most of wire drifted in
10-Aug	222 11					wind blown snow, other wires still buried, 2cm of fresh snow now
	Total	1508		1102 6		

AS4

6-Jun	157 38					
7-Jun	158.43	4	0 323	1.4		OVC, crusty ice layer at top 2cm of snowpack, dry underneath
8-Jun	159 39	-1	0.343	-0 2		
12-Jun	163 52	16	0.491	5 5		ST6, melting snow conditions, v little sign of drifting
14-Jun	165.47	37	0.557	18.2	0 69	v low cloud, v wet snow
18-Jun	169 40	42	0.528	23 6	0 65	Clr, hard +crusty surf, 19cm down to si
20-Jun	171 46	11	0 581	6 0	0 71	CU cloud cover, 9cm deep snow v wet, major formation of si since 18th, rough, bubbly ice surf
22-Jun	173 44	23	0.599	13.2	0.63	CS, sun dim vis, crystalline semi-saturated surf
24-Jun	175.51	45	0.574	27 1	0.65	v light snow falling, snow slippery and slushy, crystals smaller
26-Jun	177 43	3	0.335	1.9	0.75	sun not vis, surf patchy fresh and old snow/ice (60% fresh)
28-Jun	179 43	1	0.546	0 3	0 65	SC cloudy, saturated, crystally melting si, ice crystal shower occurring
30-Jun	181 42				0.34	sunny, 60% snow cover, remainder is darker melting si, tot saturated
4-Jul	185 46	83	*0.900*	62 0	0.47	ST, sunny breaks, crunchy ice surf sim to AS6, good flow in channels, si melting

6-Jul	187 47	67	*0.900*	50.5	0 46	AC broken, no snow left, v dry surf, slushy, wet snow N and W of stn, about 5cm melting si
8-Jul	189.47	78	*0 900*	58 8	0.41	bright sun, 3cm white porous ice above wet ice, ponding water, no si left
10-Jul	191.52	107	*0.900*	80 0	0.41	Clr, lots of cryoc. 6-11cm deep, 1-6cm diam, dry crunchy like AS6, 11cm to hard ice, wt=5cm
12-Jul	193 44	82	*0.900*	61.3	0 43	SC50-OVC, dry, porous surf, smaller crystal size than AS8, a few sat patches, wt=5cm
14-Jul	195.40	75	*0.900*	56.5	0.40	clr, cryoc 9-14cm deep, wt=5cm, crunchy white surf
16-Jul	197 47	95	*0.900*	71.0	0.48	ST cloudy, tons of cryoc holes 7-12 cm deep, dry porous 4cm thick, wt=4cm, bits of dirt on surf
19-Jul	200 51	125	*0.900*	103.1	0 38	ST OVC, sun breaking, cryoconite 8cm, wt=4cm, surf flecked w dirt, crunchy and porous
22-Jul	203 46	66	*0 900*	54 2		FOG, cryoc 6-8cm, wt=6cm, saturated blue areas = 40%
24-Jul	205 47	55	*0.900*	48 4	0.39	OVC40ST, numerous c to 8cm, wt=4-6cm, surf part wet, rough surf, dry porous surf 1cm, dark ice below (sat)
26-Jul	207 47	44	*0.900*	36 3	0 41	OVCSC, c holes to 10cm, wt=6cm, merging holes forming minor chnls, bumpy topo, white crystally surf is 1-2cm
28-Jul	209 47	44	*0.900*	38 5	0.44	OVC-AC, many c holes to 9-12cm, wt=7cm, white crystalline surf specked w dirt, few sm dirt patches, sm flow near
30-Jul	211 48	39	*0.900*	32 2	0.42	bright sun, = micro + normal c holes, some to 16cm, wt=6cm, surf dry + crunchy, sm crystals than AS6, sat below 2cn
1-Aug	213.46	84	*0 900*	63 3	0 30	sun v bright, var cloud, surf sat many areas, flecked w dirt, few c holes to 7cm, wt=5cm, crystally dry surf 1cm
3-Aug	215 47	16	*0 900*	13 2		STOVC, 0 5cm fresh snow, lg # of c holes still showing thru
10-Aug						wires buried 15-33cm snow depth, v wind blown and fairly dense
	Total	1243		926 1		

AS5

6-Jun	157 39					
7-Jun	158 44	1	0 463	0 5		no crusty ice later, v little melt
8-Jun	159 40	0	0.317	0 0		
12-Jun	163 48	11	0.342	3 4		AC/ST, snow soft + surf melting, minor signs of drifting from yesterday
14-Jun	165 44	49	0 404	16.8	0.67	snow v slushy, topp 7cm sat , under that are ice layers and hoar
19-Jun	170 39	45	*0.440*	18 2		ice surf crusty from last nite, 2cm ice crust under snow
20-Jun	171 44	1	0 468	0 6	0 63	OVC, crusty ice surf 1cm thick, 27cm snow to ice, surf not yet wet
22-Jun	173 43	13	0 405	5 9	0 57	CS, bit of sun getting thru, porous dry ice at surf
24-Jun	175 51	53	0 546	21 3	0 68	S--, wt=5cm
26-Jun	177 42	2	0 335	1 3	0 74	dark cloud totally obscurring sun, 60% coverage of drifted fresh snow, only 0 5cm deep
28-Jun	179 43	2	0 546	0 7		S surf wet and melting, smaller crystals than at AS6
30-Jun	181 43	65	0 694	35 7	0 49	sunny, 90% snow cover, a few really slushy areas, but not as wet as AS4, melting snow
4-Jul	185 67	*80*	*0 825*	55 5		slushy, likely melting superimposed ice
6-Jul	187 43	48	*0 900*	39 9	0.52	AC cloudy, thin 3cm abl surf, remnant snow, melting si
8-Jul	189 44	76	*0 900*	57 3	0 40	sm puff of AC passed by sun, some crunchy abl ice, some snow, flow at 6cm si gone
10-Jul	191 51	106	*0 900*	79 8	0 32	Clr, porous ice, some areas sat at surf, 12cm thick porous stuff, wt=5cm, a few cryoconite
12-Jul	193 43	85	*0 900*	63 5	0 40	SC50-OVC quite dirty around, cryoc , wt=4cm, var dry porous
14-Jul	195 39	85	*0 900*	63 5	0 39	Clr, cryoc up to 12cm deep, wt=2cm, porous ice surf 4cm thick, darker sat ice just under surf
16-Jul	197 47	102	*0 900*	76 5	0 44	ST/AS OVC, lots of cryoc 8-14cm deep dry porous layer 4cm thick, wt=5cm, sm bit of surf flow in channel
19-Jul	200 50	128	*0 900*	105 3	0 35	ST OVC, some sun breaking, surf flecked w dirt, flow on ice, few cryoconite,lots of rx appearing just E of stn
22-Jul	203 43	75	*0 900*	62 2		FOG R-, surf flow, wt=4cm redrilled 1 stake and hole remained dry
24-Jul	205 47	52	*0 900*	45 5	0 38	OVC40ST many cryoc all sizes dry porous surf=2cm thick, surf dirtier at 7cm down rough ice surf in area
26-Jul	207 44	43	*0 900*	35 5	0 39	OVCSC R-, many c holes merging to form dirty patches, white crystal surf v thin=2cm not as porous as before

28-Jul	209 47	53	*0 900*	46 1	0 40	AC/AS + lower OVC, many dirt patches, sm trickle of strm thru stn, merging c holes, white crunchy to 5cm wt=1-8cm
1-Aug	213 46	123	*0 900*	101 5	0 31	sun behind SC + var, surf crystalline + sat in sections, flow in stn, v little c holes, surf dirty, loose crystals 2cm var surf
3-Aug	215 47	21	*0 900*	17 6		OVCST, 0 5cm new snow, stream in stn iced over, dirty areas still exposed to E of stn
10-Aug	222 09					wind-packed snow, variable depths from 15-43cm at stn
	Total	1319		953 7		

AS6

	-1 00					
12-Jun	163 43		0.476			
14-Jun	165 39	30	0 480	14 3	0 64	5000 OVC-, snow v wet, ice surf 14cm below snow surf
18-Jun	169 55	31	0 553	14 7	0 63	Clr, snow depth=10cm, snow/ice interface wet, hard crust due to freezing overnite
20-Jun	171 43	4	0 532	2 0	0 55	OVC, snow depth=6-9cm, ice surf smooth below and wet (new), snow surf crunchy
22-Jun	173 42	14	*0.500*	7 6	0 5[illegible]	CS, large grains, porous, hard, crystally, chunks bonded together, porous to 13cm
24-Jun	175.50	8	0 458	4 0	0.61	S- or ice crystals falling, porous, lg grain crystal ice 8cm thick
26-Jun	177 40	-7	0.335	-3 1	0 67	OVC, sun partially vis, 25% fresh snow cover in area, fresh snow=1.5-2cm
28-Jun	179 42	2	0.665	0.7	0 62	sun bright behind SC, fresh snow v wet + 0 5cm thick, more saturated here, porous lg crystal ice
30-Jun	181 43	54	*0 900*	35 9	0 37	sunny, AC1, crystal, icy porous surf, saturated at depth, fresh snow gone
2-Jul	183.47	55	*0.900*	41 5		lg crystal, frozen ice, saturated below 4 cm and flow occurring there
4-Jul	185 44	25	*0 900*	20 6	0 49	ST OVC, but breaking, 4cm v porous dry ice, saturated at 11cm
6-Jul	187.43	64	*0 900*	48 3	0 47	AC completely blocking sun, 8cm dry ablation surf, wt at 15cm
8-Jul	189 43	82	*0 900*	61 5	0 37	some AC, 10cm unsaturated porous ice, wt=10cm, dirtier surf here shown in cryoconite holes
10-Jul	191 50	129	*0 900*	96 5	0.34	Clr, 1/2 stn is wet ice, 1/2 dry, surf has some dirt, dry, crunchy surf is 9cm thick
12-Jul	193 43	103	*0 900*	77 5	0.32	SC 5000-OVC, hard, porous whitish ice w/ smoother sat blue ice, glacier darker, porous stuff=4cm
14-Jul	195 67	90	*0.900*	67 3	0 39	Clr, mostly micro-cryoc., white crystal surf 6 cm thick, lg area speckled w/ dirt, not as sat as previously
16-Jul	197.46	74	*0.900*	55.3	0.49	ST cloudy, lots of micro-cryoc , surf flecked w/ dirt, high porosity layer 3-6cm thick at surf, no vis flow near stn
19-Jul	200 48	136	*0.900*	112.5	0 38	ST10, but lifting, half of ice is whiter and porous, half saturated darker ice, albedo = 33% over darker ice
22-Jul	203 42	85	*0.900*	70.4		FOG, 50/50 porous and hard saturated ice, only 2-3cm cryoconite
24-Jul	205.46	73	*0.900*	63 9	0.35	OVC40ST breaking, lots of micro-cryoc dry crystalline ice=1cm, saturated in other areas
26-Jul	207 43	45	*0 900*	37 1	0 42	OVCSC R-, micro c holes everywhere, surf dry crystalline and v loose w lg crystals, wt=2-3cm, dirt in holes down 10cm
28-Jul	209.46	51	*0 900*	44 6	0 40	AC/AS OVC, surf much wetter + dirtier, many micro c holes, surf whitish + crunchy, lg crystals 4cm thick, sat below
30-Jul	211 48	29	*0 900*	23.7	0.42	sun bright, more c hole than AS8, crunchy white surf but sm size crystals than AS8, dirt fleckd, sm surf flow, wt=8cm
1-Aug	213 44	108	*0.900*	80 8	0.30	sun havoc + SC, surf here icy sat to surf, few bits chunky ice 1cm thick, lots of micro c hole, speckd w dirt, no lg c hole
3-Aug	215 46	20	*0 900*	16.2	0 67	OVCST, 0 5cm fresh S, melt chnl to S trickling, few c holes showing but most are covered in snow
10-Aug	222 06					wind packed snow, a few bare patches in view of stn, but snow 19-33cm deep at stn
	Total	1305		993 7		

AS7

12-Jun	163 44		0 481			

14-Jun	165 40	39	0.530	18 8	0 69	sun dimly vis, ST 5000, wet +slushy snow, 13cm deep
18-Jun	169.54	27	0.546	14.1	0.72	CLR, snow 4cm deep
20-Jun	171 42	-4	*0 470*	-2 2	0 50	puff of cloud over sun, CU, rapidly changing, 1cm ice layer at 5cm depth, snow 9cm deep, surf not wet, but has been
22-Jun	173 42	19	*0.550*	8.9	0.59	CS, thin, crunchy snow crust
24-Jun	175 48	17	0.563	9 4	0.61	S-, trace of fresh snow on surf, crystalline slush under blue patch of snow nearby (melting si) albedo = 50%
26-Jun	177.39	-25	0 546	-14.3	0 61	AS8, 20% thin fresh snow cover, porous ice surf, lg crystals
28-Jun	179 42	-16	0 651	-8 6	0 64	BKN, sun not vis, not as much fresh snow, v crystalline, melting si
30-Jun	181.44	42	*0.630*	27 1	0 47	sunny, crystal slush, porous lg grain, some melting si
4-Jul	185 43	75	*0 650*	47 0	0.51	ST10, 2cm of lg crystal white dry ice on v saturated darker ice, si gone
6-Jul	187.42	50	0.634	32 7	0.53	AC, cloudy, slush flow remnants at #3-9, rest is harder ice
8-Jul	189 42	87	*0 900*	54.9	0.43	bright sun, bit of CI around, 5cm dry abl surf, good flow in melt streams, well-drained
10-Jul	191 48	103	*0.900*	77 3	0 45	Clr, not as porous as AS8, surf dry + crunchy, smooth ice 8cm below, wt=3cm, cryoconite 12-18cm deep
12-Jul	193 42	87	*0 900*	65 5	0 43	var 50-OVC, icy+slippery surf, 3-4cm cryoc , some crystalline surf 1cm thick, wt=4cm
14-Jul	195 38	61	*0 900*	46 0	0 39	Clr, cryoc 6-11cm deep, wt=4cm, surf v hard and crunchy dry and 4cm thick
16-Jul	197 46	84	*0 900*	62 8	0 52	ST cloudy, crunchy white + clean surf, 10-14cm deep cryoc , wt=4cm
19-Jul	200 48	138	*0.900*	113 6	0 45	ST OVC, sun dim vis, cryoc. to 8cm, wt at surf, hard almost slippery surf, denser ice than AS8
22-Jul	203 42	69	*0.900*	56 7		FOG, sm bits of porous ice, mostly harder whitish ice, wet, cryoc to 6cm, wt=surf , good flow in channels
24-Jul	205 46	61	*0 900*	53 1	0 46	OVC35ST breaking, surf fairly clean xcpt for rx nearby, thin porous surf=1cm, c holes to 7cm, wt=surf
26-Jul	207 43	45	*0 900*	37 4	0 45	OVCSC sun brightly vis, surf whiter, 3cm thick, crystals drier, sm c holes to 10cm wt=1cm, not much dirt evident
28-Jul	209 46	47	*0 900*	41 1	0 45	sun under AC band OVC, surf fairly clean, micro c holes in ice 5-8cm, lg hole at stn 50*20cm and 15cm deep w water
1-Aug	213 44	135	*0 900*	111 1	0 36	sun dim vis, pesky SC cloud, surf icy + slippery here, few c holes but to 10cm bit of crystally ice left, most dense ice
3-Aug	215 46	18	*0 900*	14 9		FOG, 0 5-1cm S, chnl to N of stn doing great pulse drainage, surf v white xcpt for odd rx c holes iced over 3cm down
10-Aug	*222 05*					wind swept and only 0-2cm snow at stn
	Total	1157		867 2		

AS8

12-Jun	163 46		0 386			
14-Jun	165 42	27	0 491	10 3	0 64	sun mostly visible, surf v soft and collapses when touched, only surf is wet
18-Jun	169 52	13	0 440	6 2	0 59	Clr, snow=4cm deep
20-Jun	171 40	4	*0 420*	1 6	0 43	changing cloud conditions, snow=2cm deep icy at surface
22-Jun	173 40	10	*0 380*	4 3	0 58	CS ice surf finely rippled si surf exposed 2 5cm of si formed
24-Jun	175 47	10	*0 350*	3 9	0 67	S-, crystally slushy stuff over wet, slushy ice, melting si
26-Jun	177 39	-6	0 335	-2 1	0 71	OVC, sun dim vis, fresh S surf on 40% area rest is hard, crunchy, loosely bonded ice albedo crusty snow/ice=67%
28-Jun	179 40	-8	0 556	-2 6	0 62	cloudy, AC, not as much snow (1 5cm) and wet
30-Jun	181 46	64	*0 900*	35 6	0 50	mostly sunny, dry porous crunchy ice at surf fairly white, si gone
2-Jul	183 47	70	*0 900*	52 8		no snow patches left, lg crystal porous ice hard and 7 cm thick
4-Jul	185 42	25	*0 900*	20 6	0 53	ST10 6cm of huge crystal surf hard water table 7cm below
6-Jul	187 42	57	*0 900*	42 8	0 50	AC, sun not vis 7cm dry ice surf wt at 11cm no snow left
8-Jul	189 40	75	*0 900*	56 5	0 35	some AC around v porous 7cm crystalline abl ice 8cm of water under that
10-Jul	191 48	115	*0 900*	86 3	0 36	Clr v lg crystal porous 21cm dug easy w/ shovel wt=6cm

12-Jul	193 42	81	*0 900*	50 1	0 38	var 50-OVC, dry porous ice surf 13cm to firmer ice, wt=8cm, minor flow nearby
13-Jul	194 88	55	*0 900*	41 3		stakes melting out
14-Jul	195 71	30	*0 900*	22 5		SC8 redrilled stakes
16-Jul	197 44	64	*0 900*	47 8	0 49	ST cloudy, lots of microcryoconite 15cm deep, really loose porous ice, wt=11cm
17-Jul	198 43	38	*0 900*	31 4		crystal broken porous stuff
19-Jul	200 47	84	*0 900*	63 0	0 36	ST OVC, surf specked w dirt, but cleaner than AS9 hard ice lg porous crystals wt=5cm
22-Jul	203 40	45	*0 900*	36 9		FOG, white, crystalline and porous surf , wt=8cm, lots of micro cryoconite
24-Jul	205 44	62	*0 900*	54 5	0 42	OVC3000ST, not many cryoc dry porous ice for 5cm, wt=9cm, sm surf flow, surf rel clean
26-Jul	207 43	43	*0 900*	35 8	0 45	OVCSC, R-, v lg crystals, dry surf=2cm thick, wt=7cm, harder ice at 10cm, micro c holes
28-Jul	209 44	47	*0.900*	41 1	0 36	sun just behind AC, surf v por + crumbly, crystal ice surf to 10cm, few c holes to 11cm, wt=6-11cm flow under surf
30-Jul	211 48	27	*0 900*	22.6	0 45	sun bright, many micro c holes, surf quite clean, v lg crunchy chunky crystal ice to 7cm, wt=8cm, v little surf flow
1-Aug	213 43	111	*0 900*	91 9	0 29	sun on edge of cloud, dirtier than last visit, crunchy + crystally, wt=0, lg crystals loosely bonded 8cm thick, wt=7cm
10-Aug	222 04					wind-blown snow, snow only 1-10cm deep at stn
	Total	1145		854 8		

AS9

12-Jun	163 48		0.419			
14-Jun	165 43	16	0 423	6 8	0 74	sun very dimly visible, upper 2-5cm wet snow, snow-ice interface dry
18-Jun	169 52	6	0 440	2 7	0 69	Clr, hard crustly layer 1cm thick at surf, ice layer at 10cm, dry granular below that
20-Jun	171 39	2	0 380	1 0	0 61	thin CU obscuring sun, 26cm deep snow, hard ice layer on top 1cm thick, loose hoar below
22-Jun	173 39	13	0.475	4 8	0 62	thin Cl, hard granular, rippled snow surf
24-Jun	175 46	-32	0 486	-15 2	0 76	S, 1cm fresh snow on older, wet snow
26-Jun	177 38	-19	0 345	-9.4	0 80	OVC, orb of sun vis, fresh snow is patchy from 0-5cm deep, 70% area is fresh snow, albedo on older snow = 76%
28-Jun	179 39	-31	0 556	-10 6	0 75	ST, fresh snow 2 5 cm thick and wet
30-Jun	181.47	61	0 563	33 9	0 53	SC cloud in front of sun, ice surf wet, snow 16 cm deep, flow in ice
2-Jul	183 43	55	*0 650*	31 2		OVC, hard, crusty stuff, trickle of flow nearby
4-Jul	185.42	25	*0.792*	16 0	0 57	ST overcast, sun dim vis, v saturated and slushy, 5cm to ice layer
6-Jul	187 38	43	*0.900*	34.1	0.44	AC cloudy, 9cm of porous dry surf ice, wt=16cm, bits of snow around, si starting to ablate
8-Jul	189 39	60	*0.900*	44.8	0 38	puff of AC, 10cm of grainy stuff, saturated, many more channels on both sides of stn
10-Jul	191 47	114	*0.900*	85.3	0 34	Clr, crunchy porous ice, cryoconite to 16cm, wt=8cm, a few streams, si all gone
12-Jul	193 39	88	*0 900*	65.8	0 36	OVC5000, cryoc 15cm deep, 0 1-20cm wide, dry porous surf 10cm deep, wt=6cm, surf becoming dirtier
14-Jul	195 38	80	*0.900*	59 8	0 30	Clr, crystalline + crunchy, micro-cryoc , some 8cm deep, wt=9cm
16-Jul	197 43	91	*0.900*	68 0	0 44	OVC, ST moving in, surf much dirtier, many sm cryoconite holes to 14cm deep, wt=9cm, porous ice 5cm
19-Jul	200 46	117	*0 900*	96 8	0 34	ST OVC, lots of cryoc , mostly sm, quite dirty ice surf, some flow in channels, wt=4-5cm
23-Jul	204 48	117	*0.900*	96 3		OVC5000ST, surf v dirty, surf flow in channels, v hard crunchy surf, numerous cryoc holes, some coalescing
24-Jul	205.38	25	*0.900*	20.4	0 35	OVC3000ST, surf same as yest
26-Jul	207 42	40	*0.900*	33 3	0.33	OVCST sun v dimly vis, c holes to 11cm, wt=7cm, trickle of flow by stn, surf flecked w dirt, white porous is 4-5cm thicl
28-Jul	209 43	54	*0 900*	47 5	0 28	sunny, some clouds whipping by, surf specked w dirt, most micro c holes to 7cm wt=5cm
30-Jul	211 47	46	*0.900*	38 0	0 33	sun bright Cl-, micro c holes, wt=8cm, trickle of flow thru stn which froze last nite, 3cm thin loose crystally ice
1-Aug	213 43	97	*0.900*	73 0	0 24	sun briefly behind SC, surf quite dirty, stream flowing thru stn, sm melted c holes, white crystally ice at surf=2cm

3-Aug	215 43	20	*0.900*	16 2		FOG/ST, 0 5cm fresh, slightly packy snow, sm amount of flow in channel to N
10-Aug	222 01					wind-packed snow, some areas blown free, depths from 1-14cm at stn
	Total	1087		840 2		

AS10

13-Jun	164 48		0.411			
18-Jun	169 51	7	0.454	3 0	0 72	Clr, blowing snow, hard layer 10cm thick, below it is granular
21-Jun	172 42	4	*0 470*	1 7		snow very crusty
24-Jun	175 43	-15	0 542	-7 2	0 86	S-, wet snow on ground
26-Jun	177 68	-13	*0 400*	-7 0		fresh snow ranges from 1-6 cm deep, not drifted too much
27-Jun	178 65	-19	*0.400*	-7 6		OVC, S-, fresh snow at stn
30-Jun	181 48	96	0.511	38 5		some new snow still on surf, 7 cm wet snow then dry, crystally stuff
5-Jul	186 55	212	*0 750*	108 4		snow 18cm deep, v wet surf
7-Jul	188 48	71	*0 750*	53 5		slush, 16cm deep, ponded water all around
9-Jul	190 56	136	*0.750*	102 0		slushy, grainy snow 5cm melting si slush
13-Jul	194 40	177	*0 900*	133 0		dry porous ice, bit crumbly, #4-10 in meltwater channel, crevasse by stn has filled in w/ ice, si likely gone
14-Jul	195 35	27	*0 900*	20 0	0.48	Clr, white, crunchy snow (hardened last night)
15-Jul	196 46	39	*0 900*	29 3		river flowing under #4,10 but down a lot, dry, crunchy surf
16-Jul	197 43	30	*0 900*	22 3	0 53	AS OVC, ST forming over pk, surf porous + hard, 3cm thick, micro-cryoconite
17-Jul	198 43	33	*0 900*	27 5		little trickle in channel under wires, cryoconite 10-12cm deep
19-Jul	200 38	55	*0 900*	41 0	0 42	some CU, low ST whipping by, crystal hard stuff, num cyroc 24cm diam and 1mm diam , 15cm deep, wt=7cm
23-Jul	204 43	94	*0 900*	77 3		OVC, ST/AS, lg c to 20cm diam + 12-14cm deep wt=9cm, crunchy surf, 4cm crunchy stuff on top sat por ice under
26-Jul	207 39	45	*0 900*	37 4	0 43	OVCST breaking, many well-dev c holes, still surf flow in channel, white dry crystalline surf, stream in stn only a trickle
28-Jul	209 39	37	*0 900*	32 1	0 41	CU/SC forming BKN, c holes 15cm, stream trickling under porous ice, wt=4-10cm, rough surf
29-Jul	210 48	15	*0.900*	12 4		AC/CI, mist/fog forming and dissipating
30-Jul	211 47	33	*0.900*	27 5	0 47	v little cloud, thin CI, many c holes, dirt in channel thru stn and bit of trickle crunchy lg crystal ice
1-Aug	213 40	83	*0 900*	62 0	0 41	STOVC, surf flecked w lots of dirt, c holes lg some dry to 11cm, wt=8-5cm, surf dry crunchy, chnls flowing well
3-Aug	215 42	15	*0 900*	12 1	0 64	S-, STOVC, 1cm fresh snow, channel thru stn iced over but still flow, lg channel to N flowing well
	Total	1162		819 0		

AS11

13-Jun	164 51		0 348			
18-Jun	169 50	13	0 440	4 6	0 59	surf hard + icy 2cm thick soft dry snow underneath
24-Jun	175 43	-15	0 335	-6 6	0 86	ST + S fresh snow surface

28-Jun	179 72	-8	*0 500*	-2 8		fresh snow 4-5cm deep
5-Jul	186 56	261	*0 550*	130 5		firn at 56cm, 77cm to glacier ice, wet only to firn
7-Jul	188 64	90	*0 600*	49 5		depth to ice = 74cm, 12cm of water in snowpit
13-Jul	194 94	416	*0 650*	249 6	0 63	glacier in shade, v wet, ponded water in slush, snow 8-10cm deep, good flow in slus
19-Jul	200 39	175	*0 900*	113 8	0 47	FOG, melting si and saturated drier than last time and streams well developed winter snow all gone
23-Jul	204 43	75	*0 900*	67 8		OVC ST/AS, v slushy melting si, 6cm dry, 4cm wet, harder ice below that, some flow in chnls, fairly clean surf
28-Jul	209 39	69	*0 900*	62 4	0 40	ST- puffs infront sun, hardish crust surf 9cm thick melting si, wet si under, v clean surf, lg areas crusty/mushy si
30-Jul	211 40	18	*0 900*	16 2	0 47	OVC- CI, quite sunny, clean white ice, crusty slushy melting si10cm, slushy underneath si under
2-Aug	214 52	77	*0.900*	69 0		melting si 4-5cm, surf v white v wet, some harder coarse ice showing thru fog around and temp falling (melting s i)
	Total	1171		754 0		

AS12

13-Jun	164 52		0 310			
18-Jun	169 47	2	0 521	0 7	0 71	very windy, blowing snow, sunny, icy crust on surf, crunchy layer at 18cm, dry loose snow (hoar) below that
24-Jun	175 40	-44	0 264	-22 8	0 84	ST, sun dim vis, fresh snow (3cm) over wet snow
28-Jun	179 71	-28	*0 300*	-7 3		fresh snow (9cm), top is wet
7-Jul	188 63	285	*0.500*	85 5		snow 21-27cm deep, si surf wet, water flowing on surf of ice in places
13-Jul	194 97	300	*0.650*	150 2	0 56	grainy snow 5cm, v wet surf under, AC7, sm supragl streams flowing
19-Jul	200 43	127	*0 900*	82 6	0 50	OVC ST, areas of cryoconite development, dry, crystally hard ice, some slushy melting si on which albedo taken
23-Jul	204 46	84	*0 900*	75 3		OVC50ST, well-dev c up to 16cm deep crystally ice + dirt is 12cm below white, slushy surf, 3 snow patches by Qalliq
28-Jul	209 42	76	*0 900*	68 7	0 46	ST puffs but clr, lots of c holes, dry crusty white surf 7cm, mushy melting si under, still patch of snow up by Qalliq
30-Jul	211 42	27	*0 900*	24 6	0 49	OVC- CI, maj c holes and macro, flow in chnls, ice layer fr last nite, flow below surf, wt=8cm, c hole=11cm, stn fairly clr
2-Aug	214 63	164	*0 900*	147 6		two stakes melted out, much cryoc here, so ice surf really 5-12cm lower, fog moving in and out
		995		605 1		

Notes.

Density values in italics are estimates (always 0.9g/cm3 for ice)
Cloud heights are given in feet a.s.l.
Water table (wt) is the depth in the glacier ice at which standing or flowing water is present
C holes are cryoconite holes, measured by depth (cm)
Si is superimposed ice

APPENDIX J

GRAPH OF ALBEDO AT AS1-12

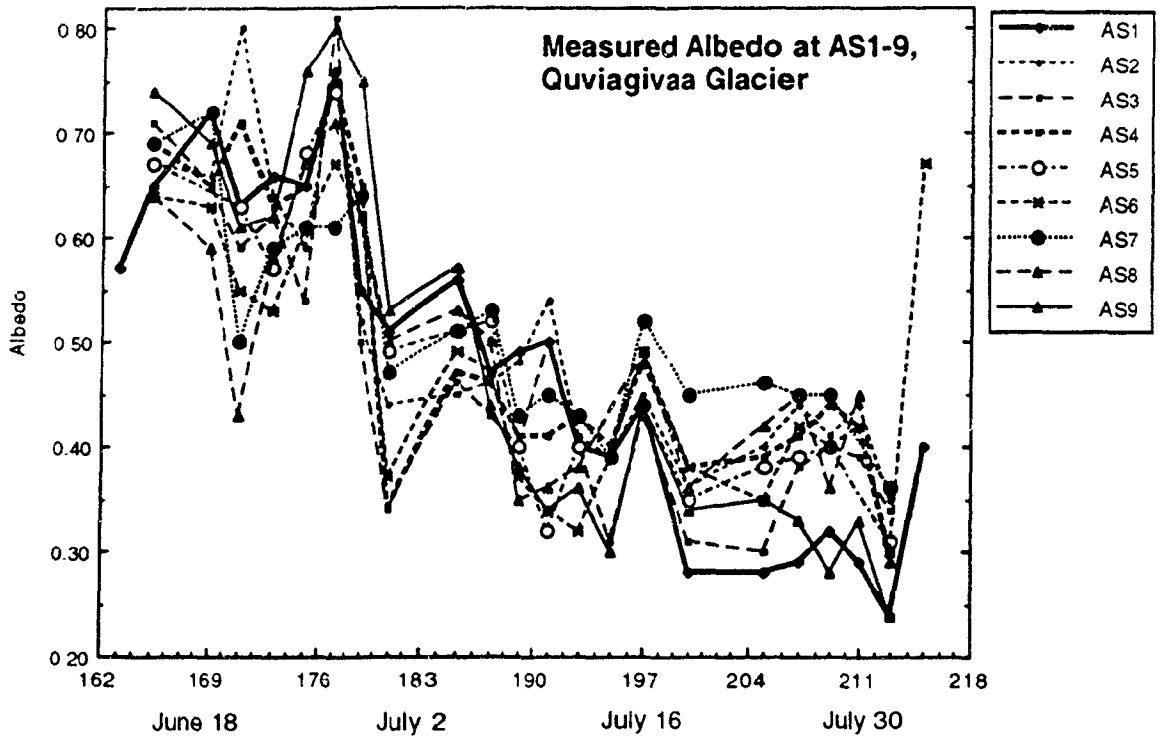
Measured Albedo at AS1-9,
Quviagivaa Glacier
Albedo
0 80
0 70
0 60
0 50
0.40
0.30
0 20
162
169
176
183
190
197
204
211
218
June 18
July 2
July 16
July 30
AS1
AS2
AS3
AS4
AS5
AS6
AS7
AS8
AS9

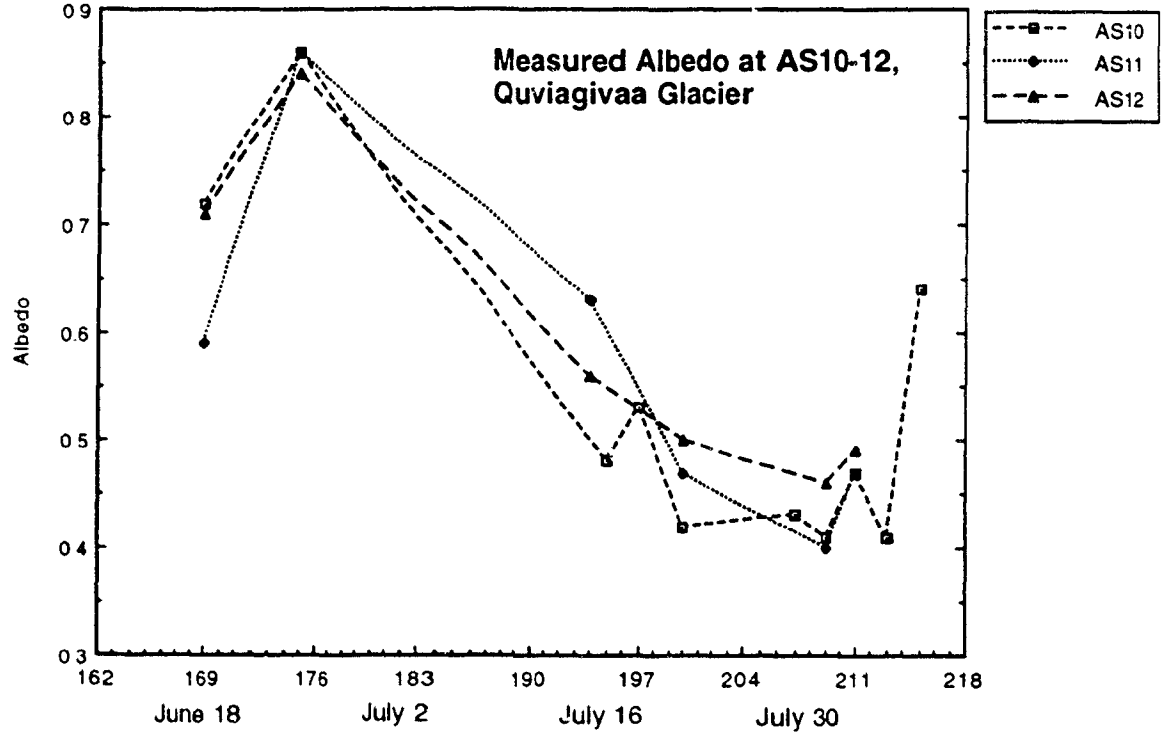
Measured Albedo at AS10-12,
Quviagivaa Glacier
Albedo
0 9
0 8
0 7
0.6
0 5
0 4
0 3
162
169
176
183
190
197
204
211
218
June 18
July 2
July 16
July 30
AS10
AS11
AS12

APPENDIX K

PLOTS OF ABLATION VERSUS DISCHARGE FOR AS1-12

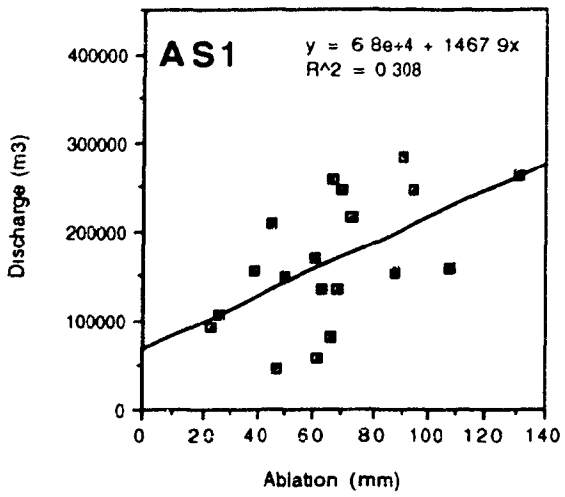
AS1
y = 6 8e+4 + 1467 9x
R^2 = 0 308
Discharge (m3)
Ablation (mm)

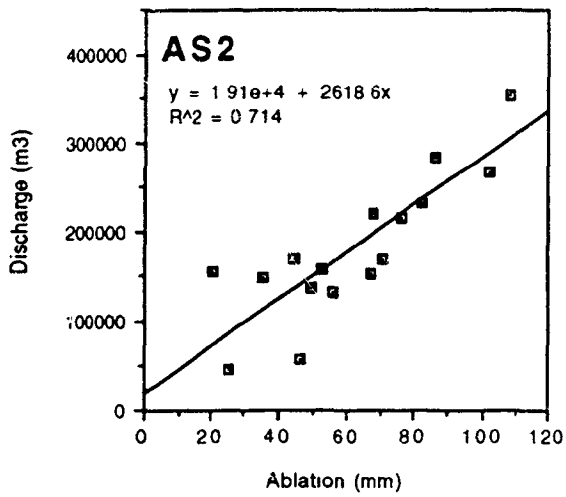
AS2
y = 1 91e+4 + 2618 6x
R^2 = 0 714
Discharge (m3)
Ablation (mm)

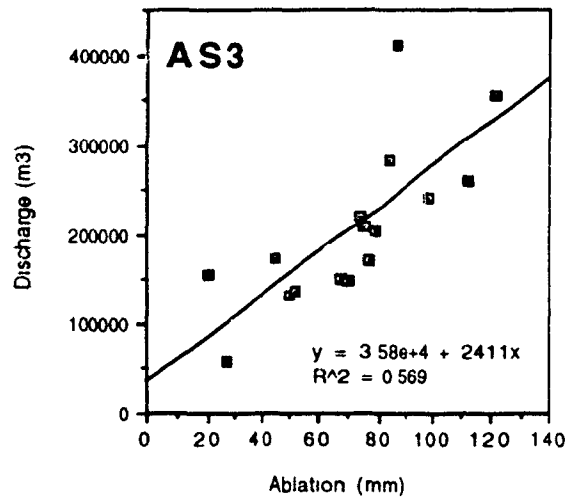
AS3
y = 3 58e+4 + 2411x
R^2 = 0 569
Discharge (m3)
Ablation (mm)

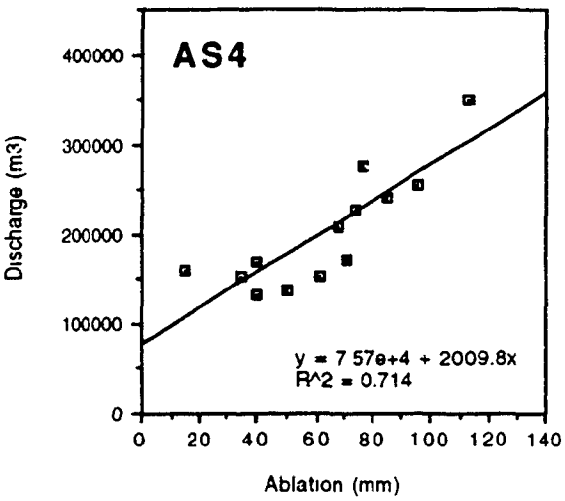
AS4
y = 7 57e+4 + 2009.8x
R^2 = 0.714
Discharge (m3)
Ablation (mm)

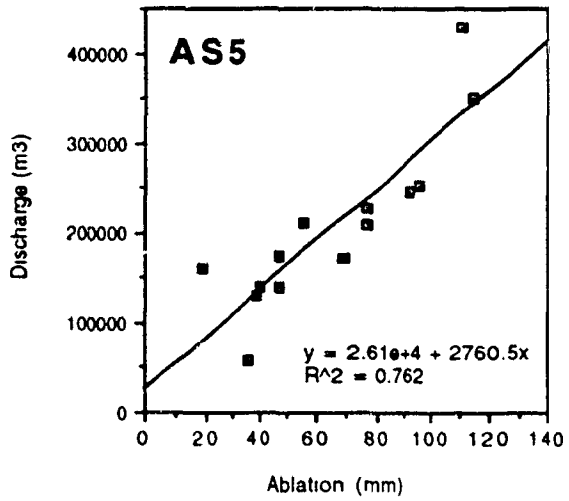
AS5
y = 2.61e+4 + 2760.5x
R^2 = 0.762
Discharge (m3)
Ablation (mm)

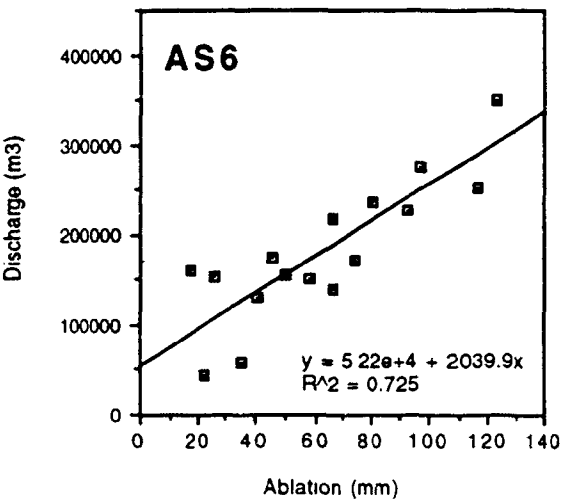
AS6
y = 5 22e+4 + 2039.9x
R^2 = 0.725
Discharge (m3)
Ablation (mm)

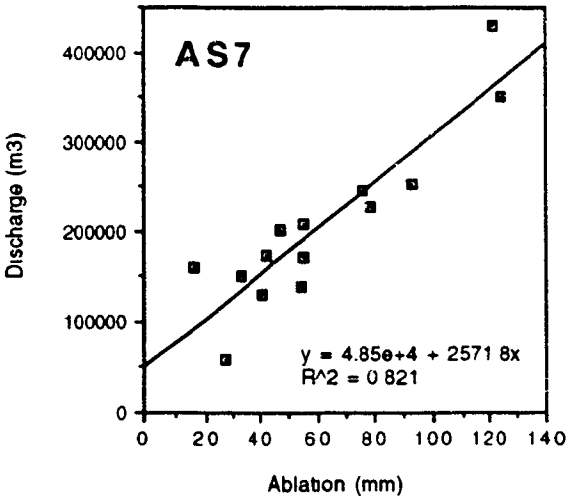
AS7
y = 4.85e+4 + 2571 8x
R^2 = 0 821
Discharge (m3)
Ablation (mm)
0
100000
200000
300000
400000
0 20 40 60 80 100 120 140

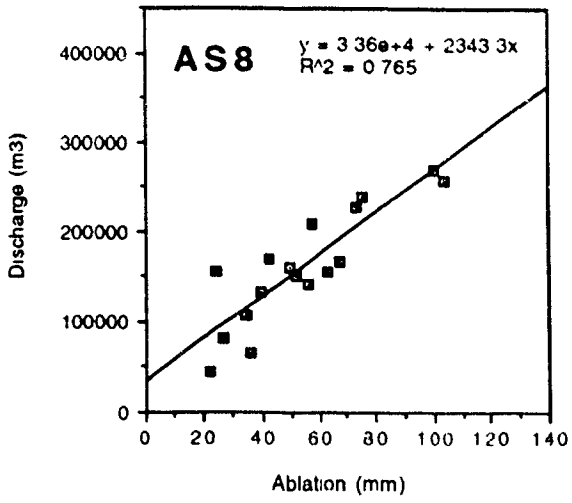
AS8
y = 3 36e+4 + 2343 3x
R^2 = 0 765
Discharge (m3)
Ablation (mm)
0
100000
200000
300000
400000
0 20 40 60 80 100 120 140

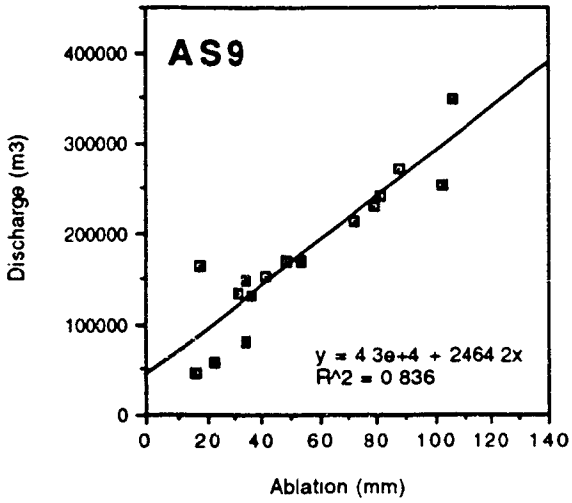
AS9
y = 4 3e+4 + 2464 2x
R^2 = 0 836
Discharge (m3)
Ablation (mm)
0
100000
200000
300000
400000
0 20 40 60 80 100 120 140

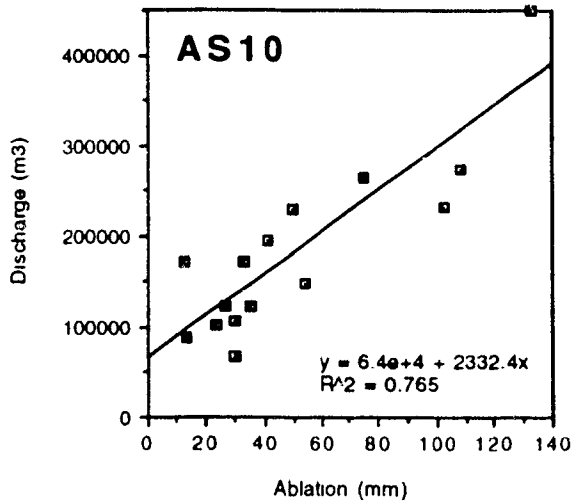
AS10
y = 6.4e+4 + 2332.4x
R^2 = 0.765
Discharge (m3)
Ablation (mm)
0
100000
200000
300000
400000
0 20 40 60 80 100 120 140

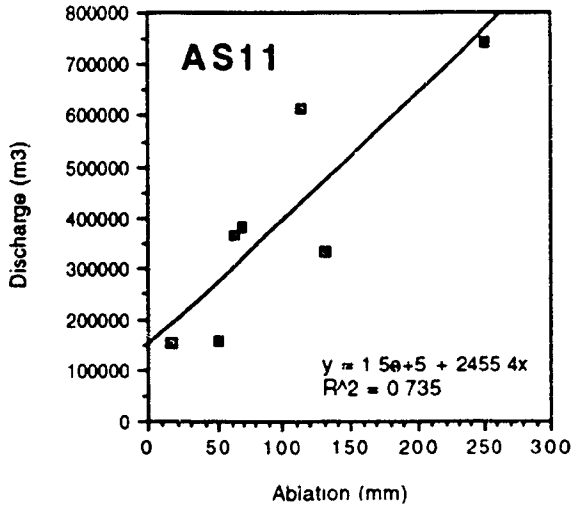
AS11
y = 1 5e+5 + 2455 4x
R^2 = 0 735
Discharge (m3)
Ablation (mm)
0
100000
200000
300000
400000
500000
600000
700000
800000
0 50 100 150 200 250 300

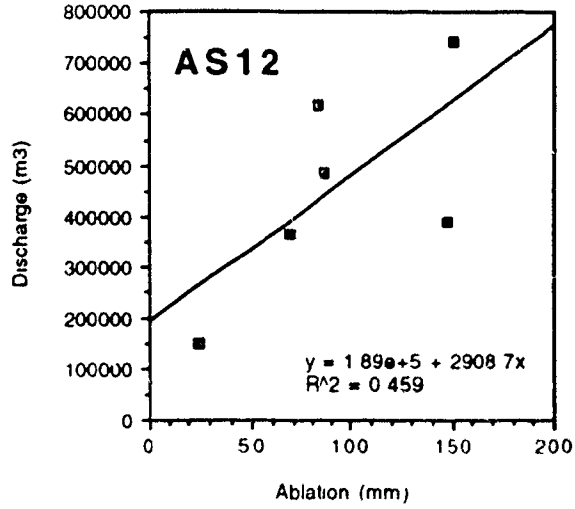
AS12
y = 1 89e+5 + 2908 7x
R^2 = 0 459
Discharge (m3)
Ablation (mm)
0
100000
200000
300000
400000
500000
600000
700000
800000
0 50 100 150 200

APPENDIX L

PLOTS OF ABSORPTIVITY FOR AS1-10

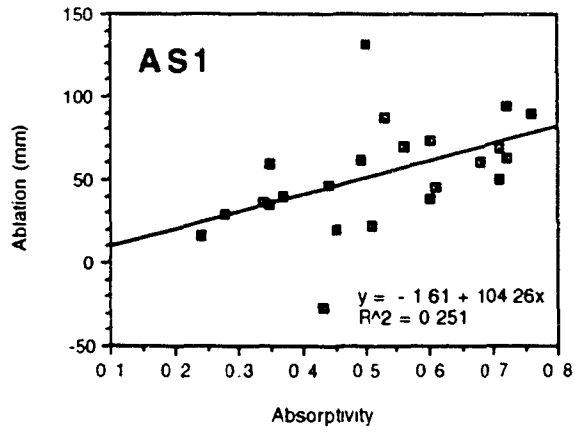
AS1
Ablation (mm)
Absorptivity
y = - 1 61 + 104 26x
R^2 = 0 251

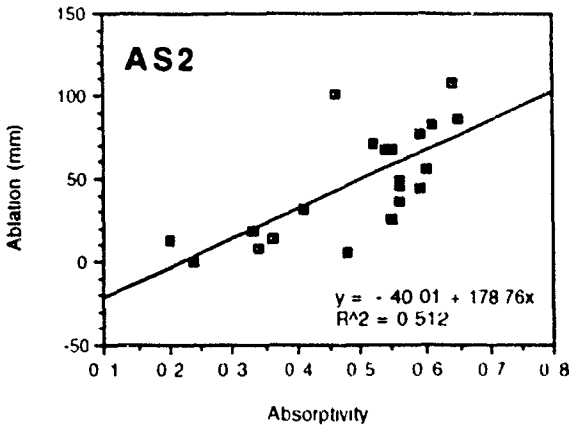
AS2
Ablation (mm)
Absorptivity
y = - 40 01 + 178 76x
R^2 = 0 512

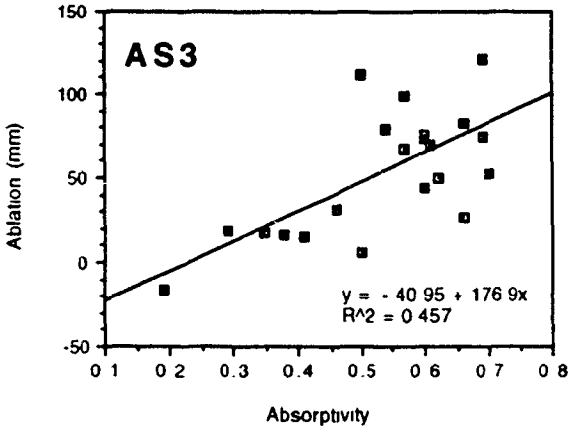
AS3
Ablation (mm)
Absorptivity
y = - 40 95 + 176 9x
R^2 = 0 457

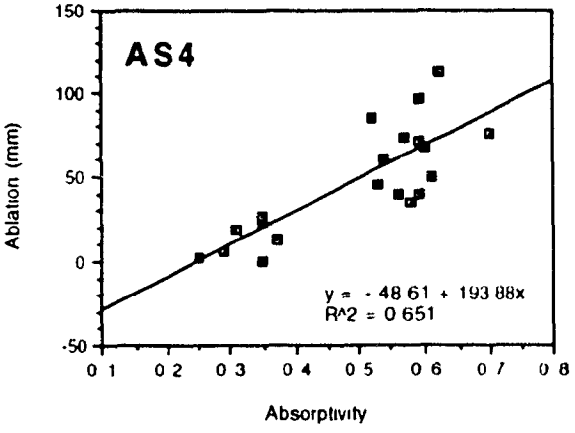
AS4
Ablation (mm)
Absorptivity
y = - 48 61 + 193 88x
R^2 = 0 651

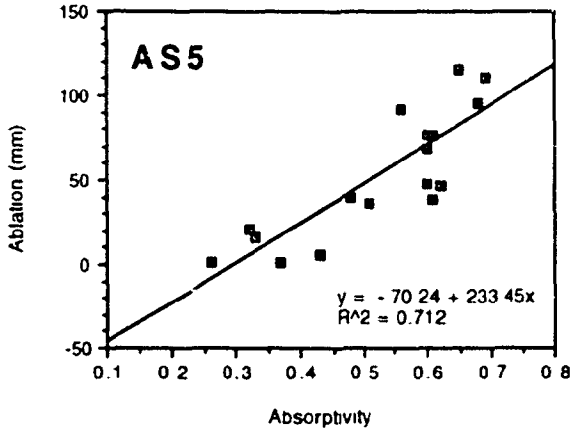
AS5
Ablation (mm)
Absorptivity
y = - 70 24 + 233 45x
R^2 = 0.712

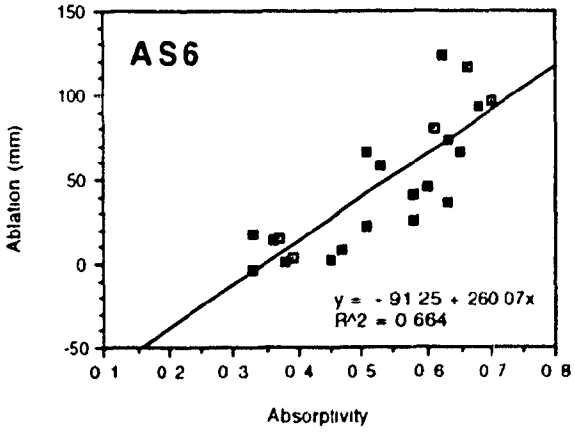
AS6
Ablation (mm)
Absorptivity
y = - 91 25 + 260 07x
R^2 = 0 664

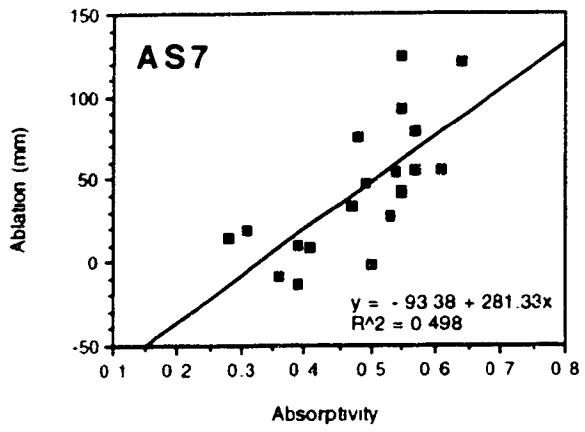
AS7
Ablation (mm)
Absorptivity
y = - 93 38 + 281.33x
R^2 = 0 498

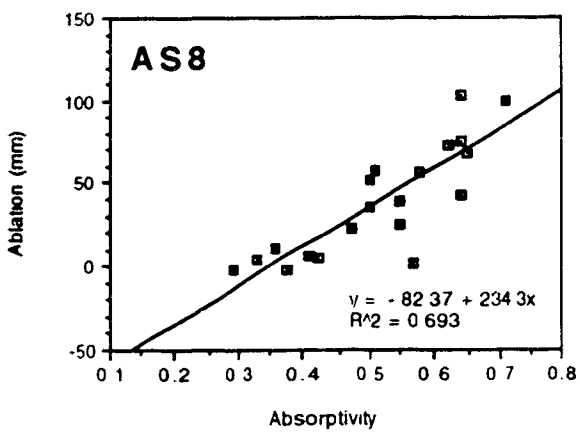
AS8
Ablation (mm)
Absorptivity
y = - 82 37 + 234 3x
R^2 = 0 693

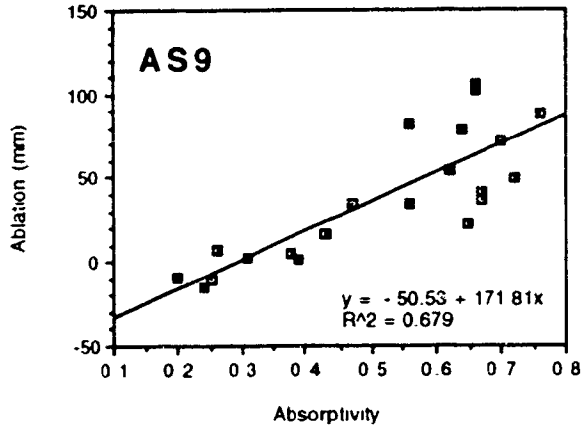
AS9
Ablation (mm)
Absorptivity
y = - 50.53 + 171 81x
R^2 = 0.679

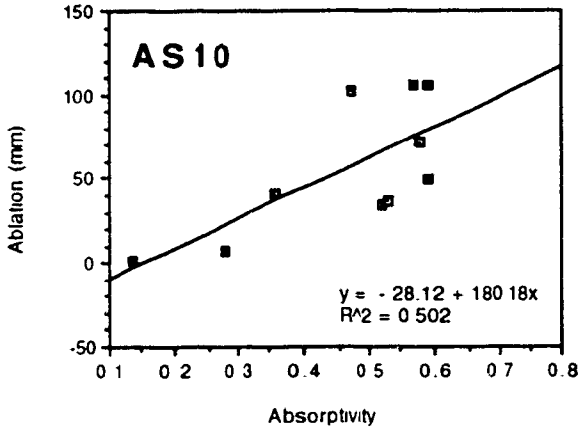
AS10
Ablation (mm)
Absorptivity
y = - 28.12 + 180 18x
R^2 = 0 502

APPENDIX M

AN ANALYSIS OF THE AUGUST, 1993 SNOWSTORM

An Analysis of the August, 1993 Snowfall

The 1993 melt season ended on August 2, and the 1993-94 accumulation season began abruptly on August 3 with a snowfall event. Snow, high winds, and sub-zero temperatures persisted from August 3 up to and including August 11, at which time the glacier camp was abandoned for the season. A snow depth survey carried out on the snout of the glacier (560-850m a.s.l.) on August 10 determined an average snow depth of 26cm and a range of depths from 0-98cm. The pattern of accumulation after strong winds from the southeast and east on August 8-9 respectively, produced an accumulation that closely resembles the pattern of the previous spring, with highest accumulation at the terminus, and lower accumulation on the central snout. The following table shows data collected during the August 10 snow survey for eight transects across the snout of the glacier.

Quviagivaa Glacier snow survey, August 10, 1993

Transect	# of meas.	Average depth (cm)	Range (cm)	Standard Dev. (cm)
1	12	46	22-98	22
2	5	24	10-31	8
3	7	22	1-41	12
4	14	23	11-31	6
5	14	30	17-43	9
6	14	14	0-39	13
7	14	23	4-37	10
8	28	23	0-54	13
Total	103	26	0-98	17

Using a minimum average density for wind blown snow of 0.35g cm^{-3} (Patterson, 1981), the average accumulation for the snout is 92mm, which represents 30% of the total accumulation for the 1992-93 season. Snow depths ranging from 40-50cm at the meteorological station on August 11 suggest that

the average accumulation for the entire glacier at this time could be as high as 130mm water equivalent, or 43% of the measured 1992-93 winter mass balance. For the eastern Fosheim Peninsula, Koerner (1979) shows an average value of snow accumulation of 150mm, based on cores for the period of 1962-1973. These findings suggest the potential importance of late summer snowfall for glacier mass balance.

References quoted in Appendix M

Koerner, R.M. (1979). Accumulation, ablation, and oxygen isotope variations on the Queen Elizabeth Islands ice caps, Canada. Journal of Glaciology. **22** (86): 25-41.

Paterson, W.S.B. (1981). The Physics of Glaciers. 2nd Edition, Oxford: Pergamon Press Ltd. 380p.

APPENDIX N

QUVIAGIVAA CREEK RATING CURVES

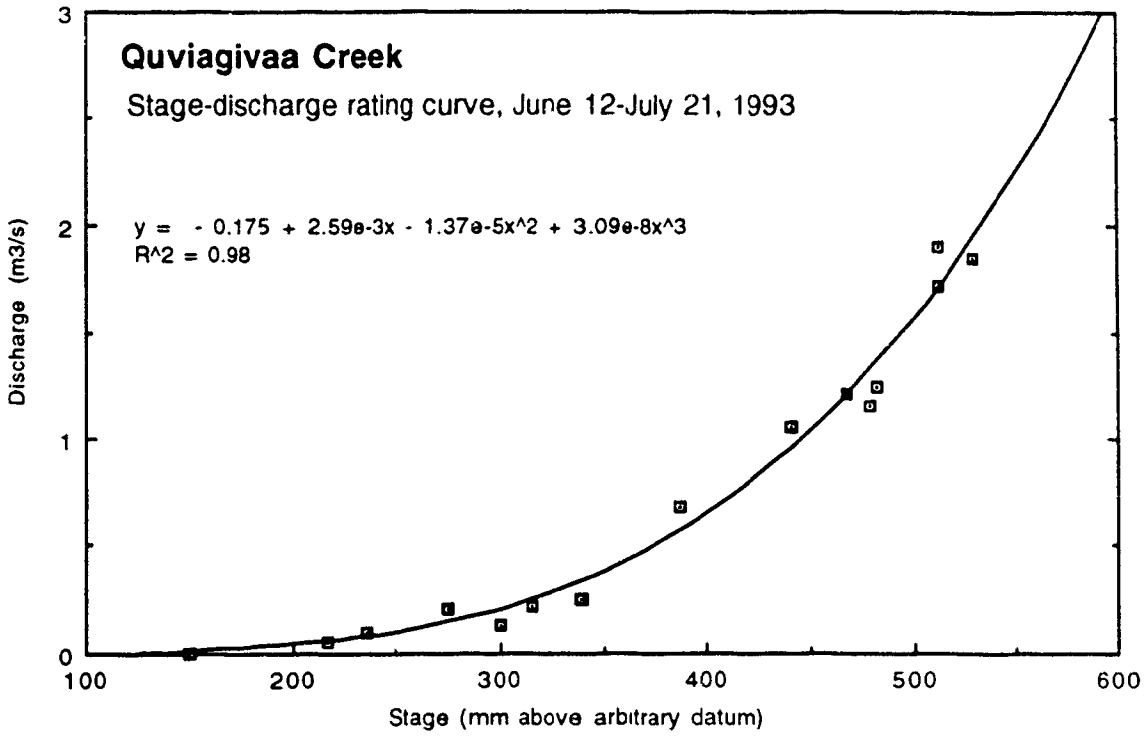
Quviagivaa Creek
Stage-discharge rating curve, June 12-July 21, 1993
y = - 0.175 + 2.59e-3x - 1.37e-5x^2 + 3.09e-8x^3
R^2 = 0.98
Discharge (m3/s)
Stage (mm above arbitrary datum)
0
1
2
3
100
200
300
400
500
600

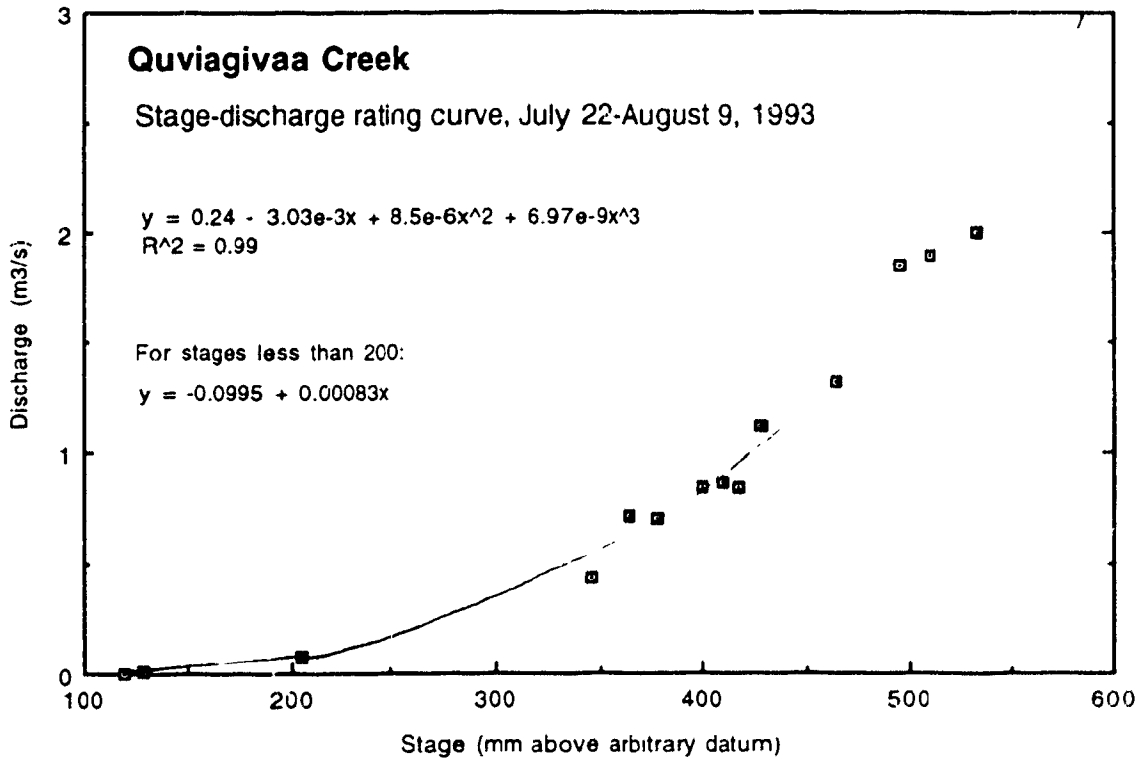
Quviagivaa Creek
Stage-discharge rating curve, July 22-August 9, 1993
y = 0.24 - 3.03e-3x + 8.5e-6x^2 + 6.97e-9x^3
R^2 = 0.99
For stages less than 200:
y = -0.0995 + 0.00083x
Discharge (m3/s)
Stage (mm above arbitrary datum)
0
1
2
3
100
200
300
400
500
600

APPENDIX O

QUVIAGIVAA CREEK DISCHARGE RECORD

Quviagivaa Creek Discharge Record, 1993

Date	Av Discharge (m3/s)	Total Discharge (m3)
13-Jun	0.0185	1598
14-Jun	0 0464	4009
15-Jun	0.0437	3776
16-Jun	0.0623	5383
17-Jun	0.0769	6644
18-Jun	0.0888	7672
19-Jun	0.1387	11984
20-Jun	0.2035	17582
21-Jun	0.1782	15396
22-Jun	0.1876	16209
23-Jun	0.3214	27769
24-Jun	0.2607	22524
25-Jun	0.1315	11362
26-Jun	0.0862	7448
27-Jun	0.1086	9383
28-Jun	0.2156	18628
29-Jun	0.4776	41265
30-Jun	0.8825	76248
1-Jul	0.9175	79272
2-Jul	0.2084	18006
3-Jul	0.3303	28538
4-Jul	0.7588	65560
5-Jul	0.9608	83013
6-Jul	0.7978	68930
7-Jul	1.2015	103810
8-Jul	1.3406	115828
9-Jul	1.4590	126058
10-Jul	1.4299	123543
11-Jul	1.3388	115672
12-Jul	1.2105	104587
13-Jul	1.2646	109261
14-Jul	1.2570	108605
15-Jul	1.4675	126792
16-Jul	1.1913	102928
17-Jul	1.3421	115957
18-Jul	1.3876	119889
19-Jul	1.5142	130827
20-Jul	1.5948	137791
21-Jul	1.7935	154955
22-Jul	0.9156	79110
23-Jul	0.7904	68288
24-Jul	0.6393	55235
25-Jul	0.8299	71703
26-Jul	1.1252	97217
27-Jul	0.8872	76654
28-Jul	0.9460	81734
29-Jul	0.8155	70459
30-Jul	1.2251	105849
31-Jul	1.8423	159175

Date	Av Discharge (m3/s)	Total Discharge (m3)
1-Aug	1.4129	122075
2-Aug	0.7206	62260
3-Aug	0.2430	20995
4-Aug	0.0747	6454
5-Aug	0.0570	4925
6-Aug	0.0420	3629
7-Aug	0.0333	2877
8-Aug	0.0266	2298